AD_____

Award Number: W81XWH-11-1-0580

TITLE: Targeting Microglia to Prevent Post-Traumatic Epilepsy

PRINCIPAL INVESTIGATOR: Daniel S. Barth

CONTRACTING ORGANIZATION: The Regents of the University of Colorado
Boulder, CO 80303-1058

REPORT DATE: July 2014

TYPE OF REPORT: Final report

PREPARED FOR: U.S. Army Medical Research and Materiel Command
Fort Detrick, Maryland 21702-5012

DISTRIBUTION STATEMENT: Approved for Public Release;
Distribution Unlimited

# REPORT DOCUMENTATION PAGE

*Form Approved*
*OMB No. 0704-0188*



| 1. REPORT DATE | 2. REPORT TYPE | 3. DATES COVERED |
|---|---|---|
| July 2014 | Final | 1 Jul 2011 - 30 Jun 2014 |

**4. TITLE AND SUBTITLE**
Targeting Microglia to Prevent Post-traumatic Epilepsy

**5a. CONTRACT NUMBER**

**5b. GRANT NUMBER**
W81XWH-11-1-0580

**5c. PROGRAM ELEMENT NUMBER**

**6. AUTHOR(S)**
Daniel S. Barth

E-Mail: dbarth@psych.colorado.edu

**5d. PROJECT NUMBER**

**5e. TASK NUMBER**

**5f. WORK UNIT NUMBER**

**7. PERFORMING ORGANIZATION NAME(S) AND ADDRESS(ES)**
The Regents of the University of Colorado
Boulder, CO 80303-1058

**8. PERFORMING ORGANIZATION REPORT NUMBER**

**9. SPONSORING / MONITORING AGENCY NAME(S) AND ADDRESS(ES)**
U.S. Army Medical Research and Materiel Command
Fort Detrick, Maryland 21702-5012

**10. SPONSOR/MONITOR'S ACRONYM(S)**

**11. SPONSOR/MONITOR'S REPORT NUMBER(S)**

**12. DISTRIBUTION / AVAILABILITY STATEMENT**
Approved for Public Release; Distribution Unlimited

**13. SUPPLEMENTARY NOTES**

**14. ABSTRACT**
The purpose of this research project is to explore anti-epileptogenic strategies in and animal model of post-traumatic epilepsy (PTE) using lateral fluid percussion injury (LFPI). Our focus is on attenuating damaging effects of hyperexcitability in the brain induced by inflammation resulting from glial cell immune responses to trauma. We are exploring two drugs, MN166 and SLC022, that are known to suppress post-traumatic glial activation and thus inflammation to evaluate their effectiveness in preventing epileptogenesis in the LFPI model of PTE. In the first project year we developed a high-speed video/EEG recording and analysis system for rapid quantification of chronically recorded epileptiform activity in multiple (24-32) subjects. With this system we became expert in identifying epileptiform versus normal video/EEG activity in the rodent and discovered an important source of artifact currently being interpreted in other published reports as seizure activity. We developed a pilocarpine model of temporal lobe epilepsy to explore the effectiveness of glial cell (neuroimmune) attenuation in preventing or limiting epileptogenesis (development of epilepsy) in this rapidly developing model. We explored numerous changes in the LFPI model to produce earlier developing signs of epilepsy, increasing the probability of succeeding in our long-term study of epileptogenesis following traumatic brain injury. Perhaps the most important outcome of this work was the negative finding that much published work concerning PTE with the LFPI model has not properly examined controls. Both injured and uninjured rats display spike-wave discharge (SWD) that, unlike previous reports, are not seizures. The actual incidence of seizures with LFPI may be extremely low, suggesting the need for a better model. Finally, we discovered and published results concerning development of post-traumatic anxiety in our brain injured animals that we could effectively prevent with peri-injury and post-injury administration of glial attenuating drug, MN-166, the same drug we hope to use for prevention of epileptogenesis in the future.

**15. SUBJECT TERMS**
Post-traumatic epilepsy, traumatic brain injury, neuroinflammation, neuroimmune

| 16. SECURITY CLASSIFICATION OF: | | | 17. LIMITATION OF ABSTRACT | 18. NUMBER OF PAGES | 19a. NAME OF RESPONSIBLE PERSON |
|---|---|---|---|---|---|
| a. REPORT | b. ABSTRACT | c. THIS PAGE | | | USAMRMC |
| U | U | U | UU | 175 | 19b. TELEPHONE NUMBER *(include area code)* |

**TABLE OF CONTENTS:**

**INTRODUCTION:**

Post-traumatic epilepsy (PTE) is a common result of traumatic closed head injury. The development of epilepsy (epileptogenesis) can take many months to several years before the appearance of behavioral seizures. Compared to other forms of epilepsy, PTE is particularly resistant to antiseizure medication once it has developed and there are currently no therapeutic interventions to prevent or attenuate epileptogenesis. The purpose of this research project is to explore anti-epileptogenic strategies in and animal model of PTE using lateral fluid percussion injury (LFPI). Our focus is on attenuating damaging effects of hyperexcitability in the brain induced by inflammation resulting from glial cell immune responses to trauma. We are exploring two drugs, MN166 and SLC022, that are known to suppress post-traumatic glial activation and thus inflammation to evaluate their effectiveness in preventing epileptogenesis in the LFPI model of PTE. If successful, our results could have accelerated impact on translation to preventing PTE in war fighters since one of these drugs (MN166) has already been approved by the FDA and is in clinical trials for human neuropathic pain studies.

**KEYWORDS:**

Post-traumatic epilepsy, neuroimmune, seizure, traumatic brain injury, pilocarpine, epileptogenesis

**OVERALL PROJECT SUMMARY:**

**YEAR 1**

There were two objectives for year one of this project. The first was to construct a custom video/EEG acquisition/analysis system. The second was to record sensory evoked potentials and spontaneous EEG from acutely anesthetized animals receiving LPS applied directly to the cortical surface to evaluate the effectiveness of MN166 in reducing microglial TLR-4-mediated hyperexcitability.

*Progress on objective 1:* The custom video/EEG acquisition and analysis system is complete and fully functional (**Fig. 1**). This consists of two racks with 16 recording chambers each. Each recording chamber was custom made and consists of a 12" diameter and 24" high plastic cylinder equipped with a 7 channel electrode harness that is attached on one end to chronic screw electrodes on each rat and on the other end to a slip-ring swivel connector, permitting recording with unimpeded movement. Each recording chamber is also equipped

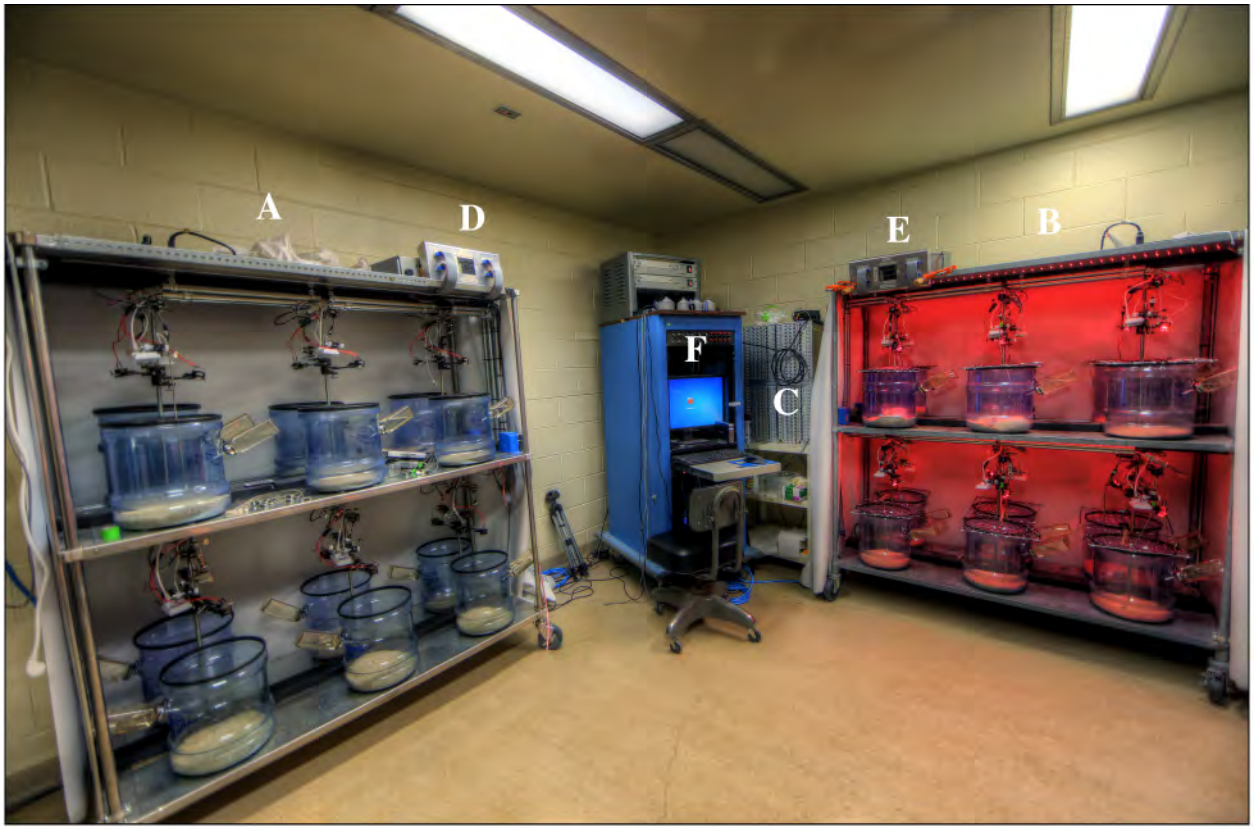


**Fig. 1.** Wide angle view of chronic recording rigs used for video/EEG of 24 (max 32) rats simultaneously. A&B) Dual level platforms holding 6 chambers per level. Each chamber consists of a containment vessel, swivel electrode harness and video camera (shown in higher resolution in next figure). All cameras are IP survailence cameras multiplexed through high speed internet switches on the top of each rig. C) 64 channel EEG amplifier used for our first recordings. D&E) These have now been replaced by 2 custom made 64 channel EEG amps of much smaller dimension. F) Rack cabinet with power supplies and DAQ computer.

with a dedicated surveillance camera (Axis M1011) for recording video. We chose cameras that are designed for internet protocol (IP) recording because they can easily be multiplexed through a wired or wireless router and use compression (H264) to reduce bandwidth (**Fig. 2**), which is critically important for chronic video/EEG recording and analysis. Each chamber is also equipped with DC (light emitting diode) lighting for day (white) and night (red) video recording without disturbing sleep cycles. Two compact 64-channel EEG amplifier systems (designed by the P.I.) were also constructed (one for each rack) to buffer signals before digitization and computer storage. The digital acquisition software was written by the P.I. in Visual Basic and provides a flexible means of logging EEG and simultaneous video for each rat in date/time registered folders. The need to

log video along with EEG posed a particular challenge due to the bandwidth of video and the need to precisely time-lock the signal to each rat's EEG. This problem was solved in part through using IP cameras as noted above. The final solution to the problem was to use computers capable very large RAM storage so 30 minute trials of temporally contiguous EEG could be sampled without interrupt from all rats while spooling video to disk and finally writing the EEG at the end of each trial while the cameras are paused. This data collection hardware/software was finished early and has been fully functional for several months, permitting us to get a head start on chronic video/EEG recording.

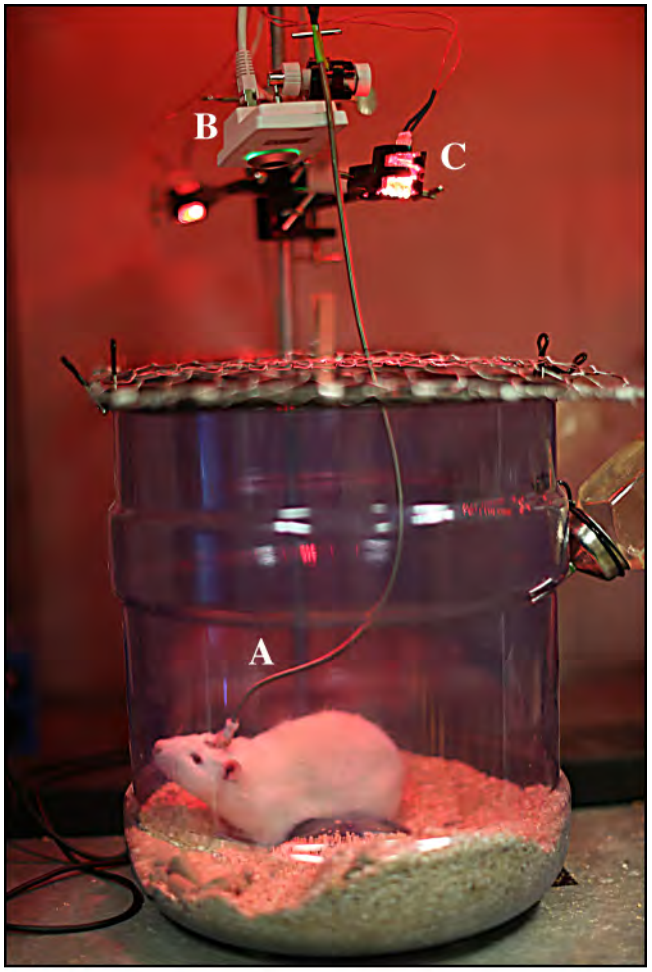


**Fig. 2** Close up view of single recording chamber. A) EEG channel plug for rat head mount attached to flexible electrode harness and slip-ring commutator. B) Survailence camera (1 per rat) providing highly compressed H264 images to limit band-width demands. C) High intensity red LEDs for night recording.

Our analysis hardware and software for the video/EEG data has also been completed and is fully functional. This turned out to be the most challenging part of the project since there is presently no commercially available software that permits extremely rapid inspection of these enormous data sets recorded 24/7 from large numbers of animals. The hardware finally chosen consists of PCs designed for gaming, providing very fast numerical and video processing at moderate cost. Video data is displayed on two high-resolution monitors mounted in tandem, permitting visual inspection of 30 min of EEG in a single page. All data analysis software was written by the P.I. in the MatLab environment and, to our knowledge, exceeds anything commercially or privately available for exploring these large data sets. From the P.I.'s previous experience of the pitfalls of automated analysis of epileptiform EEG data, the design principal of the present software was to permit initial rapid visual inspection of all data, and to use automated analysis only for subsequent quantification of suspected epileptiform events. As noted above, EEG data for a given rat is rapidly presented in 30 min blocks. The operator can rapidly zoom in on suspected epileptiform events and precisely mark their latency with a mouse click for event logging and subsequent quantification. Zooming also defines a time window within which clicking on a trace plays the video clip associated with that window for verification of seizures. Thus, unlike existing review software, our program permits quasi-random access to the data accompanied by user defined video review. This software has now been in extensive use and meets our design goal of reviewing a full one-day data set in 5-10 min. Since we finished the data collection and analysis system ahead of schedule, we have had several months to begin looking at spontaneous recordings from normal and brain damaged rats (noted below). This has prompted two additions to the software for quantifying results. The first was designed for automated epileptic spike detection. Typical spike detection programs commercially available are based on attempting to use universal spike descriptors (i.e. amplitude, rise-time, etc.) to separate spikes from noise. These approaches, while easier to implement, suffer from numerous false positives and noise. The approach we took instead was to take advantage of our ability to rapidly visually identify sub-sets of spikes for each rat individually, and from these make a rat specific average spike template that is sequentially matched to the actual data using a covariance measure that is thresholded to separate signal from noise. This approach is quite accurate, and with our fast processors, can count spikes over many days of data in under an

hour. We have also added a feature to the software that employs a touch screen to permit rapid but manual identification and quantification of more prolonged epileptiform events such as seizures and seizure like artifacts (noted below) for subsequent video verification. The speed of this quantification is achieved by using foot pedals to signal the event type and a wand on the touch screen to mark event time and duration. A brief video demonstration of this analysis software was provided to our Science Officer, Dr. Jordan D. Irvin, and is downloadable at http://dl.dropbox.com/u/11873936/SoftwareDemo1.wmv. We will also be presenting this work at The 2012 Military Health System Research Symposium held 13-16 August 2012 in Fort Lauderdale, Florida. The abstract for this presentation is included in Appendix. We feel our video/EEG data collection/analysis system should serve not just our own research but is sufficiently unique, fast, and inexpensive to be useful for emergency and post-emergency monitoring of soldiers suffering traumatic brain injury in the battlefield.

*Progress on objective 2:* The second objective of this first year project was to determine the efficacy of attenuating glial cell activation (using MN-166 and SLC022) in decreasing acute hyperexcitability of the brain induced by lipopolysacharride (LPS) applied directly to the cerebral cortex of anesthetized rats. Upon initial investigation we realized that anesthesia was having an unacceptable and variable influence on cortical excitability induced by LPS. Thus, while we could suppress excitability through glial attenuation, these results were confounded by additional suppressive anesthesia effects. Particularly troublesome was the fact that the effect of various anesthesia regimes we tried (ketamine/xylazine, xylazine alone, isoflurane, urethane) had highly variable effects in both increasing or decreasing the response to LPS independent of glial modulating treatment. With permission of our Scientific Officer, we decided to abandon this study in order to devote our time instead to accelerating work on unanesthetized animals. This turned out to be a good decision for several reasons:

1) We got a head start on examining chronic video/EEG recording from rats with and without lateral fluid percussion injury (LFPI). We were able to examine these initial recordings with unprecedented accuracy since our software relies on visual as opposed to automatic review. It immediately became apparent to us that both our control and LFPI rats displayed a repertoire of EEG patterns associated with chewing, grooming etc., which

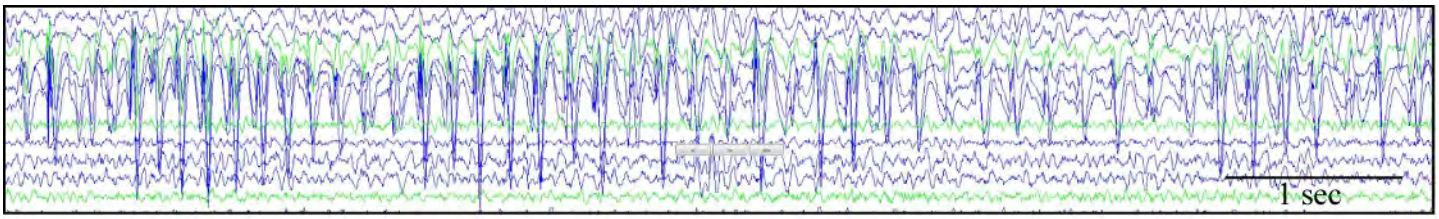


**Fig. 3.** Typical theta activity recorded from rat sensorimotor cortex during "bruxing" and "eye boggling".

are normal artifacts that we are now expert in recognizing. However, an unexpected finding was that both the LFPI and the control rats displayed pronounced runs of spike-wave discharge (SWD; Fig. 3). This drew our attention because the SWD we recorded was similar in frequency, amplitude, and duration to Epileptiform Electrographic Events (EEE) previously associated exclusively with LFPI[1,2]. By examining restrained animals with high resolution video and simultaneous EEG, it became apparent that the SWD was not epileptiform but was instead associated with behavioral arrest followed by "bruxing", also referred to as "vacuous chewing"[3,4], and "eye boggling", both activities that rats perform normally to dull the front incisors as well as when they are under stress. Please see video clip at http://dl.dropbox.com/u/11873936/BruxingBoggling.wmv displaying such behavior in relation to the EEG shown in Figure 3. While this discovery sounds trivial, it is actually at the center of a very recent controversy concerning what can be safely considered to be post-traumatic epileptiform activity in LFPI rats (see [2] and[5] for point/counter-point).

2) In reviewing our initial chronic recordings we realized that we needed more experience discerning normal from epileptiform activity. To this end we received approval to conduct a pilot study using a pilocarpine model of temporal lobe epilepsy. This model involves injecting animals with lithium followed by pilocarpine (a muscarinic receptor agonist) which induces acute status epilepticus for several hours[6]. Status is followed by a "silent period" of several weeks where epileptiform spikes may be recorded, and then the appearance of regular

temporal lobe seizures. We began an initial study in 8 rats using this model and have just started to see seizures at the 4-week time-point following status. Thus, this brief study has served its purpose of familiarizing us with chronic video/EEG recording and analysis of spikes and seizures. However, having succeeded with this model, it provides us with an ideal opportunity to test the effectiveness of glial attenuation in preventing epileptogenesis presumed to occur during the one month silent period before chronic seizures occur. This study in underway and should provide us with valuable insights concerning prevention of epileptogenesis in this more rapidly developing model before proceeding with LFPI animals and a much prolonged (many months) silent period.

3) Finally, our early start on chronic recording led to an unexpected serendipitous finding concerning post-traumatic anxiety. In piloting LFPI rats, we noticed that brain damaged animals displayed behaviors suggesting increased anxiety when placed in the recording chamber. We pursued this by performing an experiment using a controlled stressor (foot shock) and measuring freezing behavior (the rats natural defensive behavior to danger). Indeed, our LFPI animals showed a reliable over-reaction to stress when compared to controls, suggesting an animal model of post-traumatic anxiety. Most important, we found that glial attenuation with peri-injury administration of MN-166 completely prevented development of post-traumatic anxiety. While not directly related to post-traumatic epilepsy, we believe the enhanced post-traumatic anxiety is reflective of increased excitability of limbic structures due to injury-induced neuroinflammation. In this way, our serendipitous discovery holds promise for our epilepsy studies. This work is now published[7] and the manuscript is included in Appendix.

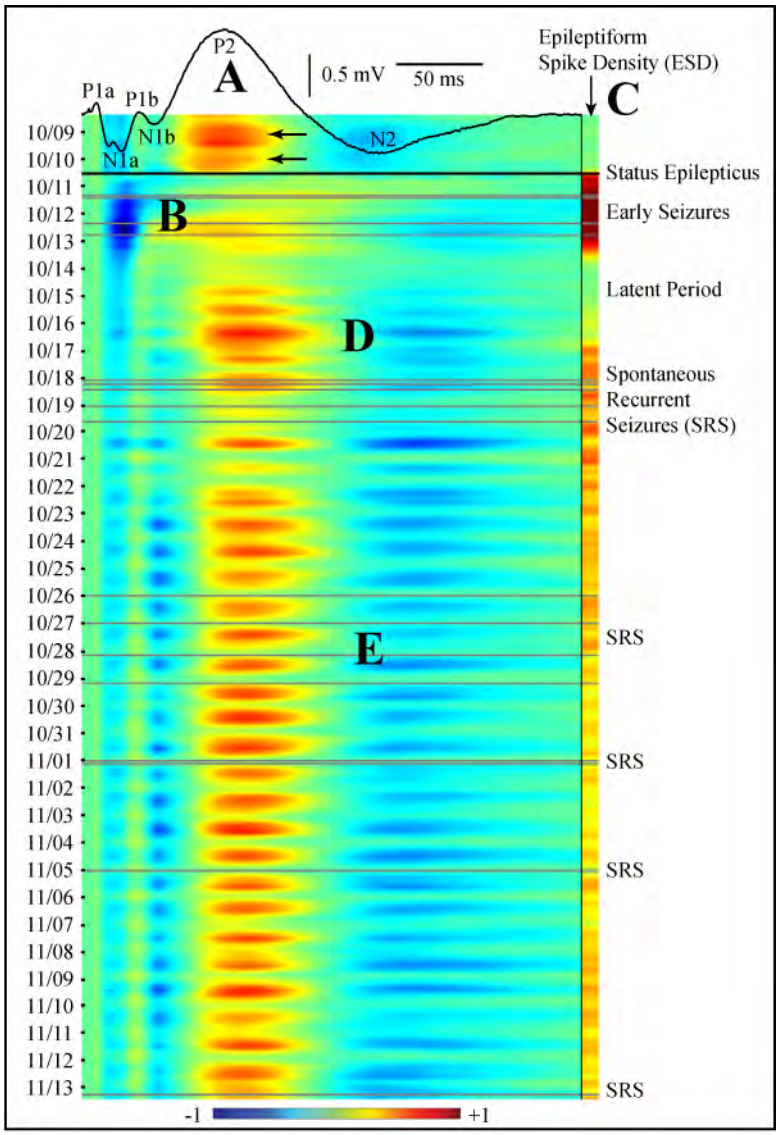


**Fig. 4.** Auditory evoked potentials (AEP) and epileptiform spike density (ESD) recorded from auditory cortex. A) AEP waveform before status epilepticus (SE). B) Early seziures before epileptogenesis. C) ESD. D) The epileptogenic "silent" or "latent" period. E) End of the latent period and appearance of spontaneous recurrent seizures (SRS).

**YEAR 2**

There were three objectives for year two of this project. The first was to test the efficacy of MN166 in reducing microglial TLR4-mediated hyper-excitability, epileptiform spiking, and seizures in the pilocarpine model of temporal lobe epilepsy. The second was to test more rostral fluid percussion injury over motor cortex with increased impact pressures for its effectiveness in producing short term (1-2 month) epileptiform spiking. The third was to begin testing the efficacy of MN166 and SLC022 as anti-epileptogenic compounds in PTE induced by lateral fluid percussion injury (LFPI), beginning in year two and continuing through year three.

*Progress on objective 1:* Success with the pilocarpine model has exceeded what we initially planned. An unexpected discovery was that by recording auditory evoked potentials (AEP) every 30 minutes 24/7, we could develop a reliable (and new) biomarker that sensitively indexes excitability changes during epileptogenesis (previously regarded as the "silent" or "latent" period where changes in the brain could not be monitored due to a lack of seizures). The shape and amplitude of the AEP waveform undergoes dramatic and stereotyped changes compared to pre-pilo baseline following status epilepticus (SE), providing a window on changes and treatment efficacy prior to appearance of the first spontaneous recurrent seizure (SRS). AEPs recorded at 30 minute intervals for approximately one month following SE (from a screw electrode directly above auditory cortex) are shown in Figure 4. The archetypal AEP waveform begins with early fast waves reflecting intra-laminar cortical excitation (Fig. 4A; P1a-N1b) followed by inhibitory slow waves (Fig. 4A; P2-N2). The amplitudes of these components remain stable over the 2-day pre-SE baseline, with a detectable circadian fluctuation of the P2 amplitude (Fig. 4A; arrows). AEP morphology is grossly altered by SE, resulting in a prominent increase in the N1a amplitude (Fig. 4B; 10/11 – 10/13) and attenuation of the P2-N2 slow wave, suggesting decreased inhibition during SE and early seizures. Epileptiform spike density (ESD; Fig. 4C) is maximum during this same period. Both the AEP and ESD are suppressed during the earliest part of the latent period but begin to increase several days before the first SRS (Fig. 4D; 10/18). For weeks following the first SRS, spike density is variable but reveals no distinct temporal pattern and shows no temporal relationship to the occurrence of subsequent SRS. By contrast, the AEP amplitude fluctuation evolves into a more prominent circadian rhythm, particularly noticeable in the inhibitory slow waves, which are regularly suppressed for several hours in the early morning. SRS, when they do occur, are time-locked to these periods when inhibition is presumably minimal (Fig. 4E; 10/19-20, 10/26-29, 11/01, 11/05, 11/13). We have performed similar recordings in 10 rats so far and have found very similar AEP changes in both auditory cortex and hippocampus (which responds to auditory stimuli). We have logged changes in the AEP out to 3 months after SE. We consistently find progressive changes before the first SRS (allowing us to monitor excitability changes and thus epileptogenesis during the latent period) as well as change after the first SRS, demonstrating continued epileptogenesis during subsequent seizures. This later point is particularly important since it is currently a matter of some debate whether epileptogenesis is essentially complete by the first SRS or continues, warranting continued anti-epileptogenic treatment well into the seizure period. Our data strongly suggest the later conclusion.

We continued our work with biomarker analysis in the pilocarpine model and looking at the effect of glial cell suppressant MN166 following SE on epileptogenesis (indexed by seizures as well as AEP and ESD changes). What we saw was promising. Two groups of rats are under study, receiving daily injections of MN166 (10 mg/kg in corn oil; N=8) or vehicle (N=7) beginning at the termination of SE and continuing for up to 30 days. 70% (5 out of 7) of the vehicle treated rats developed chronic seizures with the average latency from SE to the first seizure of 15.5 days (Fig. 5; red traces). Both the success rate and duration of the latent period are consistent with the published literature using this model. In contrast, only 12% (1 out of 8) rats receiving MN166 have had seizures (Fig. 5; black trace). Even with this low N and short duration of recording, the seizure rates in vehicle rats are significantly greater ($p=0.045$) than those treated with MN166 post-SE. These results suggested that anti-inflammatory treatment may at least have an anti-seizure effect. However, we were encouraged that the 3 treated rats that we had the opportunity to monitor out to 40-50 days post-SE (Fig. 5; oval) continued to show no seizures. These rats therefore remained seizure free for 10-20 days after MN166 was stopped, approaching the 15.5-day latency period for control rats, suggesting that epileptogenesis may have been attenuated. While we did not quantify AEP or ESD in these rats, it should be noted that all of the rats (including the MN166 treated one) that showed seizures also displayed prominent epileptiform spiking whereas this was not seen in any of the seizure free rats. Our work on Objective 1 with the pilocarpine model resulted in an R01 grant proposal to the NIH on anti-epileptogenesis in this model (see Appendix), a preproposal to the CDMRP to further develop our biomarkers for epileptogenesis with this model using optogenetic stimulation of hippocampus and cortex (see Appendix), and an abstract submission to Society for Neuroscience meeting (see Appendix). The preproposal to CDMRP was not followed by a request for full application. The NIH proposal was not funded on the first round but is under revision based on information we have obtained from the 3rd year of this project see below).

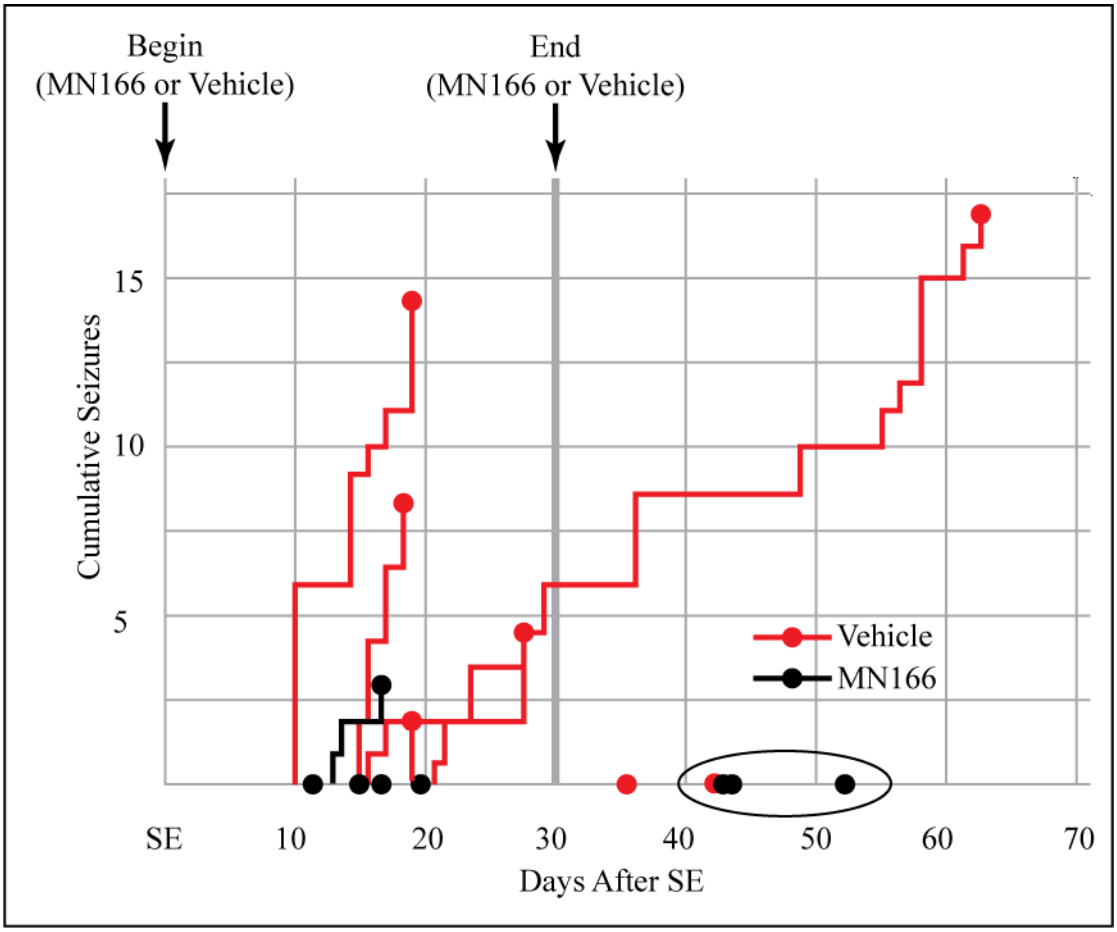


**Fig. 5.** Cumulatve seizures following SE in MN166 treated (black) and untreated Vehicle (red) rats.

*Progress on objective 2:*

Success with modifying the LFPI model so that it would yield short-term epileptiform spikes and seizures took longer than we initially planned. At the time of our first year progress report, we had discovered that Epileptiform Electrographic Events (EEE) previously associated exclusively with LFPI[1,2] were actually SWD that occurs normally in Sprague-Dawley rats (this fact has not been recognized by other investigators). We therefore changed our injury site to a more rostral location reported by Curia et al.[8] to yield higher success rates for spikes and eventual seizures. To our disappointment, the more rostral location performed no better. No animals displayed either epileptiform spikes or seizures, but all displayed SWD (regarded as EEE by others), which we have now concluded is largely artifactual and seen as frequently in control as in injured animals. While this is a negative finding, it has important implications for the field, since there is now an ongoing controversy concerning what can be safely considered to be post-traumatic epileptiform activity in LFPI rats (see [2] and[5] for point/counter-point). All of our results challenge the findings of D'Ambrosio and colleagues and support the contention of Dudek and Bertram that most of what is being reported for LFPI is not epilepsy. Worse, because of this, treatments are being devised for preventing PTE (based on SWD instead of spikes and seizures) that we feel are not necessarily related to seizures (epilepsy) as an endpoint (for a recent example of this, see [9]).

We have changed our impact location based on work by Pitkanen's group[10] demonstrating that very severe impact LFPI injury that includes entorhinal cortex may have a higher chance of developing epileptiform spikes and seizures. Instead of using such severe impact, we moved our impact location caudally and ventrally to directly target entorhinal cortex (the cortical gateway to the hippocampus). This new location looked promising

in that we saw some epileptiform spikes (no seizures) from these animals, something we could not record in any of our medial or rostral impact locations. We also noted that the hippocampal AEP at this new location is grossly altered from normal in the same way as our pilocarpine animal post-SE, with lower amplitude and prolonged temporal components. This discovery was promising in that the entorhinal cortex had been demonstrated in humans and in other animal models of epilepsy to be directly involved in epileptogenesis. In humans, entorhinal cortex is on the inferior temporal lobe and highly exposed to potential trauma. In rats, this same area is in a caudal and ventral region which is difficult to access in vivo, perhaps explaining why it has been largely ignored in favor of more accessible dorsal locations by others studying LFPI.

*Related additional studies for Year 2:*

1) As noted in our first project year progress report, we also made an unexpected serendipitous discovery concerning post-traumatic anxiety, that brain damaged animals displayed behaviors suggesting increased anxiety when placed in the recording chamber. We hypothesized that, regardless of the failure of this injury to reliably produce epilepsy, it did result in limbic hyperexcitability reflected in anxiety-like symptoms. In the first year, we found that glial attenuation with peri-injury administration of MN166 completely prevented development of post-traumatic anxiety. In this second year, we discovered that MN166 treatment, delayed until one month post-injury when anxiety symptoms had completely developed, had the effect of reversing post-traumatic anxiety. This was a surprising result suggesting that the neuroinflammatory sequelae to injury are enduring, representing a self-sustaining neuropathy that can be effectively extinguished with delayed glial modulation. This work has been submitted for publication (see Appendix). This work served as preliminary data for a proposal to the Department of Defense Broad Agency Announcement for Extramural Medical Research (see Appendix). The proposal was reviewed favorably and our responses to their memorandum for responses to external scientific review is presently under consideration.

2) We received a separate seed grant from the Autism Speaks Foundation to examine possible links between autism and epilepsy based on a common neuroinflammatory mechanism. Based on our experience in video/EEG epilepsy monitoring from the present project, we were able to perform far more advanced electrophysiology on this study than originally planned. The result in short was that we discovered a new (and the only) model of autism/epilepsy, a model that is based on a combination of the known maternal teratogens stress and terbutaline (typically taken to arrest preterm labor and closely linked to human autism). This result is quite exciting and the subject of an Idea Development proposal to the CDMRP Autism Research Program (see Appendix).

**YEAR 3**

There were two objectives for the final year of this project. The first objective was to wrap up our pilocarpine study. The second objective was to explore the effectiveness of MN166 on PTE. Progress description in this section will be briefer than the previous 2 years because they are described in manuscripts included in the Appendix.

*Progress on objective 1:*

We concluded our pilocarpine/biomarker study of epileptogenesis. We dropped the MN166 intervention component because, while promising, we found it difficult to establish a window of intervention using immune suppression that did not also result in high mortality. While establishing this window will be a necessary challenge for future work, we moved ahead with the hippocampal auditory evoked potential biomarker alone since this is a very useful method for examining changes in excitability during the otherwise silent period of epileptogenesis. A draft of the manuscript for submission to Epilepsia is included in the Appendix. The final version awaits the results of advanced pattern classification in process by our colleague in CU Dept. of Electrical Engineering, Dr. Francois Meyer, who is expert in signal processing. The summary from the manuscript is included here.

*Purpose:* In temporal lobe epilepsy (TLE), an initial precipitating injury is typically followed by a seizure free epileptogenic period of months to years before the appearance of spontaneous and recurring seizures. This period of post-traumatic epileptogenesis is often referred to as the "latent" or "silent" period due to a seemingly normal behavioral state (i.e. absence of non-convulsive and convulsive seizures). While the silent period offers and ideal interval for possible intervention and epilepsy prevention, there is a need for biomarkers that can index epileptogenesis prior to appearance of spontaneous seizures and facilitate anti-epileptogenic strategies.
*Methods:* Instead of passively monitoring the brain's spontaneous activity during the silent period, we actively monitored excitability changes in the hippocampus using chronically recorded auditory evoked field potentials (hAEP) in lithium/pilocarpine model of TLE in the rat. We applied pattern classification methods to identify distinct phases of epileptogenesis across animals.
*Results:* hAEP displayed highly repeatable changes in waveform morphology during the silent period leading up to and continuing beyond the first spontaneous seizure. Pattern classification accurately universally identified phases of epileptogensis based on morphological changes in the hAEP across rats. The hAEP could also predict a subset of rats that did not develop seizures.
*Conclusions:* Sensory stimulation combined with pattern classification methods can serve as a sensitive and generalizable biomarker to chart epileptogensis before spontaneous seizures and to predict the probability of seizure development in acquired epilepsy.

*Progress on objective 2:*
Our struggle in getting seizures with the LFPI model continued through the final year of this project and thus impeded our objective to examine the effect of neuroimmune modulation on epileptogenesis. However, there are two very important outcomes of this struggle. The first is that, as we suspected at the end of Year 2, epileptiform electrographic events (EEE) reported as seizures by D'Ambrosio and colleagues are in fact not seizures, but are instead spike-wave discharges (SWD) that turn out to be common in most Spraque-Dawley rats >6 months of age (it should be noted that Sprague-Dawley rats are the strain used in all LFPI studies to date). Proper controls were not examined in these previous studies or this would have been discovered and invalidated the model. In a related point, we conclude that the LFPI model rarely if ever results in epilepsy at least at the impact locations used by these previous studies and is therefore not a useful animal model of PTE. To quantify our results from 2 years attempting to get this model to work with over 90 rats (LFPI and control), we developed a pattern recognition method based of the Support Vector Machine. This worked very well. A completed manuscript of these results, coauthored with Dr. Edward Dudek, is provided in the Appendix. This manuscript is being submitted to Brain. A summary of the manuscript follows.
*Purpose:*
Spike-and-wave discharges (SWD) have been reported in the electrocorticogram of rats undergoing lateral fluid percussion injury (LFPI), a leading model of post-traumatic epilepsy, and thought to reflect early appearing non-convulsive and convulsive seizures. However, it has been reported that SWD are observed in uninjured Sprague-Dawley rats used as controls in these and other models of acquired epilepsy. The presence of SWD in control rats raises the possibility of confounds in the interpretation of results from acquired epilepsy models.
*Methods:*
The present study quantified features of SWD episodes throughout the lifetime of normal "control" rats with the objective of distinguishing normal brain activity from that heralding the development of non-convulsive and convulsive seizures. These results were compared to the same timeline in brain-injured rats receiving moderate to severe LFPI. A support vector machine was trained on the fully developed SWD of each rat and used to detect and quantify subsequent events.
*Results:*
A majority of older (8-12 month) control rats displayed large-amplitude and frequent SWD events at frontal and parietal recording sites. Earlier recordings in the same rats also revealed clear SWD at 3-6 months that were of shorter duration and less frequent, and "larval" SWD detected as early as 1 month. The incidence and temporal features of SWD quantified for control rats were indistinguishable in LFPI animals, including a marked increase in the frequency of occurrence, duration and amplitude with age.
*Conclusions:*

These results suggest that SWD may not unambiguously reflect seizures following moderate to severe LFPI. Additionally, none of our LFPI rats developed convulsive seizures across 12 months of video/EEG monitoring, suggesting that when SWD are excluded as epileptiform events, the incidence of epilepsy in this model can be very low.

*Related additional studies for Year 3:*
We completed two related studies.
1) Our manuscript concerning delayed neuroimmune modulation to reverse post-traumatic anxiety-like behavior was submitted and is now published in Neurotrauma[11]. This paper is included in the Appendix.

2) Our recent experience with rodent models of epilepsy led to an unplanned collaboration with Drs. Svenja Knappe and John Kitching at NIST to test a miniature room temperature atomic magnetometer they developed for recording of epileptiform discharge. Our results demonstrated a remarkable sensitivity of their device for recording single epileptic spikes in a rat model. These results are exciting in that they lead the way to scalp attachable magnetrodes that will permit mobile magnetoencephalographic (MEG) telemetry of seizures in humans for presurgical evaluation. We have submitted this work for consideration by Nature Neuroscience. A draft of the manuscript is included in the Appendix.

**KEY RESEARCH ACCOMPLISHMENTS:**

- Completed and tested chronic video/EEG recording hardware and software.
- Developed high speed, random access, video/EEG review and analysis software.
- Achieved expertise in identifying normal and epileptiform EEG patterns in chronic recording.
- Discovered key discrepancy in current literature concerning “epileptiform” spike-wave discharge (SWD).
- Began pilocarpine model of temporal lobe epilepsy to test prevention of epileptogenesis.
- Discovered and published effect of glial attenuation on post-traumatic anxiety.
- Discovered a unique biomarker for epileptogenesis in the pilocarpine model using AEPs.
- Obtained promising preliminary results suggesting MN166 blocking of epileptogenesis in pilo model.
- Discovered that impact injuries to entorhinal cortex may be a very productive model of PTE.
- Discovered and publishing effect of delayed glial attenuation on post-traumatic anxiety.
- Discovered a new (and the only) animal model of autism and epilepsy.
- Discovered that the LFPI model of post-traumatic epilepsy does not in fact yield seizures at the typical impact locations used by another leading research group, and that the seizures they report are actually SWD common in both injured and uninjured animals.

**CONCLUSION:**

*Achievements:* In the first year of this project, we constructed and tested all hardware for chronic video/EEG recording of 24 animals (expandable to 32). Software for logging video/EEG in a time-locked manner has been completed and is in use. Software for the extremely rapid quasi-random review and analysis of video/EEG data has been completed and is in use. We have been using this system to examine normal and brain damaged animals for the past several months. From this work we have discovered that what has been interpreted by others as pathological theta activity is also prominent in normal animals during "vacuous chewing" and we have entered into a very recent controversy in the field about what constitutes a valid post-traumatic epileptic seizure. We have developed a pilocarpine model of temporal lobe epilepsy and have begun recording epileptic spikes and seizures in this model. We will be conducting a study to determine if epileptogenesis (what goes on during the 1 month silent period before regular seizures evolve) can be attenuated or prevented with attenuation of glial activation using MN-166. Finally, we serendipitously discovered that LFPI produces post-traumatic anxiety that can be prevented with administration of MN-166 peri-injury.

In the second project year, we developed an auditory evoked potential biomarker for changes in brain excitability during the post-SE "silent period" and discovered progressive excitability changes continuing well past the first spontaneous seizure. We are now beginning the study to explore effects of glial attenuation with MN166 in blocking epileptogenesis in this model. Our further examination of more rostral impact locations in the LFPI model has led us to the firm conclusion that this model as it stands in not appropriate for studying PTE, at least temporal lobe epilepsy, which is always the locus of PTE in humans. However, we have had promising results using a far more caudal impact location over entorhinal cortex (the cortical gateway to the hippocampus). We will use this new model in the project year to examine effects of MN166 on short term spiking and PTE. We extended our serendipitous discovery of LFPI induced post-traumatic anxiety to demonstrating that we can reverse fully developed anxiety symptoms after they had fully developed using glial attenuation. Finally, we were able to leverage our experience with 24/7 epilepsy monitoring developed in this project to perform similar recording in a seed grant project from Autism Speaks to examine the relationship between autism and epilepsy in an animal model (the two pathologies are remarkably comorbid in the human population). This led to the recent discovery of a new (and only) animal model of autism/epilepsy based on combined maternal stress and terbutaline.

In the final year of the project, we wrapped up our pilocarpine study of hippocampal auditory evoked potentials as a biomarker for epileptogenesis. We also concluded that the LFPI model of PTE, at least at the impact locations used by another leading group investigating this model, do not result in seizures. SWD reported by this other group as seizures are equally common in injured and un-injured Spraque-Dawley rats and are not influenced by even severe injury.

*So what:* 1) Our data collection and analysis hardware/software comprises a unique and inexpensive approach to chronic monitoring of post-traumatic brain activity that is ideal, not just for the present research, but for emergency battlefield-related medical monitoring. For this reason, our results will be presented at this years MHSRS Symposium. Virtually nothing is known about epileptogenesis following traumatic brain injury in humans due in large part to the fact that video/EEG monitoring is rarely performed post-injury in the absence of a behavioral seizure. Our hardware/software system should be pursued as a tool for making this not only feasible but routine. 2) Our SWD that has been identified as post-traumatic seizures turns out to be quite timely and important because there are currently attempts to use SWD as a unique sign of early epileptogenesis and to develop drugs that might suppress this activity instead of waiting for development of actual seizures. We hope to have resolved this issue so the field of anti-epileptogenesis drugs does not head in the wrong direction. We are collaborated with epilepsy researcher, Dr. Edward Dudek at the University of Utah, on this effort and hope these results will set the PTE research back on course. 3) Our work with the pilocarpine model, while not directly related to post-traumatic epilepsy, could represent a major advance in the field if we are able to block or attenuate epileptogenesis in this more rapidly developing model. Our discovery of an auditory evoked biomarker to probe brain excitability changes during epileptogenesis will provide new insight into the effect of treatment in the pilocarpine and LFPI models, and should also be translatable to humans since auditory evoked

potentials are easily recorded non-invasively. 5) Our unexpected finding that LFPI produces an animal model of post-traumatic anxiety, and that this development can be prevented by early attenuation of post-injury brain inflammation, may have extremely important implications for post-traumatic stress disorder (PTSD) experienced by many of our war fighters after head injury. It suggests that a strong component of PTSD may in fact be directly produced by the injury and not just the psychological setting within which it occurs. It also opens the way to potential future intervention. The additional discovery that PTSD-like behavior can be reversed by glial attenuation well after injury is perhaps even more important since it opens the possibility that developed PTSD in the veteran population may actually be treated. We are currently awaiting word from the DoD on funding to separately pursue this discovery. Finally our related collaboration with investigators at NIST to test their microfabricated atomic magnetrode for MEG measurements of epilepsy should lead to neuromagnetic telemetry of human epileptic seizures during presurgical evaluation.

**INVENTIONS, PATENTS AND LICENCES:**

- Completed an Invention Disclosure Form so that our Technology Transfer Office can investigate whether the video/EEG review and analysis software is patentable or at least can be protected with a copyright.

**PUBLICATIONS, ABSTRACTS, AND PRESENTATIONS:**

**1) Lay Press: N/A**

**2) Peer-Reviewed Scientific Journals:**

Rodgers KM, Bercum FM, McCallum DL, Rudy JW, Frey LC, Johnson KW, et al. Acute Neuroimmune Modulation Attenuates the Development of Anxiety-Like Freezing Behavior in an Animal Model of Traumatic Brain Injury. J. Neurotrauma. 2012 ed. 2012 Apr 26. PMCID: PMC3390983

Rodgers KM, Deming YK, Bercum FM, Chumachenko SY, Wieseler JL, Johnson KW, et al. Reversal of established traumatic brain injury-induced, anxiety-like behavior in rats after delayed, post-injury neuroimmune suppression. J. Neurotrauma. 2014 Mar 1;31(5):487–97. PMCID: PMC3934516

Rodgers KM, Dudek FE, Barth DS. Spike-Wave Discharges versus Seizures after Fluid Percussion Injury in Sprague-Dawley Rats. (submitted).

Alem O, Benison AM, Barth DS, Kitching J, Knappe S. Magnetoencephalography of epilepsy with a microfabricated atomic magnetometer. (submitted).

Benison AM, Meyer F, Bercum FM, Rodgers KM, Smith Z, Barth DS. Morphological Alterations in Chronically Recorded Hippocampal Auditory Evoked Potentials as a Novel Biomarker of Epileptogenesis. (in preparation).

**3) Invited Articles: N/A**

**4) Abstracts:**

Wieseler, J.L., Stone, K.N., Rodgers, K., McFadden, A., Maier, S.F., Barth, D.S., Watkins, L.R. 2012. Modeling post-traumatic headache: lateral fluid percussion injury and facial allodynia. Program No. 177, New Orleans, LA: Society for Neuroscience.

Benison, A.M., Smith, Z., Barth, D.S. 2012. Involvement of insular auditory cortex in negative affective ultrasonic vocal communication in rats. Program No. 364, New Orleans, LA: Society for Neuroscience.

Rodgers, K.M., Bercum, F.M., Johnson, K.W., Watkins, L.R., Barth, D.S. 2012. Glial modulation with Ibudilast (MN166) attenuates neuroinflammation and autistic-like behaviors in the Terbutaline model of autism spectrum disorder (ASD) in rats. Program No. 443, New Orleans, LA: Society for Neuroscience.

Rodgers, K.M., Bercum, F.M., Rudy, J.W., Frey, L.C., Johnson, K.W., Watkins, L.R., Barth, D.S. 2012. Acute post-injury neuroimmune suppression reduces anxiety-like behavior following lateral fluid percussion injury in rats. Program No. 555, New Orleans, LA: Society for Neuroscience.

Benison, A.M., Rodgers, K.M., Bercum, F.M., Smith, Z., Barth, D.S. 2013. Hippocampal auditory evoked potentials in conjunction with continuous long-term video-EEG monitoring reveals novel biomarkers for epileptogenesis in the lithium-pilocarpine model of epilepsy in rats. Program No. 51, San Diego, CA: Society for Neuroscience.

Rodgers, K.M., Dudek, F.E., Barth, D.S. 2014. Pattern recognition quantification of spike-and-wave discharge in normal and brain injured Sprague-Dawley rats. Program No. 311, Washington, DC: Society for Neuroscience.

Benison, A.M., Alem, O., Knappe, S., Kitching, J., Barth, D.S. 2014. A micro-fabricated atomic magnetometer for magnetoencephalography of epilepsy. Program No. 314, Washington, DC: Society for Neuroscience.

**PERSONNEL SUPPORTED BY THIS PROJECT:**

Daniel Barth
Alex Benison
Krista Rodgers
Florencia Bercum
Zach Smith

**REPORTABLE OUTCOMES:**

- A Very High Speed System for Video/EEG Monitoring and Quantification of Post-traumatic Epileptogenesis. Software and hardware system designed and developed by Barth, DS.

**OTHER ACHEIVEMENTS:**

- Alex Benison received his Ph.D. this year and Krista Rodgers will be receiving her Ph.D. this Fall. Both will be continuing on as a post-doctoral fellows on this project. The last year of their doctoral work was supported by this award.
- Admitted 2 new graduate students, Florencia Bercum and Zachary Smith, who will be working on this project during the final year.
- Submitted pre-proposal and then full proposal in response to a USAMRMC Broad Agency Announcement for a new project entitled: “The Prevention and Treatment of Post-traumatic Anxiety Through Neuroimmune Modulation”, based on the serendipitous discovery made in the present project. Still under review.
- Submitted an Idea Development pre-proposal to the CDMRP Autism Research Program for a new project entitled: “ASD and Epilepsy: The First Animal Model to Examine Common Neuro-inflammatory Mechanisms and Neuro-immune Treatment”.
- Submitted an Investigator-Initiated Research pre-proposal to the Peer Reviewed Medical Research Program for a new project entitled: “Sensory and Optogenetically Evoked Biomarkers to Study Post-traumatic Epileptogenesis”.

**REFERENCES:**


1. D'Ambrosio R, Hakimian S, Stewart T, Verley DR, Fender JS, Eastman CL, et al. Functional definition of seizure provides new insight into post-traumatic epileptogenesis. Brain. Oxford University Press; 2009 Oct;132(Pt 10):2805–21. PMCID: PMC2759339

2. D'Ambrosio R, Miller JW. What Is an Epileptic Seizure? Unifying Definitions in Clinical Practice and Animal Research to Develop Novel Treatments. Epilepsy Currents. 2010 May;10(3):61–6.

3. Rosales VP. Emotional stress and brux-like activity of the masseter muscle in rats. The European Journal of Orthodontics. 2002 Feb 1;24(1):107–17.

4. Zeredo J, Kumei Y, Shibazaki T, Yoshida N. Biting behavior induced by acute stress in the rat during experimental tooth movement. noldus.com.

5. Dudek FE, Bertram EH. Counterpoint to “What Is an Epileptic Seizure?” By D’Ambrosio and Miller. Epilepsy Currents. 2010 Jul 8;10(4):91–4. PMCID: PMC2912541

6. Curia G, Longo D, Biagini G, Jones RSG, Avoli M. The pilocarpine model of temporal lobe epilepsy. J. Neurosci. Methods. 2008 Jul 30;172(2):143–57. PMCID: PMC2518220

7. Rodgers KM, Bercum FM, McCallum DL, Rudy JW, Frey LC, Johnson KW, et al. Acute Neuroimmune Modulation Attenuates the Development of Anxiety-Like Freezing Behavior in an Animal Model of Traumatic Brain Injury. J. Neurotrauma. 2012 ed. 2012 Apr 26. PMCID: PMC3390983

8. Curia G, Levitt M, Fender JS, Miller JW, Ojemann J, D apos Ambrosio R. Impact of Injury Location and Severity on Posttraumatic Epilepsy in the Rat: Role of Frontal Neocortex. Cereb Cortex. 2011 Jun 16;21(7):1574–92. PMCID: PMC3116737

9. D'Ambrosio R, Eastman CL, Darvas F, Fender JS, Verley DR, Farin FM, et al. Mild passive focal cooling prevents epileptic seizures after head injury in rats. Ann Neurol. 2013 Feb;73(2):199–209. PMCID: PMC3608748

10. Kharatishvili I, Pitkanen A. Association of the severity of cortical damage with the occurrence of spontaneous seizures and hyperexcitability in an animal model of posttraumatic epilepsy. Epilepsy Res. 2010 Jun;90(1-2):47–59.

11. Rodgers KM, Deming YK, Bercum FM, Chumachenko SY, Wieseler JL, Johnson KW, et al. Reversal of established traumatic brain injury-induced, anxiety-like behavior in rats after delayed, post-injury neuroimmune suppression. J. Neurotrauma. 2014 Mar 1;31(5):487–97. PMCID: PMC3934516

**APPENDICES:**

Attached are:

1) Copy of our recent manuscript concerning post-traumatic anxiety.

2) An abstract submitted to MHSRS reporting our video/EEG recording analysis system.

3) Abstract presented at 2013 Society for Neuroscience conference reporting results from our pilocarpine studies.

4) Idea Development proposal to the CDMRP Autism Research Program

5) Proposal to the Department of Defense Broad Agency Announcement for Extramural Medical Research to continue our work with preventing and treating PTSD.

6) Investigator-Initiated Research pre-proposal to Peer Reviewed Medical Research Program to develop our biomarkers for epileptogenesis using both auditory evoked responses and responses from optogenetic stimulation of hippocampus and auditory cortex.

7) Manuscript to be submitted to Epilepsia concerning the hippocampal auditory evoked potential biomarker work.

8) Manuscript published by J. Neurotrauma concerning our recent discovery of delayed reversal of PTSD-like symptoms.

9) Manuscript submitted to Brain concerning SWD in injured and un-injured Sprague-Dawley rats.

10) manuscript submitted to Nature Neuroscience concerning MEG with a microfabricated atomic magnetometer.

11) Two abstracts for presentation at the 2014 meeting of the Society for Neuroscience.

Journal of Neurotrauma

Journal of Neurotrauma: http://mc.manuscriptcentral.com/neurotrauma

# Acute neuroimmune modulation attenuates the development of anxiety-like freezing behavior in an animal model of traumatic brain injury.



| | |
|---|---|
| Journal: | *Journal of Neurotrauma* |
| Manuscript ID: | NEU-2011-2273.R1 |
| Manuscript Type: | Regular Manuscript |
| Date Submitted by the Author: | 24-Feb-2012 |
| Complete List of Authors: | Rodgers, Krista; University of Colorado, Psychology and Neuroscience<br>Bercum, Florencia; University of Colorado, Psychology and Neuroscience<br>McCallum, Danielle; University of Colorado, Psychology and Neuroscience<br>Rudy, Jerry; University of Colorado, Psychology and Neuroscience<br>Frey, Lauren; University of Colorado Denver, Neurology<br>Johnson, Kirk; MediciNova, Inc.,<br>Watkins, Linda; University of Colorado, Psychology and Neuroscience<br>Barth, Daniel; University of Colorado, Psychology and Neuroscience |
| Keywords: | INFLAMMATION, TRAUMATIC BRAIN INJURY, ANIMAL STUDIES |
| | |

# Acute neuroimmune modulation attenuates the development of anxiety-like freezing behavior in an animal model of traumatic brain injury.

**Krista M. Rodgers, M.A.[1], Florencia M. Bercum, B.A.[1], Danielle L. McCallum, B.A. [1], Jerry W. Rudy, Ph.D. [1], Lauren C. Frey, M.D.[2], Kirk W. Johnson, Ph.D.[3], Linda R. Watkins, Ph.D.[1] and Daniel S. Barth, Ph.D.[1]**

[1]Department of Psychology and Neuroscience, University of Colorado, Boulder, CO, U.S.A., [2]Department of Neurology, University of Colorado Denver, and Colorado Injury Control Research Center, Denver, CO, U.S.A., [3]MediciNova, Inc., La Jolla, CA, U.S.A.

Running title: Neuroinflammation and post-traumatic anxiety.

Table of contents title: Neuroimmune modulation of anxiety behavior in a rat model of TBI.

**Authors**

Krista M. Rodgers

University of Colorado, Department of Psychology and Neuroscience, UCB 345

Boulder, CO 80309, USA

Phone: 303-492-0359, Fax: 303-492-2967, Email: Krista.Rodgers@colorado.edu

Florencia M. Bercum

University of Colorado, Department of Psychology and Neuroscience, UCB 345

Boulder, CO 80309, USA

Phone: 303-492-0359, Fax: 303-492-2967, Email: fbercum@gmail.com

Danielle L. McCallum

University of Colorado, Department of Psychology and Neuroscience, UCB 345

Boulder, CO 80309, USA

Phone: 303-492-0359, Fax: 303-492-2967, Email: Danielle.Mccallum@Colorado.EDU

Jerry W. Rudy

University of Colorado, Department of Psychology and Neuroscience, UCB 345

Boulder, CO 80309, USA

Phone: 303-492-3306, Fax: 303-492-2967, Email: Jrudy@colorado.edu

Lauren C. Frey

University of Colorado Denver School of Medicine, Department of Neurology

Aurora, CO 80045, USA

Phone: 720-848-2080, Email: Lauren.Frey@ucdenver.edu

Kirk W. Johnson

MediciNova, Inc.

4350 La Jolla Village Drive, Suite 950

La Jolla, CA, 92122, USA

Phone: 858-373-1500, Fax: 858-373-7000, Email: kjohnson@medicinova.com

Linda R. Watkins

University of Colorado, Department of Neurology

Boulder, CO 80309, USA

Phone: 303-492-7034, Fax: 303-492-2967, Email: Linda.Watkins@Colorado.EDU

Daniel S. Barth, PhD. (Corresponding author)

University of Colorado, Department of Psychology and Neuroscience, UCB 345

Boulder, CO 80309, USA

Phone: 303-492-0359, Fax: 303-492-2967, Email: dbarth@psych.colorado.edu

**Abstract**

Chronic anxiety is a common and debilitating result of traumatic brain injury in humans. While little is known about the neural mechanisms of this disorder, inflammation resulting from activation of the brain's immune response to insult has been implicated in both human post-traumatic anxiety and in recently developed animal models. In this study, we used a lateral fluid percussion injury (LFPI) model of traumatic brain injury in the rat and examined freezing behavior as a measure of post-traumatic anxiety. We found that LFPI produced anxiety-like freezing behavior accompanied by increased reactive gliosis (reflecting neuroimmune inflammatory responses) in key brain structures associated with anxiety: the amygdala, insula and hippocampus. Acute peri-injury administration of Ibudilast (MN166), a glial cell activation inhibitor, suppressed both reactive gliosis and freezing behavior, and continued neuroprotective effects were evidenced several months post-injury. These results support the conclusion that inflammation produced by neuroimmune responses to traumatic brain injury play a role in post-traumatic anxiety, and that acute suppression of injury-induced glial cell activation may have eventual promise for prevention of post-traumatic anxiety in humans.

**Key Words**

TBI, LFPI, PTSD, neuroinflammation

## Introduction

The long-term consequences of traumatic brain injury (TBI) include heightened risk of neuropsychiatric disorders, of which anxiety disorders are the most prevalent (Rao and Lyketsos, 2000; Moore et al., 2006; Vaishnavi et al., 2009). Studies of the etiology of anxiety disorders implicate exaggerated responses of the amygdala and insula (Rauch et al., 1997; Simmons et al., 2006; Stein et al., 2007; Shin and Liberzon, 2010; Carlson et al., 2011), impaired inhibition of medial prefrontal cortex and anterior cingulate (Davidson, 2002; Shin et al., 2006; Milad et al., 2009; Shin and Liberzon, 2010) and decreased hippocampal volume (Bremner et al., 1995; Sapolsky, 2000; Shin et al., 2006). Yet, whether and how TBI induces neurochemical, structural, and functional abnormality in these structures is poorly understood.

There is increasing evidence that excessive inflammatory actions of the neuroimmune system may contribute to the development of anxiety disorders following TBI (Spivak et al., 1997; Gasque et al., 2000; Tucker et al., 2004; Shiozaki et al., 2005; von Känel et al., 2007; Hoge et al., 2009). Microglial cells are the first line of defense and primary immune effector cells in the CNS and respond immediately to even small pathological changes from damaged cells, producing proinflammatory cytokines and toxic molecules that compromise neuronal survival (Gehrmann, 1996; Gonzalez-Scarano and Baltuch, 1999; Aloisi, 2001; Town et al., 2005). This rapid microglial response often precedes the more delayed, yet prolonged activation of astrocytes and is thought to be involved with the onset and maintenance of astrogliosis (Graeber and Kreutzberg, 1988; McCann et al., 1996; Hanisch, 2002; Iravani et al., 2005; Herber et al., 2006; Zhang et al., 2010). It has been well established that microglia and astrocytes are activated during the innate immune response to brain injury, leading to the expression of high

levels of proinflammatory cytokines, most notably interleukin-1 beta (IL-1β), interleukin-6 (IL-6) and tumor necrosis factor alpha (TNF-α). While glial activation is typically neuroprotective (Aloisi, 2001; Farina et al., 2007), the chronic inflammatory responses and exaggerated proinflammatory cytokine levels observed following injury initiate neurotoxic processes resulting in secondary tissue damage (Gasque et al., 2000; Simi et al., 2007; Hailer, 2008; Lehnardt, 2010), neuronal death (Sternberg, 1997; Brown and Bal-Price, 2003; Schmidt et al., 2005; Beattie et al., 2010), secondary injury cascades (Bains and Shaw, 1997; Cernak et al., 2001b, a; Ansari et al., 2008a, b) and neuronal hyperexcitability (Hailer, 2008; Riazi et al., 2008; Rodgers et al., 2009; Beattie et al., 2010), all of which may contribute to the dysfunction of brain regions associated with anxiety.

Recently developed animal models of post-traumatic anxiety (O'Connor et al., 2003; Vink et al., 2003; Fromm et al., 2004; Sönmez et al., 2007; Wagner et al., 2007; Jones et al., 2008; Baratz et al., 2010; Liu et al., 2010) permit examination of the possible contributions of brain inflammation. Tests of post-traumatic anxiety in these models have typically included standard measurements of exploratory preference in mildly stressful environments, such as an open-field or elevated-plus testing apparatus. However, it has been frequently noted that measures of exploratory preference may be confounded by a marked overall decrease in exploration in brain-injured animals (O'Connor et al., 2003; Vink et al., 2003; Fromm et al., 2004). Decreased exploration cannot be attributed to TBI-induced motor deficits since numerous studies report only transient (~ 1 week) deficits following trauma (Yan et al., 1992; Taupin et al., 1993; Dixon et al., 1996; Fassbender et al., 2000; Goss et al., 2003; Cutler et al., 2005; Cutler et al., 2006b; Cutler et al., 2006a; Kline et al., 2007; Wagner et al., 2007; Bouilleret et al., 2009; Frey et al., 2009; Baratz et al., 2010; Liu et al., 2010). Rather, TBI-induced decreases in

exploration have been attributed to the indirect effects of freezing (a primary component of the rodent's natural defensive behavior repertoire; Blanchard and Blanchard, 1988), suggesting an abnormally heightened response to stress in brain-injured rats (O'Connor et al., 2003; Vink et al., 2003; Fromm et al., 2004).

Based on these results, we tested the hypothesis that trauma-induced innate immune responses contribute to the development of anxiety-like behaviors in rats by directly examining freezing responses to a minor (novel environment) and major (foot-shock) stressor following Lateral Fluid Percussion Injury (LFPI; a clinically relevant animal model of human closed head injury). We also tested the effectiveness of a glial cell activation inhibitor, Ibudilast (MN166), in attenuating post-injury freezing behavior and reducing reactive gliosis in brain regions associated with hyperexcitability in anxiety disorders.

## Materials and Methods

Sixty adult viral-free male Sprague-Dawley rats (275-325g; Harlan Laboratories, Madison, WI) were housed in pairs in temperature (23 ± 3 °C) and light (12:12 light:dark) controlled rooms with *ad libitum* access to food and water. All procedures were performed in accordance with University of Colorado Institutional Animal Care and Use Committee guidelines for the humane use of laboratory rats in biological research. Rats were randomly assigned to 1 of 10 groups (n = 6/group). Six groups (surgically naïve, sham operated, sham operated+vehicle, sham operated+MN166, LFPI+vehicle and LFPI+MN166) were shocked immediately after behavioral testing at 1 month post-surgery (sham operation or LFPI in the experimental rats). Surgically naïve rats received no injections or surgery, whereas sham operated rats received surgery but were not injected, the final 4 groups received sham or LFPI surgery and either vehicle injections or MN166 treatment. Another 4 groups (sham operated+vehicle, sham operated+MN166, LFPI+vehicle and LFPI+MN166) were run separately in a sucrose preference test to assess anhedonia (the inability to experience pleasure, a core symptom of human depression) without exposure to stressors (anxiety tests and foot shock).

*Lateral Fluid Percussion Injury.* LFPI rats were anesthetized with halothane (4% induction, 2.0-2.5% maintenance) and mounted in a stereotaxic frame. The lateral fluid percussion injury used in this study has been described previously (McIntosh et al., 1989; Thompson et al., 2005; Frey et al., 2009) utilizing a PV820 Pneumatic PicoPump (World Precision Instruments, Inc., Sarasota, FL) to deliver standardized pressure pulses of air to a standing column of fluid. A 3.0 mm diameter craniotomy was centered at 3 mm caudal to bregma and 4.0 mm lateral of the sagittal suture, with the exposed dura remaining intact. A

female Luer-Loc hub (inside diameter of 3.5 mm) was secured over the craniotomy with cyanoacrylate adhesive. Following hub implantation, the animal was removed from the stereotaxic frame and connected to the LFPI apparatus. The LFPI apparatus delivered a moderate impact force (2.0 atmospheres; 10 ms). The injury cap was then removed, scalp sutured and the rats returned to their home cages for recovery. Sham operated rats underwent identical surgical preparation, but did not receive the brain injury.

*Ibudilast (MN166) administration.* MN166 (MediciNova, San Diego, CA) is a relatively non-selective phosphodiesterase inhibitor with anti-inflammatory actions via glial cell attenuation, which has been found to reduce glia-induced neuronal death through the suppression of nitric oxide, reactive oxygen species, and proinflammatory mediators (Mizuno et al., 2004; Rolan et al., 2009). Treated rats received a 5-day dosing regimen of once-daily MN166 injections (10 mg/kg, 1 ml/kg subcutaneously in corn oil) 24 hr prior to LFPI, the day of surgery and LFPI, and 3 days following LFPI. Weight was recorded prior to each dosing and treatment administered at the same time each day to maintain constant levels across a 24 hr period. Dose selection was based on prior animal pharmacology results (Ellis AL, SFN, 2008) showing MN166 to be safe and well tolerated, yielding plasma concentration-time profiles commensurate with high dose regimens in clinical development. MN166 administered via this regimen yields plasma and CNS concentrations that are linked to molecular target actions including, most potently, macrophage migration inhibitory factor (MIF) inhibition (Cho et al., 2010) and, secondarily, PDE's -4 and -10 inhibition (Gibson et al., 2006). The relevance of MIF inhibition in disorders of neuroimmune function such as neuropathic pain has recently been well demonstrated (Wang et al., 2011). Such dosing regimens have clearly been linked to glial attenuation in other animal models (Ledeboer et al., 2007), and the anti-inflammatory actions of

MN166 have recently been shown to suppress cerebral aneurysms in a dose-dependent manner (Yagi et al., 2010).

*Tests of motor, vestibular and locomotive performance.* Baseline testing of motor, vestibular and locomotive performance in all groups was conducted immediately prior to surgery and again, following a 1-week recovery period. These tests included ipsilateral and contralateral assessment of forelimb and hindlimb use to assess motor function, locomotion, limb use and limb preference (Bland et al., 2000; Bland et al., 2001), toe spread to assess gross motor response (Nitz et al., 1986), placing to assess visual and vestibular function (Schallert et al., 2000; Woodlee et al., 2005), catalepsy rod test to assess postural support and mobility (Sanberg et al., 1988), bracing to assess postural stability and catalepsy (Schallert et al., 1979; Morrissey et al., 1989) and air righting to assess dynamic vestibular function (Pellis et al., 1991b; Pellis et al., 1991a). Scoring ranged from 0 (severely impaired) to 5 (normal strength and function). The individual test scores were summed and a composite neuromotor score (0–45) was then generated for each animal. In addition to the composite neuromotor score, limb-use asymmetry was assessed during spontaneous exploration in the cylinder task, a common measure of motor forelimb function following central nervous system injury in rats (Schallert et al., 2000; Schallert, 2006) and post-injury locomotor activity was assessed through distance traveled on a running wheel, both tasks were scored for 5 minutes under red light (~90 lux).

*Behavioral measures.* A novel environment was used to assess freezing behavior in response to a minor stressor (Dellu et al., 1996). The environment consisted of a standard rat cage with one vertically and one horizontally striped wall. No aversive stimuli were introduced in this context and no conditioning occurred. Rats were tested (5 minutes) and the percent of

freezing behavior was assessed. Freezing was defined as the absence of movement except for heart beat/respiration, and was recorded in 10 sec intervals.

Freezing behavior in the novel environment was measured before and after administration of a foot shock in a separate shock apparatus. The shock apparatus consisted of two chambers placed inside sound-attenuating chests. The floor of each chamber consisted of 18 stainless steel rods (4 mm diameter), spaced 1.5 cm center-to-center and wired to a shock generator and scrambler (Colbourn Instruments, Allentown, PA). An automated program delivered a 2-sec/1.5 mA electric shock. Rats were transported in black buckets and shocked immediately upon entry to chambers. Following shock, rats were returned to their home cages.

A sucrose preference test was also performed in separate groups of rats that did not receive foot-shock or testing in the novel environment. This task is commonly used to measure anhedonia in rodent models of depression (Monleon et al., 1995; Willner, 1997). The sucrose preference task was included because anxiety and depression share high rates of co-morbidity in humans (Moore et al., 2006) and was assessed as a possible confound to freezing behavior, due to possible co-occurrence of depression-like behavior. Rats were first habituated to sucrose solution, and were tested during the dark phase of the light/dark cycle to avoid the food and water deprivation necessary when testing during the light phase. Day 1 and day 2 consisted of habituation, day 3 and day 4 were baseline (averaged) and day 5 was the first test day. The rats were presented with two pre-weighted bottles containing 2% sucrose solution or tap water for a period of 4 hours. Thirty minutes into the task the bottles were swapped to force preference and counter for placement effects. Total sucrose intake and sucrose preference (sucrose intake/(sucrose intake + water intake * 100) were measured.

*Timeline for behavioral testing:* Following a 2-week recovery period from sham operation or LFPI in experimental animals, all groups except those to be evaluated for sucrose preference were tested in the novel context. Testing was performed at 2 weeks, 1, 2 and 3 months post-surgery. Shock was delivered after behavioral testing was completed at the 1 month time-point. Tests for sucrose preference were performed at 2 weeks, 1 month and 3 months post-surgery with no intervening foot-shock.

*Immunohistochemistry:* Immunoreactivity for OX-42 (targets CD11b/c, a marker of microglial activation) and glial fibrillary acidic protein (GFAP; a marker of astrocyte activation) was measured using an avidin-biotin-horseradish peroxidase (ABC) reaction (Loram et al., 2009). Brain sections (12 μm) were cut on a cryostat and mounted onto poly-L-lysine-coated slides and stored at -80 °C. Sections were post-fixed with 4% PFA for 15 min at room temperature, then treated with 0.03% $H_2O_2$ for 30 min at room temperature. The sections were incubated at 4 °C overnight in either mouse anti-rat OX-42 (1:100; BD Biosciences Pharmingen, San Jose, CA) or mouse anti-pig GFAP (1:100; MP Biomedicals, Aurora, OH). The next day, sections were incubated at room temperature for 2 h with biotinylated goat anti-mouse IgG antibody (1:200; Jackson ImmunoResearch, West Grove, PA). Sections were washed and incubated for 2 h at room temperature in ABC (1:400 Vector Laboratories, Burlingame, CA) and reacted with 3', 3-diaminobenzidine (DAB; Sigma-Aldrich, St. Louis, MO). Glucose oxidase and β-D-glucose were used to generate hydrogen peroxide. Nickelous ammonium sulfate was added to the DAB solution to optimize the reaction product. Sections were air-dried over night and then dehydrated with graded alcohols, cleared in Histoclear and coverslipped with Permount (Fisher Scientific, Fairlawn, NJ). Densitometric analysis was performed using Scion Image software.

*Image Analysis:* Slides were viewed with an Olympus BX-61 microscope, using Olympus Microsuite software (Olympus America, Melville, NY) with bright-field illumination at 10X magnification. Images were opened in ImageJ, converted into gray scale and rescaled from inches to pixels. Background areas were chosen in the white matter or in cell-poor areas close to the region of interest (ROI). The number of pixels and the average pixel values above the set background were then computed and multiplied, giving an integrated densitometric measure (integrated gray level). Four measurements were made for each ROI; the measurements were then averaged to obtain a single integrated density value per rat, per region. All measurements were taken while blind to treatment group.

*Statistical Analyses:* Results are expressed as mean ± SEM. Analyses for all behavioral variables used analysis of variance (ANOVA) with repeated measures (time after injury), and treatment as the independent variable. The integrated density from the histology was only conducted at one time point and utilized one-way ANOVAs to compare regions between groups. Data were analyzed using SPSS® Statistics software and, in all cases, statistical significance was set at $p < 0.05$.

**Results**

Neuromotor composite scores of the brain-injured groups (LFPI+MN166, LFPI+vehicle) did not significantly differ from controls ($F(3,20) = 0.803$, $p = 0.508$). Rats in all groups consistently received normal scores on forelimb and hindlimb use, toe spread, placing, catalepsy rod, bracing, and air righting tests, indicating no impairments in motor, vestibular or locomotive functioning due to TBI. There were also no significant between group differences in limb-use asymmetry observed for contralateral ($F(5,29) = 0.544$, $p = 0.741$) and ipsilateral ($F(5,29) = 0.428$, $p = 0.826$) forelimb use during vertical exploratory behavior in the cylinder task,

indicating no limb-use bias due to injury (Fig. 1A). No significant between group differences were found in locomotor performance evidenced by distance traveled during the running wheel activity ($F(5,29) = 0.069$, $p = 0.996$), revealing no post-injury impairments in locomotion (Fig. 1B). Nor were there significant between group differences in the sucrose preference task ($F(3,21) = 0.338$, $p = 0.798$), indicating no impairments in hedonic states post-injury.

Despite normal motor, vestibular and locomotive function, LFPI produced large increases in freezing behavior when rats were placed in a novel context (Fig. 2; $F(5,30) = 9.539$, $p < 0.0001$). Exposed only to this minor stressor (i.e. at 2 week and 1 month post-injury measurements conducted prior to shock), LPFI rats injected with either MN166 or vehicle (Fig. 2; white and black bars, respectively) froze approximately twice as long as naïve or sham operated rats (Fig. 2; light and dark grey bars, respectively; $p < 0.01$). At 2 and 3-month measurement times, following the additional major stressor of shock (Fig. 2; arrows), freezing in both naïve and sham operated rats remained constant at approximately 10%. Freezing in LFPI rats treated with MN166 remained consistently higher than these controls ($p < 0.001$), but, while appearing higher compared to earlier post-injury measurements in the same animals, this increased freezing compared to naïve and sham operated rats before (1 month) and following (2 month) shock did not reach significance ($p=0.316$). By contrast, LFPI+vehicle rats nearly doubled their freezing time to approximately 50% (Fig. 2; black bars) compared to pre-shock values ($p < 0.001$), freezing approximately twice as long as LFPI+MN166 rats ($p < 0.001$) and 5 times as long as naïve and sham operated controls ($p < 0.001$) at the 2 and 3 month post-injury measurement times.

The behavioral effects of injections alone, independent of LFPI, are reflected in sham surgery groups with injections of either MN166 or vehicle (Fig. 2; narrow and broad diagonal

lines, respectively). Sham operated rats tended to freeze more than un-injected naïve and sham operated controls, reaching significance for both groups at the 2 and 3-month measurement points ($p < 0.01$) and suggesting that injections alone are aversive and can contribute to subsequent freezing. However, even at pre-shock measurement points, LFPI animals that received the same injections of MN166 or vehicle froze significantly more than injected controls ($p < 0.01$), indicating substantial enhancement of freezing produced by LFPI. This effect became more apparent following shock, where LFPI+vehicle rats froze twice as long as the injected controls ($p < 0.001$). By contrast, LFPI+MN166 rats were not distinguishable from either injected control group following shock, suggesting that their elevated freezing compared to naïve and sham operated animals was the result of injections alone and that MN166 eliminated the exaggerated freezing response to shock characterizing LFPI+vehicle rats.

OX-42 and GFAP immunoreactivity (reflecting microglia and astrocytic activation) was assessed in the insula, amygdala and hippocampus in brain-injured rats for comparison to sham operated and surgically naïve rats. Representative images (40X), showing GFAP immunoreactivity in several of these regions, are shown in Figure 3, revealing normal astrocyte morphology in surgically naïve and sham operated rats. LFPI+vehicle rats showed clear signs of reactive astrocytes (Fig. 3; bottom row). LFPI rats treated with MN166 (Fig. 3; third row) were difficult to differentiate from sham operated or surgically naïve control groups.

Densitometry of GFAP labeling in all areas examined confirmed that activation of astrocytes was significantly greater in LFPI compared to all other groups in insula (Fig. 4A; left bars; $F(3,19) = 13.17$, $p < 0.0001$), amygdala (Fig. 4B; left bars; $F(3,18) = 7.54$, $p < 0.002$) and hippocampus (Fig. 4C; left bars; $F(3,15) = 8.47$, $p < 0.002$). In contrast, no differences in GFAP labeling were observed between surgically naïve, sham operated and LFPI+MN166 groups in

any of the regions examined. While MN166 treated LFPI rats were not distinguishable from surgically naïve or sham operated controls, post-hoc analyses revealed that LFPI+vehicle rats had significantly greater astrocyte activation in all 3 brain regions as compared to controls (Fig. 4A-C): insula ($p < 0.002$ vs. surgically naive, sham operated and LFPI+MN166), amygdala ($p < 0.02$ vs. surgically naive, sham operated and LFPI+MN166) and hippocampus ($p < 0.03$ vs. surgically naive, sham operated and LFPI+MN166).

Analysis of GFAP immunoreactivity in sub-regions of the insula (Fig. 4A; right bars), amygdala (Fig. 4B; right bars), and hippocampus (Fig. 4C; right bars), also revealed no differences between surgically naïve, sham operated and LFPI+MN166 groups. As in the regional analysis, LFPI+vehicle rats showed increased astrocyte activation over controls in most sub-regions examined. In the insula, LFPI+vehicle rats showed significantly increased GFAP labeling in agranular ($F(3,19) = 16.778$, $p < 0.0001$), dysgranular ($F(3,19) = 6.042$, $p < 0.005$) and granular ($F(3,19) = 5.277$, $p < 0.008$) regions, as compared to control groups. In the amygdala, GFAP labeling in LFPI+vehicle rats was significantly increased in the BLA ($F(3,18) = 4.050$, $p < 0.023$) and CE ($F(3,18) = 5.012$, $p < 0.011$) nuclei, as compared to controls. LFPI+vehicle rats also showed increased GFAP expression in the hippocampus, but this was only significant in CA3 ($F(3,18) = 3.810$, $p < 0.03$) and approached significance in CA1 ($F(3,17) = 3.234$, $p = 0.055$).

LFPI+vehicle rats also showed significantly increased microglia activation compared to control groups, as measured by OX-42 labeling, but this was restricted to the insula (Fig. 4D; $F(3,19) = 5.59$, $p < 0.007$). Analysis of sub-regions of the insula also revealed increases in microglial activation for LFPI+vehicle rats, and post-hoc comparisons showed that LFPI alone significantly increased OX-42 labeling in agranular ($F(3,19) = 11.186$, $p < 0.0001$), granular

(F(3,18) = 3.740, p < 0.03), and approaching significance (F(3,19) = 2.742, p < 0.072) in dysgranular areas. No differences in OX-42 labeling were observed between surgically naïve, sham operated and LFPI+MN166 groups in any insular regions examined. No significant between group differences were found in OX-42 expression for the amygdala or hippocampus.

## Discussion

These data suggest a link between injury-induced brain inflammation and post-traumatic anxiety. Rats with LFPI display freezing responses to the minor stress of a novel environment that is 2-3 times normal and which, unlike controls, is nearly doubled by the delivery of a major foot-shock stressor. LFPI also results in marked reactive gliosis in brain regions associated with anxiety. The possibility that post-traumatic brain inflammation and gliosis may contribute to anxiety-like behavior observed here, is supported by the effects of glial-cell activation inhibitor MN166. MN166 reduces reactive gliosis and TBI-induced freezing behavior, rendering these animals histologically and behaviorally indistinguishable from naïve and sham operated controls. To our knowledge, this is the first study to report pharmacological immunosuppression resulting in the reduction of anxiety-like behaviors following TBI.

*A possible mechanism for neuroimmune induced post-traumatic anxiety.*

Our finding of prolonged reactive gliosis in brain structures including, but likely not confined to, the hippocampus, amygdala and insular cortex, suggests that these structures may contribute to the persistent enhanced freezing of our brain-injured animals in reaction to a novel environment. All three structures have been implicated in rodent research investigating the pathogenesis of anxiety (Davis, 1992; Davis et al., 1994; Davidson, 2002; Vyas et al., 2004; Paulus and Stein, 2006; Rauch et al., 2006; Canteras et al., 2010) and fear behavior in the rat (Sullivan, 2004; Rosen and Donley, 2006; Milad et al., 2009; Liu et al., 2010).

The mechanisms by which immune responses may contribute to dysfunction of these structures remain to be determined. It is well established that LFPI in the rat results in activation of microglia and astrocytes as part of the innate immune response to insult. A number of studies

indicate that LFPI-induced reactive gliosis follows a distinct time-course, beginning with predominant microglia activation that peaks within a week (Hill et al., 1996; Nonaka et al., 1999; Grady et al., 2003; Gueorguieva et al., 2008; Clausen et al., 2009; Yu et al., 2010) but continues for several weeks and overlaps later with persistent astrocytic activation (D'Ambrosio et al., 2004; Yu et al., 2010). Microglia are resident macrophages and first responders to pathogens and neuronal insults in the CNS. They react rapidly, leading to activation of astrocytes and prolonged disruption of neuronal function (Iravani et al., 2005; Herber et al., 2006; Zhang et al., 2009; Zhang et al., 2010). Several lesion paradigms have also shown rapid microglial response followed by delayed astrocyte reaction (Gehrmann et al., 1991; Dusart and Schwab, 1994; Frank and Wolburg, 1996; McCann et al., 1996; Liberatore et al., 1999).

Our results support this well-documented temporal relationship suggesting that microglial activation precedes astrocytic activation and plays a role in the onset and maintenance of astrogliosis (Graeber and Kreutzberg, 1988; McCann et al., 1996; Hanisch, 2002; Iravani et al., 2005; Herber et al., 2006; Zhang et al., 2010). This time-course is consistent with behavioral freezing responses in the present study, appearing rapidly within 2 weeks but persisting unabated for the 3-month post-injury measurement period. It is also consistent with our immunohistochemistry results, indicating injury-induced astrocytic activation in all 3 regions of interest, insula, amygdala and hippocampus at 3 months post-injury, but less activation of microglia, only significant in the insula. The lower levels of microglia expression are likely due to assessment at 3 months post-injury.

Trauma-related reactive gliosis is well known to result in the release of high levels of pro-inflammatory cytokines, specifically tumor necrosis factor-□ (TNF-□□(Taupin et al., 1993; Fan et al., 1996; Lloyd et al., 2008), interleukin-1 beta (IL-1□□(Taupin et al., 1993; Fan et al.,

1995; Fassbender et al., 2000; Yan et al., 2002; Lloyd et al., 2008), and interleukin-6 (IL-6; (Taupin et al., 1993; Yan et al., 2002; Lloyd et al., 2008), which are central mediators of neuroinflammation following head injury (Fan et al., 1995; Rothwell and Hopkins, 1995; Rothwell and Strijbos, 1995; Fan et al., 1996; Simi et al., 2007). Release of these pro-inflammatory cytokines, particularly IL-1β and TNF-α, pathologically increases neuronal excitability in all brain regions where it has been measured (Riazi et al., 2008; Schafers and Sorkin, 2008; Rodgers et al., 2009; Beattie et al., 2010; Maroso et al., 2010). While neuronal excitability and proinflammatory cytokine levels were not measured in the present study, neuroinflammation has been implicated in neuronal excitability of amygdala and insular cortex and anxiety-like behavior by others using c-Fos labeling (Abrous et al., 1999; Ikeda et al., 2003; Kung et al., 2010). These same regions have also consistently been reported to be hyperexcitable in human imaging data across a variety of anxiety disorders (Rauch et al., 1997; Shin et al., 2006; Simmons et al., 2006; Stein et al., 2007; Shin and Liberzon, 2010; Carlson et al., 2011).

*Attenuation of post-traumatic anxiety with MN166.*

Meta-analysis of the impact of pharmacological treatments on behavioral, cognitive, and motor outcomes after traumatic brain injury in rodent models (Wheaton et al., 2011) indicates that of 16 treatment strategies evaluated to date, improved cognition and motor function have been reported, but almost no treatments have improved behaviors related to psychiatric dysfunction in general and anxiety in specific. Exceptions to this are recent promising reports of treatments such as magnesium sulphate to limit excitotoxic damage (Vink et al., 2003; Fromm et al., 2004; O'Connor, 2003, 533-41) and resevatrol to limit excitotoxicity, ischemia, hypoxia (Sönmez et al., 2007), both increasing open field exploration (resulting from decreased freezing) and therefore presumably decreasing post-injury anxiety.

Glial targeted immunosuppression has also been found to be neuroprotective following TBI in rodents, resulting in increased structural preservation and improved functional outcomes (Hailer, 2008); including recent reports that MN166 significantly attenuated brain edema formation, cerebral atrophy and apoptosis in neuronal cells following ischemic brain injury in rats, increasing neuronal survival rates (Lee et al., 2011). MN166 may reduce neuronal damage in regions involved in anxiety, mitigating the role of glial activation, neurotoxicity and hyperexcitability in the subsequent development of anxiety-like behaviors. While not focused on post-traumatic anxiety, MN166 has been found to reduce intracellular calcium accumulation (Yanase et al., 1996), apoptosis, functional damage and passive avoidance behaviors following a transient ischemia model in rats (Yoshioka et al., 2002). Increasing evidence supports neuroinflammation, chronic inflammatory responses, proinflammatory cytokines, neuronal hyperexcitability, and secondary injury cascades in the pathophysiology of post-traumatic anxiety. The mechanisms of the effect of MN166 on TBI-induced anxiety-like behavior are not fully known. However, the results of this study provide evidence of a neuroprotective role for MN166 in attenuating and perhaps preventing development of post-traumatic anxiety.

Further establishing a relationship between TBI, neuroimmune responses, neurocircuitry and anxiety disorders, is important to further understand the sequelae of TBI and to the development of effective treatment strategies. The development of anxiety disorders following TBI is a complex and multifaceted problem, and finding treatments that work will require multifaceted approaches. The injury itself initiates many complex biological events including glial activation, breakdown of the blood brain barrier, excitotoxicity and chronic neuroinflammation. While primary injury often cannot be prevented, it may be possible to reduce secondary injury, leading to better functional and behavioral recovery following TBI. The

present results, using peri-injury treatment with MN166 to prevent post-traumatic freezing behavior, not only suggest a role for neuroimmune inflammation in anxiety physiology, but similarly successful results with post-injury treatment could introduce a promising and clinically realistic translational possibility for prevention of post-traumatic anxiety in humans.

**Acknowledgements**

US Army Medical Research and Material Command grant PR100040, Craig Hospital Gift Fund, University of Colorado Innovative Seed Grant, Autism Speaks Pilot Study grant 7153, and National Institutes of Health grant NS36981 to DSB, and National Institutes of Health grants DA024044, DA01767 to LRW.

**Author Disclosure Statement**

Krista M. Rodgers: No competing financial interests exist.

Florencia M. Bercum: No competing financial interests exist.

Danielle L. McCallum: No competing financial interests exist.

Jerry W. Rudy: No competing financial interests exist.

Lauren C. Frey: No competing financial interests exist.

Kirk W. Johnson: Chief science officer of MediciNova, Inc., the pharmaceutical firm providing MN166 for this research.

Linda R. Watkins: No competing financial interests exist.

Daniel S. Barth: No competing financial interests exist.

## References

Abrous DN, Rodriguez J, le Moal M, Moser PC, Barneoud P (1999) Effects of mild traumatic brain injury on immunoreactivity for the inducible transcription factors c-Fos, c-Jun, JunB, and Krox-24 in cerebral regions associated with conditioned fear responding. Brain research 826:181-192.

Aloisi F (2001) Immune function of microglia. Glia 36:165-179.

Ansari MA, Roberts KN, Scheff SW (2008a) Oxidative stress and modification of synaptic proteins in hippocampus after traumatic brain injury. Free Radic Biol Med 45:443-452.

Ansari MA, Roberts KN, Scheff SW (2008b) A time course of contusion-induced oxidative stress and synaptic proteins in cortex in a rat model of TBI. J Neurotrauma 25:513-526.

Bains JS, Shaw CA (1997) Neurodegenerative disorders in humans: the role of glutathione in oxidative stress-mediated neuronal death. Brain Res Brain Res Rev 25:335-358.

Baratz R, Rubovitch V, Frenk H, Pick CG (2010) The influence of alcohol on behavioral recovery after mTBI in mice. J Neurotrauma 27:555-563.

Beattie MS, Ferguson AR, Bresnahan JC (2010) AMPA-receptor trafficking and injury-induced cell death. Eur J Neurosci 32:290-297.

Bland ST, Pillai RN, Aronowski J, Grotta JC, Schallert T (2001) Early overuse and disuse of the affected forelimb after moderately severe intraluminal suture occlusion of the middle cerebral artery in rats. Behav Brain Res 126:33-41.

Bland ST, Schallert T, Strong R, Aronowski J, Grotta JC (2000) Early exclusive use of the affected forelimb after moderate transient focal ischemia in rats : functional and anatomic outcome. Stroke 31:1144-1152.

Bouilleret V, Cardamone L, Liu YR, Fang K, Myers DE, O'Brien TJ (2009) Progressive brain changes on serial manganese-enhanced MRI following traumatic brain injury in the rat. J Neurotrauma 26:1999-2013.

Bremner JD, Randall P, Scott TM, Bronen RA, Seibyl JP, Southwick SM, Delaney RC, McCarthy G, Charney DS, Innis RB (1995) MRI-based measurement of hippocampal volume in patients with combat-related posttraumatic stress disorder. Am J Psychiatry 152:973-981.

Brown GC, Bal-Price A (2003) Inflammatory neurodegeneration mediated by nitric oxide, glutamate, and mitochondria. Mol Neurobiol 27:325-355.

Canteras NS, Resstel LB, Bertoglio LJ, Carobrez Ade P, Guimaraes FS (2010) Neuroanatomy of anxiety. Curr Top Behav Neurosci 2:77-96.

Carlson JM, Greenberg T, Rubin D, Mujica-Parodi LR (2011) Feeling anxious: anticipatory amygdalo-insular response predicts the feeling of anxious anticipation. Soc Cogn Affect Neurosci 6:74-81.

Cernak I, Wang Z, Jiang J, Bian X, Savic J (2001a) Ultrastructural and functional characteristics of blast injury-induced neurotrauma. J Trauma 50:695-706.

Cernak I, Wang Z, Jiang J, Bian X, Savic J (2001b) Cognitive deficits following blast injury-induced neurotrauma: possible involvement of nitric oxide. Brain Inj 15:593-612.

Cho Y, Crichlow GV, Vermeire JJ, Leng L, Du X, Hodsdon ME, Bucala R, Cappello M, Gross M, Gaeta F, Johnson K, Lolis EJ (2010) Allosteric inhibition of macrophage migration inhibitory factor revealed by ibudilast. Proc Natl Acad Sci U S A 107:11313-11318.

Clausen F, Hanell A, Bjork M, Hillered L, Mir AK, Gram H, Marklund N (2009) Neutralization of interleukin-1beta modifies the inflammatory response and improves histological and cognitive outcome following traumatic brain injury in mice. Eur J Neurosci 30:385-396.

Cutler SM, Vanlandingham JW, Stein DG (2006a) Tapered progesterone withdrawal promotes long-term recovery following brain trauma. Exp Neurol 200:378-385.

Cutler SM, Pettus EH, Hoffman SW, Stein DG (2005) Tapered progesterone withdrawal enhances behavioral and molecular recovery after traumatic brain injury. Exp Neurol 195:423-429.

Cutler SM, VanLandingham JW, Murphy AZ, Stein DG (2006b) Slow-release and injected progesterone treatments enhance acute recovery after traumatic brain injury. Pharmacol Biochem Behav 84:420-428.

D'Ambrosio R, Fairbanks JP, Fender JS, Born DE, Doyle DL, Miller JW (2004) Post-traumatic epilepsy following fluid percussion injury in the rat. Brain 127:304-314.

Davidson RJ (2002) Anxiety and affective style: role of prefrontal cortex and amygdala. Biological psychiatry 51:68-80.

Davis M (1992) The role of the amygdala in fear and anxiety. Annu Rev Neurosci 15:353-375.

Davis M, Rainnie D, Cassell M (1994) Neurotransmission in the rat amygdala related to fear and anxiety. Trends Neurosci 17:208-214.

Dellu F, Mayo W, Vallee M, Maccari S, Piazza PV, Le Moal M, Simon H (1996) Behavioral reactivity to novelty during youth as a predictive factor of stress-induced corticosterone secretion in the elderly--a life-span study in rats. Psychoneuroendocrinology 21:441-453.

Dixon CE, Bao J, Long DA, Hayes RL (1996) Reduced evoked release of acetylcholine in the rodent hippocampus following traumatic brain injury. Pharmacol Biochem Behav 53:679-686.

Dusart I, Schwab ME (1994) Secondary cell death and the inflammatory reaction after dorsal hemisection of the rat spinal cord. Eur J Neurosci 6:712-724.

Ellis AL WJ, Brown K, Blackwood C, Ramos K, Starnes C, Maier SF, and Watkins LR (SFN, 2008) Characterization of exaggerated pain behavior and glial activation in a novel rat model of spinal cord injury.

Fan L, Young PR, Barone FC, Feuerstein GZ, Smith DH, McIntosh TK (1995) Experimental brain injury induces expression of interleukin-1 beta mRNA in the rat brain. Brain Res Mol Brain Res 30:125-130.

Fan L, Young PR, Barone FC, Feuerstein GZ, Smith DH, McIntosh TK (1996) Experimental brain injury induces differential expression of tumor necrosis factor-alpha mRNA in the CNS. Brain Res Mol Brain Res 36:287-291.

Farina C, Aloisi F, Meinl E (2007) Astrocytes are active players in cerebral innate immunity. Trends Immunol 28:138-145.

Fassbender K, Schneider S, Bertsch T, Schlueter D, Fatar M, Ragoschke A, Kuhl S, Kischka U, Hennerici M (2000) Temporal profile of release of interleukin-1beta in neurotrauma. Neurosci Lett 284:135-138.

Frank M, Wolburg H (1996) Cellular reactions at the lesion site after crushing of the rat optic nerve. Glia 16:227-240.

Frey LC, Hellier J, Unkart C, Lepkin A, Howard A, Hasebroock K, Serkova N, Liang L, Patel M, Soltesz I, Staley K (2009) A novel apparatus for lateral fluid percussion injury in the rat. J Neurosci Methods 177:267-272.

Fromm L, Heath DL, Vink R, Nimmo AJ (2004) Magnesium attenuates post-traumatic depression/anxiety following diffuse traumatic brain injury in rats. J Am Coll Nutr 23:529S-533S.

Gasque P, Dean YD, McGreal EP, VanBeek J, Morgan BP (2000) Complement components of the innate immune system in health and disease in the CNS. Immunopharmacology 49:171-186.

Gehrmann J (1996) Microglia: a sensor to threats in the nervous system? Res Virol 147:79-88.

Gehrmann J, Schoen SW, Kreutzberg GW (1991) Lesion of the rat entorhinal cortex leads to a rapid microglial reaction in the dentate gyrus. A light and electron microscopical study. Acta Neuropathol 82:442-455.

Gibson LC, Hastings SF, McPhee I, Clayton RA, Darroch CE, Mackenzie A, Mackenzie FL, Nagasawa M, Stevens PA, Mackenzie SJ (2006) The inhibitory profile of Ibudilast against the human phosphodiesterase enzyme family. Eur J Pharmacol 538:39-42.

Gonzalez-Scarano F, Baltuch G (1999) Microglia as mediators of inflammatory and degenerative diseases. Annu Rev Neurosci 22:219-240.

Goss CW, Hoffman SW, Stein DG (2003) Behavioral effects and anatomic correlates after brain injury: a progesterone dose-response study. Pharmacol Biochem Behav 76:231-242.

Grady MS, Charleston JS, Maris D, Witgen BM, Lifshitz J (2003) Neuronal and glial cell number in the hippocampus after experimental traumatic brain injury: analysis by stereological estimation. J Neurotrauma 20:929-941.

Graeber MB, Kreutzberg GW (1988) Delayed astrocyte reaction following facial nerve axotomy. J Neurocytol 17:209-220.

Gueorguieva I, Clark SR, McMahon CJ, Scarth S, Rothwell NJ, Tyrrell PJ, Hopkins SJ, Rowland M (2008) Pharmacokinetic modelling of interleukin-1 receptor antagonist in plasma and cerebrospinal fluid of patients following subarachnoid haemorrhage. Br J Clin Pharmacol 65:317-325.

Hailer NP (2008) Immunosuppression after traumatic or ischemic CNS damage: it is neuroprotective and illuminates the role of microglial cells. Prog Neurobiol 84:211-233.

Hanisch UK (2002) Microglia as a source and target of cytokines. Glia 40:140-155.

Herber DL, Maloney JL, Roth LM, Freeman MJ, Morgan D, Gordon MN (2006) Diverse microglial responses after intrahippocampal administration of lipopolysaccharide. Glia 53:382-391.

Hill SJ, Barbarese E, McIntosh TK (1996) Regional heterogeneity in the response of astrocytes following traumatic brain injury in the adult rat. J Neuropathol Exp Neurol 55:1221-1229.

Hoge EA, Brandstetter K, Moshier S, Pollack MH, Wong KK, Simon NM (2009) Broad spectrum of cytokine abnormalities in panic disorder and posttraumatic stress disorder. Depress Anxiety 26:447-455.

Ikeda K, Onaka T, Yamakado M, Nakai J, Ishikawa TO, Taketo MM, Kawakami K (2003) Degeneration of the amygdala/piriform cortex and enhanced fear/anxiety behaviors in sodium pump alpha2 subunit (Atp1a2)-deficient mice. The Journal of neuroscience : the official journal of the Society for Neuroscience 23:4667-4676.

Iravani MM, Leung CC, Sadeghian M, Haddon CO, Rose S, Jenner P (2005) The acute and the long-term effects of nigral lipopolysaccharide administration on dopaminergic dysfunction and glial cell activation. Eur J Neurosci 22:317-330.

Jones NC, Cardamone L, Williams JP, Salzberg MR, Myers D, O'Brien TJ (2008) Experimental traumatic brain injury induces a pervasive hyperanxious phenotype in rats. Journal of neurotrauma 25:1367-1374.

Kline AE, Wagner AK, Westergom BP, Malena RR, Zafonte RD, Olsen AS, Sozda CN, Luthra P, Panda M, Cheng JP, Aslam HA (2007) Acute treatment with the 5-HT(1A) receptor agonist 8-OH-DPAT and chronic environmental enrichment confer neurobehavioral benefit after experimental brain trauma. Behav Brain Res 177:186-194.

Kung JC, Chen TC, Shyu BC, Hsiao S, Huang AC (2010) Anxiety- and depressive-like responses and c-fos activity in preproenkephalin knockout mice: oversensitivity hypothesis of enkephalin deficit-induced posttraumatic stress disorder. J Biomed Sci 17:29.

Ledeboer A, Hutchinson MR, Watkins LR, Johnson KW (2007) Ibudilast (AV-411). A new class therapeutic candidate for neuropathic pain and opioid withdrawal syndromes. Expert Opin Investig Drugs 16:935-950.

Lee JY, Cho E, Ko YE, Kim I, Lee KJ, Kwon SU, Kang DW, Kim JS (2011) Ibudilast, a phosphodiesterase inhibitor with anti-inflammatory activity, protects against ischemic brain injury in rats. Brain research.

Lehnardt S (2010) Innate immunity and neuroinflammation in the CNS: the role of microglia in Toll-like receptor-mediated neuronal injury. Glia 58:253-263.

Liberatore GT, Jackson-Lewis V, Vukosavic S, Mandir AS, Vila M, McAuliffe WG, Dawson VL, Dawson TM, Przedborski S (1999) Inducible nitric oxide synthase stimulates dopaminergic neurodegeneration in the MPTP model of Parkinson disease. Nat Med 5:1403-1409.

Liu YR, Cardamone L, Hogan RE, Gregoire MC, Williams JP, Hicks RJ, Binns D, Koe A, Jones NC, Myers DE, O'Brien TJ, Bouilleret V (2010) Progressive metabolic and structural cerebral perturbations after traumatic brain injury: an in vivo imaging study in the rat. J Nucl Med 51:1788-1795.

Lloyd E, Somera-Molina K, Van Eldik LJ, Watterson DM, Wainwright MS (2008) Suppression of acute proinflammatory cytokine and chemokine upregulation by post-injury administration of a novel small molecule improves long-term neurologic outcome in a mouse model of traumatic brain injury. J Neuroinflammation 5:28.

Loram LC, Harrison JA, Sloane EM, Hutchinson MR, Sholar P, Taylor FR, Berkelhammer D, Coats BD, Poole S, Milligan ED, Maier SF, Rieger J, Watkins LR (2009) Enduring reversal of neuropathic pain by a single intrathecal injection of adenosine 2A receptor agonists: a novel therapy for neuropathic pain. The Journal of neuroscience : the official journal of the Society for Neuroscience 29:14015-14025.

Maroso M, Balosso S, Ravizza T, Liu J, Aronica E, Iyer AM, Rossetti C, Molteni M, Casalgrandi M, Manfredi AA, Bianchi ME, Vezzani A (2010) Toll-like receptor 4 and high-mobility group box-1 are involved in ictogenesis and can be targeted to reduce seizures. Nat Med 16:413-419.

McCann MJ, O'Callaghan JP, Martin PM, Bertram T, Streit WJ (1996) Differential activation of microglia and astrocytes following trimethyl tin-induced neurodegeneration. Neuroscience 72:273-281.

McIntosh TK, Vink R, Noble L, Yamakami I, Fernyak S, Soares H, Faden AL (1989) Traumatic brain injury in the rat: characterization of a lateral fluid-percussion model. Neuroscience 28:233-244.

Milad MR, Pitman RK, Ellis CB, Gold AL, Shin LM, Lasko NB, Zeidan MA, Handwerger K, Orr SP, Rauch SL (2009) Neurobiological basis of failure to recall extinction memory in posttraumatic stress disorder. Biological psychiatry 66:1075-1082.

Mizuno T, Kurotani T, Komatsu Y, Kawanokuchi J, Kato H, Mitsuma N, Suzumura A (2004) Neuroprotective role of phosphodiesterase inhibitor ibudilast on neuronal cell death induced by activated microglia. Neuropharmacology 46:404-411.

Monleon S, D'Aquila P, Parra A, Simon VM, Brain PF, Willner P (1995) Attenuation of sucrose consumption in mice by chronic mild stress and its restoration by imipramine. Psychopharmacology (Berl) 117:453-457.

Moore EL, Terryberry-Spohr L, Hope DA (2006) Mild traumatic brain injury and anxiety sequelae: a review of the literature. Brain injury : [BI] 20:117-132.

Morrissey TK, Pellis SM, Pellis VC, Teitelbaum P (1989) Seemingly paradoxical jumping in cataleptic haloperidol-treated rats is triggered by postural instability. Behav Brain Res 35:195-207.

Nitz AJ, Dobner JJ, Matulionis DH (1986) Pneumatic tourniquet application and nerve integrity: motor function and electrophysiology. Exp Neurol 94:264-279.

Nonaka M, Chen XH, Pierce JE, Leoni MJ, McIntosh TK, Wolf JA, Smith DH (1999) Prolonged activation of NF-kappaB following traumatic brain injury in rats. J Neurotrauma 16:1023-1034.

O'Connor CA, Cernak I, Vink R (2003) Interaction between anesthesia, gender, and functional outcome task following diffuse traumatic brain injury in rats. J Neurotrauma 20:533-541.

Paulus MP, Stein MB (2006) An insular view of anxiety. Biological psychiatry 60:383-387.

Pellis SM, Whishaw IQ, Pellis VC (1991a) Visual modulation of vestibularly-triggered air-righting in rats involves the superior colliculus. Behav Brain Res 46:151-156.

Pellis SM, Pellis VC, Teitelbaum P (1991b) Air righting without the cervical righting reflex in adult rats. Behav Brain Res 45:185-188.

Rao V, Lyketsos C (2000) Neuropsychiatric sequelae of traumatic brain injury. Psychosomatics 41:95-103.

Rauch SL, Shin LM, Phelps EA (2006) Neurocircuitry models of posttraumatic stress disorder and extinction: human neuroimaging research--past, present, and future. Biological psychiatry 60:376-382.

Rauch SL, Savage CR, Alpert NM, Fischman AJ, Jenike MA (1997) The functional neuroanatomy of anxiety: a study of three disorders using positron emission tomography and symptom provocation. Biological psychiatry 42:446-452.

Riazi K, Galic MA, Kuzmiski JB, Ho W, Sharkey KA, Pittman QJ (2008) Microglial activation and TNFalpha production mediate altered CNS excitability following peripheral inflammation. Proc Natl Acad Sci U S A 105:17151-17156.

Rodgers KM, Hutchinson MR, Northcutt A, Maier SF, Watkins LR, Barth DS (2009) The cortical innate immune response increases local neuronal excitability leading to seizures. Brain 132:2478-2486.

Rolan P, Hutchinson M, Johnson K (2009) Ibudilast: a review of its pharmacology, efficacy and safety in respiratory and neurological disease. Expert Opin Pharmacother 10:2897-2904.

Rosen JB, Donley MP (2006) Animal studies of amygdala function in fear and uncertainty: relevance to human research. Biol Psychol 73:49-60.

Rothwell NJ, Strijbos PJ (1995) Cytokines in neurodegeneration and repair. Int J Dev Neurosci 13:179-185.

Rothwell NJ, Hopkins SJ (1995) Cytokines and the nervous system II: Actions and mechanisms of action. Trends Neurosci 18:130-136.

Sanberg PR, Bunsey MD, Giordano M, Norman AB (1988) The catalepsy test: its ups and downs. Behav Neurosci 102:748-759.

Sapolsky RM (2000) Glucocorticoids and hippocampal atrophy in neuropsychiatric disorders. Arch Gen Psychiatry 57:925-935.

Schafers M, Sorkin L (2008) Effect of cytokines on neuronal excitability. Neurosci Lett 437:188-193.

Schallert T (2006) Behavioral tests for preclinical intervention assessment. NeuroRx 3:497-504.

Schallert T, De Ryck M, Whishaw IQ, Ramirez VD, Teitelbaum P (1979) Excessive bracing reactions and their control by atropine and L-DOPA in an animal analog of Parkinsonism. Exp Neurol 64:33-43.

Schallert T, Fleming SM, Leasure JL, Tillerson JL, Bland ST (2000) CNS plasticity and assessment of forelimb sensorimotor outcome in unilateral rat models of stroke, cortical ablation, parkinsonism and spinal cord injury. Neuropharmacology 39:777-787.

Schmidt OI, Heyde CE, Ertel W, Stahel PF (2005) Closed head injury--an inflammatory disease? Brain research Brain research reviews 48:388-399.

Shin LM, Liberzon I (2010) The neurocircuitry of fear, stress, and anxiety disorders. Neuropsychopharmacology : official publication of the American College of Neuropsychopharmacology 35:169-191.

Shin LM, Rauch SL, Pitman RK (2006) Amygdala, medial prefrontal cortex, and hippocampal function in PTSD. Annals of the New York Academy of Sciences 1071:67-79.

Shiozaki T, Hayakata T, Tasaki O, Hosotubo H, Fuijita K, Mouri T, Tajima G, Kajino K, Nakae H, Tanaka H, Shimazu T, Sugimoto H (2005) Cerebrospinal fluid concentrations of anti-inflammatory mediators in early-phase severe traumatic brain injury. Shock 23:406-410.

Simi A, Tsakiri N, Wang P, Rothwell NJ (2007) Interleukin-1 and inflammatory neurodegeneration. Biochem Soc Trans 35:1122-1126.

Simmons A, Strigo I, Matthews SC, Paulus MP, Stein MB (2006) Anticipation of aversive visual stimuli is associated with increased insula activation in anxiety-prone subjects. Biological psychiatry 60:402-409.

Sönmez U, Sönmez A, Erbil G, Tekmen I, Baykara B (2007) Neuroprotective effects of resveratrol against traumatic brain injury in immature rats. Neurosci Lett 420:133-137.

Spivak B, Shohat B, Mester R, Avraham S, Gil-Ad I, Bleich A, Valevski A, Weizman A (1997) Elevated levels of serum interleukin-1 beta in combat-related posttraumatic stress disorder. Biol Psychiatry 42:345-348.

Stein MB, Simmons AN, Feinstein JS, Paulus MP (2007) Increased amygdala and insula activation during emotion processing in anxiety-prone subjects. Am J Psychiatry 164:318-327.

Sternberg EM (1997) Neural-immune interactions in health and disease. J Clin Invest 100:2641-2647.

Sullivan RM (2004) Hemispheric asymmetry in stress processing in rat prefrontal cortex and the role of mesocortical dopamine. Stress 7:131-143.

Taupin V, Toulmond S, Serrano A, Benavides J, Zavala F (1993) Increase in IL-6, IL-1 and TNF levels in rat brain following traumatic lesion. Influence of pre- and post-traumatic treatment with Ro5 4864, a peripheral-type (p site) benzodiazepine ligand. J Neuroimmunol 42:177-185.

Thompson HJ, Lifshitz J, Marklund N, Grady MS, Graham DI, Hovda DA, McIntosh TK (2005) Lateral fluid percussion brain injury: a 15-year review and evaluation. Journal of neurotrauma 22:42-75.

Town T, Nikolic V, Tan J (2005) The microglial "activation" continuum: from innate to adaptive responses. J Neuroinflammation 2:24.

Tucker P, Ruwe WD, Masters B, Parker DE, Hossain A, Trautman RP, Wyatt DB (2004) Neuroimmune and cortisol changes in selective serotonin reuptake inhibitor and placebo treatment of chronic posttraumatic stress disorder. Biol Psychiatry 56:121-128.

Vaishnavi S, Rao V, Fann JR (2009) Neuropsychiatric problems after traumatic brain injury: unraveling the silent epidemic. Psychosomatics 50:198-205.

Vink R, O'Connor CA, Nimmo AJ, Heath DL (2003) Magnesium attenuates persistent functional deficits following diffuse traumatic brain injury in rats. Neurosci Lett 336:41-44.

von Känel R, Hepp U, Kraemer B, Traber R, Keel M, Mica L, Schnyder U (2007) Evidence for low-grade systemic proinflammatory activity in patients with posttraumatic stress disorder. Journal of psychiatric research 41:744-752.

Vyas A, Pillai AG, Chattarji S (2004) Recovery after chronic stress fails to reverse amygdaloid neuronal hypertrophy and enhanced anxiety-like behavior. Neuroscience 128:667-673.

Wagner AK, Postal BA, Darrah SD, Chen X, Khan AS (2007) Deficits in novelty exploration after controlled cortical impact. Journal of neurotrauma 24:1308-1320.

Wang F, Xu S, Shen X, Guo X, Peng Y, Yang J (2011) Spinal macrophage migration inhibitory factor is a major contributor to rodent neuropathic pain-like hypersensitivity. Anesthesiology 114:643-659.

Wheaton P, Mathias JL, Vink R (2011) Impact of pharmacological treatments on outcome in adult rodents after traumatic brain injury: a meta-analysis. J Psychopharmacol.

Willner P (1997) Validity, reliability and utility of the chronic mild stress model of depression: a 10-year review and evaluation. Psychopharmacology (Berl) 134:319-329.

Woodlee MT, Asseo-Garcia AM, Zhao X, Liu SJ, Jones TA, Schallert T (2005) Testing forelimb placing "across the midline" reveals distinct, lesion-dependent patterns of recovery in rats. Exp Neurol 191:310-317.

Yagi K, Tada Y, Kitazato KT, Tamura T, Satomi J, Nagahiro S (2010) Ibudilast inhibits cerebral aneurysms by down-regulating inflammation-related molecules in the vascular wall of rats. Neurosurgery 66:551-559.

Yan F, Li S, Liu J, Zhang W, Chen C, Liu M, Xu L, Shao J, Wu H, Wang Y, Liang K, Zhao C, Lei X (2002) Incidence of senile dementia and depression in elderly population in

Xicheng District, Beijing, an epidemiologic study. Zhonghua Yi Xue Za Zhi 82:1025-1028.

Yan HQ, Banos MA, Herregodts P, Hooghe R, Hooghe-Peters EL (1992) Expression of interleukin (IL)-1 beta, IL-6 and their respective receptors in the normal rat brain and after injury. Eur J Immunol 22:2963-2971.

Yanase H, Mitani A, Kataoka K (1996) Ibudilast reduces intracellular calcium elevation induced by in vitro ischaemia in gerbil hippocampal slices. Clin Exp Pharmacol Physiol 23:317-324.

Yoshioka M, Suda N, Mori K, Ueno K, Itoh Y, Togashi H, Matsumoto M (2002) Effects of ibudilast on hippocampal long-term potentiation and passive avoidance responses in rats with transient cerebral ischemia. Pharmacol Res 45:305-311.

Yu I, Inaji M, Maeda J, Okauchi T, Nariai T, Ohno K, Higuchi M, Suhara T (2010) Glial cell-mediated deterioration and repair of the nervous system after traumatic brain injury in a rat model as assessed by positron emission tomography. J Neurotrauma 27:1463-1475.

Zhang D, Hu X, Qian L, O'Callaghan JP, Hong JS (2010) Astrogliosis in CNS pathologies: is there a role for microglia? Mol Neurobiol 41:232-241.

Zhang D, Hu X, Qian L, Wilson B, Lee C, Flood P, Langenbach R, Hong JS (2009) Prostaglandin E2 released from activated microglia enhances astrocyte proliferation in vitro. Toxicol Appl Pharmacol 238:64-70.

## Figure Captions

**Figure 1.** Cylinder task and running wheel activity at 1 week post-injury. **(A)** LFPI rats mean number of spontaneous forelimb placements (ipsilateral and contralateral) during exploratory activity in the cylinder test did not differ from controls at 1 week post-injury. A reduction was seen in contralateral limb-use in injured rats, but this reduction did not reach significance (p=0.741). **(B)** LFPI rats mean change in distance traveled in the running wheel activity did not significantly differ from controls at 1 week post-injury. Data represent mean ± SEM.

**Figure 2.** Freezing behavior in a novel context. Both surgically naïve and sham operated rats froze approximately 5-10% at post-surgical measurement points before (2 weeks and 1 month) after (2 and 3 month) foot-shock (arrow). In contrast, LFPI rats froze significantly longer (~20%) than these controls before shock. After shock, untreated LFPI rats (LFPI-vehicle) nearly doubled in time freezing (~50%) whereas treated LFPI rats (LFPI+MN166) showed only a slight increase (~25%) that did not reach significance (p=0.316). The effect of injections alone (Sham+Mn166 and Sham+vehicle) were to increase freezing behavior compared to un-injected naïve and sham operated rats, particularly at the 2 and 3 month post-shock measurement points where freezing in these rats could not be distinguished from LFPI rats treated with MN166. Data represent mean ± SEM.

**Figure 3.** Representative images depicting GFAP immunoreactivity (reflecting astrocytic activation) assessed in the hippocampus, amygdala and insula at 3 months post-injury. LFPI rats injected with vehicle showed clear signs of reactive astrocytes (bottom row), while naïve and sham operated rats appeared to have normal astrocyte morphology. LFPI rats treated with

MN166 (third row) were difficult to differentiate from surgically naïve and sham operated groups.

**Figure 4.** Regional and sub-regional analyses of microglial and astroglial activation in hippocampus, amygdala and insula at 3 months post-injury. **(A-C)** LFPI vehicle injections induced a significant increase in GFAP labeling in all three regions, compared to surgically naïve, sham operated and LFPI+MN166 treated rats. **(D)** In the insula, OX-42 activation was greater in LFPI rats compared to surgically naïve, sham operated and LFPI+MN166 treated rats. There were no significant differences found between surgically naïve, sham operated and LFPI+MN166 treated rats in either analysis. Data represent mean± SEM integrated densities of immunoreactivity.

## Figure Captions

**Figure 1.** Cylinder task and running wheel activity at 1 week post-injury. **(A)** LFPI rats mean number of spontaneous forelimb placements (ipsilateral and contralateral) during exploratory activity in the cylinder test did not differ from controls at 1 week post-injury. A reduction was seen in contralateral limb-use in injured rats, but this reduction did not reach significance (p=0.741). **(B)** LFPI rats mean change in distance traveled in the running wheel activity did not significantly differ from controls at 1 week post-injury. Data represent mean ± SEM.

**Figure 2.** Freezing behavior in a novel context. Both surgically naïve and sham operated rats froze approximately 5-10% at post-surgical measurement points before (2 weeks and 1 month) after (2 and 3 month) foot-shock (arrow). In contrast, LFPI rats froze significantly longer (~20%) than these controls before shock. After shock, untreated LFPI rats (LFPI-vehicle) nearly doubled in time freezing (~50%) whereas treated LFPI rats (LFPI+MN166) showed only a slight increase (~25%) that did not reach significance (p=0.316). The effect of injections alone (Sham+Mn166 and Sham+vehicle) were to increase freezing behavior compared to un-injected naïve and sham operated rats, particularly at the 2 and 3 month post-shock measurement points where freezing in these rats could not be distinguished from LFPI rats treated with MN166. Data represent mean ± SEM.

**Figure 3.** Representative images depicting GFAP immunoreactivity (reflecting astrocytic activation) assessed in the hippocampus, amygdala and insula at 3 months post-injury. LFPI rats injected with vehicle showed clear signs of reactive astrocytes (bottom row), while naïve and sham operated rats appeared to have normal astrocyte morphology. LFPI rats treated with MN166 (third row) were difficult to differentiate from surgically naïve and sham operated groups.

**Figure 4.** Regional and sub-regional analyses of microglial and astroglial activation in hippocampus, amygdala and insula at 3 months post-injury. **(A-C)** LFPI vehicle injections induced a significant increase in GFAP

labeling in all three regions, compared to surgically naïve, sham operated and LFPI+MN166 treated rats. **(D)** In the insula, OX-42 activation was greater in LFPI rats compared to surgically naïve, sham operated and LFPI+MN166 treated rats. There were no significant differences found between surgically naïve, sham operated and LFPI+MN166 treated rats in either analysis. Data represent mean± SEM integrated densities of immunoreactivity.

Fig.1

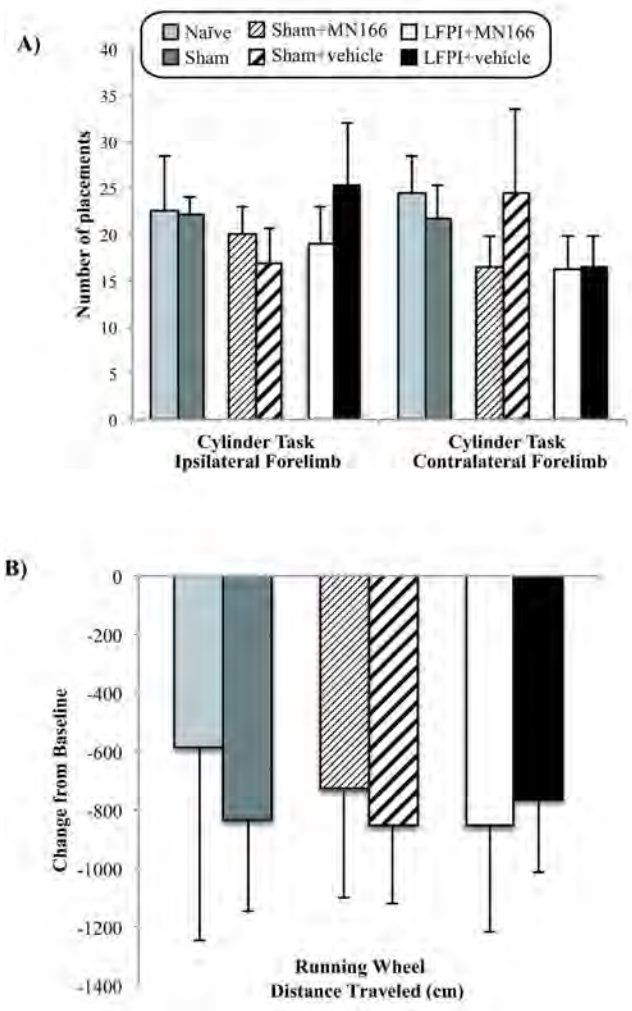


216x296mm (300 x 300 DPI)

Fig.2

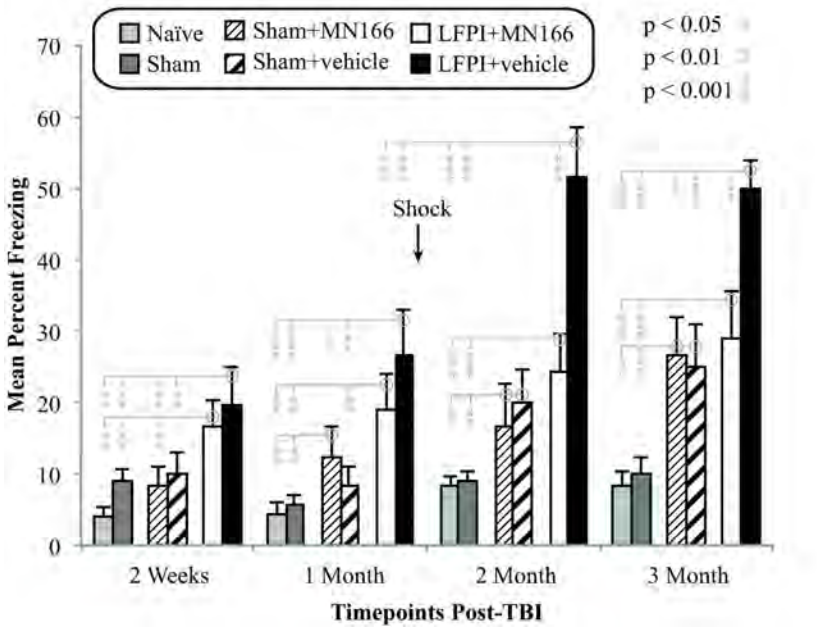


159x171mm (300 x 300 DPI)

Fig.3

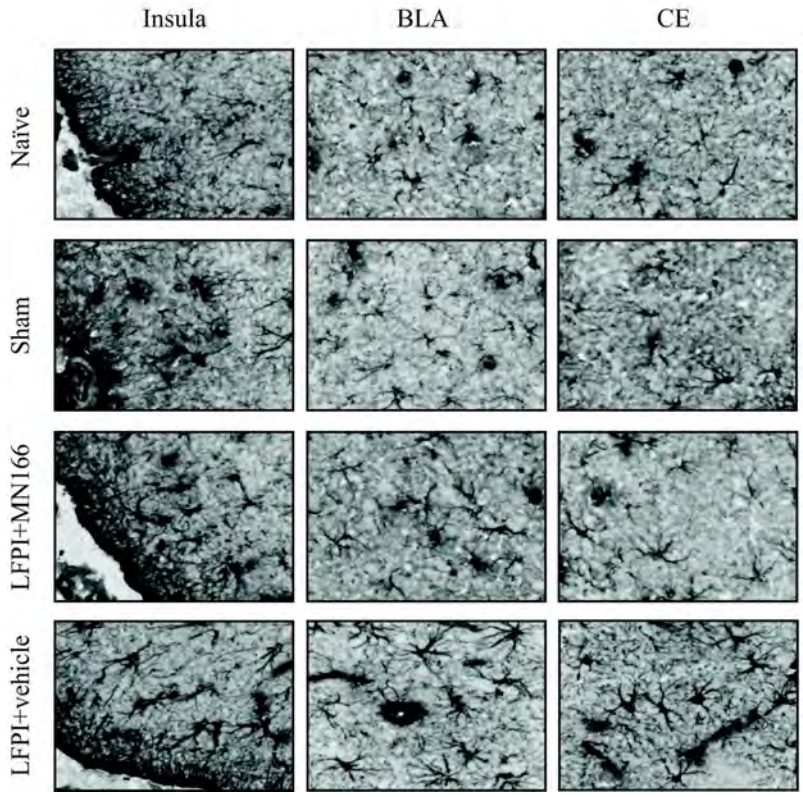


175x191mm (300 x 300 DPI)

Fig.4

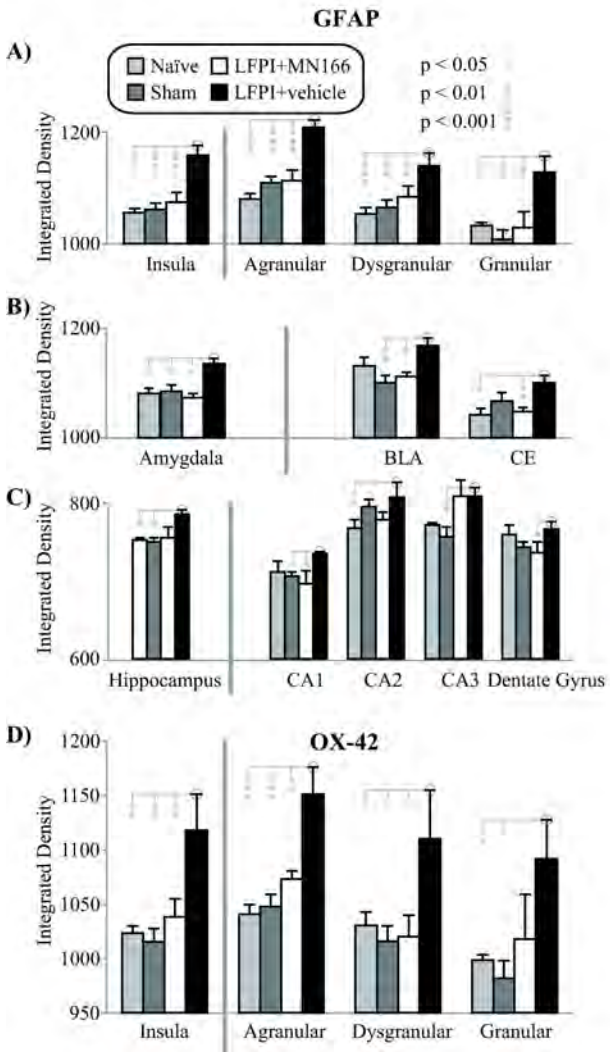


207x296mm (300 x 300 DPI)

Title of Study: **A Very High Speed System for Video/EEG Monitoring and Quantification of Post-traumatic Epileptogenesis**

**This abstract is being submitted for (check one):**

( X) Oral presentation or poster display
( ) Oral presentation only
( ) Poster display only

**This presentation represents:**

(X ) Quantitative research ( ) Qualitative research
( ) Research utilization ( ) Combined methods
( ) Clinical innovation

**Consideration for Young Investigators' Forum (check one):** ( ) YES (X ) NO

**Research Topic**: Traumatic brain injury / Healthcare informatics and medical systems

**If selected, the presenter will be**: Daniel Barth

**A Very High Speed System for Video/EEG Monitoring and Quantification of Post-traumatic Epileptogenesis**

**Daniel S. Barth, Ph.D.**

**PURPOSE/AIMS:** The overall goal of this project is to examine the role of brain inflammation in the development of post-traumatic epilepsy (PTE), and to prevent PTE with newly developed drugs that modulate the brain's immune system following injury. We use a lateral fluid percussion injury (LFPI) in the rat, a widely accepted animal model of closed head traumatic brain injury (TBI) experienced by war fighters in the battlefield. Since our major goal is to prevent the development of PTE (epileptogenesis), our first challenge was to devise methods by which we could unambiguously identify electrical (EEG) and behavioral (video) biomarkers of the epileptic brain prior to appearance of the first seizure. This is a daunting task given the vast quantities of long-term video/EEG that must be recorded and analyzed from a large number of animals.

**DESIGN:** To this end, during the first project year, we developed a unique system for recording, visually reviewing, and quantifying video/EEG from up to 32 animals in parallel.

**POPULATION/SAMPLE STUDIED:** Sprague Dawley rats with and without LFPI to the parietal and motor cortex are presently under investigation.

**METHOD(S):** We designed and constructed a unique recording system, based on compact amplifiers and miniature surveillance cameras, that is inexpensive, durable, and performs at a low bandwidth, permitting storage and review of large amounts of data recorded continuously for weeks.

**DATA ANALYSIS:** The most innovative component of the system is our specially designed software that permits very fast and interactive visual examination and event identification of hours of video/EEG data in minutes. The driving principle behind this software is that the human visual system is far more skilled and reliable than automated systems for identifying epileptiform events in the EEG and validating these events with video-recorded behavior. The core of our software is a graphical user interface that makes this possible for minimally trained users.

**FINDINGS:** Our system is now allowing us to precisely identify potential EEG biomarkers during epileptogenesis, when intervention may be possible. The system is also allowing us to statistically quantify both abnormal and normal EEG activity from long-term recording in animal models of TBI.

**CONCLUSIONS/RECOMMENDATIONS:** It is now possible to record and visually analyze long-term video/EEG data following brain trauma at a minimum cost and with sufficient speed and accuracy to make statistical analysis of normal and pathological EEG biomarkers possible for the first time.

**IMPLICATIONS:** We have begun analyzing epileptogenesis in LFPI and in a pilocarpine model. We have identified archetypical patterns in the normal EEG that could be easily mistaken for epileptiform. This knowledge will serve as critical foundation for studying the effects of neuro-immune modulating compounds following trauma in preventing epileptogenesis during the second project year. We also anticipate an unplanned application to military medicine to detect potential post-traumatic neurological disturbance and facilitate return to duty decisions.

**FROM/TO TIME PERIOD OF STUDY: 07/01/11 to 06/30/12**

**FUNDING: CDMRP #PR100040**

**For presentation at SFN 2013**

Hippocampal auditory evoked potentials in conjunction with continuous long-term video-EEG monitoring reveals novel biomarkers for epileptogenesis in the lithium-pilocarpine model of epilepsy in rats.

Acquired temporal lobe epilepsy in humans and in animal models has typically been characterized by an initiating traumatic event (brain trauma, status epilepticus, etc.) followed by a latent or "silent" period lasting weeks to many months during which epileptogenesis is presumed to occur; a period terminated by the appearance of spontaneous recurrent seizures (SRS) and the establishment of chronic epilepsy. Yet, there has been recent evidence suggesting that, while the latent period is behaviorally silent, there may be electrographic changes both spontaneous and evoked that reflect neural circuit and cellular alterations underlying epileptogenesis, and that epileptogenesis may continue well past presentation of initial SRS.

The objective of the present study was to compare biomarkers of epileptogenesis in the lithium-pilocarpine (status epilepticus; SE) rat model using regular (2 epochs/hr) hippocampal auditory evoked potentials (HAEP) to probe excitability changes, continuous spectral analysis of hippocampal and cortical EEG, automated epileptiform spike density (ESD) analysis, and continuous movement analysis based on video optical flow. Of these measures, HEAP were by far the most sensitive and reliable biomarker, showing marked and stereotyped alterations in morphology and amplitude during the latent period. Interestingly, HEAP morphology continued to change weeks or even months after the animals began having SRS, suggesting that epileptogenesis continued well after the latent period. In addition there was a circadian rhythm to the amplitude of HEAP, as well as EEG delta/theta power, and movement, with a higher probability for seizures during the late dark phase accompanying HEAP suppression. These results indicate that chronic HEAP recording may be a useful tool for actively probing the hippocampal system in order to reveal changes in its underlying physiology accompanying epileptogenesis during the latent and post-latent periods.

Idea Development proposal to the CDMRP Autism Research Program

**Research Idea:** This proposal directly addresses two FY13 ARP Areas of Interest. We will examine conditions co-occurring with ASD (examining neuroinflammation in our newly developed animal model of comorbid ASD and epilepsy, **AIM 1**) and validate new or existing therapeutic targets (using anti-inflammatory micro-glia suppressant compounds, that are safe for eventual translation to human use, to prevent limbic hyper-excitability associated with ASD/epilepsy, **AIM 2**).

**How the research addresses a central problem in ASD:** The close association between ASD and epilepsy has been recognized for decades [1,2]. Early investigations of electroencephalographic (EEG) abnormalities in autistic children spearheaded the concept of ASD as a neurological as opposed to purely psychiatric disorder [2,3], and subsequently established the epileptiform characteristics of these abnormalities, revealing a remarkably comorbid syndrome. The link between ASD and epilepsy may hold important clues to the etiology of both disorders, and suggests that in some cases they may share a common neurological basis. While genetics no doubt play a substantial predisposing role [4,5], there are converging lines of evidence that the maternal environment during pregnancy may also be of paramount importance; prenatal exposure to specific environmental factors markedly increases risk, and may establish a dynamic neuropathy resulting in autistic behavior and seizures. Little can be done to alter genetic predisposition, however, a better understanding of prenatal environmental factors could lead to improved strategies for decreasing risk and for intervention.

**Ideas and reasoning on which the proposed project is based:** The neurobiological basis for ASD remains largely unknown, but recent research strongly supports contributions of genetic, environmental, neurological, *and immunological* factors [6-10]. Immune dysfunction is a remarkably consistent finding in ASD, proposed as a critical mechanism for ASD pathogenesis [11]. Yet, most studies note abnormal elevations of blood-born immune activation markers. Only recently have neuroinflammatory processes also been described in the cerebral cortex and white matter in ASD [9]. Neuroinflammation in ASD is characterized by marked "reactive gliosis", where astrocytes, and particularly microglia cells, release proinflammatory cytokines as part of the innate immune response to stress, toxins, infection, and apoptosis. This finding is pivotal because these cytokines are known to be massively excitatory to neurons, potentially triggering excitotoxic cascades in the developing brain that could result in abnormal development and in *chronic hyperexcitability* [12]. Remarkably, 30% of children with ASD develop chronic epilepsy and 50-90% show sub-clinical epileptiform spikes by adolescence [13-16]. Similarly, approximately 30% of children with epilepsy are also diagnosed with ASD [17]. The role of glial cytokines in *epilepsy* is under intense investigation [18].

**Preliminary Data:** Our laboratory has recently completed two studies through a seed grant funded by Autism Speaks Foundation and one study concerning post-traumatic epilepsy funded by DoD, providing data leading to this idea development proposal. First, we discovered that bacterial activation of microglia (induced by lipopolysaccharide; LPS) produces seizures [19] and microglia suppressant drugs inhibit development of epilepsy in a lithium/pilocarpine model. Thus, neuroinflammation can induce seizures and immuno-modulation has anti-epileptogenic properties. Second, we replicated findings of Zerrate and colleagues [20] using the known ASD teratogen, terbutaline (used to arrest pre-term labor and associated with increased concordance for autism in dizygotic twins), to produce ASD-like behavior in rats and discovered microglia suppressant drugs prevent development of these behaviors, again suggesting the role of neuroinflammation in ASD and immuno-modulation as a potential therapeutic target. Finally, we have recently succeeded in developing an animal model of ASD *and* epilepsy. We discovered that maternal stress combined with terbutaline results in ASD like behavior more severe than either treatment alone, and only the combination results in development of chronic epilepsy. This animal model of ASD/epilepsy will serve as an ideal platform for testing the following hypotheses.

**Hypotheses:** Given, A) the close association between ASD and immune dysfunction, B) recent evidence for elevated innate immune responses and proinflammatory cytokine levels in the ASD cortex, C) epidemiological linkage between ASD, brain hyperexcitability, and epilepsy, D) strong evidence linking microglia activation with increased brain excitability and seizures and E) our recent discovery that combining two known neuroinflammatory teratogens results in ASD-like behaviors and development of chronic spontaneous recurrent seizures (the hallmark of epilepsy), we hypothesize that a core mechanism underlying both pre- and postnatal neuro-developmental disorders in ASD is chronic neuroimmune induced hyperexcitability. If true this would predict that small molecule microglia suppressant drugs, capable of crossing into the brain, would suppress release of inflammatory cytokines and attenuate pre- and postnatal hyperexcitability and neurodegeneration in our maternal stress + terbutaline model of ASD/epilepsy.

**Specific Aims:**

**Aim 1**) Develop the maternal stress + terbutaline model of ASD/Epilepsy and establish baseline biomarkers for neuroinflammation, ASD–like behavior, and epileptogenesis.

**Aim 2)** Examine the effectiveness of acute glial suppression on behavioral, functional, and histological end-points established in Aim 1, with the objective of demonstrating effectiveness in preventing or attenuating ASD/epilepsy development.

**Research Plan:**

**Aim 1)** Four groups of 5 pregnant rats will be obtained at embryonic day two (E2). Dams will be randomly assigned to two stressed and two non-stressed groups. Prenatal stress will be administered daily from (E4) until delivery. On (E4), (E11) and (E18) dams will be placed in a fear conditioning chamber and shocked (0.5 mA, 2 sec duration, delivered at 60 and 120 sec) and re-exposed daily to the fear-conditioning chamber for 5 min. Non-stressed dams will be left undisturbed in their home cages. At birth, male pups from each group will be randomized and redistributed, allowing each dam to foster no more than one pup from their own litter. Pups from entire litters will be divided into 4 experimental groups, 1 maternally stressed and 1 unstressed group receiving subcutaneous injections of terbutaline hemisulfate (10 mg/kg) and the other stressed and unstressed groups receiving equivalent volumes of saline (1 ml/kg) on postnatal day (PN) 2 through 5. Pups will be maintained until adolescence (2 mo), receive behavioral tests (ultrasonic vocalizations, freezing in a novel environment, open field social interaction, acoustic pre-pulse inhibition, exploratory behavior, locomotor and repetitive/stereotypic activity). Pups will then be implanted with one SS screw electrode over primary auditory cortex and one bipolar electrode in dorsal hippocampus and attached to a head mount for chronic tethered video/EEG recording. Along with EEG, averaged auditory evoked potentials (AEP) will be recorded every 30 minutes. Continuous recordings will be performed for 3 months. Animals will then be sacrificed and immuno-reactivity assessed with markers of microglia (OX-42) and astrocytes (GFAP). Video/EEG recordings will be analyzed for seizures and epileptiform spiking using custom software written by the P.I. and already in use in our laboratory. AEP amplitude and morphology changes will also be tracked to probe for changes in brain excitability (similar to systematic AEP waveform changes we have noted for our pilocarpine epilepsy model during the development of chronic epilepsy). Between group comparisons of long-term differences in activity level (our preliminary studies showed marked hyperactivity in autistic rats) will also be performed using optical flow analysis of the video records. Aim 1 will provide foundational baseline biomarkers of ASD/epilepsy for comparison to treatment groups in Aim 2. We expect it will require 1 year to complete Aim 1.

**Aim 2)** Procedures for Aim 2 will be the same as Aim 1, except that 4 additional groups will be included, receiving daily s.c. injections of MN166 (Ibudilast) or vehicle alone for a 5 day period following the last terbutaline/saline injection. MN166 is a well-documented cyclic AMP phosphodiesterase inhibitor that crosses the blood brain barrier and effectively suppresses microglia activated cytokine release by antagonizing TLR4 receptors [21]. We have used this acute dosing regime in our preliminary studies to effectively to block development of ASD-like behavior in the terbutaline (alone) model and also to interrupt epileptogenesis in the lithium/pilocarpine model. We expect MN166 to effectively block or at least attenuate development of ASD-like behavior and epilepsy in Aim 2. We expect it will require 2 years to complete Aim 2.

**Impact:** The ideas developed here should have a major scientific impact on the CNS mechanisms of ASD by linking, for the first time, innate neuro-immune inflammation to potentially epileptiform hyperexcitability and degenerative neuro-development. It has been established in recent epilepsy research that innate immune responses lower thresholds for seizures and that epileptiform hyperexcitability induces innate immune responses and inflammatory cytokine release, establishing a potentially destructive positive feedback loop for chronic epileptogenesis. We expect the results of the ASD/epilepsy model developed here to provide an essential bridge between positive results in epileptology to our understanding of ASD pathophysiology. While the proposed work has some risk, our expectations are backed by promising preliminary data in both the autism and epilepsy fields. Success here could have a very rapid impact on outcomes of individuals with ASD. While there are several immuno-suppressant anti-inflammatory drugs we could have chosen to evaluate, we chose MN166 because it can be orally administered, crosses the blood-brain barrier, and has no known detrimental side effects in humans (it has been used in Asia for years to treat bronchial asthma). MN166 is also currently under FDA clinical trials for treatment of chronic pain in humans [21,22]. Finally, we chose MN166 because we have preliminary indications of a powerful preventive effect in the development of post-traumatic epilepsy in the rat. If successful, we expect this work to be rapidly translatable to use as a potential drug for prenatal prevention of ASD and/or for postnatal prevention of associated epilepsy, potential behavioral interference due to hyperexcitability, and continued developmental regression from excitotoxicity in the immunoreactive ASD brain.

**Innovation:** To our knowledge, this is the first and only ASD - epilepsy - neuroinflammation animal model to be developed. We are combining ASD/epilepsy, ASD/innate immunity, and epilepsy/innate immunity, all very active but, until now, separate areas of research. Based on our preliminary work in post-traumatic epilepsy prevention, we are specifically targeting microglial suppression as a unique path for ASD prevention and/or treatment, which, if successful, will present a completely novel and we think extremely productive paradigm for ASD research. We also add novel biomarkers (AEP and Optical Flow Movement analysis) to other behavioral and electrophysiological measures to monitor the progress of brain excitability and treatment effects. Finally, this work represents a unique combination of electrophysiological, behavioral, histological, (Barth) and immunological (Watkins) methodologies for examining mechanisms and prevention in a novel animal model of ASD/epilepsy.

**Statement of Work (SOW)**

**Task (specific aim) 1.** Test the efficacy of proximal (within 24 hr. of injury) MN166 treatment on development of post-traumatic anxiety: **(timeframe, months 1-22)**

**1a.** Animal use approval for all experiments. University of Colorado Institutional Animal Care and Use Committee. **(timeframe, months 1-2)**

**1b.** Perform preliminary studies of lateral fluid percussion injury (LFPI) impact pressures required to reliably produce mild and severe TBI and associated post-traumatic anxiety. **(timeframe, months 3-7)**

**Assay->** Behavioral measures of post-traumatic anxiety (freezing in novel environment, open field and elevated plus exploration) will have been quantified for mild and severe TBI and statistically compared to our existing LFPI model of moderate TBI.

**1c.** Perform motor and behavioral testing of 8 groups (10 rats each: Sham-operated/vehicle-injected, Sham-operated*/MN166-injected*, mildTBI*/vehicle-injected*, mildTBI/MN166-injected, moderateTBI*/vehicle-injected, moderateTBI/MN166-injected, severeTBI*/vehicle-injected, severeTBI/MN166-injected) receiving MN166 treatment at 24 hr. post-injury. **(timeframe, months 8-13)**

**Assay->** Motor testing will have been performed prior to and following Sham-Operated or TBI, along with behavioral testing before foot-shock and after foot-shock at 2 weeks, 1, 2, 3 and 6 month intervals.

**1d.** Prepare and submit progress report #1 to DoD. **(timeframe, month 12)**

**1e.** Perform immunohistochemistry of all experimental groups. **(timeframe, months 14-18)**

**Assay->** Densitometry will have been performed on GFAP and OX-42 stained sections of all rats.

**1f.** Statistically analyze and prepare graphical representations of results. **(timeframe, months 19-20)**

**Assay->** Analyzed data from sub-aims 1c and 1e shall have been converted to figures for publication.

**1g.** Submit and revise manuscript for publication. **(timeframe, months 21-22)**

**Assay->** A manuscript describing results for task 1 shall be finished and submitted for publication in a peer refereed scientific journal.

**Milestone #1:** Demonstration that early treatment with MN166 prevents or attenuates post-traumatic anxiety in mild, moderate, and perhaps severe TBI.

**Task (specific aim) 2.** Test the efficacy of delayed (1 mo. post-injury) MN166 treatment on existing post-traumatic anxiety: **(timeframe, months 23-36)**

**2a.** Perform motor and behavioral testing of 8 groups (10 rats each: Sham-operated/vehicle-injected, Sham-operated*/MN166-injected*, mildTBI*/vehicle-injected*, mildTBI/MN166-injected, moderateTBI*/vehicle-injected, moderateTBI/MN166-injected, severeTBI*/vehicle-injected, severeTBI/MN166-injected) receiving MN166 treatment at 1 mo. post-injury. **(timeframe, months 23-28)**

**Assay->** Motor testing will have been performed prior to and following Sham-Operated or TBI, along with behavioral testing before foot-shock and after foot-shock at 1-month through 6-month intervals.

**2b.** Prepare and submit progress report #2 to DoD. **(timeframe, month 24)**

**2c.** Perform immunohistochemistry of all experimental groups. **(timeframe, months 29-32)**

**Assay->** Densitometry will have been performed on GFAP and OX-42 stained sections of all rats.

**2d.** Statistically analyze and prepare graphical representations of results. **(timeframe, months 33-34)**

**Assay->** Analyzed data from sub-aims 1c and 1d shall have been converted to figures for publication.

**2e.** Submit and revise manuscript for publication. **(timeframe, months 35-36)**

**Assay->** A manuscript describing results for task 1 shall be finished and submitted for publication in a peer refereed scientific journal.

**2f.** Prepare and submit final progress report to DoD. **(timeframe, month 36)**

**Milestone #2:** Demonstration that delayed treatment with MN166 reverses or attenuates established post-traumatic anxiety in mild, moderate, and perhaps severe TBI.

## 1) BACKGROUND

**Post-traumatic anxiety is a leading and devastating consequence of human traumatic brain injury (TBI).** Traumatic brain injury (TBI) has been described as the signature injury of the wars in the Middle East, where improvised explosive devices, suicide bomb blasts, and other combat related head trauma have seen a marked increase. This precipitous rise is highly correlated with a substantial increase of war fighters suffering from chronic post-traumatic stress disorder (PTSD), of which post-traumatic anxiety is the dominant symptom. In the general public, TBI is also a rising health concern, with approximately 1.7 million people in the United States alone sustaining a TBI each year and more than 5.3 million living with TBI-related disabilities. In addition to physical, cognitive and behavioral impairments, the long-term consequences of TBI include increased risk of neuropsychiatric disorders, of which anxiety disorders are by far the most prevalent, with rates ranging from 10-70% across studies (1, 2).

**There is a lack of effective treatment for post-traumatic anxiety**. Clinical trials to date have failed to reveal an effective treatment for post-traumatic anxiety. This is due in part to the considerable overlap in symptoms and high rates of co-occurrence between TBI and anxiety disorders (3-7). Co-morbid TBI/Anxiety has only been recently acknowledged as a clinical syndrome and there is a lack of research-based evidence addressing pharmacological approaches to treatment, as studies focusing on affective disorders typically exclude patients with a history of TBI and vice versa (6). The 3 primary pharmacological agents used to treat anxiety (anti-depressants, anticonvulsants, and anxiolytics) all lack evidence for treating co-morbid TBI/Anxiety (6, 8).

**The neurophysiology of post-traumatic anxiety is poorly understood.** Failure to develop adequate treatment for post-traumatic anxiety is also due to poor understanding of its neurophysiological basis. Studies of the etiology of anxiety disorders implicate exaggerated responses of the amygdala and insula (9-13), impaired inhibition of medial prefrontal cortex and anterior cingulate (12, 14-16) and decreased hippocampal volume (15, 17, 18). Several studies have shown greater activation of bilateral amygdala and insula in patients with a variety of anxiety disorders, including obsessive/compulsive disorder, phobia and post-traumatic stress disorder (PTSD) (9-13). Specifically related to PTSD, magnetic resonance imaging (MRI) studies have reported structural, neurochemical and functional abnormalities of medial prefrontal cortex in patients with PTSD, including anterior cingulate cortex (12, 15). Functional neuroimaging has also shown diminished responses in medial prefrontal cortex, which is thought to play a role in an array of anxiety disorders. Neuroimaging studies of the hippocampus have found decreased volumes in patients with PTSD, which is thought to be a risk factor for the development of pathological stress responses (15, 17, 18). Yet, in spite of substantial human neuroimaging reports, the *cellular mechanisms* potentially leading to TBI-induced neurochemical, anatomical, and functional abnormality in these structures are poorly understood.

**Neuroimmune inflammation may play a key role in post-traumatic anxiety** and as been largely ignored in developing treatments. Extensive literature indicates that inflammation produced by neuroimmune responses to TBI could be fundamental to the neurophysiology of post-traumatic anxiety (19-24). It is well established that post-traumatic inflammatory mediators activate microglia and astrocytes during the innate immune response to injury, leading to the expression of high levels of proinflammatory cytokines, most notably interleukin 1 beta, “IL-1β”, interleukin 6, “IL-6”, and tumor necrosis factor-α, “TNF-α” (22, 25-28). Given that these cytokines participate in autonomic, neuroendocrine and behavioral responses to brain injury, destabilize neurotransmitter release and re-uptake, negatively impact neuronal integrity and survival, and initiate neurotoxic processes, they may contribute to functional alterations of brain areas involved in post-traumatic anxiety (29-31).

Glial activation is normally neuroprotective (26, 32); however, the *chronic* inflammatory responses and exaggerated proinflammatory cytokine levels observed following injury initiate neurotoxic processes resulting in secondary tissue damage (20, 33-35), neuronal death (29, 36-38), secondary injury cascades (39-43) and neuronal hyperexcitability (28, 34, 38, 44). There is substantial support for chronic inflammation following TBI.

Both human and animal studies have shown that neuroinflammation is an ongoing process that persists for months to years following the injury (45-48). The ongoing inflammatory response to tissue injury may contribute to damage and dysfunction in brain regions associated with anxiety, as TBI has been found to induce both acute and chronic neurodegeneration that could be caused by delayed cellular death pathways initiated by complex signaling cascades in activated glial cells (49, 50). Several new lines of evidence support this hypothesis: (a) innate immune responses triggered by TBI (20, 34, 35), (b) resultant prolonged post-traumatic release of proinflammatory cytokines by activated glial cells (29, 33, 51, 52), (c) chronic peripheral elevations of proinflammatory cytokines in patients with PTSD and panic disorder (19, 21, 23, 24), (d) increased levels of activated microglia and astrocytes, IL-1β, TNF-α and IL-6 following controlled cortical impact and weight drop injury in rats (53-56), (e) increased anxiety-like behavior (57-60), and (f) elevated plasma corticosterone concentrations (61) when these cytokines are administered centrally or systemically in rats. Overall, these findings provide evidence for a potential role of the neuroimmune system in the pathophysiology of post-traumatic anxiety. Our over-riding hypothesis is that suppression of injury-induced glial cell activation may have eventual promise for attenuation of the development of post-traumatic anxiety *or treatment of existing post-traumatic anxiety* in humans, a hypothesis supported by our preliminary data indicating a powerful prophylactic effect of glial suppressant drugs on development of post-traumatic anxiety and the ability to reverse post-traumatic anxiety in an animal model we have developed.

**Animal models of post-traumatic anxiety have only very recently been developed to study mechanisms and interventions.** In light of the high prevalence and clinical impact of post-traumatic anxiety in human TBI and our poor understanding of its mechanisms and treatment, it is surprising that psychiatric sequelae of brain trauma have been largely overlooked in animal research, which has focused instead on sensory/motor and cognitive deficit models (62). However, there have been recent seminal reports by Vink and colleagues (63-65) of post-traumatic anxiety-like behavior in rats using an impact-acceleration model of diffuse TBI and noting significant decreases in open field exploration due to freezing (a natural defensive fear response of rats). Several other groups have since reported similar post-traumatic anxiety in rodents using a variety of TBI methods, post-injury measurement time-points, and behavioral measures (66-70). Freezing behavior was not measured directly in these studies, although freezing was consistently reported to cause decreased exploratory behavior in the open field test (63-65), suggesting a dominant fear response that is associated with pathological anxiety. In none of studies could freezing be attributed to injury induced motor deficits since there are only transient (~ 1 week) motor deficits following fluid percussion (69, 73-76) as well as controlled cortical impact (67, 70, 77-83) injuries in the rat. Particularly relevant to the present proposal concerned with animal models of post-traumatic anxiety resulting from battlefield brain trauma, is the recent work by Ahler's group at the Operational and Undersea Medicine Directorate Naval Medical Research Center (71). Independent of our recently published results of post-traumatic anxiety induced by lateral fluid percussion injury (LFPI) in rats (72), they discovered that blast exposure in rats results in increased anxiety and enhanced contextual fear conditioning, both of which are PTSD-related behavioral traits. These findings are exciting because, similar to our work, brain trauma was induced during anesthesia, indicating a purely physiological component to resulting post-traumatic anxiety (as opposed to confounds introduced by additional psychological trauma during injury). Furthermore, the physiological basis of the post-traumatic anxiety in this study appeared to predominantly involve the amygdala (we have found involvement of amygdala, insula and hippocampus in our work). Thus, two distinct animal models of post-traumatic anxiety, blast injury and LFPI, have independently been shown to result in very similar behavioral and physiological symptoms, greatly increasing our confidence in the validity, reproducibility and generalizability of the animal work in this field.

**Preliminary Work**

As mentioned above, we have recently developed a rodent model of post-traumatic anxiety (84) that directly measures freezing in a novel environment as the *most* reliable index of abnormal/pathological anxiety induced by LFPI. Other measures of anxiety, such as open field and elevated plus maze exploration, showed results that trended in the same direction but did not reach significance with the number of rats examined in these studies. With this model of LFPI induced freezing behavior, we have collected compelling preliminary

data indicating a major role of glial activation in insula, amygdala and hippocampus in the development of post-traumatic anxiety.

In this preliminary work we attenuated the proinflammatory response of glial cells to LFPI using a well documented, cyclic AMP phosphodiesterase inhibitor, MN166 ("Ibudilast"; 3-isobutyryl-2-isopropylpyrazolo-[1,5-a]pyridine). MN166 has a documented suppression of pro-inflammatory responses by microglia *in vitro* and *in vivo*, tolerability, and long duration of action (64). Systemic or central administration attenuates nerve injury-induced astrocytic and microglial activation and also suppresses expression of the cytokines IL-1β, IL-6 and TNFα *in vivo*. MN166 partitions roughly 1:1 plasma:brain in rats (65) with a half-life nearly the same in both plasma and CNS tissues ~1hr after a single injection and ~8hr following a multi-day regimen wherein the drug has reached steady state in both compartments (65, 66). It attenuates the activation of brain microglia following *in vivo* administration in the rat (64, 67). At concentrations of 10 mg/kg, onset of glial attenuation with MN166 in rats is within 24 hr. and durable for >24 hr. (64, 65, 68-70). Interestingly it has recently been shown that MN166 administration can increase the anti-inflammatory cytokine IL-10 expression close to 40 fold in vivo (71). It is therefore likely that much of the glial inhibitory actions of MN166 are a result of the MN166 mediated increase in IL-10 release. The only known effects of MN166 on neurons are indirect via glial actions (72). Based on clear evidence from animal studies indicating a role of glial cells in pathological pain states, MN166 is currently under the FDA approved Phase 2 clinical trials in the treatment of neuropathic pain. It was chosen for use in our preliminary studies (and in the present proposal) because it is an orally available, blood-brain barrier permeable, glial activation inhibitor (based on microglial and astrocyte activation marker suppression). MN166 also has a long history of safety in humans and has been used widely for over 15 years in Japan to treat post-stroke dizziness and asthma (72). Finally, recent controlled studies indicate that it is well tolerated in healthy adults (73). Thus, potential future translation of this compound for eventual use in human post-traumatic anxiety is not as distant as other unexplored compounds.

A major outcome of our preliminary work is that we discovered peri-injury application of MN166 has the powerful effect of attenuating post-traumatic glial activation (in amygdala and insular cortex, brain regions closely associated with anxiety in humans and animals) and preventing development of post-traumatic anxiety-like behavioral symptoms. Additionally, our data indicate that ongoing post-traumatic anxiety-like behavior may be due to a chronic inflammatory response that can be effectively reversed by a brief (5-day) treatment of MN166 *once anxiety-like symptoms have fully developed at 1 month post-injury*. Our key results are summarized below.

**Fig. 1**

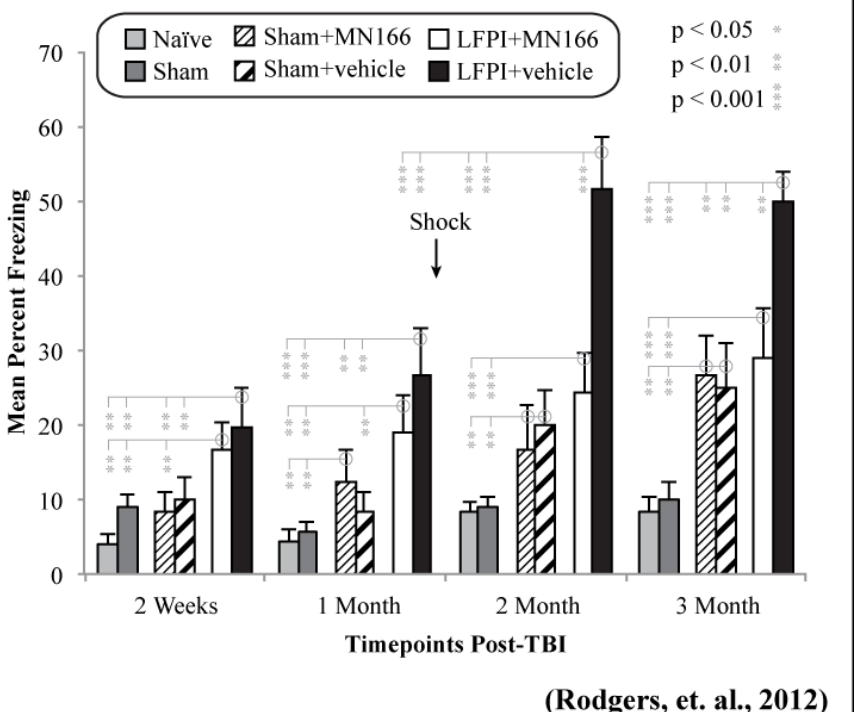


**(Rodgers, et. al., 2012)**

**Preliminary Study 1: Evidence for prevention of post-traumatic anxiety with peri-injury glial attenuation**

***Glial attenuation reduces freezing behavior in the novel context***. Our initial study focused on the effectiveness of attenuating injury-induced neuroinflammation on preventing the development of post-traumatic anxiety, using daily MN166 injections beginning 1 day before LFPI, the day of LFPI, and continuing for 3 days following injury. The justification for beginning injections before injury was based on the approximately 24 hr. required for MN166 to maximally attenuate glial activation. Despite normal motor, vestibular and locomotive function, LFPI produced large increases in freezing behavior

when rats were placed in a novel context (**Fig. 1**). Exposed only to this minor stressor (i.e. at 2 week and 1 month post-injury measurements conducted prior to shock), LPFI rats injected with either MN166 or vehicle (**Fig. 1**; white and black bars, respectively) froze approximately twice as long as naïve or sham operated rats (**Fig. 1**; light and dark grey bars, respectively). At 2- and 3-month measurement times, following the additional major stressor of shock (**Fig. 1**; arrows), freezing in the novel context (testing was not performed in the shock chamber to avoid confounds of conditioned fear) in both naïve and sham operated rats remained constant at approximately 10%. Freezing in LFPI rats treated with MN166 remained consistently higher than these controls, but, while appearing higher compared to earlier post-injury measurements in the same animals, this increased freezing compared to naïve and sham operated rats before (1 month) and following (2 month) shock did not reach significance. By contrast, LFPI+vehicle rats nearly doubled their freezing time to approximately 50% (**Fig. 1**; black bars) compared to pre-shock values, freezing approximately twice as long as LFPI+MN166 rats and 5 times as long as naïve and sham operated controls at the 2- and 3-month post-injury measurement times. The behavioral effects of injections alone, independent of LFPI, are reflected in sham surgery groups with injections of either MN166 or vehicle (**Fig. 1**; narrow and broad diagonal lines, respectively). Sham operated rats tended to freeze more than un-injected naïve and sham operated controls, reaching significance for both groups at the 2- and 3-month measurement points and suggesting that injections alone are aversive and can contribute to subsequent freezing. However, even at pre-shock measurement points, LFPI animals that received the same injections of MN166 or vehicle froze significantly more than injected controls, indicating substantial enhancement of freezing produced by LFPI. This effect became more apparent following shock, where LFPI+vehicle rats froze twice as long as the injected controls. By contrast, LFPI+MN166 rats were not distinguishable from either injected control group following shock, suggesting that their elevated freezing compared to naïve and sham operated animals was the result of injections alone and that MN166 eliminated the exaggerated freezing response to shock characterizing LFPI+vehicle rats.

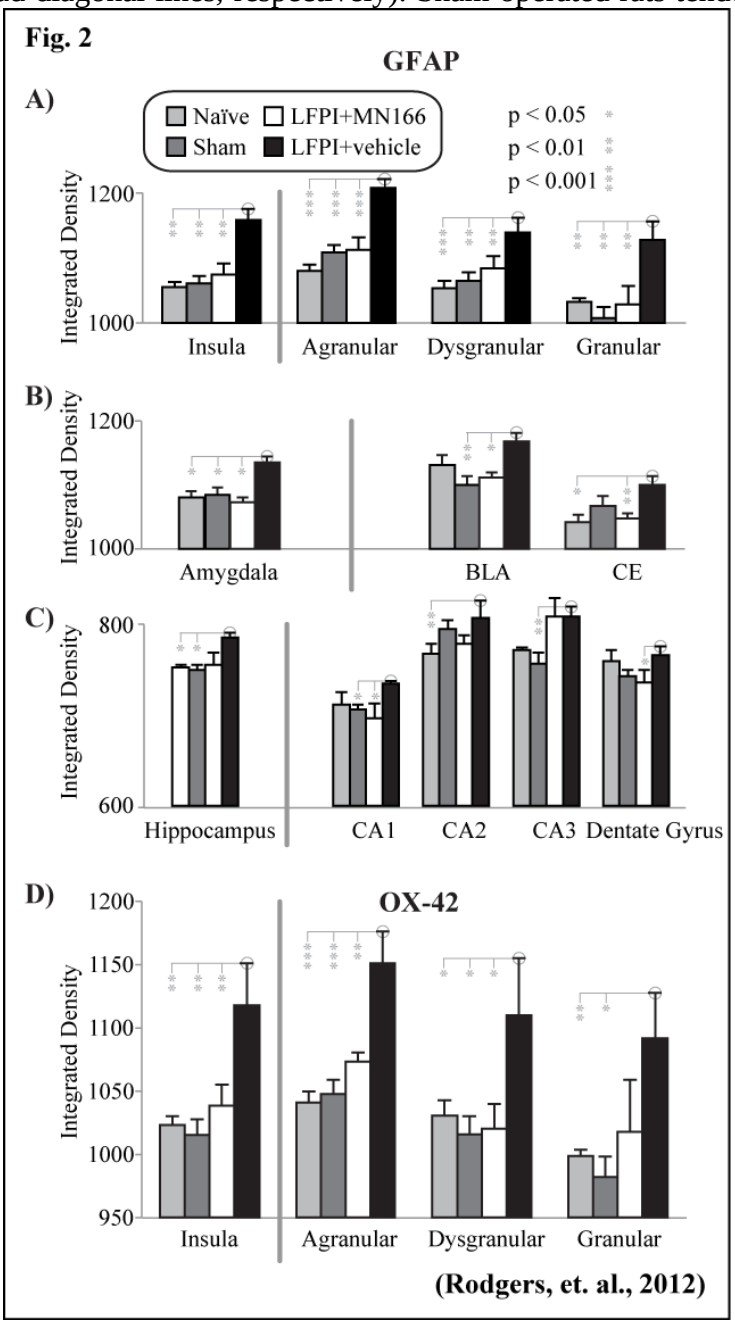


***Reactive gliosis in hippocampus, amygdala and insula at 3 months post-injury.*** Consistent with our behavioral results suggesting a role for LFPI induced neuroinflammation in post-traumatic anxiety, LFPI rats with only vehicle injections (**Fig. 2**; black bars) displayed a pattern of increased glial fibrillary acidic protein (GFAP), indicating reactive astrocytes in insula (**Fig. 2A**), amygdala (**Fig. 2B**) and hippocampus (**Fig. 2C**). By contrast, GFAP labeling in LFPI rats receiving MN166 injections (**Fig. 2**; white bars) were not distinguishable from surgically naïve (**Fig. 2**; light grey bars) or sham operated (**Fig. 2**; dark grey bars) animals, indicating a significant reduction in injury-induced astrogliosis due to MN166 treatment. OX-42 (a microglial marker) activation was also greater in the insular cortex of LFPI rats compared to surgically naïve, sham operated and

LFPI+MN166 treated animals (**Fig. 2D**). There were no significant differences found between surgically naïve, sham operated and LFPI+MN166 treated rats in either analysis.

***Astrocyte morphology 3 months post-injury***. **Figure 3** shows representative images depicting GFAP immunoreactivity assessed in the hippocampus, amygdala and insula at 3 months post-injury. LFPI rats injected with vehicle showed clear signs of reactive astrocytes (bottom row), while naïve and sham operated rats appeared to have normal astrocyte morphology. LFPI rats treated with MN166 (third row) were difficult to differentiate from surgically naïve and sham operated groups.

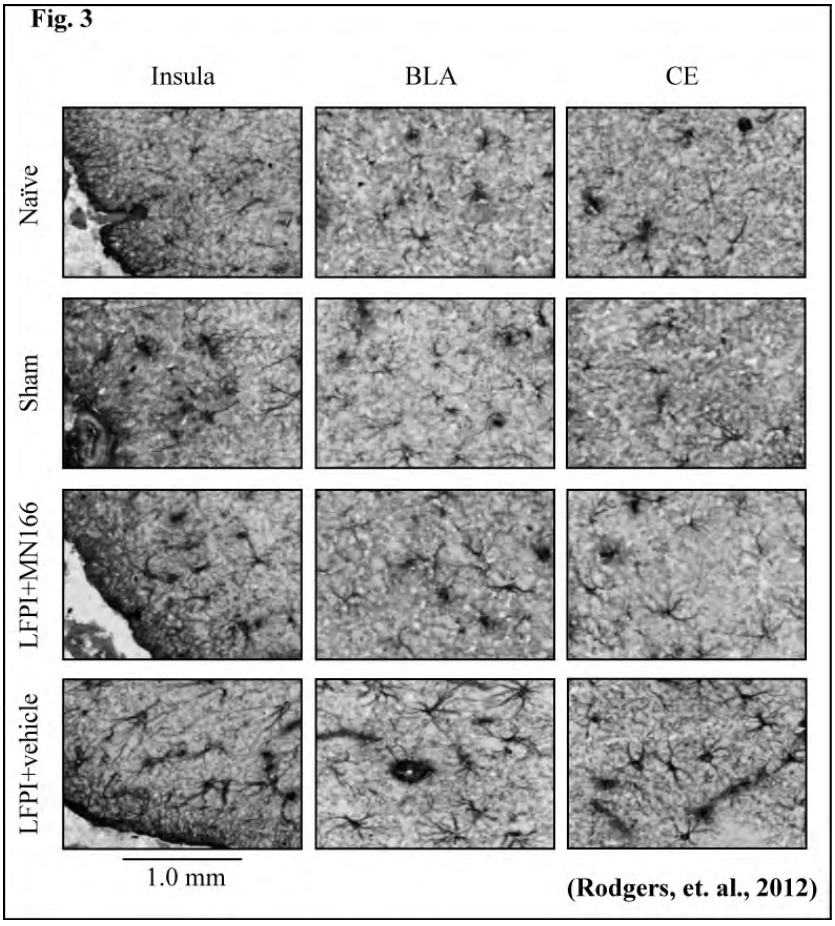


**Preliminary Study 2: Evidence for treatment of post-traumatic anxiety with post-injury glial attenuation**

***Glial attenuation reduces established freezing behavior in the novel context.*** This experiment differed from Study 1 in that post-shock freezing behavior was permitted to fully develop out to 1 month post-injury before treatment. Sham operated rats (**Fig. 4**; dark and light grey bars) froze approximately 25% before treatment with MN166 or vehicle, while LFPI rats (**Fig. 4**; black and white bars) froze at significantly higher rates (~60%) in the novel context. Following treatment, LFPI+MN166 rat's freezing behavior was reduced to (~25%) compared to LFPI+vehicle rats (~50%). This effect was significant at 3 months, and remained so through 6 months following injury. Freezing in Sham+MN166 and Sham+vehicle rats could not be distinguished from LFPI+MN166 treated rats at all time-points following treatment, while LFPI+vehicle injected rats froze significantly more than both sham groups at all post-treatment time-points with the exception of LFPI+vehicle and Sham+vehicle, which did not differ at the 4 month and

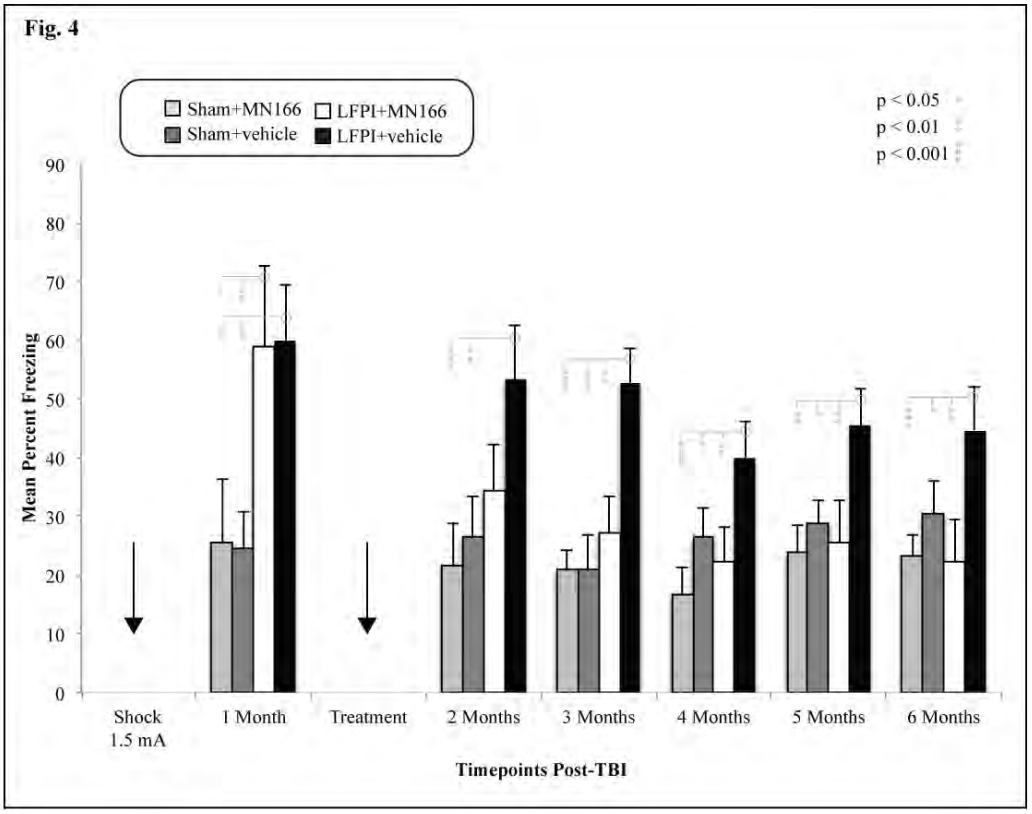

6 month time-points. Thus, MN166 injections after full development of post-traumatic anxiety had the effect of long-term reversal of anxiety symptoms, suggesting a reversible but otherwise prolonged and perhaps chronic neuro-inflammatory condition maintaining post-traumatic anxiety in untreated LFPI animals.

***Reactive gliosis is reduced in amygdala and insula 6 months post-injury.*** Immunohistochemistry supports the possibility of chronic inflammation in untreated rats. LFPI+vehicle rats had significant increases in GFAP labeling in both insula and amygdala (**Fig. 5A & B,** respectively; black bars), indicating higher astroglial activation compared to sham operated and LFPI+MN166 treated rats. In the central amygdala (CE), microglial activation (**Fig. 6**; OX-42) was also greater in LFPI+vehicle injected rats compared to both sham operated groups and LFPI+MN166 treated rats, and was approaching significance for basolateral amygdala (BLA).

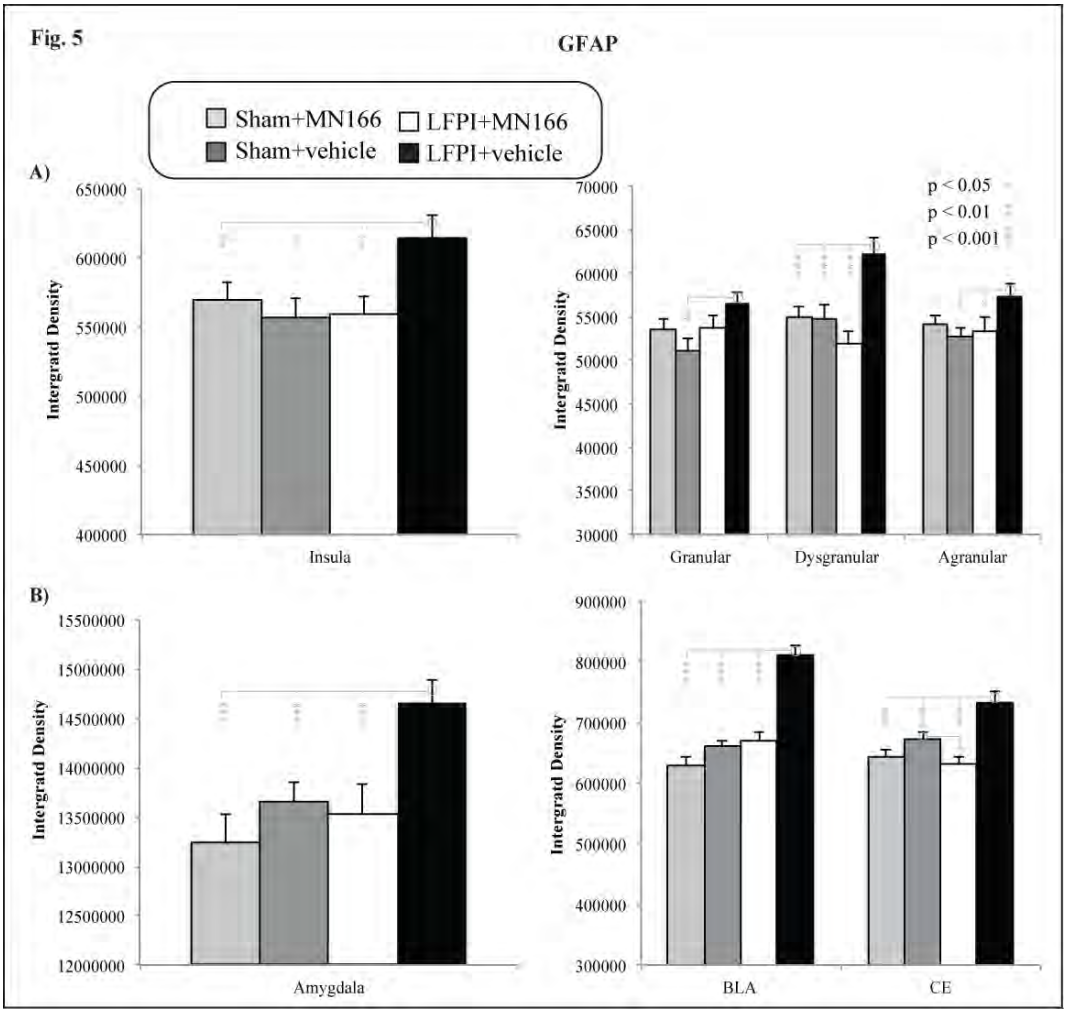


***Astrocyte morphology 6 months post-injury.*** **Figure 7** shows representative images depicting GFAP immunoreactivity assessed in the amygdala and insula at 6 months post-injury. LFPI rats injected with vehicle showed clear signs of reactive astrocytes (bottom row), while sham operated rats appeared to have normal astrocyte morphology (top rows). LFPI rats treated with MN166 (third row) were difficult to differentiate from sham operated groups.

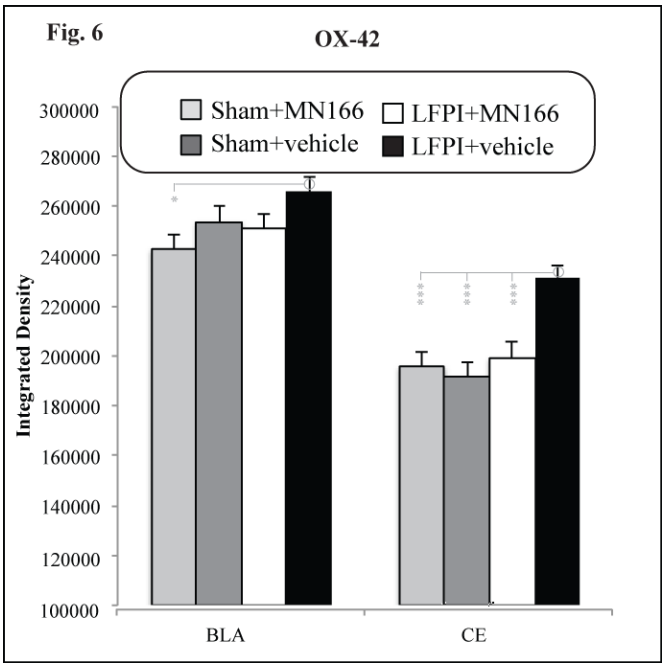


***Relevence of our preliminary results to other work and the present proposal.*** Our first study demonstrates that LFPI induces anxiety-like behaviors in an animal model of post-traumatic anxiety. Further, we show the involvement of neuroinflammation by attenuating the behaviors and trauma-induced changes in reactive gliosis through MN166 based immunosuppression. Peri-injury administration results in a marked reduction in anxiety behaviors, which we suspect is due to attenuation of the inflammatory response post-injury, as astroglial and microglial activation is significantly reduced in the amygdala and insula, brain regions

consistently implicated in anxiety in both rats and humans. This study is the first report of successfully reducing trauma-induced anxiety-like behavior based on immunosuppression. Lastly, this study validates the use of LFPI to induce anxiety-like behavior following experimental TBI in rats and introduces a model useful for exploring basic mechanisms of post-traumatic anxiety observed in humans.

Our second study replicates the finding of LFPI-induced increases in post-traumatic anxiety and shows that acute treatment with MN166 results in a reduction of post-traumatic anxiety and reactive gliosis in brain regions important to the development of anxiety. However, this study critically expands the clinical relevance of our previous findings because treatment was administered one month post-injury and the reductions in anxiety-like behavior persisted out to six months. The findings of elevated astroglial and microglial levels at time-points this long post-injury supports the hypothesis of chronic neuroinflammation in anxiety disorders following TBI. The results also broaden the critical treatment window for those with post-traumatic anxiety disorders and suggest neuroinflammation as a possible treatment target long after injury and behavior have been established. This is of potential clinical importance because studies indicate that prevalence rates continue to increase years after injury (87-89). Evidence for long-term risk in the development of post-traumatic anxiety documented in a study of TBI patients assessed 30 years following injury indicate that almost half (48.3%) of TBI participants develop a psychiatric disorder following injury, and almost half (23.3%) of the reported disorders are anxiety disorders, thus showing the importance of psychiatric follow-up and chronic treatment management after injury (89).

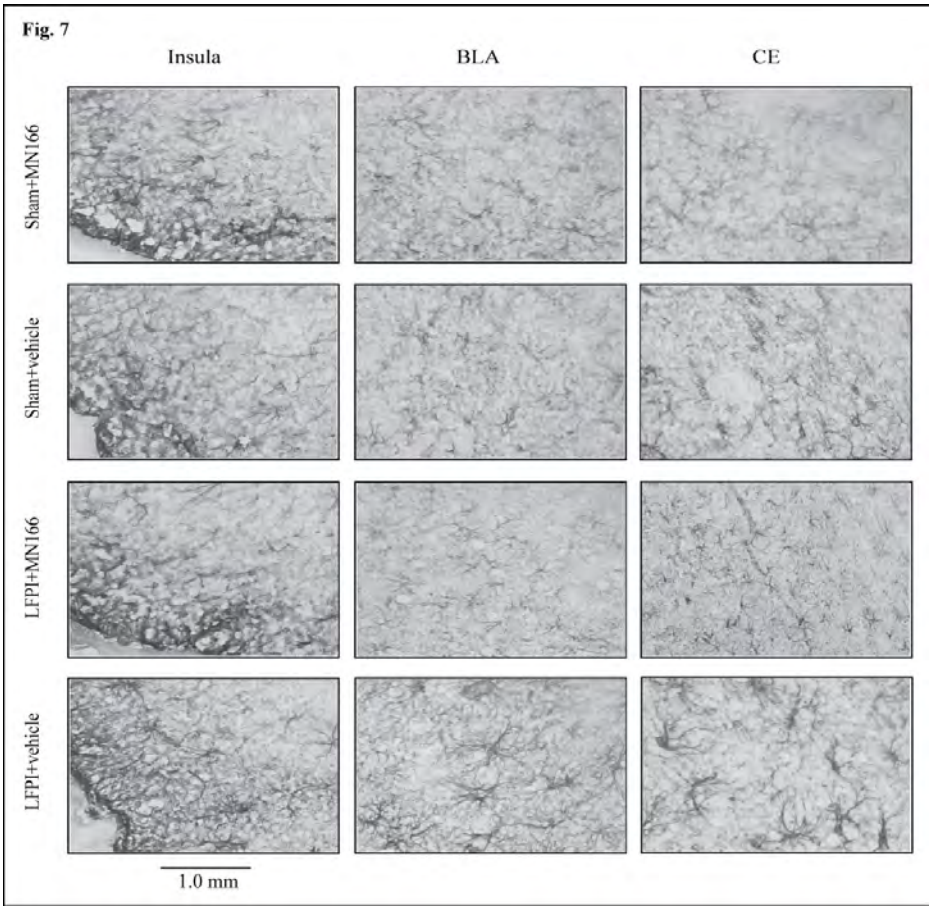


Very few animal studies have reported success in treating post-traumatic anxiety. A recent meta-analysis (1989-2009, including 91 treatments and over 200 pre-clinical studies) assessed the impact of pharmacological agents on cognitive, motor and behavioral outcomes in rats following TBI, and the results revealed that almost no treatment improves behavioral outcomes, including anxiety, depression and aggression (90). Three studies that have been found to be effective in reducing anxiety-like aftermaths following TBI, as evidenced by increased exploratory behavior in open field and elevated plus tests in treated animals, utilized magnesium, resveratrol and progesterone (66, 79, 85). Although the mechanism of action for magnesium treatment is unknown, the neuroprotective effect is likely due to reductions in glutamate excitotoxicity, mitochondrial damage, and apoptosis (91). Resveratrol is a potent polyphenol with many antioxidant properties, which have been shown to decrease oxidative stress following TBI. Resveratrol has also been found to be neuroprotective against excitotoxicity, ischemia, and hypoxia (66). Progesterone is thought to protect against glutamate excitotoxicity by interacting with inhibitory $GABA_A$ receptors and through modulation of excitatory neurotransmitter (kainite, glycine, serotonin, and acetylcholine) receptors (91).

However, while the above treatments show reductions in anxiety-like behavior following TBI, all treatments require rapid administration (within 30 min – 6 h post-injury) reducing the therapeutic window to the day of injury. Additionally, pre-clinical studies utilizing animals have consistently failed to translate a successful pharmacological intervention to date, likely because highly controlled investigations may not be

reflective of clinical trial designs. Pre-clinical studies tend to only include one injury severity (91). Another weakness in pre-clinical trials in animals is pre-treatment or very early interventions (30 min – 6 hours), in spite of evidence that many molecular, biochemical and immunological changes occur for many months to years following injury, and that clinical intervention may not be possible at such early stages of TBI. To better understand the pathophysiology of post-traumatic anxiety, pre-clinical treatments need to target longer treatment windows with range of injury severities. Our proposed project will attempt to overcome many of these limitations by focusing on delayed MN166 treatment and targeting mild, moderate and severe injuries, to extend our preliminary findings of neuroprotective immunosuppression on functional and immunological outcomes following TBI.

**Uniqueness**. We have developed a novel animal model of post-traumatic anxiety, using LFPI induced freezing behavior as a direct measure of fear responses. With this model, we show the first empirical proof of the theoretical concept that neuroinflammation plays a key role in post-traumatic anxiety and that a powerful post-injury intervention for post-traumatic anxiety development can be effected through brief peri-injury MN166 treatment. Our results represent a paradigm shift, challenging present attempts to treat post-injury anxiety symptoms, and moving instead toward preventing the development of post-traumatic anxiety in the first place by acutely suppressing the extreme and potentially chronic inflammatory response that TBI produces. Finally, and perhaps most exciting from both a scientific, clinical and military standpoint, we have preliminary evidence that acute treatment with MN166 at 1 month post-injury (after post-traumatic anxiety symptoms have fully developed), instead of at the time of injury, has the pronounced and long-term effect of reversing post-traumatic anxiety, which becomes indistinguishable from control animals. This finding suggests that post-traumatic anxiety is due in part to an ongoing chronic neuroinflammatory state, which may be disrupted by brief suppression of glia activation. To our knowledge, neuroimmune modulation as a means of post-traumatic anxiety prevention/treatment at time-points this late post-injury have never been tried before now. These results from our animal model form the basis of the present proposal to explore, for the first time, mechanisms of neuroimmune brain inflammation in the prevention and treatment of post-traumatic anxiety

## 2) HYPOTHESES

**Hypothesis 1) Post-traumatic anxiety *prevention* across injury severity**. We hypothesize that attenuating glial cell activation with MN166 4 days following mild, moderate, or severe LFPI will result in corresponding attenuation of anxiety, suggesting a preventative strategy for post-traumatic anxiety. Our expectations are based on the demonstrated success of peri-injury treatment in this model using moderate LFPI. They are also based on our success in reversing post-traumatic anxiety when already established at 1 month post-injury. Since our preliminary work was based on moderate LFPI, we expect significant if not equal improvement in post-traumatic anxiety symptoms with severe LFPI and equal if not better results with mild LFPI. Success with proximal post-injury treatment would present a far more clinically relevant finding for preventing post-traumatic anxiety and associated neuro-trauma without the need for pre-treatment. To test this hypothesis, we will examine the effects of LFPI and acute post-injury MN166 treatment on freezing behavior tested in a novel environment at 2 weeks, 1, 2, 3 and 6 months post-trauma.

**Hypothesis 2) Post-traumatic anxiety *treatment* across injury severity**. We hypothesize that post-traumatic brain inflammation is an ongoing, chronic process contributing to prolonged anxiety-like behavior, and that glial attenuation with administration of MN166 1 month following mild or severe LFPI, after the development of both behavioral and functional symptoms, will reverse or at least attenuate these symptoms, suggesting a treatment strategy for established post-traumatic anxiety. We have already had success at reversing established post-traumatic anxiety with treatment beginning at 1 month post-injury, this was evidenced out to long-term time-points, 6 months post-injury (**Fig. 4**). To test this hypothesis in mild and severe injury severities, we will use the same animal model and behavioral/histological evaluations as Hypothesis 1, but will delay treatment with MN166 until 1 month post-injury, when post-traumatic anxiety has fully developed. To test this hypothesis, we will examine the effects of LFPI and acute post-injury MN166 treatment post-traumatic anxiety-like behavior at 1-month through 6-months post-trauma.

## 3) TECHNICAL OBJECTIVES

The hypotheses outlined above lead to 2 specific aims addressing the following questions:

**AIM 1)** Can acute neuroimmune suppression begun 4 days following TBI prevent or at least attenuate development of post-traumatic anxiety and associated neuroinflammation? If so, is the effect long term (out to 6 months) and is prevention differentially effective for mild, moderate and severe TBI?

**AIM 2)** Can acute neuroimmune suppression begun 1 month following TBI reverse or at least attenuate ongoing post-traumatic anxiety and possible chronic neuroinflammation? If so, is the effect long term (out to 6 months) and is treatment differentially effective for mild, moderate and severe TBI?

## 4) PROJECT MILESTONES

We expect by the end of this 3 year project period to have determined: 1) the role of trauma-induced neuroinflammation in the development and/or maintenance of post-traumatic anxiety, 2) whether brain structures typically associated with anxiety in humans and in animal models reveal reactive gliosis in response to mild, moderate and severe injury, and 3) whether reduction of glial activation with MN166 holds promise for prevention and/or reversal of post-traumatic anxiety related symptoms.

As detailed in our Statement of Work, we expect to reach the first milestone of **AIM 1** within the second year of work. **Milestone #1:** Demonstration that early treatment with MN166 prevents or attenuates post-traumatic anxiety in mild, moderate, and perhaps severe TBI. We base this estimate on time required to perform preliminary studies of LFPI impact pressures required to reliably produce mild and severe TBI associated with post-traumatic anxiety (months 1-7), subsequent data collection for the first experiment (months 8-13; see 6 month procedural timeline for AIM 1; **Fig. 8**), followed by histology (months 14-18), data analysis (months 19-20), and publication (months 21-22). We expect to reach the second milestone on **AIM 2** by the end of the 3$^{rd}$ project year. **Milestone #2:** Demonstration that delayed treatment with MN166 reverses or attenuates established post-traumatic anxiety in mild, moderate, and perhaps severe TBI. This estimate is based on the 6-month procedural timeline for AIM 2 (months 23-28; **Fig. 9**), and additional time required for histology, data analysis, and publication (months 29-36).

## 5) MILITARY SIGNIFICANCE

Traumatic brain injury (TBI) has been described as the signature injury of the wars in the Middle East, where improvised explosive devices, suicide bomb blasts, and other combat related head trauma have seen a marked increase. This precipitous rise is highly correlated with a substantial increase of war fighters suffering from chronic PTSD, of which post-traumatic anxiety is the dominant symptom. There is considerable overlap in symptoms and high rates of co-occurrence between PTSD and post-traumatic anxiety. Soldiers reporting TBI are at very high risk for long-term mental and physical health problems in general, and the high rates of TBI and post-traumatic anxiety pose a particularly significant concern for the long-term health of U.S. veterans. A greater understanding of their interaction is critical to the treatment of Active Duty, Reserve, National Guard, and Veteran soldiers affected by TBI with psychiatric morbidity.

Our proposed project is directly relevant to two main USAMRMC research areas of interest. The first concerns the Combat Casualty Care Research Program (CCCRP) in that we plan to investigate the effectiveness of an orally available pharmacological intervention to limit the immediate, short- and long-term impairments that follow traumatic brain injury. The drug we will investigate, Ibudilast (MN166), is intended to mitigate post-injury neural and immune cell over stimulation, brain inflammation, resultant cell loss and neurologic dysfunction (resulting in post-traumatic anxiety). We will specifically explore the effectiveness of proximal (4-day) post-injury administration of MN166 on preventing/attenuating post-traumatic anxiety, an application well suited to first responders. MN166 is currently in FDA approved clinical trials for human pain management, so its potential translation to military treatment of post-traumatic anxiety would be far more facilitated compared to other potential neuroimmune suppressant compounds.

Our project is also directly relevant to 2 objectives of the Military Operational Medicine Research Program (MOMRP) under the categories of 1) Injury Prevention and Reduction, and 2) Psychological Health and Resilience, in that we focus on reducing the negative impact of concussion/mild traumatic brain injury by

elucidating underlying mechanisms of post-traumatic anxiety associated with PTSD (neuroinflammation) and focusing on potential implementation of evidence-based prevention (immediate post-injury administration of MN166 to prevent post-traumatic anxiety) and treatment techniques (reversal of post-traumatic anxiety symptoms with neuroimmune attenuation well after post-traumatic anxiety symptoms have developed).

In this project, we will use an animal model of head trauma and post-traumatic anxiety to explore both its neurobiology and a means of prevention and treatment using suppression of inevitable trauma-induced brain inflammation. If successful, we expect our results to make a major scientific advance in understanding how post-traumatic anxiety occurs. But more importantly to injured soldiers, the drug we will test for prevention can be administered orally (i.e. pills), has been used for years in Asia (primarily for asthma treatment) with no known side effects, and, as noted above, is currently approved by the FDA for clinical trials concerning use in human chronic pain. Therefore our success should lead to very rapid translation of this work to a practical and effective prevention/attenuation of post-traumatic anxiety in battlefield emergency medicine, and treatment of already developed post-traumatic anxiety in the large Veteran population. This work has an urgent immediacy in that, not only are conflict induced brain injuries and cases of post-traumatic anxiety on the rise, but there is an unrelenting increase of the burden on Veteran health delivery with no effective treatment in sight. Finally, we expect success of this work to lead to additional experiments examining the effect of immunosuppression on other very common TBI-induced cognitive and motor disorders, which follow closely behind post-traumatic anxiety as major blast-injury related disabilities resulting from combat.

**6) PUBLIC PURPOSE (written in laymen's terms)**

Head trauma that can result from battlefield, sporting or automobile accidents frequently produces long-term injury to the brain. Patients with these brain injuries report not only a decreased ability to think and move properly, but also often report a profound and long-term feeling of anxiety that has devastating consequences to their employment and quality of life. While such post-traumatic anxiety has long been recognized, very little is known about how it is caused by brain injury and even less is known about how to either prevent its development and/or treat its symptoms. We have recently developed an animal model of post-traumatic anxiety in rats and determined that trauma results in prolonged inflammation of the brain, similar in some ways to commonly experienced inflammation of the skin in response to damage from burns. This is important because brain inflammation is well known to cause parts of the brain to become over active. We have also discovered that if we administer drugs that briefly suppress inflammation at the time of injury, or after post-traumatic anxiety has developed, the effect is to decrease over-activity of the brain and similarly decrease anxiety-like behaviors in rats. In this project we use our animal model to better understand the areas of the brain producing post-traumatic anxiety and to establish ways of preventing its development or reversing the symptoms once they occur. We will do this by decreasing inflammation produced by brain trauma with a powerful anti-inflammatory drug called "Ibudilast" that has already proven safe for use in humans.

**7) METHODS**

**Subject groups and procedural timeline.**

*(Details of methods indicated here with an "*", are provided in "General Methods" below.)*

**AIM 1) Post-traumatic anxiety prevention.** All procedures will be performed in accordance with University of Colorado Institutional Animal Care and Use Committee guidelines for the humane use of laboratory rats in biological research. For the first hypothesis of this project, 80 adult viral-free male Sprague-Dawley rats (275-325g; Harlan Laboratories, Madison, WI) will be randomly assigned to 1 of 8 groups (10 rats each: Sham-operated/vehicle-injected, Sham-operated*/MN166-injected*, mildTBI*/vehicle-injected*, mildTBI/MN166-injected, moderateTBI*/vehicle-injected, moderateTBI/MN166-injected, severeTBI*/vehicle-injected, severeTBI/MN166-injected). Prior to TBI, baseline motor coordination testing* will be performed (**Fig. 8a**). TBI will then be induced as in our preliminary studies with LFPI* (**Fig. 8b**). At 4 days post-injury, daily subcutaneous injections of MN166* (in corn oil; 10 mg/kg) or vehicle will commence and be administered for 5 consecutive days (**Fig. 8c**). Motor testing* will be repeated following recovery and injections, beginning at 1-week post-injection (**Fig. 8d**; to eliminate the possible confound of motor impairment due to pain sensitivity from injections). The rats will be tested for % time freezing in a novel context* (minor stressor), exploration of

an open field* and elevated plus maze* at 2 weeks post-injury (**Fig. 8e**) to establish baseline behaviors before foot shock* (i.e. anxiety-like behavior induced by LFPI alone without an added major stressor). As noted earlier, in our preliminary studies, examining a smaller number of rats, open field and elevated plus maze exploration showed results that trended in the same direction as freezing in the novel environment but did not reach significance. These additional measures are included in the present studies and are expected to reach significance with the larger number of rats per group. After baseline behavioral measurements, all animals will be exposed to foot shock* (**Fig. 8f**) in another context (to ensure the absence of contextual conditioning to the novel context) before retesting for the same anxiety-like behaviors at 1, 2 and 3 and 6 months post-injury (**Fig. 8g-j**). Tissue will then be collected* for histology (**Fig. 8k)**.

**Fig. 8**

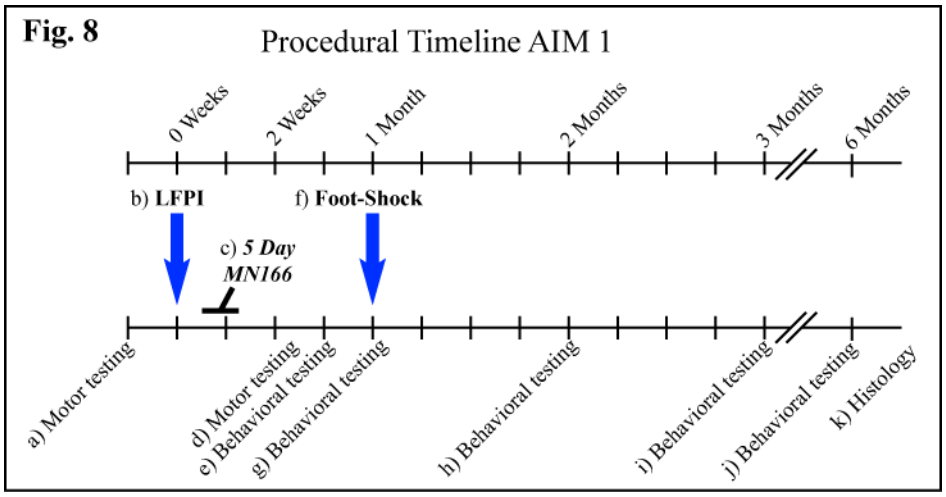


**Fig. 9**

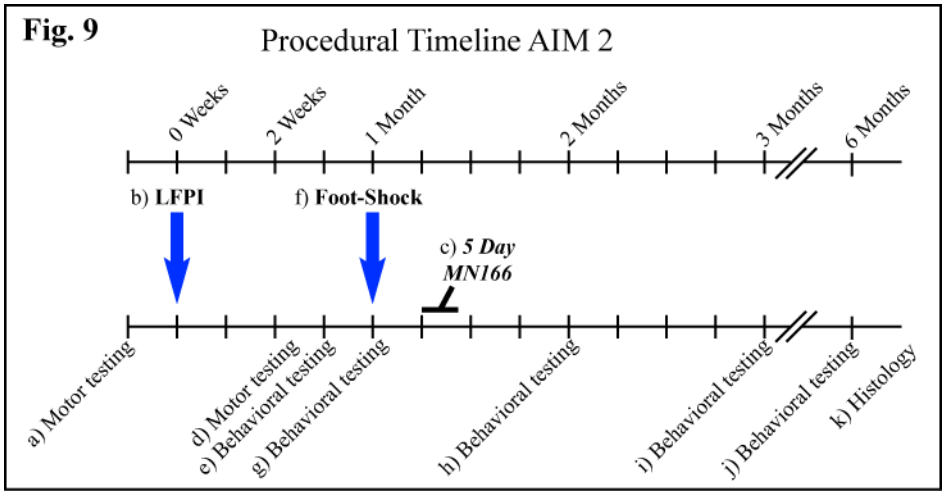


**AIM 2) Post-traumatic anxiety reversal.** To test the second hypothesis of this project, 80 adult viral-free male Sprague-Dawley rats (275-325g; Harlan Laboratories, Madison, WI) will be randomly assigned to 1 of 8 groups (10 rats each: Sham-operated/vehicle-injected, Sham-operated*/MN166-injected*, mildTBI*/vehicle-injected*, mildTBI/MN166-injected, moderateTBI*/vehicle-injected, moderateTBI/MN166-injected, severeTBI*/vehicle-injected, severeTBI/MN166-injected). Pre-injury motor testing (**Fig. 9a**), LFPI (**Fig. 9b**), post-injury motor testing (**Fig. 9d**), as well as the time-line for foot-shock (**Fig. 9f**) post-shock behavioral testing time-points (**Fig. 9h-j**) will be exactly the same as the time-line for AIM 1. However, a key difference in this experiment is that MN166 or vehicle injections will be delayed until behavioral symptoms of post-traumatic anxiety have been fully developed and tested at the 1 month post-injury time-point (**Fig. 9c**) to examine possible treatment related reversal or attenuation of anxiety-like behavior.

***General Methods.**

*Lateral Fluid Percussion Injury (LFPI).* Rats are anesthetized with halothane (4% induction, 2.0-2.5% maintenance) and mounted in a stereotaxic frame. The LFPI adapted for our preliminary studies and the present proposal is widely used to induce TBI in animal models and has been described previously (62, 74, 92) utilizing a PV820 Pneumatic PicoPump (World Precision Instruments, Inc., Sarasota, FL) to deliver standardized pressure pulses of air to a standing column of fluid. A 3.0 mm diameter craniotomy is performed, with the exposed dura remaining intact. A female Luer-Loc hub (inside diameter of 3.5 mm) is secured over the craniotomy with cyanoacrylate adhesive. Following hub implantation, the animal is removed from the stereotaxic frame and connected to the LFPI apparatus. The LFPI apparatus will then be used to deliver a mild impact force (1.0 atmospheres; 10 ms), moderate impact force (2.0 atmospheres; 10 ms), or severe impact force (3.0 atmospheres; 10 ms). The injury cap is then removed, scalp sutured and the rats returned to their home

cages for recovery. Sham operated rats undergo identical surgical preparation, but do not receive the brain injury.

*Ibudilast (MN166) administration.* MN166 (MediciNova, San Diego, CA) is a relatively non-selective phosphodiesterase inhibitor with anti-inflammatory actions via glial cell attenuation (93, 94). Treated rats receive a 5-day dosing regimen of once-daily MN166 (10 mg/kg, 1 ml/kg subcutaneously in corn oil) or vehicle (1 ml/kg subcutaneously, corn oil) injections beginning at 4 days (AIM 1) or 1 month (AIM 2) following LFPI. Weight will be recorded prior to each dosing and treatment administered at the same time each day to maintain constant levels across a 24 hr. period. Dose selection is based on prior animal pharmacology results (95), and has been shown to be safe and well tolerated, yielding plasma concentration-time profiles commensurate with high dose regimens in clinical development (96). MN166 administered via this regimen yields plasma and CNS concentrations that are linked to molecular target actions including, most potently, macrophage migration inhibitory factor (MIF) inhibition (97) and, secondarily, PDE's -4 and -10 inhibition (98). The relevance of MIF inhibition in disorders of neuroimmune function such as neuropathic pain has recently been well demonstrated (99). Such dosing regimens have clearly been linked to glial attenuation in other animal models (100). Our preliminary studies demonstrate that a dosing regime of 5 days at 10 mg/kg is well tolerated and yields significant effects.

*Neuromotor Tests.* Baseline testing of motor, vestibular and locomotive performance in all groups will be conducted immediately prior to surgery and again, at 1 week (Hypothesis 1) or 3 weeks (Hypothesis 2) following injury. These tests include ipsilateral and contralateral assessment of forelimb and hindlimb use to assess motor function, locomotion, limb use and limb preference (101, 102), toe spread to assess gross motor response (103), placing to assess visual and vestibular function (104, 105), catalepsy rod test to assess postural support and mobility (106), bracing to assess postural stability and catalepsy (107, 108) and air righting to assess dynamic vestibular function (109, 110). Scoring will range from 0 (severely impaired) to 5 (normal strength and function). The individual test scores will be summed and a composite neuromotor score (0–45) generated for each animal. In addition to the composite neuromotor score, limb-use asymmetry will be assessed during spontaneous exploration in the cylinder task, a common measure of motor forelimb function following central nervous system injury in rats (104, 111) and post-injury locomotor activity will be assessed through distance traveled on a running wheel, both tasks will be scored for 5 minutes under red light (~90 lux).

*Freezing Behavior.* A novel environment will be used to assess freezing behavior in response to a minor stressor (112). We and others have found that even though the environment cannot be considered novel after the first exposure, repeat testing at widely spaced (2-4 wk) intervals does not result in habituation of the freezing response (see **Fig. 1**) The environment will consist of a standard rat cage with one vertically and one horizontally striped wall. No aversive stimuli are introduced in this context and no conditioning should occur. Rats will be tested (5 minutes) and the percent of freezing behavior assessed. Freezing is defined as the absence of movement except for heart beat/respiration, and is recorded in 10 sec intervals.

Freezing behavior in the novel environment will be measured again following the administration of a foot shock in a separate shock apparatus. The shock apparatus consists of two chambers placed inside sound-attenuating chests. The floor of each chamber has 18 stainless steel rods (4 mm diameter), spaced 1.5 cm center-to-center and wired to a shock generator and scrambler (Colbourn Instruments, Allentown, PA). An automated program delivers a 2-sec/1.5 mA electric shock. Rats will be transported in black buckets and shocked immediately upon entry to chambers. Following shock, rats will be returned to their home cages.

*Open field exploration.* Spontaneous locomotor activities and exploratory behaviors will be evaluated using an open field testing apparatus (94). Rats will be placed facing the same direction, in the upper left corner of an open field-testing apparatus, consisting in a 40x40x40 cm Plexiglas enclosure. Rat displacements will be recorded for 10 min with a digital camera placed directly over the apparatus. The testing will begin as soon as the animal is placed in the open field. The camera will be attached to a computer running "Any-Maze Video Tracking SystemTM" (Stoelting Co., Wood Dale, IL, USA) program which tracks the animal and records its trajectory in the enclosure separated in 16 equal squares. The following parameters will be analyzed: entries into the inner arena, total distance traveled during the test period, vertical & horizontal locomotion, and freezing behavior.

*Elevated plus maze exploration.* The elevated plus maze is made of ivory Plexiglas with 50 cm long and 10 cm wide arms, elevated 50 cm above the floor. The closed arms are surrounded by a 50 cm wall. Rat displacements will be recorded for 10 min with a digital camera placed directly over the apparatus. The testing will begin as soon as the rat is placed in the central platform of the maze facing an open arm. The camera will be attached to a computer running "Any-Maze Video Tracking SystemTM" (Stoelting Co., Wood Dale, IL, USA) program which tracks the animal and records its trajectory in the enclosure. The following parameters will be analyzed: number of open arm entries, time spent in open/closed arms, distance traveled in open/closed arms, and freezing behavior.

*Immunohistochemistry.* Rats will be intracardially perfused with 0.9% saline and tissue collected, then fixed with 4% paraformaldehyde overnight at 4°C. Brain sections (20 μm) will be post-fixed with 4% PFA for 15 min at room temperature, then treated with 0.03% $H_2O_2$ for 30 min. Immunoreactivity in brain regions associated with anxiety (insula and amygdala) will be assessed for markers of microglia (CD11b/c; OX42 labeling) and astrocytes (glial fibrillary acidic protein; GFAP), using an avidin-biotin-horseradish peroxidase (ABC) reaction (113). Briefly, the sections are incubated at 4 °C overnight in either mouse anti-rat OX-42 (1:100; BD Biosciences Pharmingen, San Jose, CA) or mouse anti-pig GFAP (1:100; MP Biomedicals, Aurora, OH). The following day, sections are incubated for 2 h with biotinylated goat anti-mouse IgG antibody (1:200; Jackson ImmunoResearch, West Grove, PA). Sections are then washed and incubated for 2 h at room temperature in ABC (1:400 Vector Laboratories, Burlingame, CA) and reacted with 3', 3-diaminobenzidine (DAB; Sigma-Aldrich, St. Louis, MO). Sections are air-dried over night, dehydrated with graded alcohols, cleared in Histoclear, and cover slipped with Permount (Fisher Scientific, Fairlawn, NJ). Densitometry analysis is performed using Scion Image software.

**Analytic plan.**

*Image Analysis.* Slides will be viewed with a Nikon Ci-LE System with Motorized nosepiece, X, Y, and Z system and camera with bright-field illumination at 10X magnification. Densitometry analysis is performed using Scion Image software. Images are opened in ImageJ, converted into gray scale and rescaled from inches to pixels. Background areas are chosen in the white matter or in cell-poor areas close to the region of interest (ROI). The number of pixels and the average pixel values above the set background are then computed and multiplied, giving an integrated densitometric measure. Six measurements are made for each ROI; the measurements are then averaged to obtain a single integrated density value per rat, per region.

*Statistical analyses.* Analyses of behavioral measures will use repeated measures (time point post-injury) ANOVAs, with group assignment as the independent variable, followed by Bonferroni post hoc tests for multiple comparisons of individual time points. Immunohistochemistry data will only be collected at one time point (6 months post-injury) and one-way ANOVAs will be conducted, with group assignment as the independent variable. Differences with a *p*-value of <0.05 will be considered significant.

*Power Analysis.* Power analysis of our 8 x 5 design (group: 8 levels, and time: 5 levels), for AIM 1 & 2 (**Fig.**

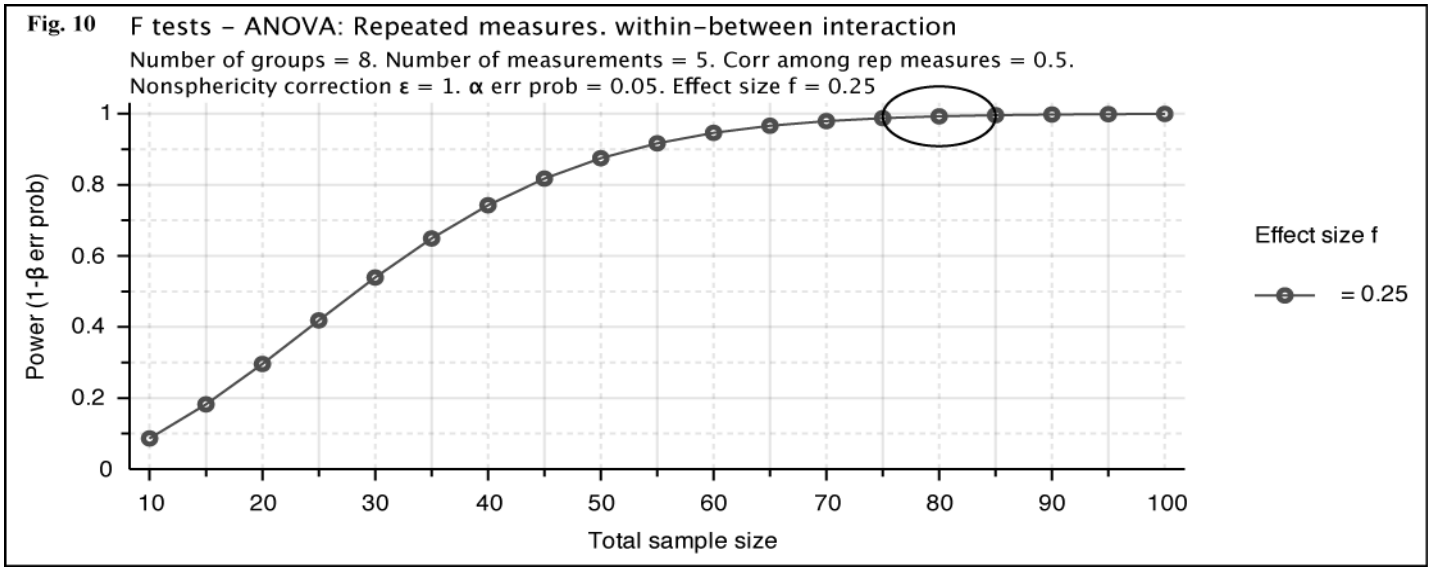

**10**) indicates that acceptable power of 0.8 can be achieved with 45 rats and the maximum power of 1.0 will be reached with N = 80 rats as planned (**Fig. 10**; oval).

**Expected challenges.**

Based on our preliminary data, we expect that moderate-severe LFPI in both AIM 1 & 2 will reliably result in increased post-traumatic anxiety behavioral symptoms in untreated LFPI rats. However, a potential challenge could be that mild TBI at the 1.0 atmosphere impact pressure does not result in anxiety-like behavior. A solution to this problem would be to increase the impact pressure to 1.5 atmospheres, which is on the higher end of mild TBI in rodent models. However, recent studies have reported anxiety-like behaviors following mild TBI (86) and collaborative work between our laboratory and Dr. Watkins's laboratory has revealed anxiety-like behavior at the 1.0 atmosphere impact pressures suggested here.

Another potential challenge could be unacceptable variability of our LFPI results due variability of the injury. This has been minimized by the use of calibrated and temporally precise pressure pulses delivered by a Pneumatic PicoPump. However, in the course of our preliminary studies, we have noted 2 sources of injury variability that we will control in the present studies. The first is direct damage to the middle cerebral artery (MCA) that results in a large sub-dural hematoma and loss of adequate blood supply to large regions of cortex. The second is rupturing of the dura, simulating a (more severe) penetrating head wound instead of the closed head injury intended by the LFPI model. To avoid MCA damage, we will use rats of 275-325 gm., which, in combination with our lateral craniotomy location, minimize this outcome. In occasional cases where the MCA can be visualized within the area of craniotomy, the rat will be immediately sacrificed and replaced. Dural rupture is apparent following LFPI as extradural bleeding. These animals will also be replaced at the time of surgery.

Motor impairments have been found following severe LFPI, and impairments such as catalepsy, could confound our behavioral measures. Early pilot studies in our laboratory revealed motor impairments following surgery; however, changing the site of injury to a more lateral location and avoiding disruption of the MCA, eliminated these deficits. We will include a series of motor coordination tests to ensure that subsequent results aren't driven by motor impairments. In addition to motor impairments, these tests will assess deficits in other systems that may affect behavior, including vestibular, visual and proprioceptive systems. Animals found to have significant neuromotor composite scores compared to baseline scores will be excluded from the study.

Finally, animals have an increased risk for infection as a result of the surgery, which would increase inflammation and potentially cause problems with our behavioral measures. Therefore, our staff and campus veterinarian will carefully monitor the animals for increases in weight loss and temperature, the two most common indicators of the presence of infection. Animals will be excluded from the study if their weight drops below 20% of their baseline weight and/or temperature increases above 39°C, guidelines given to us by our on-staff veterinarian. We practice sterile surgical techniques to minimize sources of infection, and have not had to exclude any animals due to infections in our preliminary studies.

**Expected outcomes and consequences of success/failure.**

**AIM 1) Post-traumatic anxiety prevention.**

*Benchmark for success*-> We will conclude that suppressing glial activation with acute MN166 administration is an effective means of <u>preventing</u> development of post-traumatic anxiety if anxiety behavior in LFPI-MN166 treated rats at the 6 month post-injury time-point is significantly less than LFPI-untreated rats and <u>cannot be distinguished</u> from sham-operated controls in at least one of the TBI severity levels.

*Consequence of this success*-> This outcome alone would carry promise for post-traumatic anxiety prevention and would inspire more detailed future investigation of dose–response curves to determine an optimum treatment regime (duration and dose) and critical treatment windows (how soon after TBI) for maximum preventative effect.

*Benchmark for success*-> It is possible that treatment following TBI by 4 days as planned will not be as effective in attenuating post-traumatic anxiety symptoms as that seen in our preliminary study which began

injections 1 day prior to injury. Yet, if the result of treatment in LFPI rats is post-traumatic anxiety behavior that is significantly less than untreated rats (however, significantly more than sham-operated controls), we will still consider this outcome to be a success in that any significant improvement would be of potential translational significance.
*Consequence of this success*-> The ability to significantly attenuate the development of post-traumatic anxiety in our animal model will motivate future investigation of dose–response curves as noted above to see if treatment effects can be further increased and perhaps lead to actual prevention. Depending on the success of AIM 2, it would also be critical to further evaluate combining partial prevention with subsequent treatment (i.e. with additional delayed inflammatory attenuation) to see if the combination is more effective than either approach alone. It should be emphasized that since protracted MN166 treatment is well tolerated by humans and the compound can be effectively administered orally, long duration treatment beginning soon after TBI and continuing for months post-injury could be a distinct translational possibility.
*Consequence of failure*-> It is possible that MN166 treatment at 4 days following impact will have no influence on post-traumatic anxiety at any of the TBI severity levels. While this would call our hypothesis into question, it would have no impact on the justification for our AIM 2 study since the mechanisms and efficacy of prevention may differ from those of reversal. However, if a failure in preventing behavioral symptoms was also correlated with a failure to decrease gliosis in histological analysis, it would suggest that our hypothesis may be valid but our treatment was not, indicating future examination of other glial modulating drugs (for example, SLC022; "propentofylline"; 3-methyl-1-(5-oxohexyl)-7-propyl-3,7-dihydro-1H-purine-2,6-dione) that, while not as close to human translation as MN166, could further our understanding of potential neuroimmune prevention of post-traumatic anxiety.

**AIM 2) Post-traumatic anxiety treatment/reversal.**
*Benchmark for success*-> We will conclude that attenuation of glial activation with acute MN166 administration, after behavioral symptoms of post-traumatic anxiety have developed, is an effective means of reversing post-traumatic anxiety if anxiety behavior in LFPI-treated rats at the 6 month time-point is significantly less than LFPI-untreated rats and cannot be distinguished from sham-operated controls in at least one of the TBI severity levels.
*Consequence of this success*-> As noted, this outcome is independent of the success or failure of AIM 1 since the mechanisms and timing of prevention versus reversal may differ. Successful reversal would directly motivate follow-up studies looking at much longer duration post-injury delays before treatment (we have recorded large and persistent freezing responses in our rat post-traumatic anxiety model up to 18 months post-injury) to see if potential reversal might be eventually applicable to patients with ongoing and chronic post-traumatic anxiety.
*Benchmark for success*-> Similar to our AIM 1 benchmark, it is possible that delayed treatment will significantly attenuate, but not reverse, post-traumatic anxiety behavior in this study. This outcome would not be surprising since, particularly at later time points post-injury, it is likely that ongoing brain inflammation is only one of several contributors to behavioral symptoms. There is a large body of evidence showing that increased oxidative and nitrosative stress comprise a secondary injury cascade following TBI. Permanent damage to brain structures following TBI is likely, due to increases in the production of reactive oxygen species (ROS) and reactive nitrogen species (RNS), which are initiated by inflammatory mediators following activation of immune system in response to insult (26, 42, 43) and result in oxidative damage that can disrupt neuroprotective functioning. We may succeed in interrupting further damage but not reversing that which has occurred, leaving substantial residual deficits and post-traumatic anxiety behavior.
*Consequence of this success*-> A partial reversal of post-traumatic anxiety would still be of great importance both for understanding the role of ongoing neuroimmune contributions and for possible translational studies concerned with treatment. As noted earlier, depending on the outcome of AIM 1, this result would also motivate examination of the effectiveness of combined treatment both soon after injury and at later post-injury time-points when behavioral symptoms of post-traumatic anxiety may yet emerge.
*Consequence of failure*-> Failure to find any influence of glial attenuation on reversing established post-traumatic anxiety behavior in any of the TBI severity levels would support our null hypothesis, that the

contributions of brain inflammation are no longer contributing to chronic post-traumatic anxiety at later time-points. However, as noted for AIM 1, if a failure to attenuate post-traumatic anxiety symptoms is also associated with failure to decrease gliosis, we would conclude that our treatment was ineffective and explore other glial modulating compounds that may be have more potent anti-inflammatory effects.

Investigator-Initiated Research pre-proposal to the Peer Reviewed Medical Research Program

**Topic Area:** This proposal directly addresses one FY13 PRMRP Areas of Interest, epilepsy.

**Research Idea:** Approximately 50 million people worldwide have epilepsy [1] with 100,000 new cases diagnosed annually in the United States alone [2]. Traumatic brain injury (TBI) has been described as the signature injury of modern conflicts such as those in Afghanistan and Iraq[3]. TBI is also a major cause of acquired epilepsy, with overt seizures reported in up to 50% of survivors [4] and with approximately 20% of all symptomatic epilepsies attributed to TBI [5]. In addition, unlike many other forms of symptomatic epilepsies, fully developed post-traumatic epilepsy (PTE) is particularly difficult to treat both medically and surgically[6]. One way acquired epilepsies such as PTE and temporal lobe epilepsy (TLE) are distinguished from idiopathic epilepsies is that they are typically precipitated by an identifiable brain insult (i.e. traumatic brain injury or status epilepticus), followed by a prolonged "latent" period of epileptogenesis before the appearance of the first spontaneous behavioral seizures. The epileptogenic period provides a unique opportunity for discovery of anti-epileptogenic strategies, however progress in this area of clinical research has been hindered by the lack of reliable biological identifiers that can be used to measure and quantify the progress of epilepsy or its treatment (biomarkers) during this electrographically "silent" period.

Understandably, traditional emphasis has been placed on development of anti-seizure treatments for intervention once recurrent spontaneous seizures have been clinically established[7], however, the window of intervention, prevention, or mitigation may occur during the clinically silent period of epileptogenesis (often many months to years post-insult). A change in focus from symptom mitigation, to disease prevention, may therefore be advantageous, but in order for this to happen, novel and reliable biomarkers must be developed in order to allow investigation of this clinically silent period[8]. To date, however, most research conducted during the latent period, has focused on passive brain measures such as EEG, MRI, epileptiform spike and serum analysis, or invasive measures, such as gene expression and cellular markers to assess changes in brain physiology. We postulate that failure in the development of new compounds for the prevention, and often the treatment, of epilepsy may be due, in part, to a lack of brain markers that allow scientists and clinicians to actively probe the central nervous system during epileptogenesis and thereby quantify disease progression and treatment efficacy. The establishment of active biomarkers that examine changes occurring during the epileptogenic period (and beyond) would be beneficial in two key areas; **1)** investigation of the underlying mechanisms of epileptogenesis leading to more effective treatment regimes targeting prevention **2)** use as diagnostic tools to predict the risk/probability of acquiring epilepsy in high risk patients following brain insults. Indeed, the later could prove immediately beneficial for warfighters and veterans due to the high occurrence of head trauma in modern warfare [4] , the long epileptogenic period observed in these cases (months to years), and the high cost of treatment of epilepsy once it is established estimated to cost the US government up to 15.5 billion a year [2]. In this project we will concentrate on identification of novel biomarkers, with immediate human translational feasibility that can be used as, low-cost, noninvasive, biological assays that reflect alterations in brain functionality, induced by brain insult. The long-term goal of our research plan is to discover epileptogenic biomarkers in rodent models of epilepsy that can help further uncover the inherent mechanisms underlying epilepsy, used to monitor and quantify the efficacy of novel antiepileptogenic therapies during the electrographically/clinically silent period, and which can quickly be translated to human clinical use to screen high risk military service members, veterans and beneficiaries who have received a brain insult to asses if they are at risk for developing epilepsy.

**Research Strategy:**

To this end our lab has recently uncovered a novel biomarker of epileptogenesis in the lithium-pilocarpine (Li-pilo) model of epilepsy in rats. Using chronically implanted electrodes we have measured the auditory evoked response, from a click stimulus, in both primary auditory cortex as well as in the hippocampus. The averaged auditory evoked potential from 128 clicks was collected every 30 minutes from rats under 24/7 video and electrophysiological monitoring. The auditory stimulus has a few distinct advantages as a probe of neural circuits, 1) it is non-invasive, 2) it can be presented chronically without disruption of the animals normal sleep/wake activity if the volume is at low enough levels[9], 3) it can be presented to freely moving rats, 4) due to its non-invasive nature it has translational capability. Under baseline conditions there is a highly stereotyped auditory evoked potential (AEP) in both the primary auditory cortex as well as the hippocampus. The archetypal AEP morphology in sensory responsive brain regions, reflecting normal underlying neuronal circuit function, offers a stable criterion against which later changes in brain function can be measured. By monitoring rat AEP's 24/7 in the Li-pilo model of epilepsy we have discovered that the normal archetypal morphology of these sensory evoked brain events undergoes systematic and stereotyped changes during the latent period, which predict the probability of the development of later spontaneous seizures. Chronic and progressive changes in AEP waveform during epileptogenesis in animals that eventually develop spontaneous recurrent seizure (SRS) are distinguished from the AEP in animals that never develop epilepsy in that the latter return to a near baseline state. Interestingly, in animals that develop epilepsy, the changes in morphology of the AEP (repeatably progressive changes in the latency, duration and amplitude of temporal components) continue long past the first SRS, suggesting an ongoing epileptogenic period beyond the typically defined latent period. This prolonged epileptogenic period, sensitively indexed by continued alteration of the AEP, is recently suggested in the literature[10] based on seizure progression alone, and indicates not only the possibility of progressive epi-

leptogenesis that continues beyond the first SRS, but also the potential for antiepileptogenic treatment even following the onset of SRS with a means of monitoring success. The objective of this proposal is to further explore and characterize this novel biomarker of epileptogenesis with 3 experiments.

**Specific Aim 1**: Fully characterize the morphological alternations that occur in cortical and hippocampal auditory evoked responses following brain insult from lithium-pilocarpine.

**Specific Aim 2**: Further probe the glutamatergic cell population responsible for the AEP in isolation from the auditory sensory pathway using optogenetically-evoked responses directly in the hippocampus and cortex.

**Specific Aim 3**: Probe for archetypal morphological alterations in both auditory and optogenetically evoked responses in hippocampus and cortex following brain insult from lateral fluid percussion injury.

**Experimental approach: Aim 1)** Male Sprague Dawley rats (250-300g) will be randomly assigned to three groups, 1) Li-pilo, 2) Li-saline, and 3) no-injection. All animals will then be implanted with one SS screw electrode over primary auditory cortex and one bipolar electrode in dorsal hippocampus. After a 3-week recovery from surgery, animals will be attached to a head mount for chronic tethered video/EEG recording. Along with continuous EEG, averaged auditory evoked potentials (AEP) will be recorded every 30 minutes. Following a 2 week baseline animals will receive either the Li-pilo protocol[11], the Li-pilo protocol with saline in the place of pilocarpine, or no injections. Continuous recordings will be performed for 3 months. Animals will then be sacrificed and mossy fiber sprouting (classic characteristic of epileptic hippocampus) will be assessed with Timm staining. EEG will be visually scanned for seizures and severity classified based on associated video records. Both spontaneous EEG and AEPs will be compared to baseline recording throughout epileptogenesis and beyond. EEG will be assessed for band-delimited changes in power spectral density, as well as epileptiform spike density (based on automated template matching software written by the P.I. and currently in use). Changes in AEP waveform morphology will be quantified according to component peak amplitudes, duration, and post-stimulus latency. An additional cohort of li-pilo animals will have microelectrodes chronically implanted in the hippocampus and cortex to characterize the multiunit activity (to assess changes in excitatory/inhibitory balance) associated with the components of the AEP during baseline, epileptogenesis and SRS. We expect it will require 12 months to complete Aim 1.

**Aim 2)** The li-pilo model will be used again, but optogenetically evoked local field potentials (oLFP) will be added. Three groups, similar to those in aim 1, will be used with half of each group receiving excitatory opsin ChR2 (AAV-CaMKIIa-hChR2(H134R)-EYFP) injections into the target structures (cortex and hippocampus) at the time of the surgical implantation of the electrodes, and the other half receiving a control AAV-fluorophore (AAV-CaMKIIa-EYFP). These optogenes will be targeted at the glutamatergic neuronal population using the CaMKIIa promoter. Multimode fiber optic fibers will be glued to the electrodes to allow photo-stimulation (473nM, 20-35mW/mm$^2$) of the target structures. Photo-stimulation to generate an averaged oLFP will occur every 30 minutes following auditory stimulation, for the duration of the study (3 months). Care will be taken to stimulate at frequencies known to not influence synaptic plasticity, however recent optogenetic kindling studies offer the possibility that after-discharge from high frequency stimulation could be used as an additional measure of excitability in a separate cohort[12]. Baseline and li-pilo time course and analysis will be identical to aim 1. Analysis of changes in oLFP waveform morphology will be quantified according to component peak amplitudes, duration, post-stimulus latency, and will be compared to concurrent changes in AEP morphology. An additional cohort of li-pilo/AAV-CaMKIIa-hChR2(H134R)-EYFP animals will have microelectrodes chronically implanted in the hippocampus and cortex to characterize the multiunit activity associated with the components of the oLFP during baseline, epileptogenesis and SRS. We expect it will require 12 months to complete Aim 2.

**Aim 3)** The same protocol as aim 2, but the li-pilo model will be substituted with the later fluid percussion traumatic brain injury model (LFP, a model with which we have 4 years experience[13]). The animals will be randomly assigned into 4 groups 1) LFP/AAV-ChR2, 2) shamLFP/AAV-ChR2, 3) LFP/AAV-EYFP, 4) shamLFP/AAV-EYFP. Following baseline recording of 2 weeks LFP will be delivered. Signs of epileptogenesis will be monitored using AEP and oLFP for 8 months. We expect it will require 12 months to complete Aim 3.

**Impact:** Civilian patients that receive severe TBI are 30 times more likely to develop epilepsy, and soldiers who have sustained blast injury are at even greater risk [4,6]. Because of the nature of modern conflict and the long duration of the latent period in humans (months to years), it can be expected that many veterans and active duty warfighters will develop epilepsy, in addition to those that already suffer from it [3,4]. This long latent period offers some advantages though, if AEP biomarkers can be further explored and characterized, it is very possible that they could be used to screen high-risk individuals who have been exposed to brain trauma[8]. By using a well characterized model of epilepsy (li-pilo), with a relatively short latent period and high rate of SRS, to initially characterize this novel biomarker then extending these findings to the slower model of TBI induced epilepsy (LFP), we hope to speed up the potential of this biomarker for translational use. Inexpensively measured AEP's in individuals exposed to brain trauma could lead to enhanced anti-epileptogenic strategies by identifying those individuals most vulnerable to epilepsy development before the manifestation of spontaneous seizures.

# Morphological Alterations in Chronically Recorded Hippocampal Auditory Evoked Potentials as a Novel Biomarker of Epileptogenesis

Alexander M. Benison[1], Francois Meyer[2], Florencia Bercum[1], Krista M. Rodgers[1], Zachariah Smith[1], and Daniel S. Barth[1]

[1]*Department of Psychology and Neuroscience,* [2]*Department of Electrical Engineering,*

*University of Colorado, Boulder, Colorado, U.S.A.*

Address correspondence and reprint requests to:

Daniel S. Barth

Department of Psychology and Neuroscience

University of Colorado

Campus Box 345

Boulder, CO 80309 U.S.A.

e-mail: daniel.barth@colorado.edu

Running title: *HIPPOCAMPAL AEP AND EPILEPTOGENESIS*

4000 words

6 Figs

**Summary: (300 words max)**

*Purpose:* In temporal lobe epilepsy (TLE), an initial precipitating injury is typically followed by a seizure free epileptogenic period of months to years before the appearance of spontaneous and recurring seizures. This period of post-traumatic epileptogenesis is often referred to as the “latent” or “silent” period due to a seemingly normal behavioral state (i.e. absence of non-convulsive and convulsive seizures). While the silent period offers and ideal interval for possible intervention and epilepsy prevention, there is a need for biomarkers that can index epileptogenesis prior to appearance of spontaneous seizures and facilitate anti-epileptogenic strategies.

*Methods:* Instead of passively monitoring the brain’s spontaneous activity during the silent period, we actively monitored excitability changes in the hippocampus using chronically recorded auditory evoked field potentials (hAEP) in lithium/pilocarpine model of TLE in the rat. We applied pattern classification methods to identify distinct phases of epileptogenesis across animals.

*Results:* hAEP displayed highly repeatable changes in waveform morphology during the silent period leading up to and continuing beyond the first spontaneous seizure. Pattern classification accurately universally identified phases of epileptogensis based on morphological changes in the hAEP across rats. The hAEP could also predict a subset of rats that did not develop seizures.

*Conclusions:* Sensory stimulation combined with pattern classification methods can serve as a sensitive and generalizable biomarker to chart epileptogensis before spontaneous seizures and to predict the probability of seizure development in acquired epilepsy.

Key words: Epilepsy, lithium pilocarpine, waveform, seizure, silent period, rodent, wavelet, spectral clustering

The transition from a normal biological state to an epileptic one is known as epileptogenesis. Little is known about physiological changes that occur during epileptogenesis largely because there are few biomarkers that directly or indirectly reflect these changes. The development of such biomarkers would not only facilitate research into physiological mechanisms giving rise to stages of epileptogenesis, but would also greatly expedite the development of pharmacological agents and medical devices that prevent, treat and possibly cure epilepsy[1].

Partial-onset epilepsies account for about 60% of all adult epilepsy cases, and temporal lobe epilepsy (TLE) is the most common type of partial epilepsy referred for epilepsy surgery and often refractory to antiepileptic drugs[2]. In TLE, an initial precipitating injury is typically followed by a seizure free epileptogenic period of months to years before the appearance of spontaneous and recurring convulsive seizures (the hallmark of epilepsy). The period of post-traumatic epileptogenesis is often referred to as the "latent" or "silent" period due to a seemingly normal behavioral state (i.e. absence of non-convulsive and convulsive seizures)[3]. There are, however, recent findings suggesting that this period is not electrographically silent and that the appearance of epileptiform population spikes[4-6] and high frequency oscillations[7,8] may be associated with the probability of developing epilepsy. Yet, these are passive measurements of brain function that confine analysis to the sporadic occurrence of spikes. In addition, high frequency oscillations do not appear to show progressive changes during epileptogenesis. While passive biomarkers may have a distinct predictive value heralding the appearance of spontaneous seizures, our goal was to develop a novel biomarker that could be used to continuously and *actively* probe the progression from a normal brain state to an epileptic

one.

Auditory, along with other sensory evoked potentials, can be recorded from a variety of limbic structures due to their role in sensory integration, learning, and memory[9-17]. We hypothesized that electrophysiological recordings of sensory responses in limbic regions most responsible for, and affected by, TLE could be used as a biomarker to actively quantify excitability changes during the silent period of epileptogenesis. We targeted the hippocampus for chronic monitoring in a lithium-pilocarpine animal model of TLE. This decision was based on the established role of the hippocampus in TLE and also on evidence for robust hippocampal auditory evoked potentials (hAEP) recorded from electrodes implanted in auditory responsive regions[15,16]. By dynamically probing the system with auditory stimuli (unlike perforant path electrical stimulation) we were able to establish the responsiveness of normal hippocampal sensory circuits and subsequently characterize stereotyped changes in hAEP morphology associated with epileptogenesis.

## METHODS

Twenty adult viral-free male Sprague-Dawley rats (Harlan Laboratories, Madison, WI) were housed in temperature (23 ± 3 °C) and light (12:12 light: dark) controlled rooms with *ad libitum* access to food and water. All procedures were performed in accordance with University of Colorado Institutional Animal Care and Use Committee guidelines for the humane use of laboratory rats in biological research.

### Chronic video/EEG and hAEP recording

Aseptic surgical procedures were used for all chronic preparations. Under isoflurane (Abbott Laboratories) anesthesia (2.5%), adult, male, Sprague-Dawley rats (Charles River, 250-300g) were implanted with a Teflon-coated hippocampal wire electrode (AP: -3.8 mm, ML: 1.1 mm, DV: 3.8 mm), a ground screw (AP: -1 mm, ML: 1 mm), and a reference screw over the occipital bone. Buprenorphin (0.1mg/kg, subcutaneously) was administered immediately after the surgical procedure and again every 12 hr for a 72 hr period. Following a 2-week recovery period, animals were tethered to an electrode harness (Plastics One, 363) and slip ring commutator (Plastics One, SL6C) permitting free movement for 24/7 video/EEG monitoring throughout the duration of the experiment. Spontaneous EEG signals were amplified and then digitized at 500 Hz. Chambers for chronic recording were fitted with top-mounted speakers to provide auditory click stimulation evoking hAEP. Hippocampal responses to 120 monopolar square-wave clicks (0.1 ms duration, 2 sec ISI, 45dB SPL) were amplified (10,000x), digitized (10 kHz), averaged and stored. hAEPs were collected every 30 minutes 24/7 for the entire experiment. Spontaneous EEG and video were stored for subsequent seizure detection. Chronic hAEPs were recorded from 4 groups: animals that

received lithium-pilocarpine and eventually developed spontaneous recurrent seizures (SRS) (li-pilo/SRS, n=10), a subset of animals that received li-pilo and did not develop SRS (li-pilo/non-SRS, n=3), animals that received all drug injections in the li-pilo model (lithium, scopolamine, peraldehyde and saline) where pilocarpine was substituted with the vehicle saline (Veh-drug, n=3), and animals that only had chronic electrodes implanted with no injections (control, n=4).

**Lithium Pilocarpine (li-pilo) model of TLE**

After full recovery from chronic electrode implantation (2 weeks) and an additional week of chronic recording of baseline video/EEG and hAEP, we administered an IP injection of Lithium chloride (3mEq/kg, 1ml/kg, Sigma, St. Louis, MO). Twenty hours later, an IP injection of scopolamine (1 mg/kg, 1 ml/kg, Sigma, St. Louis, MO) was given to ameliorate any peripheral muscarinic effects of pilocarpine[18]. Twenty minutes after scopolamine administration a single injection of pilocarpine hydrochloride (50 mg/kg, i.p., 1 ml/kg, Sigma) was administered. After 1 hour of status epilepticus (SE), the animals were administered an IM dose of paraldehyde (0.3mg/kg, Sigma, St. Louis, MO) to terminate convulsions. A second dose of paraldehyde was given 8-10 hours later and 5 ml of Saline co-administered sub-cutaneously with both doses. We found that paraldehyde was much more effective than diazepam for increasing survival rates and terminating convulsions. Additionally, we found that this protocol yielded a subset of animals that did not develop spontaneous recurrent seizures (SRS)[19,20] for comparison to those that did. Animals were kept on post-surgical nutritional gel (Diet Gel, Clearh2o, Portland, OR) and their water was replaced with an electrolyte sports drink for 72 hours.

Vehicle-drug animals received all drug injections except pilocarpine, which was replaced with a 0.9% saline vehicle injection.

**Seizure detection**

Visual detection of seizures was done using custom software. EEG for a given rat was displayed in 30 min blocks on high-resolution monitors. Electroencephalographic seizures were differentiated from background noise by the appearance of large-amplitude (at least three times baseline), high frequency (minimum of 5 Hz) activity, with progression of the spike frequency that lasted for a minimum of 20 s. Behavioral video data was used to determine seizure intensity on the Racine scale[21] and to confirm EEG seizure activity versus potential animal generated noise such as eating and grooming.

**Pattern classification of hAEP**

Pattern classification of hAEP was based on established methods of spectral clustering. For each rat, representative hAEP waveforms were selected for 4 experimental phases: baseline (one week period before li-pilo and SE), post-SE (two day period following SE termination), pre-SRS (1 week period prior to the first spontaneous seizure, or at 2 weeks post SE in the rats who did not have SRS), and 30 days after the first SRS. Features of the hAEP best discriminating between experimental phases were derived through differencing coefficients of the wavelet decomposition of hAEP for each phase. The dimensionality of the feature space was then reduced by computing 3 eigenvectors from a matrix representing a Gaussian similarity index between extracted feature from all pairs of hAEP for the animals used for training the pattern classifier.

**Histology**

At the termination of all experiments animals were deeply anesthetized, perfused with 2.5% paraformaldehyde and Nissl stained to verify electrode placement.

## RESULTS

### Longitudinal mapping of the hAEP

The electrode for chronic hAEP recording in the auditory responsive area of the right hippocampus[10,12-14,16] was located at Bregma -3.8 mm, 1.1 mm lateral to midline and 3.8 mm ventral in the rostral-dorsal Dentate gyrus (Fig. 1A). The averaged hAEP had a prototypical morphology beginning with a negative component peaking at approximately 40 ms (Fig. 1B; N1; baseline trace) followed by a positive component peaking at approximately 100 ms (Fig. 1B; P1; baseline trace). Color maps were computed to visualize the evolution of hAEP morphology over the duration of the experiment. Figure 1B shows a typical example of the hAEP mapped for a single rat. Successive hAEP averaged every 30 min are plotted longitudinally along the Y-axis from the start of the experiment (Fig. 1B; top) to 30 days post-SE (Fig. 1B; bottom). The map was normalized and smoothed across days for better visualization of gross changes in morphology without circadian amplitude oscillations[22]. Corresponding waveforms averaged across 72 hours from sections of baseline, post-SE, pre-SRS, and post-SRS are superimposed on the normalized map (Fig. 1B). The N1 and P1 (Fig. 1B; blue and red, respectively) remained stable over the 1-week baseline period. Immediately following SE there was a gross attenuation of hAEP (Fig. 1B; post-SE) with delayed recovery (1-2 day) and progressively increased amplitude along with broadening and increased post-stimulus latency of the amplitude peaks during the silent period of epileptogenesis (Fig. 1B; pre-SRS). Morphological changes continued after SRS had begun (Fig. 1B, post-SRS).

**Quantification of hAEP morphology changes during epileptogenesis**

Figure 2 shows chronically recorded hAEPs averaged across animals in each group (li-pilo/SRS, li-pilo/non-SRS, veh-drug and control) collapsed across 72 hours at each time point described in Figure 1B; baseline, post-SE (or post vehicle), pre-SRS (or at 10 days post vehicle injection in animals that did not develop SRS), and 30 days post-SE or vehicle. Figure 3 charts parameters quantified for the hAEP for these groups and time points.

No morphology differences across groups in the baseline hAEP were observed (Fig. 2A, Fig. 3) with notable exception of decreased P1 amplitude in no-SRS animals ($p<.01$; Fig. 2A, Fig. 3B). Compared to baseline, at 72 hours post-SE (Fig. 2B), there were characteristic changes in hAEP morphology of the li-pilo/SRS rats (Fig. 2.1B). The N1 amplitude was decreased (Fig. 3A; $p<.05$), whereas the latency (Fig. 3C; $p<.05$) and duration (Fig. 3E; $p<.05$) where increased. Similar changes were apparent in the P1 amplitude (Fig. 3B; $p<.05$), latency (Fig. 3D; $p<.01$) and duration (Fig. 3F; $p<.01$) in these animals. In the li-pilo/no-SRS group, morphology changes at 72 hours post SE (Fig. 2.2B) were restricted to in decreases in peak amplitude of the N1 (Fig. 3A; $p<.05$) and P1 (Fig. 3B; $p<.05$). No significant differences were seen in either the latencies or durations of the N1 or P1. The hAEP of the veh-drug group did not differ from baseline at this time-point except for an amplitude decrease in the N1 and P1 that approached significance ($p=.06$ and $p=.07$ respectively).

A substantial recovery of the hAEP was seen at 72 hours prior to the first SRS (11.5 ±3 days after status; Fig. 2.1C) and at 10 days post-vehicle in animals that did not develop SRS (Fig. 2.2C). In both groups, the N1 and P1 amplitudes recovered to baseline

levels. In the li-pilo/SRS group, the N1 latency (Fig. 3C) and duration (Fig. 3E) remained longer (Fig. 2.1c; arrows; $p<.01$) compared to baseline (Fig. 2.1C; light red line), as did the latency (Fig. 3D) and duration (Fig. 3F) of the P1 (Fig. 2.1c; arrows; $p<.01$). In contrast, hAEP component latencies and durations in li-pilo/no-SRS group significantly differed from the li-pilo/SRS group (Fig. 3C-F; $p<.01$) in that they had largely recovered (Fig. 2.2C; "*") with no significant differences from baseline. Morphology changes in the li-pilo/SRS group remained at 30 days post SE, whereas hAEP of the li-pilo/no-SRS, veh-drug and chronic electrode control groups were not distinguishable from baseline by the end of the experiment.

**Pattern classification of hAEP morphology changes during epileptogenesis**

This work is still underway and will be concluded this month.

**DISCUSSION (awaiting conclusion of pattern classification results)**

(summarize results)

(relate to literature)

(future studies)

The hippocampus is not privileged to primary sensory input as the perirhinal and postrhinal/parahippocampal cortices provide the major polysensory input to the hippocampus through their entorhinal connections and are the recipients of differing combinations of sensory information from primary and secondary sensory cortices [23]. Because of this serial relay of the auditory signal prior to its appearance in the hippocampus, as the hAEP, it will be critical in future studies to examine if changes occur at other locations along the auditory pathway that project both directly to the parahippocampus, such as secondary auditory cortex, and entorhinal cortex, or indirectly via other regions in the ascending auditory pathway such as, the brainstem, thalamus and primary auditory cortex. By doing simultaneous chronic recordings of these areas in conjunction with recording the hAEP, multifaceted interactions between the hippocampus and it's various input/output areas might be examined in real-time. These sensory integration areas that feed into and receive output from the hippocampus have been shown to participate in epileptogenesis [24-26] and seizure generalization [27] so studying changes in the auditory signal at various points along the ascending pathway using an evocable, biomarker could offer valuable insight into the multifaceted interactions occurring between, and among, these cortical and subcortical structures during epileptogenesis.

In order to further understand the mechanisms underlying the pathological changes predicted by the morphological changes of the hAEP, multiunit, chronic recordings as well as single unit acute studies combined with pharmacological manipulations should undertaken in order to further understand the fundamental network physiology that generates the various hAEP components. Unlike cortical sensory evoked

potentials [28-30], a very limited number of experiments have been conducted examining the anatomical and cellular generators of hippocampal sensory evoked field potentials [10,12-15,31]. Due to the relatively limited amount of basic, foundational, knowledge about the neurophysiology of the hAEP it is difficult to speculate on the principal dysfunction that leads to altered hippocampal sensory potentials, but it also offers promise that by dissecting the individual components of the hAEP and reveling how they are generated, a greater understanding of the intrinsic mechanisms of epileptogenesis may be uncovered in the process. This hints that changes in the hAEP are not just an epiphenomena correlated with the development of epilepsy, but that each individual componential change within the hAEP may also contain complex, valuable, information about the vary cellular or network alterations that underlie the transition from a non-pathological brain state to an epileptic one. Further, the fact that the the hAEP is a probe-able, physiologically relevant measure that can be evoked in both chronic and acute conditions with minimal invasiveness makes it broadly versatile in its scientific and diagnostic applications. Further discoveries about the nature of epileptogenesis may occur when this type of analysis is combined with other biomarkers such as high frequency oscillations and interictal spikes

**Acknowledgements:** This work was supported by the U.S. Army Medical Research and Material Command (grant PR100040).

**References**


1. Engel J Jr., Pitkänen A, Loeb JA, Edward Dudek F, Bertram EH III, Cole AJ, et al. Epilepsy biomarkers. Epilepsia. 2013 Aug 1;54:61–9.

2. Téllez-Zenteno JF, Hernández-Ronquillo L. A Review of the Epidemiology of Temporal Lobe Epilepsy. Epilepsy Research and Treatment. 2012;2012(5):1–5.

3. Engel J Jr. Introduction to temporal lobe epilepsy. Epilepsy Res. 1996 Dec;26(1):141–50.

4. Huneau C, Benquet P, Dieuset G, Biraben A, Martin B, Wendling F. Shape features of epileptic spikes are a marker of epileptogenesis in mice. Epilepsia. 2013 Dec;54(12):2219–27.

5. Huneau C, Demont-Guignard S, Benquet P, Martin B, Wendling F. Time-domain features of epileptic spikes as potential bio-markers of the epileptogenesis process. Conf Proc IEEE Eng Med Biol Soc. 2010;2010:6007–10. PMCID: PMC3009990

6. White A, Williams PA, Hellier JL, Clark S, Dudek FE, Staley KJ. EEG spike activity precedes epilepsy after kainate-induced status epilepticus. Epilepsia. 2010 Mar;51(3):371–83. PMCID: PMC2906396

7. Bragin A, Wilson CL, Almajano J, Mody I, Engel J. High‐frequency Oscillations after Status Epilepticus: Epileptogenesis and Seizure Genesis. Epilepsia. Wiley Online Library; 2004;45(9):1017–23.

8. Jacobs J, Staba R, Asano E, Otsubo H, Wu JY, Zijlmans M, et al. High-frequency oscillations (HFOs) in clinical epilepsy. Prog Neurobiol. 2012 Sep;98(3):302–15. PMCID: PMC3674884

9. Vinogradova OS. Hippocampus as comparator: role of the two input and two output systems of the hippocampus in selection and registration of information. Hippocampus. 2001;11(5):578–98.

10. Bellistri E, Aguilar J, Brotons-Mas JR, Foffani G, Menendez de la Prida L. Basic properties of somatosensory-evoked responses in the dorsal hippocampus of the rat. J Physiol (Lond). 2013 Feb 18. PMCID: PMC3678049

11. Kimura A, Donishi T, Okamoto K, Imbe H, Tamai Y. Efferent connections of the ventral auditory area in the rat cortex: implications for auditory processing related to emotion. Eur J Neurosci. 2007 Apr 25;25(9):2819–34.

12. Miller CL, Freedman R. The activity of hippocampal interneurons and pyramidal cells during the response of the hippocampus to repeated auditory stimuli. Neuroscience. 1995 Nov;69(2):371–81.

13. Brankack J, Buzsáki G. Hippocampal responses evoked by tooth pulp and acoustic stimulation: depth profiles and effect of behavior. Brain Res. 1986 Jul 23;378(2):303–14.

14. Foster TC, Christian EP, Hampson RE, Campbell KA, Deadwyler SA. Sequential dependencies regulate sensory evoked responses of single units in the rat hippocampus. Brain Res. 1987 Apr;408(1-2):86–96.

15. Ruusuvirta T, Astikainen P, Wikgren J, Nokia M. Hippocampus responds to auditory change in rabbits. Neuroscience. 2010 Sep 29;170(1):232–7.

16. Jirsa R, Poc P, Radil T. Hippocampal auditory evoked response threshold in the rat: behavioral modulation. Brain Res Bull. 1992 Feb;28(2):149–53.

17. Naumann RT, Kanwal JS. Basolateral amygdala responds robustly to social calls: spiking characteristics of single unit activity. J Neurophysiol. 2011 May;105(5):2389–404. PMCID: PMC3094175

18. Scorza FA, Arida RM, Naffah-Mazzacoratti MDG, Scerni DA, Calderazzo L, Cavalheiro EA. The pilocarpine model of epilepsy: what have we learned? An. Acad. Bras. Cienc. 2009 Sep;81(3):345–65.

19. Morrisett RA, Jope RS, Snead OC III. Effects of drugs on the initiation and maintenance of status epilepticus induced by administration of pilocarpine to lithium-pretreated rats. Exp Neurol. Elsevier; 1987;97(1):193–200.

20. Curia G, Longo D, Biagini G, Jones RSG, Avoli M. The pilocarpine model of temporal lobe epilepsy. J Neurosci Methods. 2008 Jul;172(2):143–57. PMCID: PMC2518220

21. Racine RJ. Modification of Seizure Activity by Electrical Stimulation .2. Motor Seizure. Electroencephalography and Clinical Neurophysiology. 1972;32(3):281–&.

22. Phillips DJ, Schei JL, Meighan PC, Rector DM. State-dependent changes in

cortical gain control as measured by auditory evoked responses to varying intensity stimuli. Sleep. American Academy of Sleep Medicine; 2011;34(11):1527.

23. Burwell RD. The parahippocampal region: Corticocortical connectivity. Ann N Y Acad Sci. 2000;911:25–42.

24. McIntyre DC, Gilby KL. Mapping seizure pathways in the temporal lobe. Epilepsia. 2008 Mar;49(s3):23–30.

25. Uva L, Librizzi L, Wendling F, de Curtis M. Propagation dynamics of epileptiform activity acutely induced by bicuculline in the hippocampal-parahippocampal region of the isolated Guinea pig brain. Epilepsia. 2005 Dec;46(12):1914–25.

26. Biagini G, D'Antuono M, Benini R, de Guzman P, Longo D, Avoli M. Perirhinal cortex and temporal lobe epilepsy. Frontiers in Cellular Neuroscience. 2013;7:130.

27. Fukumoto S-I, Tanaka S, Tojo H, Akaike K, Takigawa M. Perirhinal cortical lesion suppresses the secondary generalization in kainic acid-induced limbic seizure. Psychiatry Clin. Neurosci. 2002 Oct;56(5):561–7.

28. Barth DS, Di S. Three-dimensional analysis of auditory-evoked potentials in rat neocortex. J Neurophysiol. 1990.

29. Simpson GV, Knight RT. Multiple brain systems generating the rat auditory evoked potential. II. Dissociation of auditory cortex and non-lemniscal generator systems. Brain Res. 1993.

30. SHAW NA. The Auditory Evoked-Potential in the Rat - a Review. Prog

Neurobiol. 1988;31(1):19–45.

31. Itskov PM, Vinnik E, Honey C, Schnupp J, Diamond ME. Sound sensitivity of neurons in rat hippocampus during performance of a sound-guided task. J Neurophysiol. 2012 Apr 1;107(7):1822–34.

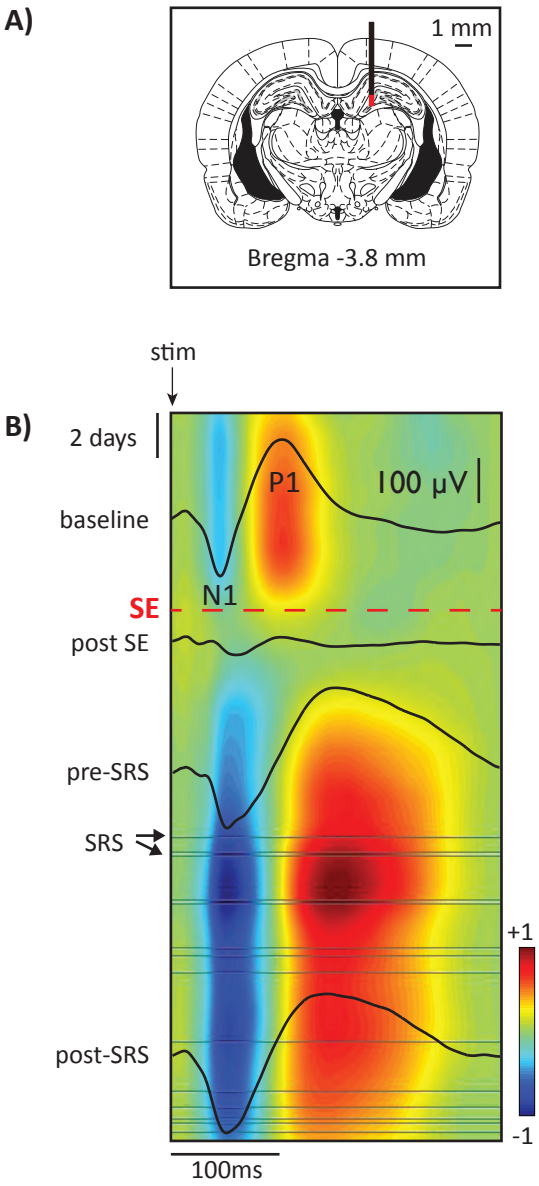
A)
1 mm
Bregma -3.8 mm
stim
B)
2 days
P1
100 µV
baseline
N1
SE
post SE
pre-SRS
SRS
+1
post-SRS
-1
100ms

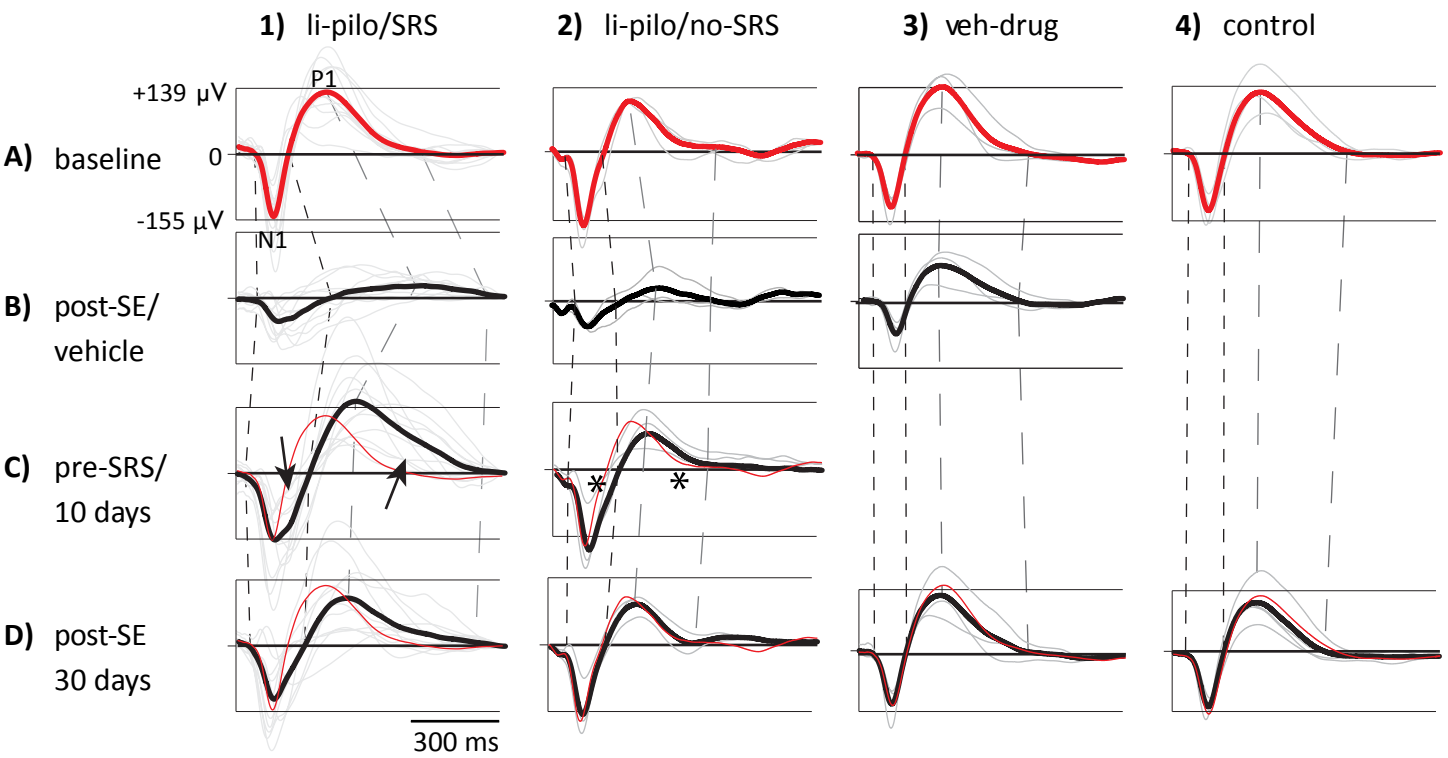
1) li-pilo/SRS
2) li-pilo/no-SRS
3) veh-drug
4) control
+139 µV
0
-155 µV
P1
N1
A) baseline
B) post-SE/ vehicle
C) pre-SRS/ 10 days
D) post-SE 30 days
300 ms

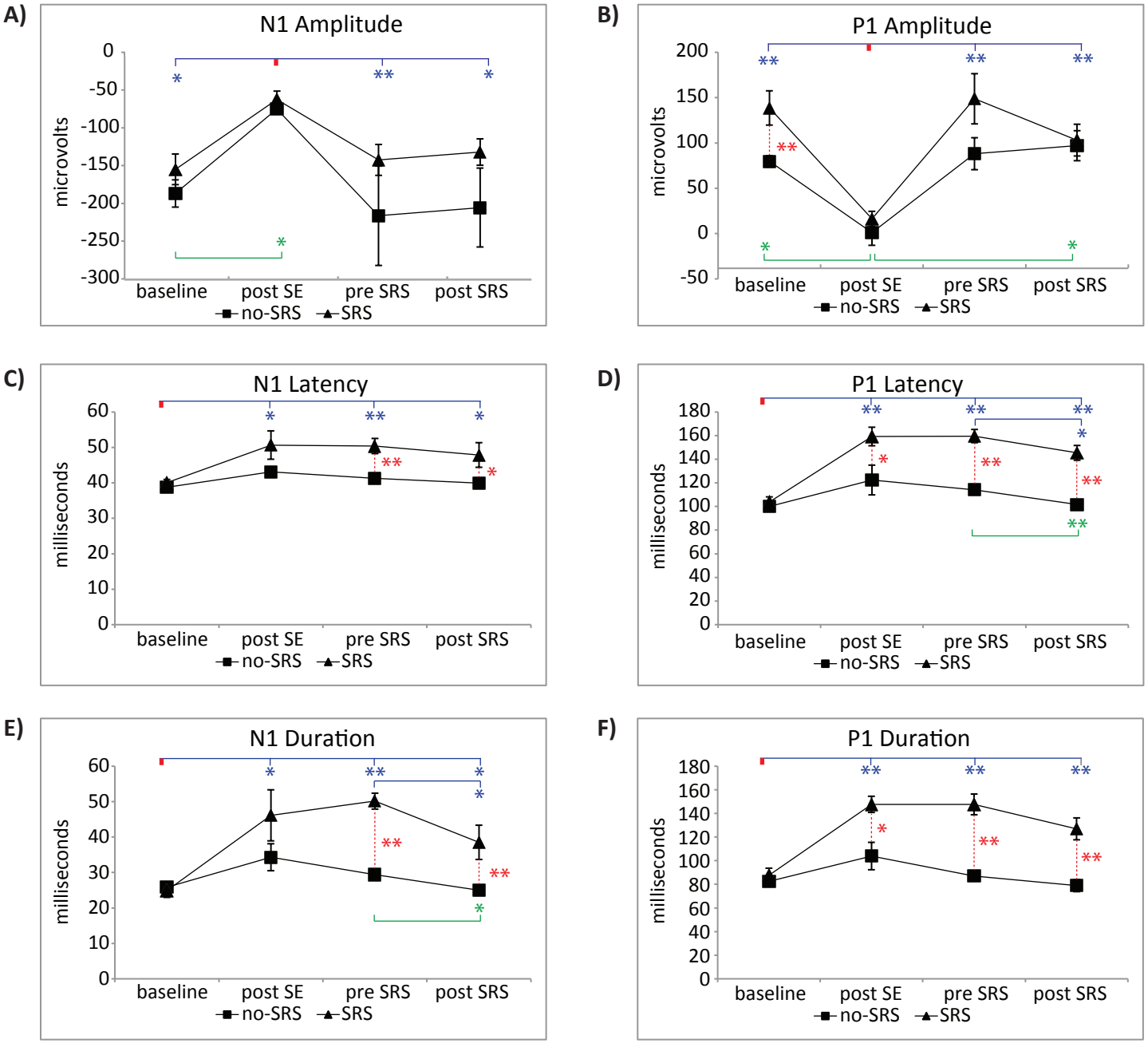
A)
N1 Amplitude
microvolts
0
-50
-100
-150
-200
-250
-300
baseline
post SE
pre SRS
post SRS
no-SRS
SRS
B)
P1 Amplitude
microvolts
200
150
100
50
0
-50
C)
N1 Latency
milliseconds
60
50
40
30
20
10
0
D)
P1 Latency
milliseconds
180
160
140
120
100
80
60
40
20
0
E)
N1 Duration
milliseconds
F)
P1 Duration
milliseconds

NEU-2013-3090-ver9-Rodgers_1P
Type: Research Article

JOURNAL OF NEUROTRAUMA XX:1–11 (XXXX XX, 2014)

DOI: 10.1089/neu.2013.3090

**Original Article**

# Reversal of Established Traumatic Brain Injury–Induced Anxiety-Like Behavior in Rats After Delayed, Postinjury Neuroimmune Suppression

Krista M. Rodgers,[1] Yuetiva K. Deming,[1] Florencia M. Bercum,[1] Serhiy Y. Chumachenko,[1] Julie L. Wieseler,[1] Kirk W. Johnson,[2] Linda R. Watkins,[1] and Daniel S. Barth[1]

## Abstract

Traumatic brain injury (TBI) increases the risk of neuropsychiatric disorders, particularly anxiety disorders. Yet, there are presently no therapeutic interventions to prevent the development of post-traumatic anxiety or effective treatments once it has developed. This is because, in large part, of a lack of understanding of the underlying pathophysiology. Recent research suggests that chronic neuroinflammatory responses to injury may play a role in the development of post-traumatic anxiety in rodent models. Acute peri-injury administration of immunosuppressive compounds, such as Ibudilast (MN166), have been shown to prevent reactive gliosis associated with immune responses to injury and also prevent lateral fluid percussion injury (LFPI)-induced anxiety-like behavior in rats. There is evidence in both human and rodent studies that post-traumatic anxiety, once developed, is a chronic, persistent, and drug-refractory condition. In the present study, we sought to determine whether neuroinflammation is associated with the long-term maintenance of post-traumatic anxiety. We examined the efficacy of an anti-inflammatory treatment in decreasing anxiety-like behavior and reactive gliosis when introduced at 1 month after injury. Delayed treatment substantially reduced established LFPI-induced freezing behavior and reactive gliosis in brain regions associated with anxiety and continued neuroprotective effects were evidenced 6 months post-treatment. These results support the conclusion that neuroinflammation may be involved in the development and maintenance of anxiety-like behaviors after TBI.

**Key words:** glial cell response to injury; inflammation; traumatic brain injury

## Introduction

Over 5.3 million people in the United States are living with traumatic brain injury (TBI)-related disabilities,[1] including anxiety disorders, which are among the most prevalent.[2–4]

The rates of a variety of anxiety disorders reported by patients with TBI are consistently elevated relative to general population rates,[3–5] and the risk for developing post-traumatic stress disorder (PTSD) remains elevated for years postinjury.[6–8] Because the temporal pattern of onset is variable and the etiology unclear, there are currently few interventions for the treatment of PTSD.

The ongoing inflammatory response after TBI is an emerging target for the treatment of post-traumatic anxiety. Extensive research has shown that chronic neuroinflammation continues for months to years after injury,[9–12] and evidence for chronic inflammation has been observed in a number of studies examining patients with PTSD, panic disorder, obsessive-compulsive disorder (OCD), and generalized anxiety disorder.[13–18] Glial activation may be involved in the development and maintenance of PTSD,[9–12] and mounting evidence supports the role of inflammatory processes in both TBI and anxiety disorders.

After injury, immune cells rapidly produce endogenous danger signals or ''alarmins,'' which function as potent effectors of innate defense and promote immune system activation by recruiting antigen-presenting cells (APCs) that relay and amplify the inflammatory response.[19] The resident APCs of the cenral nervous system (CNS) are microglia, which undergo marked recruitment and activation in response to danger signals,[20,21] triggering the onset of prolonged astrocytic activation through the production of proinflammatory cytokines, chemokines, and other proinflammatory mediators.[22,23]

Activated microglia are thought to contribute to the initiation and maintenance of astrogliosis, which is involved in neural cell damage and inhibition of regenerative responses through secretion of excessive neurotoxic substances, destabilization of neurotransmitter balance, disruption of synaptic connectivity, and excitotoxic neuronal death[24–28] and therefore may contribute to functional alterations of brain areas involved in post-traumatic anxiety.

[1]Department of Psychology and Neuroscience, University of Colorado, Boulder, Colorado.
[2]MediciNova, Inc., La Jolla, California.

Several studies have reported increased anxiety-like behavior in rodent TBI models,[29–32] including increased conditioned[33] and unconditioned[34] fear responses to both learned and novel stimuli. TBI in rodents also increases levels of activated glial cells and proinflammatory cytokines,[34–38] and administration of these cytokines increases anxiety-like behaviors.[29–32]

The aim of the present study was therefore to determine whether neuroinflammation is associated with the long-term maintenance of post-traumatic anxiety in an animal model. We examined the efficacy of delayed, immunosuppressive treatment (with a glial cell activation inhibitor, Ibudilast) in reducing anxiety-like behaviors and TBI-induced immunological damage.

## Methods

Twenty-four adult viral-free male Sprague-Dawley rats (275–325 g; Harlan Laboratories, Madison, WI) were housed in pairs in temperature- (23 ± 3°C) and light- controlled (12-h light/dark) rooms with *ad libitum* access to food and water. All procedures were performed in accord with University of Colorado (Boulder, CO) Institutional Animal Care and Use Committee guidelines for the humane use of laboratory rats in biological research. Rats were randomly assigned to the following groups ($n = 6$/group): sham + vehicle; sham + MN166; lateral fluid percussion injury (LFPI) + vehicle; and LFPI + MN166.

### *Lateral fluid percussion injury*

LFPI is the most commonly used animal model of TBI and has been shown to reliably replicate many of the pathological changes observed after human TBI, validating its use as a clinically relevant model of human TBI.[39] The LFPI used in this study has been described previously.[40] Briefly, LFPI rats were anesthetized with halothane (3% induction, 2.0–2.5% maintenance) and mounted in a stereotaxic frame. A 3.0-mm-diameter craniotomy was centered at 3 mm caudal to the bregma and 4.0 mm lateral of the sagittal suture, with the exposed dura remaining intact. A female Luer-Loc hub (inside diameter of 3.5 mm) was secured over the craniotomy with cyanoacrylate adhesive. After hub implantation, rats were removed from the stereotaxic frame and connected to the LFPI apparatus. The LFPI apparatus delivered an impact force (2.0 atmospheres; 20 ms), resulting in a moderate TBI. The injury cap was then removed, the scalp sutured, and rats were returned to their home cages for recovery. Sham-operated rats underwent identical surgical preparation, but did not receive the brain injury.

### *Ibudilast (MN166) administration*

MN166 (MediciNova, San Diego, CA) is a relatively nonselective phosphodiesterase inhibitor with anti-inflammatory actions by glial cell attenuation.[41,42] Treated rats received a 5-day dosing regimen of once-daily MN166 injections (10 mg/kg, subcutaneously), beginning at 30 days after LFPI. Weight was recorded before each dosing and treatment administered at the same time each day to maintain constant levels across a 24-h period. Dose selection was based on previous animal pharmacology results[43] showing MN166 to be safe and well tolerated, yielding plasma concentration-time profiles commensurate with high-dose regimens in clinical development. MN166 administered by this regimen yields plasma and CNS concentrations that are linked to molecular target actions, including, most potently, macrophage migration inhibitory factor (MIF) inhibition [44] and, secondarily, phosphodiesterases −4 and −10 inhibition.[45] The relevance of MIF inhibition in disorders of neuroimmune function, such as neuropathic pain, has recently been well demonstrated.[46]

### *Neuromotor tests*

Baseline testing of motor, vestibular, and locomotive performance in all groups was conducted immediately before surgery and again at 1 month after injury (Fig. 1). These tests included ipsi- and contralateral assessment of fore- and hindlimb use to assess motor function, locomotion, limb use, and limb preference,[47,48] toe spread to assess gross motor response,[49] placing to assess visual and vestibular function,[50,51] catalepsy rod test to assess postural support and mobility,[52] bracing to assess postural stability and catalepsy,[53,54] and air righting to assess dynamic vestibular function.[55,56] Scoring ranged from 0 (severely impaired) to 5 (normal strength and function). Individual test scores were summed, and a composite neuromotor score (0–45) was then generated for each animal. In addition to the composite neuromotor score, limb-use asymmetry was assessed during spontaneous exploration in the cylinder task, a common measure of motor forelimb function after CNS injury in rats,[50,57] and postinjury locomotor activity was assessed through distance traveled on a running wheel; both tasks were scored for 5 min under red light (~90 lux).

### *Behavioral measures*

The core features of anxiety in humans include feelings of apprehension or dread both with or without autonomic signs and symptoms, and in the case of post-traumatic anxiety (PTSD), also includes reexperiencing trauma, avoidant behavior, and hypervigilance.[4] The immediate shock paradigm was chosen to elicit PTSD-related traits of abnormally elevated fear responses and hypervigilance. In traditional contextual fear conditioning, rats are placed in a context and shock is delayed for a period of time, allowing for association between the contextual cues and the shock, resulting in increased freezing during later testing. However, rats that are immediately shocked upon placement in a shock chamber show no increase in freezing behavior during later testing. This phenomenon is known as the immediate shock deficit and results in failure to display contextual fear conditioning because the rats do not have time to construct a representation of the context,[58–60] indicating a lack of association between the context and shock. However, we previously found that LFPI rats show increases in freezing responses even in the absence of fear conditioning.[34] These unconditioned freezing responses may reflect pathological anxiety, which involves exaggerated fear, hypervigilance, and readiness to respond to danger or negative events,[61] because freezing behavior is part of an anticipatory response to stress or danger. Shock was chosen as the stressor because it resulted in anxiety-like freezing behavior, which is a simple reproducible response elicited as a defense reaction in both conditioned and unconditioned fearful situations.[62]

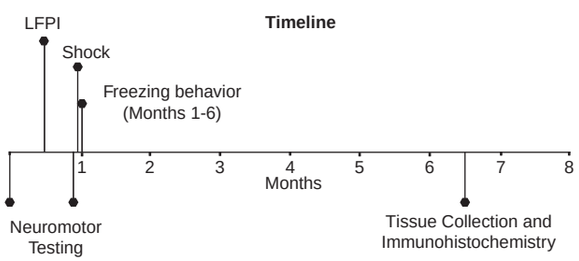


**FIG. 1.** Experimental timeline. Neuromotor testing included measures of motor, vestibular, and locomotive performance and was conducted immediately before LFPI and again at 1 month postinjury. A single shock was delivered after neuromotor testing was completed at the 1-month time point, and freezing behavior was assessed at 1 through 6 months postinjury. Tissue was then collected for immunohistochemistry. LFPI, lateral fluid percussion injury.

A novel environment was used for testing to ensure that there was no association between the context and shock, because rats were never tested in the context where the shock occurred. The novel context was a standard rat cage with one vertically and one horizontally striped wall. No aversive stimuli were introduced in this context and no conditioning occurred. Rats were tested (5 min) and the percent of freezing behavior was assessed. Freezing was defined as the absence of movement, except for heart beat/respiration, and was recorded in 10-sec intervals. Freezing behavior in the novel environment was measured after administration of a foot shock in a separate apparatus. The shock apparatus consisted of two chambers placed inside sound-attenuating chests. The floor of each chamber consisted of 18 stainless steel rods (4 mm in diameter), spaced 1.5 cm center to center and wired to a shock generator and scrambler (Colbourn Instruments, Allentown, PA). An automated program delivered a 2-sec/1.5-mA electric shock. Rats were transported in black buckets and shocked immediately upon entry to chambers. After shock, rats were returned to their home cages.

### *Timeline for behavioral testing*

Testing was performed at 1 through 6 months postinjury. A single shock was delivered after neuromotor testing was completed at the 1-month time point.

### *Immunohistochemistry*

Rats were intracardially perfused with 0.9% saline and tissue was collected, then fixed with 4% paraformaldehyde (PFA) overnight at 4°C. Tissue was transferred to a 30% sucrose phosphate-buffered saline solution for 1–2 days, then stored at −80°C. Brains were sectioned at 20 $\mu$m and mounted onto SuperFrost Plus slides (Fisher Scientific, Pittsburgh, PA) using a cryostat at −22°C. Brain sections were postfixed with 4% PFA for 15 min at room temperature, then treated with 0.3% $H_2O_2$ for 30 min at room temperature. Immunoreactivity in brain regions associated with anxiety (insula and amygdala) was assessed for markers of microglia (CD11b/c; OX42 labeling) and astrocytes (glial fibrillary acidic protein; GFAP), using an avidin-biotin-horseradish peroxidase (ABC) reaction.[63] Sections were incubated at 4°C overnight in either mouse anti-rat OX-42 (1:100; BD Biosciences Pharmingen, San Jose, CA) or mouse anti-pig GFAP (1:100; MP Biomedicals, Aurora, OH). The next day, sections were incubated at room temperature for 2 h with biotinylated goat anti-mouse immunoglobulin G antibody (1:200; Jackson ImmunoResearch, West Grove, PA). Sections were washed and incubated for 2 h at room temperature in ABC (1:400; Vector Laboratories, Burlingame, CA) and reacted with 3',3-diaminobenzidine (Sigma-Aldrich, St. Louis, MO). Sections were air-dried overnight and then dehydrated with graded alcohols, cleared in Histoclear and cover-slipped with Permount (Fisher Scientific, Fairlawn, NJ).

### *Image analysis*

Slides were viewed with an Olympus BX-61 microscope, using Olympus Microsuite software (Olympus America, Melville, NY), with bright-field illumination at 10× magnification. Densitometric analysis was performed using Scion Image software. Images were analyzed, under blinded conditions, in National Institutes of Health ImageJ (NIH; Bethesda, MD) using grayscale. Signal pixels of a region of interest (ROI) were defined as having gray values 3.5 standard deviations above the mean gray value of a cell-poor area close to the ROI. The number of pixels and the average gray values above the set background were then computed for each ROI and multiplied, giving an integrated densitometric measurement. Six measurements were made for each ROI; measurements were then averaged to obtain a single integrated density value per rat, per region.

### *Statistical analyses*

Results are expressed as mean ± standard error of the mean. Analyses for behavioral measures used analysis of variance (ANOVA) with repeated measures (time after injury) and treatment as the independent variable. The integrated density was measured at one time point (6 months postinjury) and utilized one-way ANOVAs to compare regions between groups. Tukey's honestly significant difference was used to conduct planned pair-wise comparisons to follow up significant overall ANOVAs. Data were analyzed using SPSS® Statistics software (SPSS, Inc., Chicago, IL), and, in all cases, statistical significance was set at $p < 0.05$.

## Results

LFPI-induced increases in freezing behavior were observed when rats were placed in a novel context after shock in a separate environment (Fig. 2; $F(3, 20) = 9.029$; $p = 0.001$). Exposed only to this minor additional stressor and before treatment with either MN166 or vehicle, LPFI rats (Fig. 2, white and black bars) froze approximately twice as long as sham-operated rats (Fig. 2, light and dark gray bars) at the 1-month time point: LFPI + vehicle ($p < 0.03$ vs. sham + vehicle and sham + MN166) and LFPI + MN166 ($p < 0.03$ vs. sham + vehicle and sham + MN166), whereas both LFPI groups (before treatment or vehicle) did not differ ($p = 0.94$) statistically. ◀F2

At 2 months postinjury, after treatment with MN166 or vehicle, freezing in both sham-operated groups remained constant at approximately 25%. There was a drastic reduction (25%) in freezing behavior in MN166-treated rats, with untreated LFPI + vehicle rats freezing approximately 20% more than LFPI + MN166 rats. Freezing differences between sham + vehicle and sham + MN166 control groups and LFPI + MN166-treated rats no longer reached significance ($p = 0.49$ and $p = 0.26$, respectively). Freezing behavior in vehicle-injected LFPI rats remained consistently higher than sham controls ($p < 0.03$ vs. sham + vehicle and sham + MN166), with untreated rats freezing approximately 30% more than sham-operated controls at 2 months postinjury.

At 3 through 6 months postinjury, freezing averages for sham + MN166 and sham + vehicle control groups again remained constant (20 and 25%, respectively). Freezing behavior in vehicle-injected LFPI rats remained consistently higher than drug-treated controls at all post-treatment time points (3 through 6 months; $p < 0.03$ vs. sham + MN166). Freezing behavior in untreated LFPI rats remained higher than sham + vehicle controls at the 3- and 5-month time points postinjury (3 months, $p = 0.00$; 4 months, $p = 0.10$; 5 months, $p = 0.04$; 6 months, $p = 0.13$).

The behavior of MN166-treated LFPI rats remained indistinguishable from controls. Remarkably, freezing differences between sham + MN166- and sham + vehicle-injected control groups and LFPI + MN166-treated rats did not reach significance at any of the post-treatment time points (3 through 6 months; $p > 0.30$ vs. sham + vehicle and sham + MN166). In contrast, untreated LFPI + vehicle-injected rats froze significantly more than treated rats, approximately twice that of the treated rats across all post-treatment time points (3 through 6 months; $p < 0.03$ vs. LFPI + MN166).

The behavioral effects of surgery alone, independent of LFPI, were observed in the sham + vehicle group (Fig. 2, dark gray bars). This group froze more than the sham + MN166-treated group across most time points, in spite of having no significant differences in freezing behavior at baseline. Additionally, whereas the LFPI + vehicle group did freeze more than the sham + vehicle group across the entire study, they did not statistically differ at the 4- and 6-month time points, which may reflect behavioral, immunological, and morphological damage noted by other researchers in response to craniotomy alone.[64]

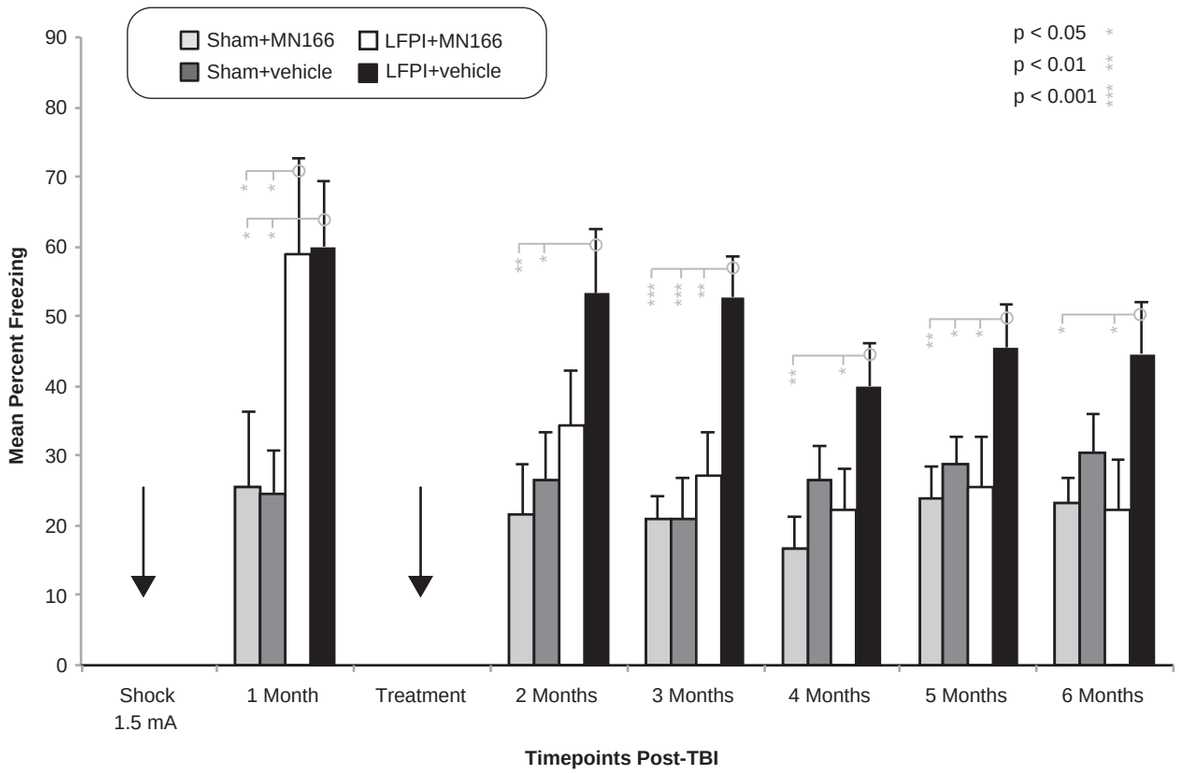


**FIG. 2.** Freezing behavior in novel context. Sham-operated rats froze approximately 25% before treatment with MN166 or vehicle, whereas LFPI rats froze at significantly higher rates (~60%), indicating greater anxiety-like behavior. After treatment, anxiety-like freezing behavior in LFPI + MN166 rats was reduced, (~25%), compared to LFPI + vehicle rats (~50%). This effect was significant at 3 months and remained through 6 months postinjury. Freezing in sham + MN166 and sham + vehicle rats could not be distinguished from LFPI + MN166-treated rats at all time points after treatment, whereas LFPI + vehicle-injected rats froze significantly more than both sham groups at all post-treatment time points, with the exception of the sham vehicle group at the 4- and 6-month time points. Data represent mean ± standard error of the mean. LFPI, lateral fluid percussion injury; TBI traumatic brain injury.

Disruption of blood vessels and nerves along the scalp suture, mechanical pressure of the drill, and atmospheric exposure when the bone flap is removed can alter vascular physiology and lead to structural and functional impairments after surgery alone.[64,65] Though traditional sham control groups are the standard in TBI research, these results suggest that injury resulting from surgery may increase freezing behavior, although sham + MN166-treated rats showed reductions in freezing behavior from baseline, which does indicate efficacy of MN166 treatment in reducing behavioral effects resulting from craniotomy alone. However, based on these results, future studies will need to include naïve or anesthesia-only controls to determine whether MN166 treatment can reduce anxiety-like freezing behavior to levels of uninjured controls.

LFPI-induced freezing responses were not influenced by motor, vestibular, or locomotive impairments, because neuromotor composite scores of the brain-injured groups (LFPI + MN166 and LFPI + vehicle) did not significantly differ from controls ($F(3, 20) = 0.383$; $p = 0.766$). Rats in all groups consistently received normal scores on fore- and hindlimb use, toe spread, placing, catalepsy rod, bracing, and air righting tests, indicating no impairments in motor, vestibular, or locomotive functioning as a result of TBI. There were also no significant between-group differences in limb-use asymmetry observed for contra- ($F(3, 20) = 0.058$; $p = 0.981$) and ipsilateral ($F(3, 20) = 0.285$; $p = 0.836$) forelimb use during vertical exploratory behavior in the cylinder task, indicating no limb-use bias resulting from injury (Fig. 3A). No significant between-group differences were found in locomotor performance evidenced by distance traveled during the running wheel activity ($F(3, 20) = 0.152$; $p = 0.464$), revealing no postinjury impairments in locomotion (Fig. 3B). ◀F3

OX-42 and GFAP immunoreactivity (reflecting microglia and astrocytic activation, respectively) was assessed in the insula and amygdala in MN166- and vehicle-injected LFPI rats for comparison to sham-operated controls. Representative images (20×), showing GFAP immunoreactivity in several of these regions, are shown in Figure 4, revealing normal astrocyte morphology in both MN166- and vehicle-injected sham controls. LFPI + vehicle rats showed clear signs of reactive astrocytes (Fig. 4; bottom row), whereas LFPI rats treated with MN166 (Fig. 4, third row) were difficult to differentiate from sham-operated control groups. ◀F4

Immunohistochemistry (IHC) was conducted to assess TBI-induced increases in gliosis and efficacy of MN166 in reducing reactive gliosis in brain regions associated with anxiety. Results revealed increased GFAP labeling in both brain regions examined, confirming that astroglial activation was significantly greater in LFPI + vehicle, compared to other, groups in insula (Fig. 5A, left ◀F5

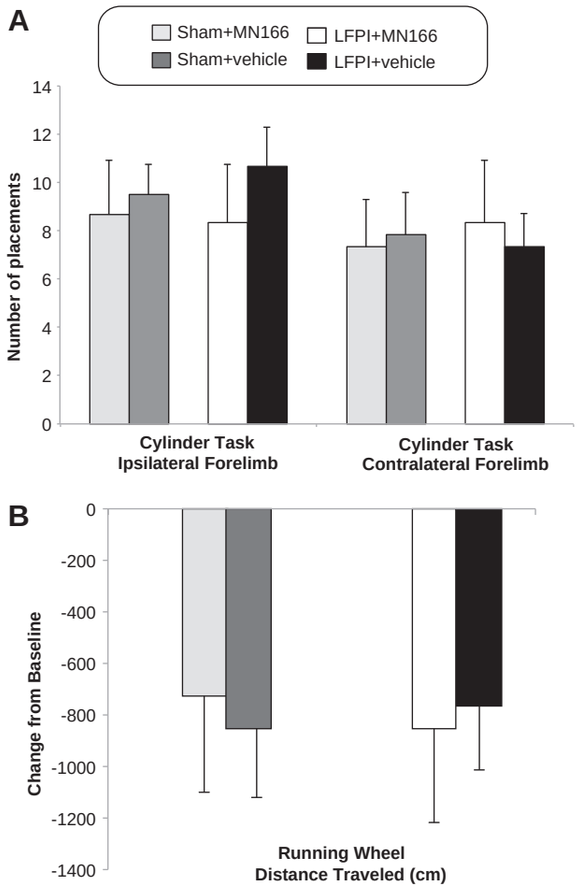


**FIG. 3.** Cylinder task and running wheel activity at 1 month postinjury. (**A**) LFPI rats mean number of spontaneous forelimb placements (ipsi- and contralateral) during exploratory activity in the cylinder test did not differ from controls at 1 month postinjury, indicating no deficits in limb use resulting from injury. (**B**) LFPI rats mean change in distance traveled in the running wheel activity did not significantly differ from controls at 1 month postinjury, indicating no impairments in locomotion resulting from injury. Data represent mean ± standard error of the mean. LFPI, lateral fluid percussion injury.

graph; $F(3, 140) = 3.761$; $p = 0.012$) and amygdala (Fig. 5B, left graph; $F(3, 140) = 6.025$; $p = 0.001$). In contrast, no differences in GFAP labeling were observed between sham-operated and LFPI + MN166 groups in either region (insula, $p > 0.60$ vs. sham + vehicle and sham + MN166; amygdala, $p > 0.40$ vs. sham + vehicle and sham + MN166). Whereas MN166-treated LFPI rats were not distinguishable from sham-operated controls, post-hoc analyses revealed that LFPI + vehicle rats had significantly greater astrocytic activation in both brain regions, as compared to controls (Fig. 5A,B, left graphs: insula, $p < 0.02$ vs. LFPI + MN166, sham + vehicle, and sham + MN166; amygdala, $p < 0.01$ vs. LFPI + MN166, sham + vehicle, and sham + MN166).

Analysis of GFAP immunoreactivity in subregions of the insula (Fig. 5A, right graph) also revealed that LFPI + vehicle rats had increased GFAP labeling in agranular ($F(3, 140) = 2.493$; $p = 0.063$), dysgranular ($F(3, 140) = 7.388$; $p = 0.000$), and granular ($F(3, 140) = 2.998$; $p = 0.033$) insular regions. No significant differences between sham-operated and LFPI + MN166 groups were found in subregions of the insula (agranular, $p > 0.70$ vs. sham + vehicle and sham + MN166; dysgranular, $p > 0.20$ vs. sham + vehicle and sham + MN166; granular, $p > 0.20$ vs. sham + vehicle and sham + MN166). Untreated, LFPI + vehicle rats had greater astrocytic activation in all three subregions, as compared to controls (Fig. 5A, right graph: agranular, $p < 0.03$ vs. LFPI + MN166 and sham + vehicle and $p = 0.079$ vs. sham + MN166; dysgranular, $p < 0.01$ vs. LFPI + MN166, sham + vehicle, and sham + MN166; granular, $p = 0.124$ vs. LFPI + MN166, $p = 0.003$ vs. sham + vehicle, and $p = 0.087$ vs. sham + MN166).

In the subregions of the amygdala (Fig. 5B, right graph), GFAP labeling in LFPI + vehicle rats was significantly increased in basolateral amagdala (BLA; $F(3, 140) = 39.154$; $p = 0.000$) and central amygdala (CE; $F(3, 140) = 12.073$; $p = 0.000$) nuclei, compared to controls. Post-hoc analyses revealed that LFPI + vehicle rats had significantly greater astrocytic activation in both subregions (CE, $p < 0.001$ vs. LFPI + MN166, sham + vehicle, and sham + MN166; BLA, $p = 0.001$ vs. LFPI + MN166, sham + vehicle, and sham + MN166). MN166-treated LFPI rats had significantly less GFAP expression than sham + vehicle controls in CE ($p = 0.03$), but did not differ from sham + MN166-treated rats ($p = 0.58$). LFPI + MN166-treated rats also did not differ from sham controls in the BLA ($p = 0.58$ vs. sham + vehicle and $p = 0.06$ vs. sham + MN166).

LFPI + vehicle rats also showed significantly increased microglial activation, as measured by OX-42 labeling, compared to control groups (Fig. 5C), but this was restricted to subregions of the amygdala, such as the CE ($F(3, 140) = 9.290$; $p = 0.000$), and also approached significance in BLA ($F(3, 140) = 2.399$; $p = 0.071$) nuclei. Post-hoc analysis revealed significant increases in microglial activation for LFPI + vehicle rats in CE ($p < 0.001$ vs. LFPI + MN166, sham + vehicle, and sham + MN166) and BLA ($p = 0.009$ vs. sham + MN166). No differences in OX-42 labeling were observed between sham-operated and LFPI + MN166 groups in amygdala, nor were any significant between-group differences found in OX-42 expression for the insula.

## Discussion

LFPI-induced anxiety-like behaviors are found at long-term, postinjury time points in untreated brain-injured rats, as compared to those treated with MN166. Pharmacological suppression of immune responses at 1 month postinjury, when anxiety-like behavior has fully developed, markedly reduces long-term behavioral and immunological impairments after TBI (out to 6 months) and restores MN166-treated rats to levels indistinguishable from sham-operated controls. These findings not only implicate chronic neuroinflammation in the development of anxiety-like behaviors after TBI, but also show that delayed treatment is capable of reversing established post-traumatic anxiety behaviors. To our knowledge, this is the first study to examine delayed immunosuppression at long-term injury time points, because other immunosuppressive treatments targeting anxiety-like behaviors have been administered before or within hours of injury.[34,37,38,66–69] These results indicate that the persistence of post-traumatic anxiety may reflect chronic neuroinflammatory neuropathy, a possibility supported by the observation of activated microglia and astrocytes, key cells mediating inflammatory processes, many years after injury in long-term survivors of TBI.[9–12]

Chronic post-traumatic neuroinflammation suggests the presence of a self-perpetuating positive feedback loop, possibly involving reactivation and further promotion of inflammatory mediators after injury in an inflammation-damage-inflammation

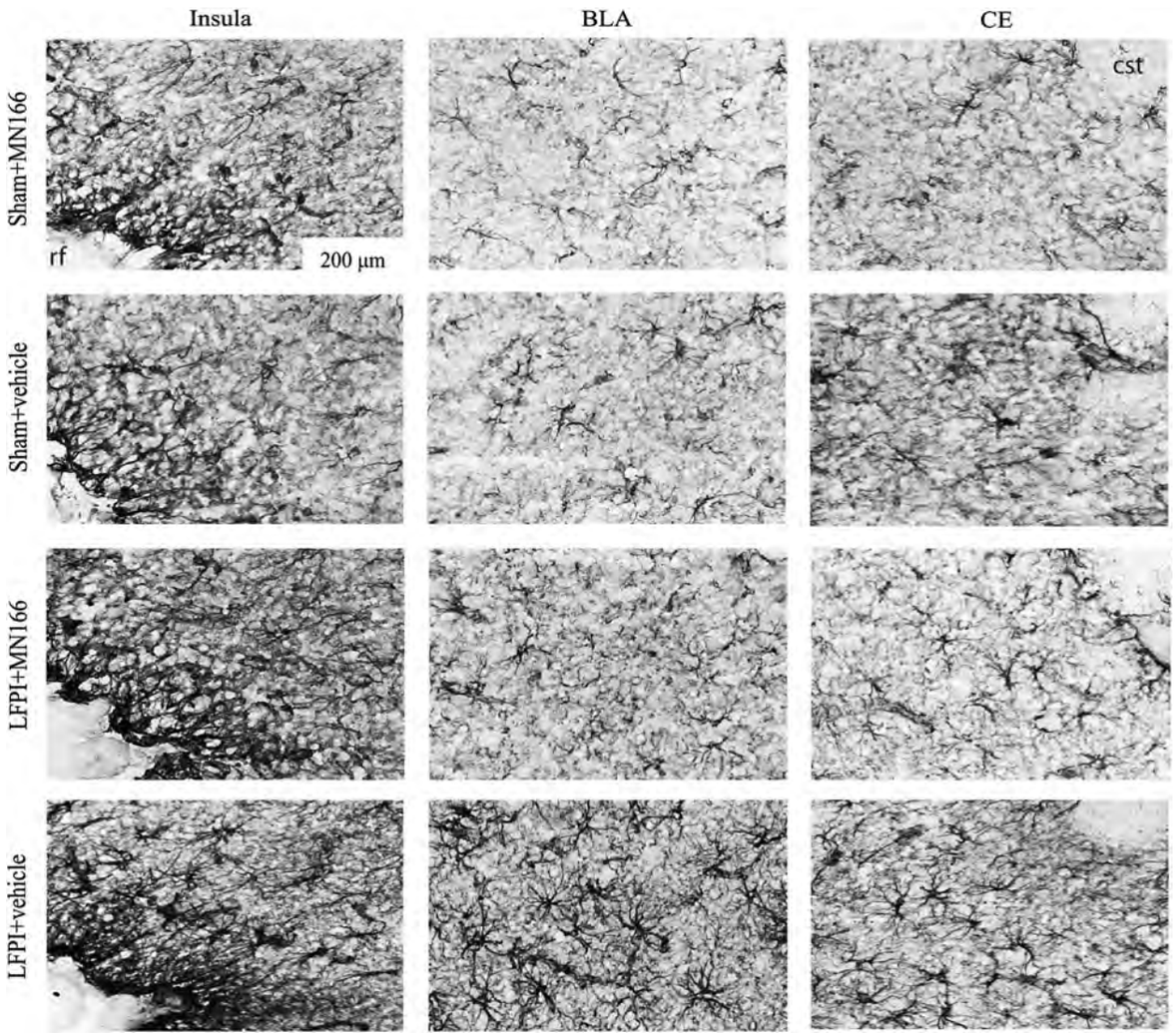


**FIG. 4.** Representative photomicrographs (20×) depicting GFAP immunoreactivity assessed in the insula and amygdala at 6 months postinjury. Vehicle-injected LFPI rats showed clear signs of reactive astrocytes (bottom row), whereas astrocytes from sham-operated rat tissue appeared to have normal morphology (top rows). LFPI rats treated with MN166 (third row) were difficult to differentiate from sham-operated groups. Rhinal fissure (rf ) and commissural stria terminalis (cst). GFAP, glial fibrillary acidic protein; LFPI, lateral fluid percussion injury.

cycle.[70] Stressed, damaged, and injured cells release endogenous danger signals, which trigger local inflammatory responses needed for tissue repair and regeneration.[21,71–73] Damage-associated molecular patterns (DAMPs) play an important role in the propagation of the proinflammatory cascade of innate immunity, promoting the release of cytokines and other inflammatory mediators.[70,74] DAMPs initiate the innate immune response through the activation of APCs, which up-regulate costimulatory and major histocompatibility complex molecules.[21,71,75] APCs respond to endogenous signals through Toll-like receptors (TLRs), which recognize a variety of DAMPs and act as pattern recognition receptors for endogenous molecules.

Microglia are the resident immunological cells and primary APCs of the CNS, remaining quiescent until activated through TLR engagement with DAMPs to perform effector inflammatory and APC functions.[76] Microglial cells contribute to neuroinflammation in response to DAMPS by secreting proinflammatory cytokines, such as interleukin (IL)-1 and tumor necrosis factor alpha (TNF-α), which amplify the inflammatory response by initiating the production of other cytokines and promoting microglial proliferation and activation of astrocytes.[70] The early phase of TBI-induced reactive gliosis has been reported to begin in with predominant microglia activation that peaks within 1 week,[28,77–82] but continues for several weeks and overlaps later with persistent astrocytic activation.[28,82,83]

Our IHC results support this time course, indicating injury-induced astrogliosis in the insula and amygdala at 6 months postinjury, but less activation of microglia (only significant in the amygdala), suggesting that microglial activation may precede astrocytic activation and modulate the onset and maintenance of astrogliosis.[27,84–88] Lower levels of microglia expression could be the result of assessment at 6 months postinjury, when microglia may have returned to a quiescent or surveying state,[28,89] whereas astrocytic activation persists in a long-lasting, self-perpetuating

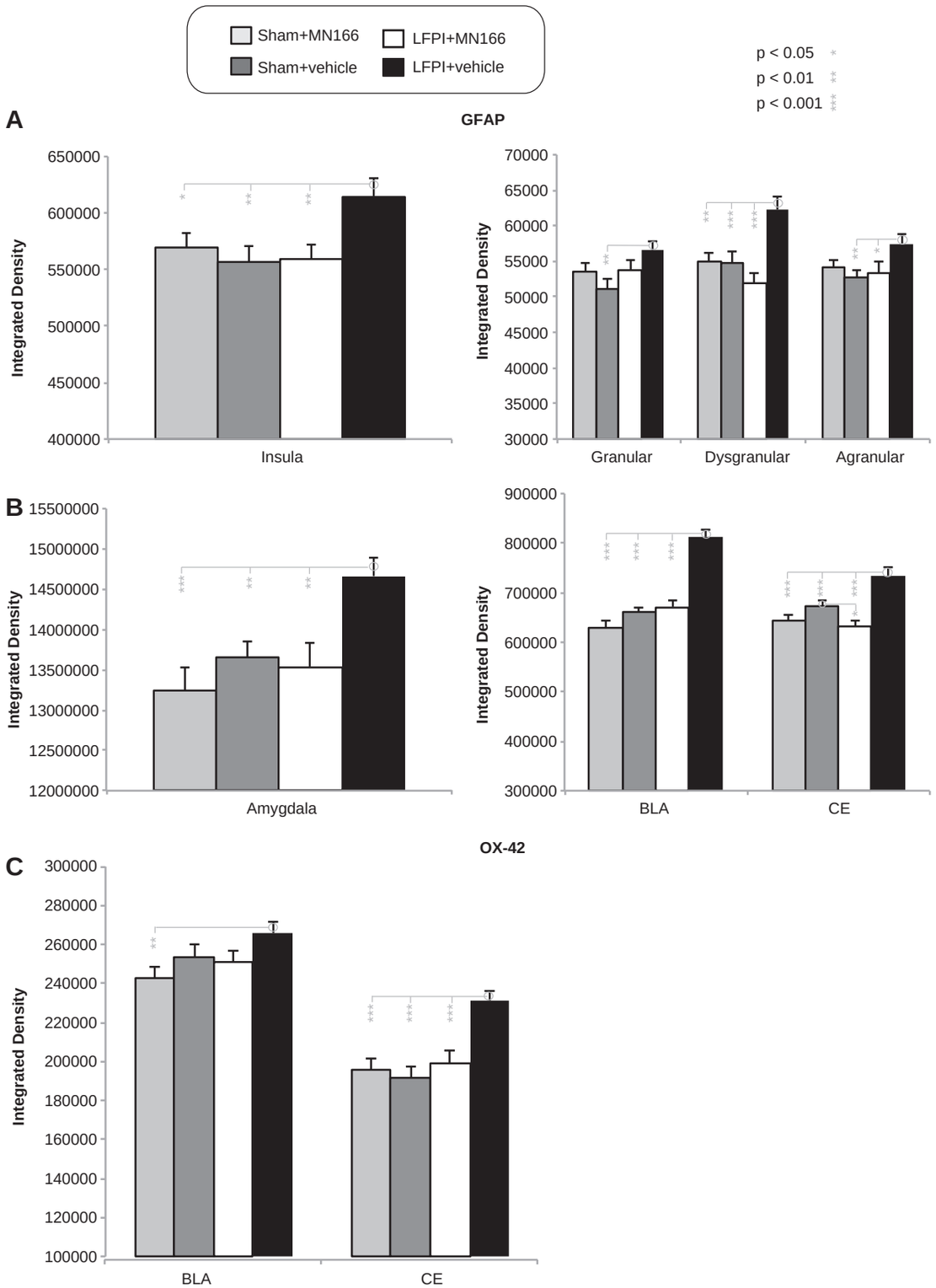


**FIG. 5.** Astro- and microglial activation in insula and amygdala at 6 months postinjury. LFPI + vehicle rats had increased reactive gliosis postinjury, as evidenced by increased glial activation, compared to controls, and treatment with MN166 reduced gliosis levels in LFPI rats to those of sham-operated controls. (**A** and **B**) LFPI + vehicle rats had significantly increased in GFAP labeling in both regions, indicating higher astroglial activation, compared to sham-operated and LFPI + MN166-treated rats. (**C**) In the CE, microglial activation was greater in LFPI + vehicle-injected rats, compared to both sham-operated groups and LFPI + MN166-treated rats, and was approaching significance in BLA. Data represent mean ± standard error of the mean. LFPI, lateral fluid percussion injury; GFAP, glial fibrillary acidic protein; CE, central amagdala; BLA, basolateral amygdala.

inflammatory response in the brain that exceeds early neuroprotection and results in neurodegenerative changes capable of continuing the inflammatory cycle.[9,27,90]

Chronic inflammation has been observed in a number of studies examining patients with trauma-related anxiety disorders, reporting increases in downstream mediators, such as peripheral elevations of TNF-$\alpha$, interferon-gamma (IFN-$\gamma$), IL-1$\beta$, and IL-6, in patients with PTSD,[13–16] elevations of TNF-$\alpha$ and IL-6 in patients with OCD,[17] and elevations in proinflammatory cytokines and chemokines (monocyte chemoattractant protein 1, macrophage inflammatory protein 1 alpha, IL-1$\alpha$, IL-1$\beta$, IL-6, IL-8, Eotaxin, granulocyte macrophage colony-stimulating factor, and IFN-$\gamma$) in individuals with panic disorder and PTSD.[18] Despite compelling evidence implicating excessive inflammatory actions and a generalized inflammatory state in the development of anxiety disorders after TBI, central measures of proinflammatory cytokine elevations specifically related to human PTSD and other anxiety disorders have not yet been performed. However, the current results provide evidence for chronic neuroinflammation in the development and maintenance of post-traumatic anxiety in an animal model, as indicated by elevated immunoreactivity in the amygdala and insula at 6 months postinjury.

The amygdala and insula have long been associated with human anxiety disorders. Studies in patients with PTSD implicate exaggerated responses of the amygdala and insula,[91–95] impaired inhibition of medial prefrontal cortex and anterior cingulate,[94,96–98] and decreased hippocampal volume.[97,99,100] Other neuroimaging reports of patients with non-trauma-related OCD and phobia, as well as those with PTSD, have revealed that aversive anticipation (a hallmark of anxiety) involves increased activation of both the amygdala and insula.[92] Evidence for the specific involvement of these brain areas in human post-traumatic anxiety is complemented by animal models, including findings of increased PTSD-related traits and increased Stathmin 1 (a protein known to increase fear responses) expression in the amygdala after blast injury,[101] increased fear conditioning and up-regulation of excitatory N-methyl-D-aspartate receptors (crucial receptors for normal fear learning and memory) in the amygdala after concussive injury,[33] and our current results showing increased anxiety-like behavior and reactive gliosis in insula and amygdala at long-term time points after LFPI. However, though these results support findings from our previous study[34] indicating increased gliosis in these areas, the insula and amygdala are not the only regions involved in anxiety and do not exclude the possibility that other regions may be contributing to the results reported here. Future studies will be aimed at characterizing the model and inclusion of other brain regions involved in human anxiety, including cingulate cortex, hippocampus, medial prefrontal cortex, locus coeruleus, and the bed nucleus of the stria terminalis.[94,97,99,102,103]

Although the exact role of the immune system in the pathogenesis of anxiety disorders after TBI remains unknown, neuroinflammation is emerging as a potential target. The present findings of treatment-related reductions in anxiety-like behaviors and reactive gliosis in brain regions associated with anxiety support the use of immunosuppression to improve functional outcome after TBI. Peri-injury and immediate postinjury immunosuppression have been found to be neuroprotective after TBI in rodents, resulting in increased structural preservation and improved functional outcomes.[104] Early administration of the immunosuppressant drugs, minocycline, statins, cyclosporin A, and FK506, have been shown to exert anti-inflammatory effects through suppression of micro- and astroglial production of IL-1$\beta$, TNF-$\alpha$, and IL-6, resulting in reduced functional deficits, cerebral edema, and brain lesion volumes,[35–38,66] improving mitochondrial preservation, reducing dendritic spine loss, and improving cognitive performance and functional motor recovery.[105,106] Our previous investigation found that peri-injury Ibudilast treatment attenuated glial cell activation at the time of injury, resulting in reduced anxiety-like behaviors and immunological impairments after LFPI. [34]

These immunosuppressant drugs all have direct inhibitory effects on microglia and astrocytes, leading to better functional recovery after TBI; however, these treatments require rapid administration and reduce the therapeutic window to the day of injury. The current work shows reversal of established anxiety-like behaviors and reactive gliosis at 1 month postinjury, delayed treatment time points that have not been tested with any other immunosuppressive interventions, in spite of substantial evidence that many molecular, biochemical, and immunological changes occur for many months after injury and that clinical intervention may not be possible at early stages of TBI. Ongoing inflammation represents a window of opportunity for therapeutic intervention to prevent progressive tissue damage, loss of function, and possibly interrupt the progression of neuropathological conditions after injury.

Our finding that delayed immunosuppression is capable of reversing established post-traumatic anxiety behaviors and immunological impairments through 6 months after TBI contributes to growing evidence that the critical window for treatment after TBI can be expanded to include those suffering from long-term TBI-related disabilities. Studies have shown that delayed treatment (24 h) with erythropoietin, a novel neuroprotective cytokine found to improve neuronal survival through attenuation of cytokine production and inflammation, improved sensorimotor functional recovery, reduced hippocampal cell loss, enhanced neurogenesis, and improved neurological outcomes after controlled cortical impact (CCI) and weight-drop rodent TBI models.[107,108] Similarly, a recent study reported reduced chronic inflammation and neurodegeneration after activation of metabotropic glutamate receptor 5 with the specific agonist, (RS)-2-chloro-5-hydroxyphenylglycine (CHPG), which has been shown to decrease microglial activation and release associated proinflammatory mediators. The study delayed treatment until 1 month after CCI in mice, delivering a single intracerebroventricular injection of CHPG. The results revealed reductions in reactive gliosis, hippocampal cell loss, reduced lesion progression, and improved motor and cognitive recovery, compared to untreated controls.[109]

Immunosuppression of chronic neuroinflammation may hold promise as a therapeutic target in treatment of established anxiety disorders after TBI. It has been shown here that inflammation produced by neuroimmune responses after injury plays a role in TBI-induced anxiety, and delayed immunosuppression leads to better functional outcomes at long-term postinjury treatment points after TBI. Delayed, postinjury suppression of glial cell activation could therefore expand the clinical window for treatment of TBI-induced anxiety disorders in humans.

## Acknowledgments

This work was supported by the U.S. Army Medical Research and Material Command (grant PR100040), the Craig Hospital Gift Fund, a University of Colorado Innovative Seed Grant, the Autism Speaks Pilot Study (grant 7153), and the National Institutes of Health (grant nos. NS36981 [to D.S.B.] and DA024044 and DA01767 [to L.R.W.].

AU1 ▶

## Author Disclosure Statement

No competing financial interests exist.

## References


1. Faul, M., Xu, L., Wald, M.M., and Coronado, V.G. (2010). *Traumatic Brain Injury in the United States: Emergency Department Visits, Hospitalizations and Deaths 2002–2006*. Available at: http://www.cdc.gov/traumaticbraininjury/pdf/blue_book.pdf. Accessed November 5, 2013.
2. Rao, V., and Lyketsos, C. (2000). Neuropsychiatric sequelae of traumatic brain injury. Psychosomatics 41, 95–103.
3. Hiott, D.W., and Labbate, L. (2002). Anxiety disorders associated with traumatic brain injuries. NeuroRehabilitation 17, 345–355.
4. Vaishnavi, S., Rao, V., and Fann, J.R. (2009). Neuropsychiatric problems after traumatic brain injury: unraveling the silent epidemic. Psychosomatics 50, 198–205.
5. van Reekum, R., Cohen, T., and Wong, J. (2000). Can traumatic brain injury cause psychiatric disorders? J. Neuropsychiatry Clin. Neurosci. 12, 316–327.
6. Morton, M.V., and Wehman, P. (1995). Psychosocial and emotional sequelae of individuals with traumatic brain injury: a literature review and recommendations. Brain Inj. 9, 81–92.
7. Deb, S., Lyons, I., Koutzoukis, C., Ali, I., and McCarthy, G. (1999). Rate of psychiatric illness 1 year after traumatic brain injury. Am. J. Psychiatry 156, 374–378.
8. Koponen, S., Taiminen, T., Portin, R., Himanen, L., Isoniemi, H., Heinonen, H., Hinkka, S., and Tenovuo, O. (2002). Axis I and II psychiatric disorders after traumatic brain injury: a 30-year follow-up study. Am. J. Psychiatry 159, 1315–1321.
9. Gentleman, S.M., Leclercq, P.D., Moyes, L., Graham, D.I., Smith, C., Griffin, W.S., and Nicoll, J.A. (2004). Long-term intracerebral inflammatory response after traumatic brain injury. Forensic. Sci. Int. 146, 97–104.
10. Streit, W.J., Mrak, R.E., and Griffin, W.S. (2004). Microglia and neuroinflammation: a pathological perspective. J. Neuroinflammation 1, 14.
11. Nagamoto-Combs, K., McNeal, D.W., Morecraft, R.J., and Combs, C.K. (2007). Prolonged microgliosis in the rhesus monkey central nervous system after traumatic brain injury. J. Neurotrauma 24, 1719–1742.
12. Ramlackhansingh, A.F., Brooks, D.J., Greenwood, R.J., Bose, S.K., Turkheimer, F.E., Kinnunen, K.M., Gentleman, S., Heckemann, R.A., Gunanayagam, K., Gelosa, G., and Sharp, D.J. (2011). Inflammation after trauma: microglial activation and traumatic brain injury. Ann. Neurol. 70, 374–383.
13. Spivak, B., Shohat, B., Mester, R., Avraham, S., Gil-Ad, I., Bleich, A., Valevski, A., and Weizman, A. (1997). Elevated levels of serum interleukin-1 beta in combat-related posttraumatic stress disorder. Biol. Psychiatry 42, 345–348.
14. Tucker, P., Ruwe, W.D., Masters, B., Parker, D.E., Hossain, A., Trautman, R.P., and Wyatt, D.B. (2004). Neuroimmune and cortisol changes in selective serotonin reuptake inhibitor and placebo treatment of chronic posttraumatic stress disorder. Biol. Psychiatry 56, 121–128.
15. Rohleder, N., Joksimovic, L., Wolf, J.M., and Kirschbaum, C. (2004). Hypocortisolism and increased glucocorticoid sensitivity of pro-Inflammatory cytokine production in Bosnian war refugees with posttraumatic stress disorder. Biol. Psychiatry 55, 745–751.
16. von Kanel, R., Hepp, U., Kraemer, B., Traber, R., Keel, M., Mica, L., and Schnyder, U. (2007). Evidence for low-grade systemic proinflammatory activity in patients with posttraumatic stress disorder. J. Psychiatr. Res. 41, 744–752.
17. Konuk, N., Tekin, I.O., Ozturk, U., Atik, L., Atasoy, N., Bektas, S., and Erdogan, A. (2007). Plasma levels of tumor necrosis factor-alpha and interleukin-6 in obsessive compulsive disorder. Mediators Inflamm. 2007, 65704.
18. Hoge, E.A., Brandstetter, K., Moshier, S., Pollack, M.H., Wong, K.K., and Simon, N.M. (2009). Broad spectrum of cytokine abnormalities in panic disorder and posttraumatic stress disorder. Depress. Anxiety 26, 447–455.
19. Pugin, J. (2012). How tissue injury alarms the immune system and causes a systemic inflammatory response syndrome. Ann. Intensive Care 2, 27.
20. Matzinger, P. (1998). An innate sense of danger. Semin. Immunol. 10, 399–415.
21. Hirsiger, S., Simmen, H.P., Werner, C.M., Wanner, G.A., and Rittirsch, D. (2012). Danger signals activating the immune response after trauma. Mediators Inflamm. 2012, 315941.
22. Gehrmann, J., Banati, R.B., and Kreutzberg, G.W. (1993). Microglia in the immune surveillance of the brain: human microglia constitutively express HLA-DR molecules. J. Neuroimmunol. 48, 189–198.
23. Gehrmann, J., Matsumoto, Y., and Kreutzberg, G.W. (1995). Microglia: intrinsic immuneffector cell of the brain. Brain Res. 20, 269–287.
24. Sternberg, E.M. (1997). Neural-immune interactions in health and disease. J. Clin. Invest. 100, 2641–2647.
25. Raison, C.L., and Miller, A.H. (2003). When not enough is too much: the role of insufficient glucocorticoid signaling in the pathophysiology of stress-related disorders. Am. J. Psychiatry 160, 1554–1565.
26. Szelenyi, J., and Vizi, E.S. (2007). The catecholamine cytokine balance: interaction between the brain and the immune system. Ann. N. Y. Acad. Sci. 1113, 311–324.
27. Zhang, D., Hu, X., Qian, L., O'Callaghan, J.P., and Hong, J.S. (2010). Astrogliosis in CNS pathologies: is there a role for microglia? Mol. Neurobiol. 41, 232–241.
28. Colangelo, A.M., Cirillo, G., Lavitrano, M.L., Alberghina, L., and Papa, M. (2012). Targeting reactive astrogliosis by novel biotechnological strategies. Biotechnol. Adv. 30, 261–271.
29. Connor, T.J., Song, C., Leonard, B.E., Merali, Z., and Anisman, H. (1998). An assessment of the effects of central interleukin-1beta, −2, −6, and tumor necrosis factor-alpha administration on some behavioural, neurochemical, endocrine and immune parameters in the rat. Neuroscience 84, 923–933.
30. Cragnolini, A.B., Schioth, H.B., and Scimonelli, T.N. (2006). Anxiety-like behavior induced by IL-1beta is modulated by alpha-MSH through central melanocortin-4 receptors. Peptides 27, 1451–1456.
31. Sokolova, E.S., Lyudyno, V.I., Simbirtsev, A.S., and Klimenko, V.M. (2007). The psychomodulatory action of subpyrogenic doses of interleukin-1beta in conditions of chronic administration to rats. Neurosci. Behav. Physiol. 37, 499–504.
32. Zubareva, O.E., and Klimenko, V.M. (2009). Long-term disorders of behavior in rats induced by administration of tumor necrosis factor during early postnatal ontogenesis. Neurosci. Behav. Physiol. 39, 21–24.
33. Reger, M.L., Poulos, A.M., Buen, F., Giza, C.C., Hovda, D.A., and Fanselow, M.S. (2012). Concussive brain injury enhances fear learning and excitatory processes in the amygdala. Biol. Psychiatry 71, 335–343.
34. Rodgers, K.M., Bercum, F.M., McCallum, D.L., Rudy, J.W., Frey, L.C., Johnson, K.W., Watkins, L.R., and Barth, D.S. (2012). Acute neuroimmune modulation attenuates the development of anxiety-like freezing behavior in an animal model of traumatic brain injury. J. Neurotrauma 29, 1886–1897.
35. Chen, S.F., Hung, T.H., Chen, C.C., Lin, K.H., Huang, Y.N., Tsai, H.C., and Wang, J.Y. (2007). Lovastatin improves histological and functional outcomes and reduces inflammation after experimental traumatic brain injury. Life Sci. 81, 288–298.
36. Li, B., Mahmood, A., Lu, D., Wu, H., Xiong, Y., Qu, C., and Chopp, M. (2009). Simvastatin attenuates microglial cells and astrocyte activation and decreases interleukin-1beta level after traumatic brain injury. Neurosurgery 65, 179–185; discussion, 185–176.
37. Homsi, S., Federico, F., Croci, N., Palmier, B., Plotkine, M., Marchand-Leroux, C., and Jafarian-Tehrani, M. (2009). Minocycline effects on cerebral edema: relations with inflammatory and oxidative stress markers following traumatic brain injury in mice. Brain Res. 1291, 122–132.
38. Homsi, S., Piaggio, T., Croci, N., Noble, F., Plotkine, M., Marchand-Leroux, C., and Jafarian-Tehrani, M. (2010). Blockade of acute microglial activation by minocycline promotes neuroprotection and reduces locomotor hyperactivity after closed head injury in mice: a twelve-week follow-up study. J. Neurotrauma 27, 911–921.
39. Thompson, H.J., Lifshitz, J., Marklund, N., Grady, M.S., Graham, D.I., Hovda, D.A., and McIntosh, T.K. (2005). Lateral fluid percussion brain injury: a 15-year review and evaluation. J. Neurotrauma 22, 42–75.
40. Frey, L.C., Hellier, J., Unkart, C., Lepkin, A., Howard, A., Hasebroock, K., Serkova, N., Liang, L., Patel, M., Soltesz, I., and Staley, K. (2009). A novel apparatus for lateral fluid percussion injury in the rat. J. Neurosci. Methods 177, 267–272.

41. Mizuno, T., Kurotani, T., Komatsu, Y., Kawanokuchi, J., Kato, H., Mitsuma, N., and Suzumura, A. (2004). Neuroprotective role of phosphodiesterase inhibitor ibudilast on neuronal cell death induced by activated microglia. Neuropharmacology 46, 404–411.
42. Rolan, P., Hutchinson, M., and Johnson, K. (2009). Ibudilast: a review of its pharmacology, efficacy and safety in respiratory and neurological disease. Expert Opin. Pharmacother. 10, 2897–2904.
43. Ellis, A.L., Wieseler, J., Brown, K., Blackwood, C., Ramos, K., Starnes, C., Maier, S.F., Watkins, L.R., and Falci, S.P. (2008). Characterization of exaggerated pain behavior and glial activation in a novel rat model of spinal cord injury. Poster from 38th Annual Meeting of the Society for Neuroscience, Washington, DC, November 15–19, 2008.
44. Cho, Y., Crichlow, G.V., Vermeire, J.J., Leng, L., Du, X., Hodsdon, M.E., Bucala, R., Cappello, M., Gross, M., Gaeta, F., Johnson, K., and Lolis, E.J. (2010). Allosteric inhibition of macrophage migration inhibitory factor revealed by ibudilast. Proc. Natl. Acad. Sci. U. S. A. 107, 11313–11318.
45. Gibson, L.C., Hastings, S.F., McPhee, I., Clayton, R.A., Darroch, C.E., Mackenzie, A., Mackenzie, F.L., Nagasawa, M., Stevens, P.A., and Mackenzie, S.J. (2006). The inhibitory profile of Ibudilast against the human phosphodiesterase enzyme family. Eur. J. Pharmacol. 538, 39–42.
46. Wang, F., Xu, S., Shen, X., Guo, X., Peng, Y., and Yang, J. (2011). Spinal macrophage migration inhibitory factor is a major contributor to rodent neuropathic pain-like hypersensitivity. Anesthesiology 114, 643–659.
47. Bland, S.T., Schallert, T., Strong, R., Aronowski, J., Grotta, J.C., and Feeney, D.M. (2000). Early exclusive use of the affected forelimb after moderate transient focal ischemia in rats: functional and anatomic outcome. Stroke 31, 1144–1152.
48. Bland, S.T., Pillai, R.N., Aronowski, J., Grotta, J.C., and Schallert, T. (2001). Early overuse and disuse of the affected forelimb after moderately severe intraluminal suture occlusion of the middle cerebral artery in rats. Behav. Brain Res. 126, 33–41.
49. Nitz, A.J., Dobner, J.J., and Matulionis, D.H. (1986). Pneumatic tourniquet application and nerve integrity: motor function and electrophysiology. Exp. Neurol. 94, 264–279.
50. Schallert, T., Fleming, S.M., Leasure, J.L., Tillerson, J.L., and Bland, S.T. (2000). CNS plasticity and assessment of forelimb sensorimotor outcome in unilateral rat models of stroke, cortical ablation, parkinsonism and spinal cord injury. Neuropharmacology 39, 777–787.
51. Woodlee, M.T., Asseo-Garcia, A.M., Zhao, X., Liu, S.J., Jones, T.A., and Schallert, T. (2005). Testing forelimb placing ''across the midline'' reveals distinct, lesion-dependent patterns of recovery in rats. Exp. Neurol. 191, 310–317.
52. Sanberg, P.R., Bunsey, M.D., Giordano, M., and Norman, A.B. (1988). The catalepsy test: its ups and downs. Behav. Neurosci. 102, 748–759.
53. Schallert, T., De Ryck, M., Whishaw, I.Q., Ramirez, V.D., and Teitelbaum, P. (1979). Excessive bracing reactions and their control by atropine and L-DOPA in an animal analog of Parkinsonism. Exp. Neurol. 64, 33–43.
54. Morrissey, T.K., Pellis, S.M., Pellis, V.C., and Teitelbaum, P. (1989). Seemingly paradoxical jumping in cataleptic haloperidol-treated rats is triggered by postural instability. Behav. Brain Res. 35, 195–207.
55. Pellis, S.M., Pellis, V.C., and Teitelbaum, P. (1991). Air righting without the cervical righting reflex in adult rats. Behav. Brain Res. 45, 185–188.
56. Pellis, S.M., Whishaw, I.Q., and Pellis, V.C. (1991). Visual modulation of vestibularly-triggered air-righting in rats involves the superior colliculus. Behav. Brain Res. 46, 151–156.
57. Schallert, T. (2006). Behavioral tests for preclinical intervention assessment. NeuroRx 3, 497–504.
58. Fanselow, M.S. (1986). Associative vs topographical accounts of the immediate shock-freezing deficit in rats: implications for the response selection rules governing species-specific defensive reactions. Learn. Motiv. 17, 16–39.
59. Rudy, J.W., and O'Reilly, R.C. (2001). Conjunctive representations, the hippocampus, and contextual fear conditioning. Cogn. Affect Behav. Neurosci. 1, 66–82.
60. Landeira-Fernandez, J., DeCola, J.P., Kim, J.J., and Fanselow, M.S. (2006). Immediate shock deficit in fear conditioning: effects of shock manipulations. Behav. Neurosci. 120, 873–879.
61. Rosen, J.B., and Schulkin, J. (1998). From normal fear to pathological anxiety. Psychol. Rev. 105, 325–350.
62. Rosen, J.B. (2004). The neurobiology of conditioned and unconditioned fear: a neurobehavioral system analysis of the amygdala. Behav. Cogn. Neurosci. Rev. 3, 23–41.
63. Loram, L.C., Harrison, J.A., Sloane, E.M., Hutchinson, M.R., Sholar, P., Taylor, F.R., Berkelhammer, D., Coats, B.D., Poole, S., Milligan, E.D., Maier, S.F., Rieger, J., and Watkins, L.R. (2009). Enduring reversal of neuropathic pain by a single intrathecal injection of adenosine 2A receptor agonists: a novel therapy for neuropathic pain. J. Neurosci. 29, 14015–14025.
64. Cole, J.T., Yarnell, A., Kean, W.S., Gold, E., Lewis, B., Ren, M., McMullen, D.C., Jacobowitz, D.M., Pollard, H.B., O'Neill, J.T., Grunberg, N.E., Dalgard, C.L., Frank, J.A., and Watson, W.D. (2011). Craniotomy: true sham for traumatic brain injury, or a sham of a sham? J. Neurotrauma 28, 359–369.
65. Olesen, S.P. (1987). Leakiness of rat brain microvessels to fluorescent probes following craniotomy. Acta Physiol. Scand. 130, 63–68.
66. Siopi, E., Llufriu-Daben, G., Fanucchi, F., Plotkine, M., Marchand-Leroux, C., and Jafarian-Tehrani, M. (2012). Evaluation of late cognitive impairment and anxiety states following traumatic brain injury in mice: the effect of minocycline. Neurosci. Lett. 511, 110–115.
67. Lee, H.F., Lee, T.S., and Kou, Y.R. (2012). Anti-inflammatory and neuroprotective effects of triptolide on traumatic brain injury in rats. Respir. Physiol. Neurobiol. 182, 1–8.
68. Kovesdi, E., Kamnaksh, A., Wingo, D., Ahmed, F., Grunberg, N.E., Long, J.B., Kasper, C.E,. and Agoston, D.V. (2012). Acute minocycline treatment mitigates the symptoms of mild blast-induced traumatic brain injury. Front. Neurol. 3, 111.
69. Lopez, N.E., Gaston, L., Lopez, K.R., Coimbra, R.C., Hageny, A., Putnam, J., Eliceiri, B., Coimbra, R., and Bansal, V. (2012). Early ghrelin treatment attenuates disruption of the blood brain barrier and apoptosis after traumatic brain injury through a UCP-2 mechanism. Brain Res. 1489, 140–148.
70. Namas, R., Ghuma, A., Hermus, L., Zamora, R., Okonkwo, D.O., Billiar, T.R., and Vodovotz, Y. (2009). The acute inflammatory response in trauma/hemorrhage and traumatic brain injury: current state and emerging prospects. Libyan J. Med. 4, 97–103.
71. Gallucci, S., and Matzinger, P. (2001). Danger signals: SOS to the immune system. Curr. Opin. Immunol. 13, 114–119.
72. Oppenheim, J.J., and Yang, D. (2005). Alarmins: chemotactic activators of immune responses. Curr. Opin. Immunol. 17, 359–365.
73. Oppenheim, J.J., Tewary, P., de la Rosa, G., and Yang, D. (2007). Alarmins initiate host defense. Adv. Exp. Med. Biol. 601, 185–194.
74. Bianchi, M.E. (2007). DAMPs, PAMPs and alarmins: all we need to know about danger. J. Leukoc. Biol. 81, 1–5.
75. Matzinger, P. (2002). An innate sense of danger. Ann. N. Y. Acad. Sci. 961, 341–342.
76. Olson, J.K., and Miller, S.D. (2004). Microglia initiate central nervous system innate and adaptive immune responses through multiple TLRs. J. Immunol. 173, 3916–3924.
77. Hill, S.J., Barbarese, E., and McIntosh, T.K. (1996). Regional heterogeneity in the response of astrocytes following traumatic brain injury in the adult rat. J. Neuropathol. Exp. Neurol. 55, 1221–1229.
78. Nonaka, M., Chen, X.H., Pierce, J.E., Leoni, M.J., McIntosh, T.K., Wolf, J.A., and Smith, D.H. (1999). Prolonged activation of NF-kappaB following traumatic brain injury in rats. J. Neurotrauma 16, 1023–1034.
79. Gueorguieva, I., Clark, S.R., McMahon, C.J., Scarth, S., Rothwell, N.J., Tyrrell, P.J., Hopkins, S.J., and Rowland, M. (2008). Pharmacokinetic modelling of interleukin-1 receptor antagonist in plasma and cerebrospinal fluid of patients following subarachnoid haemorrhage. Br. J. Clin. Pharmacol. 65, 317–325.
80. Grady, M.S., Charleston, J.S., Maris, D., Witgen, B.M., and Lifshitz, J. (2003). Neuronal and glial cell number in the hippocampus after experimental traumatic brain injury: analysis by stereological estimation. J. Neurotrauma 20, 929–941.
81. Clausen, F., Hanell, A., Bjork, M., Hillered, L., Mir, A.K., Gram, H., and Marklund, N. (2009). Neutralization of interleukin-1beta modifies the inflammatory response and improves histological and cognitive outcome following traumatic brain injury in mice. Eur. J. Neurosci. 30, 385–396.
82. Yu, I., Inaji, M., Maeda, J., Okauchi, T., Nariai, T., Ohno, K., Higuchi, M., and Suhara, T. (2010). Glial cell-mediated deterioration

and repair of the nervous system after traumatic brain injury in a rat model as assessed by positron emission tomography. J. Neurotrauma 27, 1463–1475.
83. D'Ambrosio, R., Fairbanks, J.P., Fender, J.S., Born, D.E., Doyle, D.L., and Miller, J.W. (2004). Post-traumatic epilepsy following fluid percussion injury in the rat. Brain 127, 304–314.
84. Graeber, M.B., and Kreutzberg, G.W. (1988). Delayed astrocyte reaction following facial nerve axotomy. J. Neurocytol. 17, 209–220.
85. McCann, M.J., O'Callaghan, J.P., Martin, P.M., Bertram, T., and Streit, W.J. (1996). Differential activation of microglia and astrocytes following trimethyl tin-induced neurodegeneration. Neuroscience 72, 273–281.
86. Hanisch, U.K. (2002). Microglia as a source and target of cytokines. Glia 40, 140–155.
87. Iravani, M.M., Leung, C.C., Sadeghian, M., Haddon, C.O., Rose, S., and Jenner, P. (2005). The acute and the long-term effects of nigral lipopolysaccharide administration on dopaminergic dysfunction and glial cell activation. Eur. J. Neurosci. 22, 317–330.
88. Herber, D.L., Maloney, J.L., Roth, L.M., Freeman, M.J., Morgan, D., and Gordon, M.N. (2006). Diverse microglial responses after intrahippocampal administration of lipopolysaccharide. Glia 53, 382–391.
89. Hanisch, U.K., and Kettenmann, H. (2007). Microglia: active sensor and versatile effector cells in the normal and pathologic brain. Nat. Neurosci. 10, 1387–1394.
90. Griffin, W.S., Sheng, J.G., Royston, M.C., Gentleman, S.M., McKenzie, J.E., Graham, D.I., Roberts, G.W., and Mrak, R.E. (1998). Glial-neuronal interactions in Alzheimer's disease: the potential role of a 'cytokine cycle' in disease progression. Brain Pathol. 8, 65–72.
91. Rauch, S.L., Savage, C.R., Alpert, N.M., Fischman, A.J., and Jenike, M.A. (1997). The functional neuroanatomy of anxiety: a study of three disorders using positron emission tomography and symptom provocation. Biol. Psychiatry 42, 446–452.
92. Simmons, A., Strigo, I., Matthews, S.C., Paulus, M.P., and Stein, M.B. (2006). Anticipation of aversive visual stimuli is associated with increased insula activation in anxiety-prone subjects. Biol. Psychiatry 60, 402–409.
93. Stein, M.B., Simmons, A.N., Feinstein, J.S., and Paulus, M.P. (2007). Increased amygdala and insula activation during emotion processing in anxiety-prone subjects. Am. J. Psychiatry 164, 318–327.
94. Shin, L.M., and Liberzon, I. (2010). The neurocircuitry of fear, stress, and anxiety disorders. Neuropsychopharmacology 35, 169–191.
95. Carlson, J.M., Greenberg, T., Rubin, D., and Mujica-Parodi, L.R. (2011). Feeling anxious: anticipatory amygdalo-insular response predicts the feeling of anxious anticipation. Soc. Cogn. Affect. Neurosci. 6, 74–81.
96. Davidson, R.J. (2002). Anxiety and affective style: role of prefrontal cortex and amygdala. Biol. Psychiatry 51, 68–80.
97. Shin, L.M., Rauch, S.L., and Pitman, R.K. (2006). Amygdala, medial prefrontal cortex, and hippocampal function in PTSD. Ann. N. Y. Acad. Sci. 1071, 67–79.
98. Milad, M.R., Pitman, R.K., Ellis, C.B., Gold, A.L., Shin, L.M., Lasko, N.B., Zeidan, M.A., Handwerger, K., Orr, S.P., and Rauch, S.L. (2009). Neurobiological basis of failure to recall extinction memory in posttraumatic stress disorder. Biol. Psychiatry 66, 1075–1082.
99. Bremner, J.D., Randall, P., Scott, T.M., Bronen, R.A., Seibyl, J.P., Southwick, S.M., Delaney, R.C., McCarthy, G., Charney, D.S., and Innis, R.B. (1995). MRI-based measurement of hippocampal volume in patients with combat-related posttraumatic stress disorder. Am. J. Psychiatry 152, 973–981.
100. Sapolsky, R.M. (2000). Glucocorticoids and hippocampal atrophy in neuropsychiatric disorders. Arch. Gen. Psychiatry 57, 925–935.
101. Elder, G.A., Dorr, N.P., De Gasperi, R., Gama Sosa, M.A., Shaughness, M.C., Maudlin-Jeronimo, E., Hall, A.A., McCarron, R.M., and Ahlers, S.T. (2012). Blast exposure induces post-traumatic stress disorder-related traits in a rat model of mild traumatic brain injury. J. Neurotrauma 29, 2564–2575.
102. Davis, M. (2006). Neural systems involved in fear and anxiety measured with fear-potentiated startle. Am. Psychol. 61, 741–756.
103. Samuels, E.R., and Szabadi, E. (2008). Functional neuroanatomy of the noradrenergic locus coeruleus: its roles in the regulation of arousal and autonomic function part I: principles of functional organisation. Curr. Neuropharmacol. 6, 235–253.
104. Hailer, N.P. (2008). Immunosuppression after traumatic or ischemic CNS damage: it is neuroprotective and illuminates the role of microglial cells. Prog. Neurobiol. 84, 211–233.
105. Alessandri, B., Rice, A.C., Levasseur, J., DeFord, M., Hamm, R.J., and Bullock, M.R. (2002). Cyclosporin A improves brain tissue oxygen consumption and learning/memory performance after lateral fluid percussion injury in rats. J. Neurotrauma 19, 829–841.
106. Campbell, J.N., Churn, S.B., and Register, D. (2011). Traumatic brain injury causes an FK506-sensitive loss and an overgrowth of dendritic spines in rat forebrain. J. Neurotrauma 29, 201–217.
107. Yatsiv, I., Grigoriadis, N., Simeonidou, C., Stahel, P.F., Schmidt, O.I., Alexandrovitch, A.G., Tsenter, J., and Shohami, E. (2005). Erythropoietin is neuroprotective, improves functional recovery, and reduces neuronal apoptosis and inflammation in a rodent model of experimental closed head injury. FASEB J. 19, 1701–1703.
108. Xiong, Y., Mahmood, A., Meng, Y., Zhang, Y., Qu, C., Schallert, T., and Chopp, M. (2010). Delayed administration of erythropoietin reducing hippocampal cell loss, enhancing angiogenesis and neurogenesis, and improving functional outcome following traumatic brain injury in rats: comparison of treatment with single and triple dose. J. Neurosurg. 113, 598–608.
109. Byrnes, K.R., Loane, D.J., Stoica, B.A., Zhang, J., and Faden, A.I. (2012). Delayed mGluR5 activation limits neuroinflammation and neurodegeneration after traumatic brain injury. J. Neuroinflammation 9, 43.

Address correspondence to:
*Daniel S. Barth, PhD*
*Department of Psychology and Neuroscience*
*University of Colorado*
*UCB 345*
*Boulder, CO 80309*

*E-mail:* dbarth@psych.colorado.edu

## AUTHOR QUERY FOR NEU-2013-3090-VER9-RODGERS_1P

AU1: Under Author Disclosure Statement, the statement ‘‘No competing financial interests exist’’ has been added for all authors. Please confirm that this statement is accurate.

# Spike-Wave Discharges versus Seizures after Fluid Percussion Injury in Sprague-Dawley Rats

Krista M. Rodgers[1], F. Edward Dudek[2] and Daniel S. Barth[1]

[1]*Department of Psychology and Neuroscience, University of Colorado, Boulder, CO 80309*

[2]*Department of Neurosurgery, University of Utah School of Medicine, Salt Lake City, UT 84108*

Correspondence to:

Daniel S. Barth

Department of Psychology and Neuroscience

University of Colorado

Campus Box 345

Boulder, CO 80309 U.S.A.

e-mail: daniel.barth@colorado.edu

Running title: *SPIKE-WAVE DISCHARGES VERSUS SEIZURES AFTER FPI*

## Abstract

Events with variable-duration oscillations and repetitive high voltage spikes have been recorded in the electrocorticogram (ECoG) of rats weeks and months after fluid percussion injury (FPI), a model of traumatic brain injury. These ECoG events, which have close similarities to spike-wave discharges (SWDs), have been proposed to represent non-convulsive seizures characteristic of post-traumatic epilepsy. However, SWDs have been observed in many strains, including normal Sprague-Dawley rats here, raising the possibility of previous misinterpretation of ECoG data in several animal models of acquired epilepsy.

The present study quantified features of SWD episodes throughout the lifetime of brain-injured rats receiving moderate to severe FPI. These results were compared to normal "control" rats with the objective of distinguishing normal brain activity from that heralding the development of seizures. A support vector machine was trained on the fully developed SWD of each rat and used to detect and quantify subsequent events.

Most of the older (6-12 month) control and brain-injured rats displayed large-amplitude and frequent SWD events at frontal and parietal recording sites. Earlier recordings in the same rats also revealed clear SWD at 3-6 months that were of shorter duration and less frequent, and "larval" SWD was detected as early as 1 month in both groups. All features of SWD quantified for control and experimental (FPI) rats were indistinguishable, including interruptibility by sensory stimulation, waveform morphology, and a marked increase in the frequency of occurrence, duration and amplitude with age. Additionally, none of the FPI-treated rats developed convulsive seizures across 12 months of video/EEG monitoring.

Our results suggest that SWDs are not epileptic seizures arising from the FPI-induced brain injury, because control animals had virtually identical events, and none of the FPI-treated rats developed spontaneous recurrent seizures during 12 months of video/EEG monitoring.

**Key words:** traumatic brain injury, seizure, post-traumatic epilepsy, fluid percussion injury, spike-wave

**Abbreviations:**

ECoG = electrocorticogram; FPI = fluid percussion injury; PTE = post traumatic epilepsy; SWD = spike-wave discharge

## Introduction

Traumatic brain injury is a common cause of epilepsy that is characterized by recurrent, spontaneous, convulsive (clinical) seizures that can variously be focal, generalized, or focal with secondary generalization (Haltiner *et al.*, 1997), and are difficult to treat both medically and surgically (Lowenstein, 2009). Developing strategies to prevent or treat PTE relies directly on adequate animal models, the most common of which is FPI in Sprague-Dawley rats (D'Ambrosio *et al.*, 2004; Kharatishvili *et al.*, 2006). FPI is thought to mimic closed head injury in humans (Thompson *et al.*, 2005). While it has been possible to produce convulsive, secondarily generalized seizures in the FPI model using caudal and lateral impact locations injuring the entorhinal cortex and underlying hippocampus (Kharatishvili *et al.*, 2006), investigations of mechanisms and intervention strategies for these seizures have been limited by a long post-injury latency (6-12 mo) required to achieve greater than 25% success rates. Much earlier (2 mo post-injury) and more frequent seizures have been reported with the use of rostral parasagittal impact locations targeting sensorimotor cortex (D'Ambrosio and Miller, 2010; D'Ambrosio *et al.*, 2003; 2004; 2005; 2009). These early appearing cortical seizures are subtler than convulsive episodes, and are typified by stereotyped freeze-like pauses (behavioral arrest) and facial automatisms. Their signature in the ECoG is also quite distinct from convulsive temporal lobe seizures, and is characterized by a sudden increase in voltage amplitude produced by rhythmic cortical spiking, resulting in up to 5-fold spectral power increases, particularly at 7 Hz and higher harmonics (14, 21 and 28 Hz; see Fig. 1 (D'Ambrosio *et al.*, 2004)). A particularly compelling outcome of studies using rostral parasagittal FPI is the report that these electrocortically and behaviorally distinct characteristics were never observed in sham-operated controls (D'Ambrosio *et al.*, 2004; 2005; 2009), suggesting that they are exclusive to brain-injured rats and to PTE.

Yet, this outcome is also surprising given that the electrographic and behavioral characteristics of rostral parasagittal seizures are identical to those described for high-voltage rhythmic spiking or more commonly labeled SWD in uninjured rats, including the Sprague-Dawley breed (Aldinio *et al.*, 1985; Buzsaki, Smith, *et al.*, 1990; Kaplan, 1985; Kelly *et al.*, 2001; Kharlamov *et al.*, 2003; Kleinlogel, 1985; Pearce *et al.*, 2014) used in all FPI experiments to date. SWD are quasi-periodic signals and therefore have unique spectrums with high values at a fixed fundamental frequency (typically 7-9 Hz) and at whole multiples (harmonics) of this fundamental frequency. These spectral characteristics so distinctly identify SWD (Shaw, 2004) that they have been routinely used for automated SWD detection (Hese *et al.*, 2003; Van Hese *et al.*, 2009). They are also the same as those described for cortical discharge produced by rostral parasagittal FPI (D'Ambrosio *et al.*, 2004). Additionally, SWD are invariably associated with behavioral arrest and facial automatisms (Hammond *et al.*, 1979; Kaplan, 1985; Robinson and Gilmore, 1980; Semba *et al.*, 1980; Shaw, 2004; Vanderwolf, 1975; Vergnes *et al.*, 1982). The common presence of SWD and associated behavioral arrest in uninjured Sprague-Dawley rats raises the possibility of confounds in the interpretation of results from PTE models if they are thought to also reflect seizures (for a review of this controversy, please see: (D'Ambrosio and Miller, 2010; Dudek and Bertram, 2010)). The present study quantified features of SWD episodes in control rats at 1-12 months of age with the objective of distinguishing normal brain activity from that associated with PTE. These results were compared to the same timeline in brain-injured rats receiving moderate and severe rostral parasagittal FPI.

## Materials and methods

Ninety adult viral-free male Sprague-Dawley rats (Harlan Laboratories, Madison, WI) were housed in pairs in temperature (23 ± 3 °C) and light (12:12 light: dark) controlled rooms with *ad*

*libitum* access to food and water. All procedures were performed in accordance with University of Colorado Institutional Animal Care and Use Committee guidelines for the humane use of laboratory rats in biological research. Rats were randomly assigned to the following groups: Sham operated (n = 20), Naïve (n = 20), FPI-moderate (n = 15) and FPI-severe (n = 35). To establish a temporal profile of SWD events over time, chronic video/EEG recording was performed in rats at 1-3 months only (5%), 1-6 months only (20%), 6-12 months only (50%), and 1-12 months (25%).

## Fluid percussion injury and experimental groups

The rostral parasagittal FPI used in this study has been described previously (Frey *et al.*, 2009; Rodgers *et al.*, 2012; 2014). Briefly, FPI rats were anesthetized with halothane (Abbott Laboratories; 3.5% induction, 1.5-2.0% maintenance) and mounted in a stereotaxic frame. A 3.0 mm diameter craniotomy was centered at AP, -2.0 mm and ML, 3.0 mm from the mid-sagittal suture (Fig. 1A), with the exposed dura remaining intact. A female Luer-Loc hub (inside diameter of 3.5 mm) was secured over the craniotomy with cyanoacrylate adhesive. Following hub implantation, rats were removed from the stereotaxic frame and connected to the FPI apparatus. The FPI apparatus delivered one of two impact pressures (10 ms pulse), either an impact force of 2.0 or 3.4 atm (moderate or severe injury, respectively). All rats experienced apnea following injury and were revived after 15 sec. The injury cap was then removed, scalp sutured, and the rats returned to their home cages for recovery. The righting time was approximately 10 min following injury. There was a ~10% mortality rate for severe impact pressures. Sham operated rats underwent identical surgical preparation, but did not receive the brain injury. Naïve rats only received electrode implantation surgery described below.

## Chronic video/EEG recording

One week following FPI or sham surgery, epidural bilateral stainless steel screw electrodes were implanted for ECoG recording, using septic surgical procedures for all chronic preparations. Under halothane anesthesia (3.5%), rats (post-natal days 32-34, 3 month old, or 8 month old) were implanted with bilateral screw electrodes ipsilateral and contralateral to injury (Fig. 1A) over parietal (AP, -6.0 mm, ML, 4.5 mm) and frontal (AP, 0 mm, ML, 4.5 mm) cortex, a reference screw (AP, 3.0 mm, ML, 1.0 mm), and a ground screw (AP, -7.5 mm, ML, 1.0 mm). Following a one-week recovery period, animals were tethered to an electrode harness (Plastics One, 363) and slip-ring commutator (Plastics One, SL6C) permitting free movement for 24/7 video/EEG monitoring throughout the duration of the experiment. Spontaneous EEG signals were amplified (x10000) and digitized at 500 Hz. Spontaneous EEG and video were stored for subsequent SWD event detection and related behavioral analysis.

**Semi-automated SWD detection and quantification**

ECoG data were analyzed in one-second segments. Approximately 20 segments containing SWD were visually selected for each rat at ages 1, 3, 6, 9 and 12 months. Auto-covariance functions were computed for identified segments to capture the amplitude, frequency, and waveform morphology of the SWD. Covariance functions for SWD trials and similar functions for segments containing representative noise were used to train a Support Vector Machine (Orrù *et al.*, 2012) to automatically discriminate between SWD and noise throughout 48 hours of data for each rat at each age recorded for that rat. All detected SWD events for a given 48-hour period were visually examined and artifacts deleted before the number and durations of SWD events were extracted for statistical analysis. In rats where all four electrodes were viable for comparison, recordings of 10 SWD epochs per rat were also examined to assess asynchronous versus synchronous onset. If SWD began in one electrode channel at least 100 ms

before activity could be detected in other channels, it was considered an asynchronous onset. Synchronous onsets were characterized by no detectable delay of SWD between the 4 recording electrodes. Isolated onsets were defined as SWD bursts that never spread beyond a single electrode. Behavior during automatically detected SWD was assessed for representative 48 hr periods with time-locked video. All rats were also visually observed during SWD to detect subtle behaviors (i.e. vibrissa and jaw movements).

### Convulsive seizure detection and quantification

Visual detection of potential convulsive seizures was performed using custom software. Video/EEG for a given rat was displayed in 30 min blocks on high-resolution monitors. Convulsive electroencephalographic seizures were differentiated from background noise by the appearance of large-amplitude (at least three times baseline), high frequency (minimum of 5 Hz) activity, with progression of the spike frequency that lasted for a minimum of 20 seconds. Behavioral video data was used to determine seizure intensity and to confirm EEG seizure activity versus potential animal generated noise such as eating and grooming. Seizure intensity was rated according to Racine's behavioral scale (Racine, 1972), recently modified to rate the intensity of post-traumatic seizures (D'Ambrosio *et al.*, 2004).

## Results

### FPI injury

By 5 months post-injury, FPI typically induced damage at the locus of the craniotomy (Fig. 1C; upper plates) beginning at the level of the dorsal hippocampus. Contralateral brain structures appeared to be morphologically preserved, although some ventricular enlargement could be seen in FPI rats contralateral to injury. Just caudal to the craniotomy (Fig. 1C; lower

plates) FPI induced marked structural damage, cortical atrophy, deformation and atrophy of the hippocampus and ventricular enlargement.

## Incidence of SWD events

SWD incidence rate was indistinguishable between FPI and control animals $F(1,9) = 0.321$, $p = 0.587$, across all time points post-injury. The incidence rate ranged from 66.7% - 100% at the 1-month and 3-month time points, and from 90% - 100% at the 6-month, 9-month, and 1-year time points. As noted below, while the incidence of SWD was high even at 1-3 months, the number and duration of events was far lower than at later time points.

## Pattern recognition of SWD events

Figure 2 shows a six second SWD event (Fig. 2A; red) detected in an uninjured 12-month old rat. Events such as the one depicted here were typically characterized by an abrupt (<1 sec) onset and termination (Fig. 2A; arrows), lack of post-event amplitude suppression, steady frequency of approximately 7-8 Hz, clear spike-wave morphology (Fig. 2C; S and W), and spindle-like variations in amplitude throughout the event. For automated event detection, data were analyzed in successive one-second blocks. The auto-covariance function for each block (Fig. 2B and C: dark trace) captured both the amplitude and morphology of SWD (Fig. 2C; light trace). A linear or quadratic kernel was trained on the auto-covariance functions of 20-30 visually identified one-second blocks of SWD for each rat at each age and then used to detect subsequent SWD for that animal.

## Spatiotemporal features of SWD events

A total of 470 and 510 SWD events in the FPI and control rats, respectively, were examined for isolated, asynchronous, or synchronous onset. In no animals did SWD in the 2 parietal leads precede the frontal electrodes. While right versus left asynchronous onsets in the

frontal leads were observed, a majority of SWD events in FPI and control animals began synchronously (79% and 90%, respectively). In FPI rats, 13% of SWD showed asynchronous onset starting in the right frontal electrode at the site of injury, compared to 6% starting in the left hemisphere. However, there was also a right hemisphere preference (7%) compared to the left hemisphere (2%) for SWD onset in the control animals. We recorded isolated (one electrode only) SWD in only a very small number of events for either FPI or control rats (2% and 1%, respectively). A one-way ANOVA conducted to compare the effect of injury group (FPI-injured or uninjured controls) on synchronous, left hemisphere or right hemisphere asynchronous, or isolated SWD onsets showed no significant group effects ($F(1,96) = 1.39$, $p = 0.241$, $F(1,96) = 1.46$, $p = 0.229$, $F(1,96) = 0.00$, $p = 0.997$ and $F(1,96) = 1.88$, $p = 0.174$, respectively).

**Behavioral features of SWD events**

When time-locked video was examined, SWD events detected in both uninjured and injured rats were associated with inactivity or interruption of ongoing movement. Real-time visual examination of a subset of control and FPI rats revealed that SWD were often accompanied by vibrissa extension and slight vibrational tremor, and terminated by bruxing movements of the incisors that were sometimes sufficiently intense to produce eye “boggling” (rapid movement of the eye in and out of the socket due to flexing of the masseter muscle). No events exceeding a seizure intensity score of 2 were observed.

**SWD counts and lengths as a function of age and injury**

Figure 3 exemplifies SWD in an uninjured rat recorded across 1-12 months of age. One-second samples shown here typify SWD in the majority of normal control rats across their lifespan (Fig. 3A). SWD were fully developed at 12 months with a clear spike-wave morphology. The number and duration of SWD events increased with age, but short bursts of

larval SWD could be detected even at 1 month. Despite age-related increases in the number and duration of events, the morphology and frequency, best visualized in the averaged SWD (Fig. 3B) and auto-covariance function (Fig. 3C), remained stable even when comparisons were made between 1 and 12 month records (Fig. 3; 12 month; light and dark traces, respectively).

The number ($p = 0.099$) and duration ($p = 0.132$) of SWDs did not differ between naïve and sham controls, so these groups were combined for the overall analyses. Age-related increases in the number and duration of SWD events are summarized in the grouped control and FPI rats (Fig. 4A and B). A two-way ANOVA was conducted to examine the effect of age (1 month – 12 month) and injury group on the number of SWD events. There was no significant interaction between the effects of age and injury on the number of SWD events (Fig. 4A) for any time point post-injury ($F(11,356) = 0.600$, $p = 0.700$). There was a main effect found for age, with the total number of SWD events significantly increasing with age ($F(4,356) = 2.951$, $p = 0.020$). Post-hoc comparisons showed that the older (9-12 month) FPI and control rats displayed more SWD events than the younger rats, which was statistically higher at both the 9 month ($p < 0.01$) and 1 year ($p < 0.01$) time points. However, there was not a significant main effect for injury group ($F(2,356) = 0.338$, $p = 0.713$), indicating no difference in the number of SWD events between FPI-injured and uninjured control rats.

A two-way ANOVA examining the effect of age and injury on the duration of SWD events also revealed no significant interaction (Fig. 4B; $F(11,356) = 1.259$, $p = 0.281$). A significant main effect was found for age ($F(4,356) = 7.189$, $p = 0.000$), reflecting significantly longer SWD duration as a function of age, across both groups. In both FPI and control groups SWD duration was significantly longer at the 6 month ($p < 0.05$), 9 month ($p < 0.05$), and 1 year

($p < 0.05$) time points. As with the number of SWD events, there was no main effect for injury group and SWD duration across any time point post-injury ($F(2,356) = 2.041$, $p = 0.131$).

Characterization of the SWD events by burst length in uninjured controls (Fig. 4C) showed that the number of SWD bursts declined with increasing length. SWD burst length parameters for FPI-injured rats (Fig. 4D) followed very similar age-related patterns and were not significantly different from the uninjured controls ($F(39,2379) = 1.491$, $p = 0.078$). There was not a significant main effect found for injury group ($F(39,2379) = 2.563$, $p = 0.110$). There was a significant main effect found for burst length ($F(39,2379) = 123.881$, $p = 0.000$), revealing that there were significantly more 1 sec – 3 sec SWD events than 4 sec – 20 sec events ($p < 0.010$). While the number (Fig. 4A) and duration (Fig. 4B) of SWD events increase with age, the SWD burst length decreased to include mostly 1 sec – 10 sec SWD events.

**SWD frequency, morphology, and sensory interruption as a function of injury**

SWD frequency (referring to spike repetition rate, not frequency of bursts) was consistently in the range of 7-9 Hz and did not differ between uninjured (7.7 Hz ± 0.4) and injured (7.9 Hz ± 0.3) animals (Fig. 5A). SWD morphology was also qualitatively similar between groups (Fig. 5B). In a final comparison, we used automated SWD detection to trigger an auditory stimulus (~65 dB SPL; 20 cm distance) during ongoing SWD events in a subset of 9 control and 12 FPI rats (Fig. 6). It has been noted in other studies that, unlike seizures, normal SWD may be interrupted by sensory stimulation and arousal (Buzsaki, Laszlovszky, *et al.*, 1990; Kaplan, 1985; Pearce *et al.*, 2014; Robinson and Gilmore, 1980; Semba *et al.*, 1980; Shaw, 2004; Vergnes *et al.*, 1982; Wiest and Nicolelis, 2003). Similar to these previous reports, a click had the effect of rapidly aborting ongoing SWD in our control rats (single trial example shown in Fig. 6A). Figure 6B and C shows averaged spectrograms (n=10 trials each) of click-evoked SWD

suppression for two control and two FPI rats, respectively. Note also in these spectrograms the stereotyped harmonic spectral bands for SWD marked with white lines at the fundamental frequency (7-9 Hz) and the first higher harmonic (14-18 Hz). The percent of click-evoked SWD suppression was calculated for all rats by comparing the ratio of total RMS power for two seconds before and after the click. The average suppression was 89.3±0.48% and 90.5±0.55% for the control and FPI, respectively (Fig. 6D), and did not significantly differ between the groups ($p = 0.16$).

### Convulsive seizures

None of our injured or uninjured rats developed convulsive seizures, even when measured out to 12 months of age.

## Discussion

### SWD/freezing-behavior in uninjured rats

Our results indicate that SWD events are a very common phenomenon in uninjured Sprague-Dawley rats, supporting observations of previous studies of this species (Aldinio *et al.*, 1985; Buzsaki, Smith, *et al.*, 1990; Kaplan, 1985; Kelly *et al.*, 2001; Kharlamov *et al.*, 2003; Kleinlogel, 1985; Pearce *et al.*, 2014) as well as Long Evans (Kaplan, 1985; Semba *et al.*, 1980; Shaw, 2004; Wiest and Nicolelis, 2003), Wistar (Dejean *et al.*, 2007; Kaplan, 1985; Robinson and Gilmore, 1980; Vergnes *et al.*, 1982), Hooded (Vanderwolf, 1975), Buffalo (Buzsaki, Smith, *et al.*, 1990) and Fischer (Buzsaki, Smith, *et al.*, 1990) rats. This electrographic pattern has been variously termed high-voltage rhythmic spike discharge, poly-spiking activity, sensorimotor rhythm, high voltage spindles, alpha (mu) rhythm, paroxysmal electro-clinical patterns, as well as spike-wave discharge. In addition to common waveform morphologies, there are a number of similarities between features of SWD in these reports and the present data from our control rats.

The fundamental frequencies of SWD in uninjured rats typically range from 7 - 12 Hz (Buzsaki, Smith, *et al.*, 1990; Dejean *et al.*, 2007; Hammond *et al.*, 1979; Kaplan, 1985; Marescaux *et al.*, 1984; Pearce *et al.*, 2014; Robinson and Gilmore, 1980; Semba *et al.*, 1980; Shaw, 2004; Vanderwolf, 1975; Vergnes *et al.*, 1982; Wiest and Nicolelis, 2003) and amplitudes are greater than 200 μV (Kaplan, 1985; Robinson and Gilmore, 1980; Shaw, 2004; Vergnes *et al.*, 1982). As is our data, the spectral signatures of SWD are also distinctly harmonic (Hese *et al.*, 2003; Shaw, 2004; Van Hese *et al.*, 2009), a characteristic feature of these uniquely quasi-periodic signals. SWD events are noted to start and stop abruptly (Vergnes *et al.*, 1982) and are associated with inactivity and behavioral arrest (Hammond *et al.*, 1979; Kaplan, 1985; Robinson and Gilmore, 1980; Semba *et al.*, 1980; Shaw, 2004; Vanderwolf, 1975; Vergnes *et al.*, 1982), vibrissa tremor (Buzsaki, Laszlovszky, *et al.*, 1990; Kaplan, 1985; Robinson and Gilmore, 1980; Semba *et al.*, 1980; Shaw, 2004) and facial movements (Kaplan, 1985; Robinson and Gilmore, 1980) including mastication (Buzsaki, Laszlovszky, *et al.*, 1990; Pearce *et al.*, 2014) as well as gnawing and tooth chattering (bruxing; (Semba *et al.*, 1980). Unlike other reports, we also regularly noted eye boggling at the termination of long SWD events. Authors have described SWD events that may be easily interrupted by sensory stimulation (Buzsaki, Laszlovszky, *et al.*, 1990; Kaplan, 1985; Pearce *et al.*, 2014; Robinson and Gilmore, 1980; Semba *et al.*, 1980; Shaw, 2004; Vergnes *et al.*, 1982; Wiest and Nicolelis, 2003) as in the uninjured rats we tested. Additionally, age-related increases of SWD in normal rats have been regularly observed, typically becoming fully developed after 6 months of age (Buzsaki, Laszlovszky, *et al.*, 1990; Pearce *et al.*, 2014), although poorly developed SWD (lower amplitude and ~ 1 sec duration, similar to our larval events) have been noted in animals as young as 1-2 months (Kaplan, 1985; Pearce *et al.*, 2014). SWD burst length is typically reported as several seconds, with occasional

lengths up to 30 seconds (Kaplan, 1985; Robinson and Gilmore, 1980), and increasing in length with age (Buzsaki, Laszlovszky, *et al.*, 1990). In studies where SWD event length was quantified in 4-12 month old rats (Dejean *et al.*, 2007; Shaw, 2004; Vergnes *et al.*, 1982), the average durations of 1.1 - 6 sec are comparable to 2.5 ± 0.3 sec seen in our mature animals. Similarly, total time spent in SWD averaged 8 sec/min, or 1152 sec/day, close to the 800 sec/day of SWD recorded here for 9 and 12 month old control rats (Fig. 4B). Finally, our incidence rates of SWD are comparable to, but generally higher than, those reported for mature (>6 mo) Sprague-Dawley rats at 28-89% (Buzsaki, Laszlovszky, *et al.*, 1990; Kharlamov *et al.*, 2003; Pearce *et al.*, 2014; Robinson and Gilmore, 1980), and for mature Wistar (38%) (Vergnes *et al.*, 1982) and Long-Evans (73%) (Shaw, 2004) strains. It is possible that our higher incidence numbers do not reflect a real difference between our rats and those studied by others, but were due to the use of pattern recognition and extensive review of large epochs of data, particularly for the younger rats with larval SWD.

**Absence of SWD in uninjured control rats from other FPI studies**

Both the qualitative and quantitative features of SWD in uninjured rats measured here, and in other studies, suggest that these events typify normal electrographic activity of Sprague-Dawley rats and a number of other outbred and inbred rat species, and become progressively more prevalent and prolonged with age. In this light, it is not clear why SWD were rarely noted in sham operated control animals run in previous FPI studies (D'Ambrosio *et al.*, 2004; 2005; 2009). Perhaps an insufficient number of rats were examined in this work. Yet, in an initial report, 18 sham-operated controls were recorded and SWD never observed out to 3 months of age (D'Ambrosio *et al.*, 2004). In a second study (D'Ambrosio *et al.*, 2005), only 7 of 20 control animals studied out to 7 months of age presented SWD and these events were identified as

idiopathic not by waveform, duration, or behavioral characteristics, but by their synchronous onset and larger amplitude in parietal as opposed to frontal electrodes, compared to frontal dominance noted to characterize discharge patterns in the FPI rats. Signs of behavioral arrest were not examined. Five independent control animals were used in a recent study (Curia *et al.*, 2011) with data from an additional 5 rats included from early work (D'Ambrosio *et al.,* 2005) and SWD were never seen. Assuming 20 control animals in the 2005 study were independent and not continued recording from the 2004 study (but reanalyzed for a later report (D'Ambrosio *et al.,* 2009)), this would present a total of 43 uninjured rats in 4 consecutive studies most of whom did not display any sign of SWD. Perhaps this could be due in part to the young age (3 mo) at which recording was terminated in some of the studies. Yet, while we found SWD counts were lower at the 1 and 3-month time points, with examination of 24 hr recording, multiple SWD could be identified. We could not differentiate the defined idiopathic onset pattern since all of our SWD were consistently as large or larger in the frontal leads of all rats. It is unfortunate that similar SWD were not detected in controls used for the previous FPI studies to enable direct comparisons to features in the injured animals.

**SWD/freezing-behavior events in FPI rats are not seizures**

A surprising outcome of our study is that we were not able to establish any parameter of SWD in moderate and severe brain-injured rats that uniquely differed from the uninjured control rats. Qualitative assessment of behaviors associated with SWD, such as behavioral arrest, vibrissa tremor, bruxing, and eye boggling could not be distinguished between FPI and control rats. Racine's behavioral scale (Racine, 1972), originally developed to assess the intensity of kindled seizures, has been put forward in slightly modified form to rate the intensity of post-traumatic seizures (D'Ambrosio *et al.*, 2004) such that 0 = no behavioral change (subclinical), 1

= pause in behavior, 2 = facial movements (twitching of vibrissae, sniffing, eye blinking or jaw automatisms), 3 = mild head nodding, 3.5 = severe head nodding, and 4 = myclonus. Our results suggest confounds in using this scale to assess all but the most severe seizures due to FPI since pauses in behavior (level 1) and facial movements (level 2) were consistently observed during SWD in both injured and uninjured rats. Additionally, neither our FPI or control animals displayed level 3-4 behaviors during SWD, leading us to conclude that the SWD events were either subclinical or were not seizures. Since we only examined video/behavior associated with identified SWD events, it is possible that some rats experienced level 3-4 seizures not associated with SWD. However, this is unlikely since we did visually examine all EEG from every rat on every day they were recorded and did not detect any electrical activity characteristic of convulsive seizures, events easily identified on visual analysis. This, plus the fact that ongoing SWD events in both groups could be consistently interrupted by auditory stimulation (an unlikely finding if these were seizures), and that all temporal features of SWD including spectral harmonics, onset patterns, frequency, distributions of event counts, durations, total event time, and changes in these later parameters with age, did not statistically differ between groups, leads us to conclude that FPI had no influence on SWD, did not produce PTE, and that SWD events were not seizures.

**Limitations of SWD/behavioral events as a signature of seizures**

The remarkable resilience of SWD to even severe brain damage, and its persistence in a form indistinguishable from control rats, suggests limitations in the use of SWD as an electrographic signature of seizures. Our results indicate a clear need for controls to discriminate epileptiform from benign variants of this complex in future studies of both PTE and other models of acquired epilepsy where SWD-like events have been regarded as seizures (Dube, 2006;

Rakhade *et al.,* 2011). Perhaps SWD can evolve uniquely epileptiform characteristics and transform into seizures in the FPI model, revealing a statistically significant change characterizing epileptogenesis. Indeed, it has been proposed that ictal SWD are distinguishable from non-ictal or idiopathic forms of SWD based on spatiotemporal patterns such as asynchronous onset or greater amplitude at the rostral impact location compared to parietal recording loci (D'Ambrosio *et al.,* 2004). Yet, these features appear highly variable, and, without statistical comparison to non-ictal SWD in FPI rats and in control animals, their reliability is doubtful. We always recorded larger or equal amplitude SWD in frontal electrodes, even in our control animals. Furthermore, we recorded a right hemisphere (sight of injury) bias in asynchronous onsets in both our injured and uninjured rats, albeit at a much lower incidence and shorter latencies than in previous reports. Other cortical mapping studies of SWD are in agreement with our findings, consistently showing a rostral SWD focus with asynchronous earlier onset in the peri-oral representation of somatosensory cortex (the most rostral locus) (Buzsaki *et al.,* 1988; Meeren *et al.,* 1998; 2002; van Luijtelaar *et al.,* 2011). The finding of a rostral focus has been reinforced by fMRI studies of rats inbred to produce a predominance of SWD (Blumenfeld, 2003; Nersesyan *et al.,* 2004). In the present study, it was not possible to verify a potentially ictal transformation of SWD because none of our animals developed spontaneous convulsive seizures. Our failure to elicit convulsive seizures was surprising in light of the success reported by others using FPI (Kharatishvili *et al.,* 2006). As noted by these investigators, this may indicate a marked sensitivity of the model to experimental parameters. We relied on more rostral parasagittal impact locations and performed FPI through a 3 mm diameter craniotomy, parameters reported by others to be highly successful (Curia *et al.,* 2011; D'Ambrosio *et al.,* 2004; 2005). While this resulted in a 10% mortality rate with severe impact

pressures, post-trauma apnea >15 sec that required resuscitation, and substantial brain damage evident in histology, these initial outcome measures alone may not indicate sufficient cortical and subcortical damage for epileptogenesis. In contrast to earlier reports (Curia *et al.*, 2011), recent studies suggest that more caudal and lateral impact locations with a wider (5 mm) craniotomy access may be more effective in yielding convulsive seizures and that the impact pressure wave must be sufficient to produce essential damage to entorhinal cortex and hippocampus (Kharatishvili and Pitkanen, 2010). If morphological and/or spatiotemporal changes in SWD sufficient to be conclusively defined as seizures are to be discovered, perhaps these limbic structures would also be the most productive target for recording and analysis. However, the lower success rate and long latency to seizures with this model suggests that PTE produced by FPI is much rarer than previously reported and requires long-term monitoring not conducive to efficient exploration of treatment strategies. This possibility may explain why the rostral parasagittal FPI model of PTE has received limited attention in the decade since it was first reported.

**Funding:** This work was supported by the U.S. Army Medical Research and Material Command (grant PR100040).

## References

Aldinio C, Aporti F, Calderini G, Mazzari S, Zanotti A, Toffano G. Experimental models of aging and quinolinic acid. Methods Find Exp Clin Pharmacol 1985; 7: 563–568.

Blumenfeld H. From molecules to networks: cortical/subcortical interactions in the pathophysiology of idiopathic generalized epilepsy. Epilepsia 2003; 44 Suppl 2: 7–15.

Buzsaki G, Bickford RG, Armstrong DM, Ponomareff G, Chen KS, Ruiz R, et al. Electric activity in the neocortex of freely moving young and aged rats. Neuroscience 1988; 26: 735–744.

Buzsaki G, Laszlovszky I, Lajtha A, Vadasz C. Spike-and-wave neocortical patterns in rats: Genetic and aminergic control. Neuroscience 1990

Buzsaki G, Smith A, Berger S, Fisher LJ, Gage FH. Petit mal epilepsy and parkinsonian tremor: hypothesis of a common pacemaker. Neuroscience 1990; 36: 1–14.

Curia G, Levitt M, Fender JS, Miller JW, Ojemann J, D apos Ambrosio R. Impact of Injury Location and Severity on Posttraumatic Epilepsy in the Rat: Role of Frontal Neocortex. Cereb Cortex 2011; 21: 1574–1592.

D'Ambrosio R, Fairbanks J, Fender J, Born D, Doyle D, Miller J. Posttraumatic epilepsy following fluid percussion injury in the rat. J. Neurotrauma 2003; 20: 1059–1059.

D'Ambrosio R, Fairbanks J, Fender J, Born D, Doyle D, Miller J. Post-traumatic epilepsy following fluid percussion injury in the rat. Brain 2004; 127: 304–314.

D'Ambrosio R, Fender JS, Fairbanks JP, Simon EA, Born DE, Doyle DL, et al. Progression from

frontal-parietal to mesial-temporal epilepsy after fluid percussion injury in the rat. Brain 2005; 128: 174–188.

D'Ambrosio R, Hakimian S, Stewart T, Verley DR, Fender JS, Eastman CL, et al. Functional definition of seizure provides new insight into post-traumatic epileptogenesis. Brain 2009; 132: 2805–2821.

D'Ambrosio R, Miller JW. What Is an Epileptic Seizure? Unifying Definitions in Clinical Practice and Animal Research to Develop Novel Treatments. Epilepsy Currents 2010; 10: 61–66.

Dejean C, Gross CE, Bioulac B, Boraud T. Synchronous high-voltage spindles in the cortex-basal ganglia network of awake and unrestrained rats. European Journal of Neuroscience 2007; 25: 772–784.

Dube C. Temporal lobe epilepsy after experimental prolonged febrile seizures: prospective analysis. Brain 2006; 129: 911–922.

Dudek FE, Bertram EH. Counterpoint to ‘What Is an Epileptic Seizure?’ By D’Ambrosio and Miller. Epilepsy Currents 2010; 10: 91–94.

Frey LC, Hellier J, Unkart C, Lepkin A, Howard A, Hasebroock K, et al. A novel apparatus for lateral fluid percussion injury in the rat. J. Neurosci. Methods 2009; 177: 267–272.

Haltiner AM, Temkin NR, Dikmen SS. Risk of seizure recurrence after the first late posttraumatic seizure. Arch Phys Med Rehab 1997; 78: 835–840.

Hammond EJ, Villarreal HJ, Wilder BJ. Distinction between normal and epileptic rhythms in

rodent sensorimotor cortex. Epilepsia 1979; 20: 511–517.

Hese PV, Martens J-P, Boon P, Dedeurwaerdere S, Lemahieu I, Walle RV de. Detection of spike and wave discharges in the cortical EEG of genetic absence epilepsy rats from Strasbourg. Phys. Med. Biol. 2003; 48: 1685–1700.

Kaplan BJ. The epileptic nature of rodent electrocortical polyspiking is still unproven. Exp Neurol 1985; 88: 425–436.

Kelly KM, Kharlamov A, Henntosz TM, Kharlamova EA, Williamson JM, Bertram EH, et al. Photothrombotic brain infarction results in seizure activity in aging Fischer 344 and Sprague Dawley rats. Epilepsy Res 2001; 47: 189–203.

Kharatishvili I, Nissinen JP, McIntosh TK, Pitkanen A. A model of posttraumatic epilepsy induced by lateral fluid-percussion brain injury in rats. Neuroscience 2006; 140: 685–697.

Kharatishvili I, Pitkanen A. Association of the severity of cortical damage with the occurrence of spontaneous seizures and hyperexcitability in an animal model of posttraumatic epilepsy. Epilepsy Res 2010; 90: 47–59.

Kharlamov EA, Jukkola PI, Schmitt KL, Kelly KM. Electrobehavioral characteristics of epileptic rats following photothrombotic brain infarction. Epilepsy Res 2003; 56: 185–203.

Kleinlogel H. Spontaneous EEG paroxysms in the rat: effects of psychotropic and alpha-adrenergic agents. Neuropsychobiology 1985; 13: 206–213.

Lowenstein DH. Epilepsy after head injury: an overview. Epilepsia 2009; 50 Suppl 2: 4–9.

Marescaux C, Micheletti G, Vergnes M, Depaulis A, Rumbach L, Warter JM. A model of

chronic spontaneous petit mal-like seizures in the rat: comparison with pentylenetetrazol-induced seizures. Epilepsia 1984; 25: 326–331.

Meeren HKM, Pijn JPM, Van Luijtelaar ELJM, Coenen AML, Lopes da Silva FH. Cortical focus drives widespread corticothalamic networks during spontaneous absence seizures in rats. J. Neurosci. 2002; 22: 1480–1495.

Meeren HKM, van Luijtelaar ELJM, Coenen AML. Cortical and thalamic visual evoked potentials during sleep-wake states and spike-wave discharges in the rat. Electroencephalography and Clinical Neurophysiology/Evoked Potentials Section 1998; 108: 306–319.

Nersesyan H, Hyder F, Rothman DL, Blumenfeld H. Dynamic fMRI and EEG recordings during spike-wave seizures and generalized tonic-clonic seizures in WAG/Rij rats. J. Cereb. Blood Flow Metab. 2004; 24: 589–599.

Orrù G, Pettersson-Yeo W, Marquand AF, Sartori G, Mechelli A. Using Support Vector Machine to identify imaging biomarkers of neurological and psychiatric disease: A critical review. Neuroscience & Biobehavioral Reviews 2012; 36: 1140–1152.

Pearce PS, Friedman D, Lafrancois JJ, Iyengar SS, Fenton AA, Maclusky NJ, et al. Spike-wave discharges in adult Sprague-Dawley rats and their implications for animal models of temporal lobe epilepsy. Epilepsy Behav 2014; 32: 121–131.

Racine RJ. Modification of seizure activity by electrical stimulation. II. Motor seizure. Electroencephalogr Clin Neurophysiol 1972; 32: 281–294.

Rakhade SN, Klein PM, Huynh T, Hilario-Gomez C, Kosaras B, Rotenberg A, et al. Development of later life spontaneous seizures in a rodent model of hypoxia-induced neonatal seizures. Epilepsia 2011; 52: 753–765.

Robinson PF, Gilmore SA. Spontaneous generalized spike-wave discharges in the electrocorticograms of albino rats. Brain Res. 1980; 201: 452–458.

Rodgers KM, Bercum FM, McCallum DL, Rudy JW, Frey LC, Johnson KW, et al. Acute Neuroimmune Modulation Attenuates the Development of Anxiety-Like Freezing Behavior in an Animal Model of Traumatic Brain Injury. J. Neurotrauma 2012

Rodgers KM, Deming YK, Bercum FM, Chumachenko SY, Wieseler JL, Johnson KW, et al. Reversal of established traumatic brain injury-induced, anxiety-like behavior in rats after delayed, post-injury neuroimmune suppression. J. Neurotrauma 2014; 31: 487–497.

Semba K, Szechtman H, Komisaruk BR. Synchrony among rhythmical facial tremor, neocortical 'ALPHA' waves, and thalamic non-sensory neuronal bursts in intact awake rats. Brain Res. 1980

Shaw F-Z. Is Spontaneous High-Voltage Rhythmic Spike Discharge in Long Evans Rats an Absence-Like Seizure Activity? J Neurophysiol 2004

Thompson HJ, Lifshitz J, Marklund N, Grady MS, Graham DI, Hovda DA, et al. Lateral fluid percussion brain injury: a 15-year review and evaluation. J. Neurotrauma 2005; 22: 42–75.

Van Hese P, Martens J-P, Waterschoot L, Boon P, Lemahieu I. Automatic detection of spike and wave discharges in the EEG of genetic absence epilepsy rats from Strasbourg. IEEE Trans

Biomed Eng 2009; 56: 706–717.

van Luijtelaar G, Sitnikova E, Littjohann A. On the origin and suddenness of absences in genetic absence models. Clin EEG Neurosci 2011; 42: 83–97.

Vanderwolf CH. Neocortical and hippocampal activation relation to behavior: effects of atropine, eserine, phenothiazines, and amphetamine. J Comp Physiol Psychol 1975; 88: 300–323.

Vergnes M, Marescaux C, Micheletti G, Reis J, Depaulis A, Rumbach L, et al. Spontaneous paroxysmal electroclinical patterns in rat: A model of generalized non-convulsive epilepsy. Neurosci Lett 1982; 33: 97–101.

Wiest MC, Nicolelis MAL. Behavioral detection of tactile stimuli during 7-12 Hz cortical oscillations in awake rats. Nat Neurosci 2003; 6: 913–914.

## Figure Captions

**Figure 1** ECoG montage and FPI histology. **(A)** Craniotomy for FPI (open circle) in relation to rostral (1 & 4) and caudal (2 & 3) recording sites. Reference and ground electrodes are 5 & 6, respectively. Cresyl violet stained coronal sections comparing a control **(B)** to damage typically induced by FPI **(C)** at 5 months post-injury. Sections taken from the locus of the craniotomy (upper plates) show damage in FPI rats beginning at the level of the dorsal hippocampus. Contralateral brain structures appear to be morphologically preserved, although some ventricular enlargement can be seen in FPI rats contralateral to injury. Just caudal to the craniotomy (lower plates), FPI induced marked structural damage, cortical atrophy, deformation and atrophy of the hippocampus and ventricular enlargement.

**Figure 2** Spike-wave discharge (SWD) and segmented auto-covariance function for pattern recognition. **(A)** Typical six second burst of spontaneous SWD detected by pattern recognition (red) recorded from parietal cortex of normal 12-month old Sprague-Dawley control rat. The SWD burst is analyzed in one-second segments. Note the sudden onset and termination (arrows), lack of post-burst suppression, and steady frequency and morphology typical for most SWD episodes. **(B)** Auto-covariance functions of successive one-second burst computed with lags of ± 200 ms capture the periodicity, wave-shape, and amplitude of the SWD segment as features for pattern recognition. Typical of SWD events, the amplitude of the covariance function waxes and wanes but the frequency and morphology remain steady from the beginning to the end. **(C)** Enlarged one-second segment of SWD (light trace) with scaled and superimposed auto-covariance function (dark trace) highlighting the spike (“S”) and wave (“W”) components.

**Figure 3** Evolution of spike-wave discharges (SWD) in an aging control rat. **(A)** Raw (un-averaged) SWDs at one month are typically brief (<2 sec) and occur infrequently. Both the duration and frequency of occurrence increase with age but the waveform morphology and frequency remain stable over the 12-month time-span. The stability of frequency and SWD waveform over the 12-month time-span are reflected in both the averaged SWD (n=3-5) **(B)** and auto-covariance functions **(C)** computed from the 1 sec samples shown in **(A)**, with little difference at 12 months (dark traces) compared to 1 month (light traces).

**Figure 4** Comparison of SWD events, time, and burst durations in control versus Lateral Fluid Percussion Injured (FPI) rats. **(A)** There were no significant differences found in the number of SWD events between FPI and control rats; however, older rats (9 month and 1 year) had significantly more SWD events. **(B)** The SWD duration was higher in older rats, significantly increased across 6 months, 9 months, and 1 year. As with the number of SWD events, no statistical differences were detected between FPI and control rats. **(C & D)** Young (1 and 3 month) control **(C)** and FPI **(D)** rats showed a predominance of 1-3 sec SWD bursts, with negligible bursts of longer duration. The total number of bursts was lowest in young animals. Bursts counts in both groups of rats increased with age and peaked at 9 months - 1 year, with corresponding age related increases in longer duration (>6 sec) bursts. Data represent mean ± SD.

**Figure 5** SWD frequency (repetition rate of spikes) and morphology for control versus FPI rats. **(A)** Spike frequency for both control and brain-injured rats across 12 months of age. **(B)** Exemplary averaged (n=3-5) fully developed SWD at 9-12 months age for rats receiving sham

surgery at one-month (‘sham”) and older naïve rats (implanted at 9-12 months). No morphological differences could be discerned for these 2 groups. **(C)** Similar to **(B)** but showing averaged SWD for 9-12 month FPI rats.

**Figure 6** Interruption of ongoing SWD events with acoustic stimulus. **(A)** Single raw trace of SWD recorded from a control rat, immediately aborted by click stimulus. **(B)** Computed spectrogram permitted averaging (n=10) the SWD interruption across multiple trials for two exemplary control rats. White horizontal lines indicate the fundamental frequency (lower line) and first harmonic (upper line). **(C)** Same as **(B)** but averaged spectrograms for two FPI rats. Ages of both control and FPI rats in these examples were 12 months. **(D)** Percent change of RMS power pre- and post-stimulus for the control (blue; n=9) and FPI (red; n=12) groups.

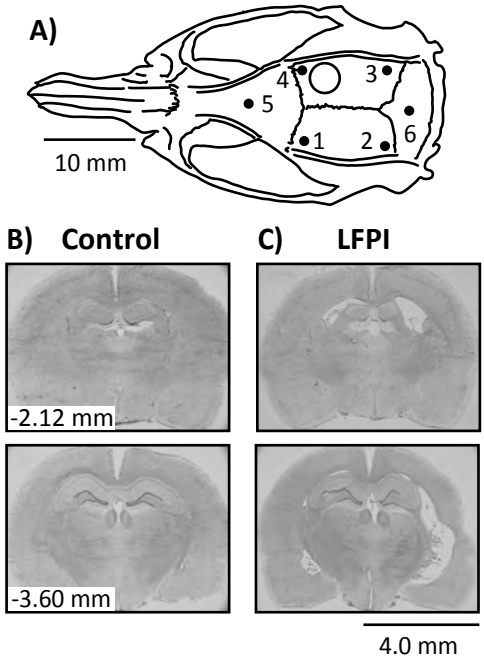
A)
4
3
5
1
2
6
10 mm
B) Control
C) LFPI
-2.12 mm
-3.60 mm
4.0 mm

FIG.2

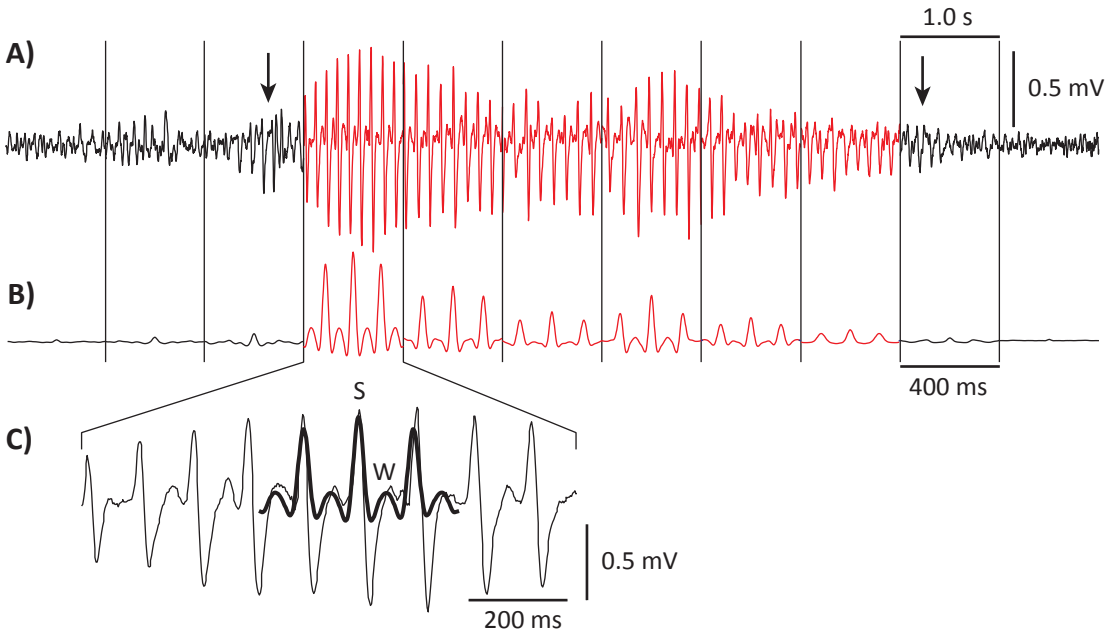

FIG.3

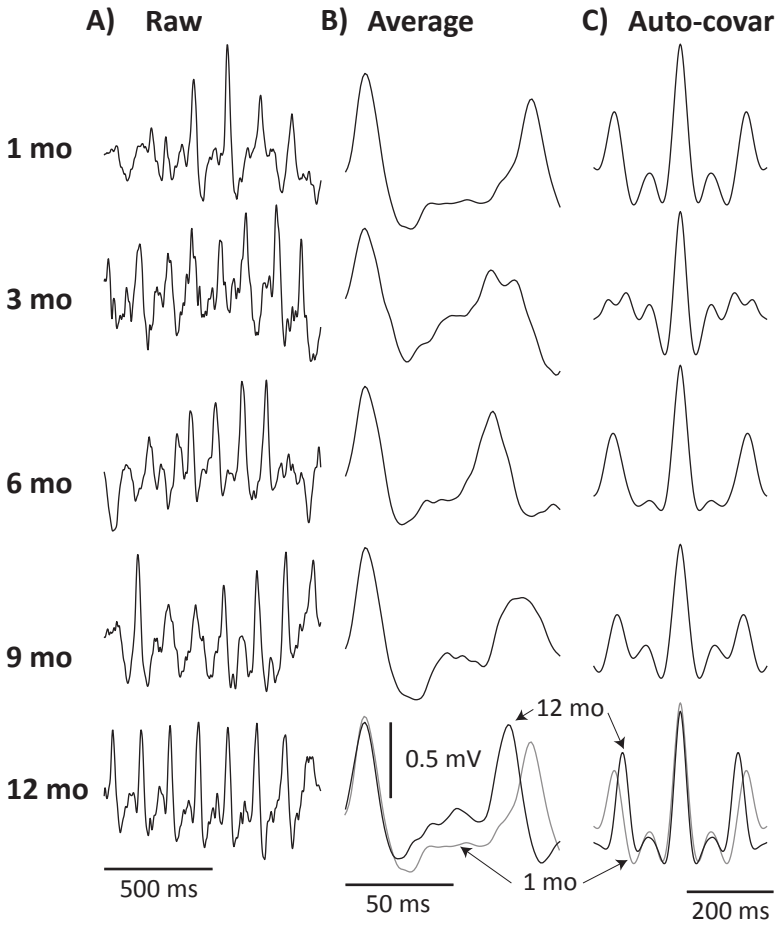
A) Raw
B) Average
C) Auto-covar
1 mo
3 mo
6 mo
9 mo
12 mo
0.5 mV
12 mo
1 mo
500 ms
50 ms
200 ms

FIG.4

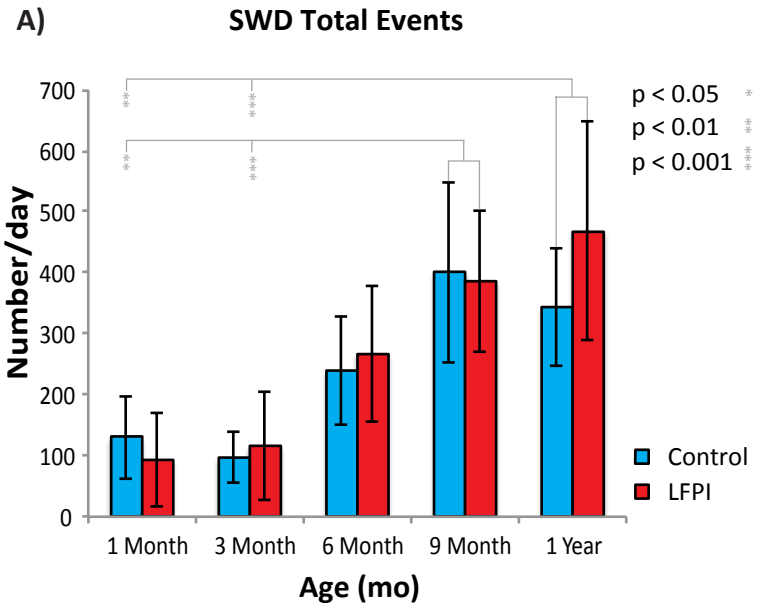
A)
SWD Total Events
Number/day
700
600
500
400
300
200
100
0
1 Month
3 Month
6 Month
9 Month
1 Year
Age (mo)
p < 0.05
p < 0.01
p < 0.001
Control
LFPI

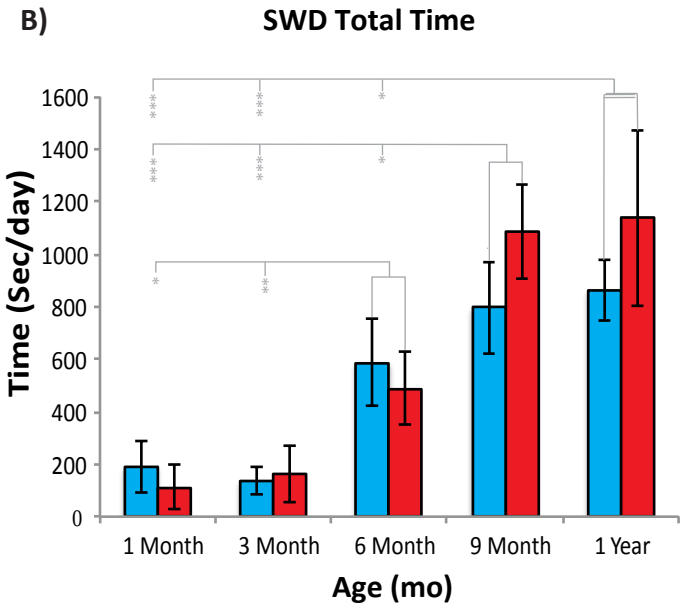
B)
SWD Total Time
Time (Sec/day)
1600
1400
1200
1000
800
600
400
200
0
1 Month
3 Month
6 Month
9 Month
1 Year
Age (mo)

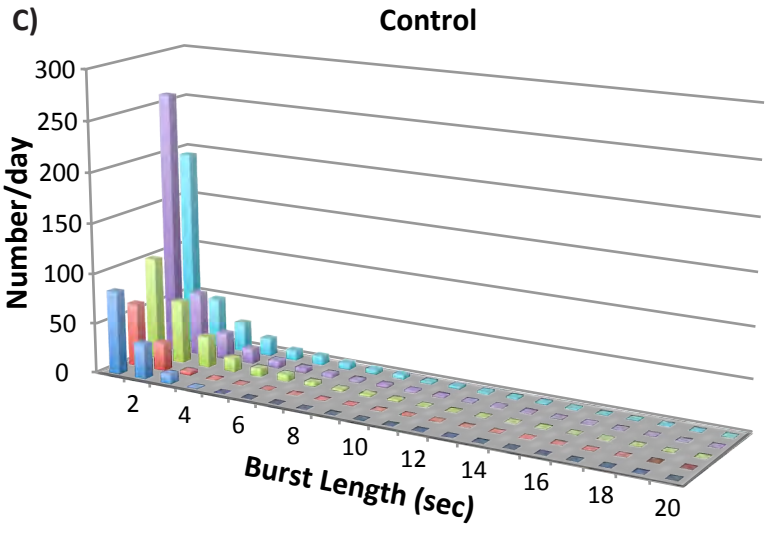
C)
Control
Number/day
300
250
200
150
100
50
0
2
4
6
8
10
12
14
16
18
20
Burst Length (sec)

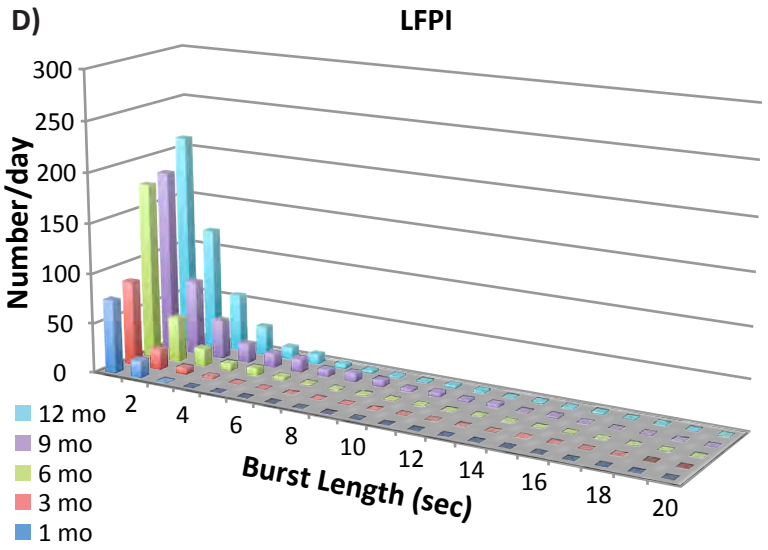
D)
LFPI
Number/day
300
250
200
150
100
50
0
2
4
6
8
10
12
14
16
18
20
Burst Length (sec)
12 mo
9 mo
6 mo
3 mo
1 mo

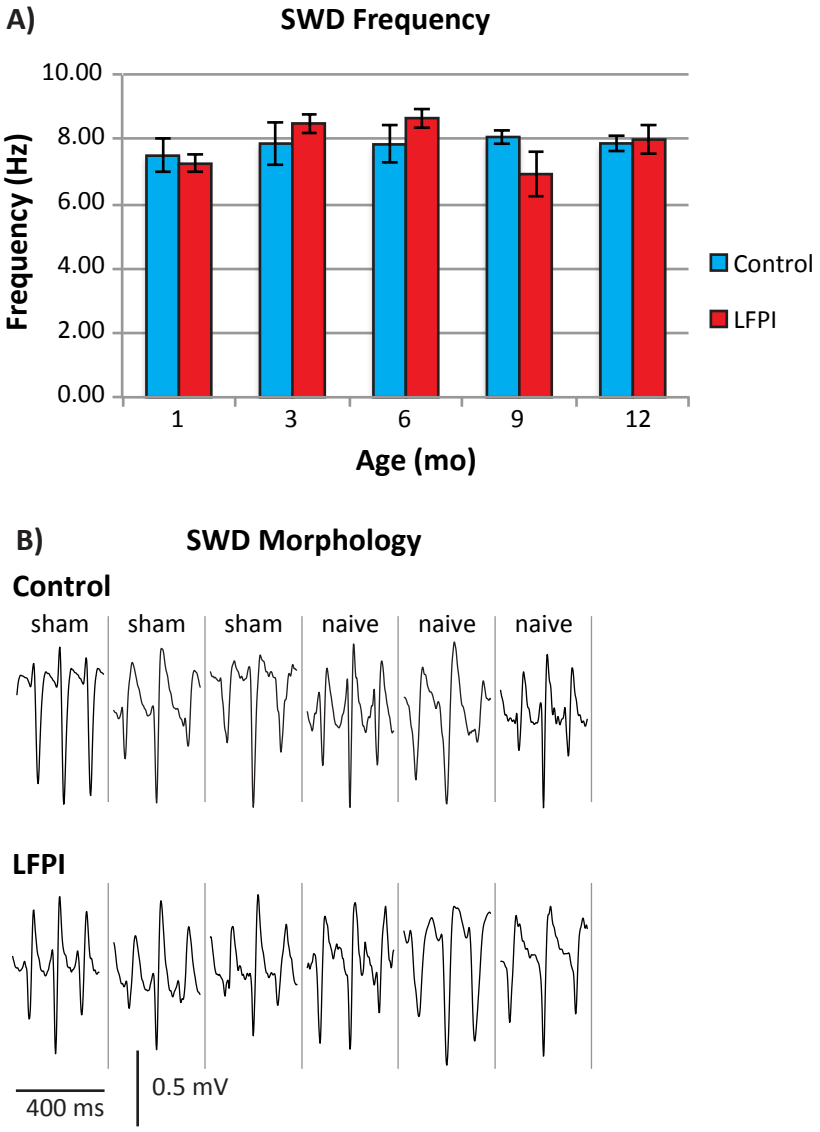
A)
SWD Frequency
10.00
8.00
6.00
4.00
2.00
0.00
Frequency (Hz)
1
3
6
9
12
Age (mo)
Control
LFPI
B)
SWD Morphology
Control
sham
sham
sham
naive
naive
naive
LFPI
400 ms
0.5 mV

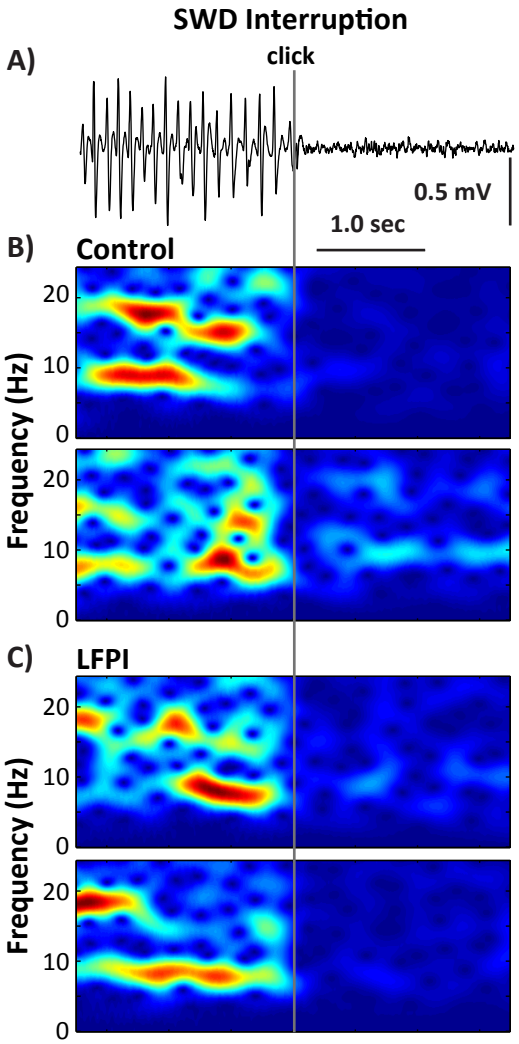
SWD Interruption
A)
click
0.5 mV
1.0 sec
B)
Control
Frequency (Hz)
20
10
0
20
10
0
C)
LFPI
Frequency (Hz)
20
10
0
20
10
0

# Magnetoencephalography of epilepsy with a microfabricated atomic magnetometer

Orang Alem[2], Alex M. Benison[1], Daniel S. Barth[1], John Kitching[2] , Svenja Knappe[1,2]

[1]Department of Psychology and Neuroscience, University of Colorado, Boulder, CO 80309

[2]Time and Frequency Division, National Institute of Standards and Technology, Boulder, CO 80305

…

We measured the magnetic signature of epileptiform discharges with high signal-to-noise ratio, using microfabricated atomic magnetometers based on laser spectroscopy of rubidium vapor and similar in size to scalp EEG electrodes. Sensitivity to neuronal currents approached that of superconducting sensors without the need for cryogenic technology. These measurements are a promising step toward the goal of high-resolution noninvasive telemetry of epileptic events in humans with seizure disorders.

…

Neuronal currents associated with brain activity produce minute extracranial magnetic fields detectable in the magnetoencephalogram (MEG), accompanied by electrical potentials recorded in the scalp electroencephalogram (EEG). Over the past 30 years there has been intense interest in MEG because, while electrical potentials are attenuated and distorted by the heterogeneous resistive properties of the cranium that compromise the spatial resolution of EEG, the skull is transparent to magnetic fields[1]. MEG has long presented the promise of providing noninvasive images of brain activity, with a spatial and temporal resolution rivaling that obtained only through penetrating the skull by use of electrodes placed within the brain.

Nowhere is the potential of MEG more clinically relevant than in the surgical treatment of human epilepsy[2,3], where the origin of seizures cannot always be adequately determined from the scalp EEG, making invasive intracranial electrical recording (electrocorticography; ECoG) necessary[4]. Yet, the use of MEG to replace invasive recording of epilepsy has remained elusive, primarily because present cryogenic technology is not suited to long-term telemetry required to capture single rare events (seizures). What is needed to fully realize the clinical potential of MEG are sensors that may be operated at room temperature, can be directly and flexibly attached to the scalp like EEG electrodes for long-term monitoring, are of sufficiently small size to permit high density placement, and most important, are capable of detecting single epileptic discharges with a sensitivity similar to invasive recording electrodes. Here, we report recording single epileptiform spikes and smaller-amplitude spontaneous brain activity, in an animal model where MEG could be directly compared to ECoG, using a microfabricated atomic magnetometer (μAM) that meets these requirements.

Atomic magnetometers, also known as optically pumped magnetometers, utilize the influence of magnetic fields on alkali atoms in a vapor. The vapor of atoms is spin-polarized by transferring the spin of resonant laser light to the atoms (**Fig. 1a**). Once the atoms (in our case Rubidium or $^{87}$Rb) are polarized, the precession, or wobble, of the electron spin can be imparted by external magnetic fields (**Fig. 1b**). Reorientation of the spins changes the light transmitted through the atomic vapor. At zero magnetic field, the light transmission is maximum, since most of the atoms are spin-polarized parallel to the transmitted light. In a non-zero transverse magnetic field the atoms precess, and the static polarization, resulting from a balance between optical pumping and precession, will not be optimally aligned with the pump light, causing a decrease in the transmission intensity (**Fig. 1c**). In order to determine the direction of the magnetic field, a small oscillating magnetic field is applied perpendicular to the light beam, and the transmitted light is demodulated with a phase-sensitive detector.

Recently it has become possible to build a practical μAM of comparable size to a standard scalp EEG electrode[5] (**Fig. 1d**), using Micro-Electro-Mechanical Systems (MEMS) technology. The use of fiber-optics and evacuated packaging[6,7] enables flexible positioning, low-power operation and the ability to position the heated sensor within a few millimeters of living tissue. The sensor head contains a $^{87}$Rb vapor cell within a vacuum package (**Fig. 1d**), keeping the outside of the sensor at room temperature while the cell is heated to 150 °C. The thin vacuum gap allows a very high-signal-to noise ratio, since the atomic vapor can be positioned within millimeters of the scalp. The vacuum package is glued to a microfabricated optical bench (**Fig. 1d**; underside of μAM) holding a ferrule with the optical fibers, along with a polarizer, beam splitter, turning mirror, and quarter-wave plate. The pump light emitted by one of the fibers is circularly polarized, transmitted through the $^{87}$Rb cell, and collected on a photodiode (removed to expose vapor cell in **Fig. 1d**).

We performed measurements in a three-layer magnetic shield made of mu-metal and containing coils to control the magnetic field environment. Figure 2 shows simultaneous recording from the μAM and from ECoG electrodes placed directly on the cortical surface of a rat. With the bottom of the μAM vacuum package pressed against the dorsal parietal skull, the center of the $^{87}$Rb cell was located approximately 3.7 mm dorsal to the left parietotemporal ridge in experiment 1 (**Fig. 2a**), or left and right parietotemporal ridges in experiment 2 (**Fig. 2d**). In experiment 1, an ECoG electrode recorded data from the pial surface (dura reflected) of the left hemisphere through a cranial window in the temporal bone 10 mm ventral to the $^{87}$Rb cell (**Fig. 2a**). In experiment 2, bilateral ECoG monitoring was performed (**Fig. 2d**). The smallest signals recorded were spontaneous transient non-epileptiform discharges associated with ketamine anesthesia[8] ("ketamine spikes"; **Fig. 2b**; "*"). The negative peaks of the ketamine spikes (280 ± 14 μV) were accompanied by similar spikes in the MEG (1.3 ± .18 pT) that could be visualized individually in the raw recording. In this figure, downward

deflections of the MEG trace reflect a dorsal tangential magnetic field component pointed caudally. Thus, during the negative ECoG spike in the left hemisphere, the caudally pointed magnetic field was consistent with that generated by dipolar intra-dendritic currents perpendicular to and directed away from the cortical surface[9], producing clockwise magnetic fields (**Fig. 2a**; circle with arrows). The signal-to-noise ratios of ketamine spikes were 9.6 ± 1.3 and 76.2 ± 10.6 in the MEG and ECoG, respectively, when noise in the live animal (sampled between spikes) was used for comparison and 18.5 ± 2.4 and 197.2 ± 10.6, respectively, compared to noise following euthanasia. Examination of recordings before and after euthanasia indicated that higher noise in the live animal was due in part to spontaneous brain activity and not from other biological sources such as respiration or cardiac artifact. Epileptiform spikes following cortical bicuculline methiodide (BMI) injection at the cranial window were approximately three times larger than ketamine spikes in the ECoG (**Fig. 2c**; 888 ± 32.7 μV; negative peak) with correspondingly large amplitude signals in the MEG (2.8 ± .18 pT). Signal to noise ratios in the MEG and ECoG of epileptiform spikes were also higher in the live (45.8 ± 1.4 and 606 ± 129.1, respectively) and euthanized (105.8 ± 20.7 and 855.6 ± 145.8, respectively) animal. Experiment 2 demonstrated the spatial resolution of μAM, with a capacity to discriminate small ketamine spikes originating in the opposite hemispheres. When we used the peaks of ~20 MEG spikes recorded above the left hemisphere (**Fig. 2g**; arrow) to time-align averages of the bilateral ECoG and MEG, the electrical and magnetic signals indicated a large source in the left hemisphere (**Fig. 2e**; lower traces), an attenuated response in the right MEG, and no response in the right ECoG (**Fig. 2e**; upper traces). The converse was true when ketamine spikes in the right MEG sensor were used for averaging (**Fig. 2f**; arrow), resulting in a large ECoG response in the right hemisphere; MEG responses also lateralized largely to the right hemisphere, and no corresponding signal in the left hemisphere ECoG (**Fig. 2f**).

The spatial resolution and sensitivity of the μAM demonstrated here is comparable to the most sensitive animal measurements of single epileptiform spikes performed with cryogenic technology[10,11]. Because the μAM operates without a cryogenic Dewar and can therefore be directly attached to the scalp as a magnetrode, its sensitivity for stationary recording of human epileptic discharge should also be comparable to present cryogenic MEG systems used in magnetically shielded environments. Yet, the small size of the μAM also makes it ideally suited to portable systems that could be worn for long-term non-stationary telemetry of brain pathology such as epileptic seizures in humans. Recent advances in scalar optically-pumped sensors have shown sensitivities below 1 $fT/Hz^{1/2}$ in centimeter-size cells[12]. Microfabrication will further reduce size while improving the dynamic range and common-mode rejection in gradiometer configurations, thus facilitating recording in unshielded or minimally shielded environments required for practical human telemetry. Further improvements in sensitivity to near the limit set by photon shot noise of 10 $fT/Hz^{1/2}$ may also enable single-trial recordings of deep brain structures in humans. While these technical improvements will facilitate the use of atomic MEG for human telemetry, the present animal recordings justify and motivate this work. The μAM represents an advance in neuro-magnetometry with the potential to realize the originally anticipated application of MEG to the non-invasive pre-surgical evaluation of human epilepsy by localizing the source of seizures.

**Supplementary Methods**

*μAM Design*

The magnetic field was sensed by the vapor of $^{87}$Rb atoms confined inside a cubic microfabricated vapor cell with internal dimensions of 1.5 mm on the side. The vapor chamber was made by dry-etching a hole into a silicon wafer and anodically bonding a 250 μm thick glass window onto each side. The atoms were confined inside the cell along with 1 amagat of nitrogen, and the cell was diced to an outside dimension of 2.5 mm. Absorptive filters were glued onto both windows and used to absorb the light from a laser at wavelength 1480 nm to heat the cell to a temperature of 150 °C. This raised the vapor pressure of the $^{87}$Rb metal in the cell, resulting in an atomic density that optimized the signal. The vacuum packaging of the cell allowed the outside surface of the sensor to remain at room temperature. This was achieved by suspending the cell on a thin web of polyimide attached to an octagonal support structure, which minimized the heat conduction to the silicon package. The octagonal assembly was attached and sealed inside a silicon package by means of anodic bonding to a glass wafer on either side. Barium getter particles placed inside the package aided to preserve the vacuum. This design achieved a minimum distance of 3.65 mm between the center of the vapor cell and the outside surface of the sensor.

The light from two diode lasers was transmitted through two 5 m long optical fibers that were terminated in a small ferrule on one end, with a distance between the two fiber faces of 125 um. The ferrule was attached to a Macor† bench that allowed the light beams to expand, be reflected by a micro-prism into a circular polarizer, and be directed toward the center of the vapor cell. Half of the heat light was absorbed by the first filter and the other half by the second. The light from the second laser was resonant with the atoms and carried the information about the magnetic field. After pumping and probing the atoms, the transmitted light was detected with a silicon photodiode bonded to a flexible polyimide backing, which carried the electrical signal to a trans-impedance amplifier.

*Principle of Operation*

The atoms were pumped and probed with a laser on resonance with the D1 transition of $^{87}$Rb at 795 nm. The light was circularly polarized to pump an orientation of the atomic spins parallel to the light beam. The atomic spins precess in a magnetic field at a well-defined frequency proportional to the amplitude of the external magnetic field. At low magnetic fields, a reorientation of the atoms results from a balance between this precession and the optical re-pumping process. A high atomic density of $^{87}$Rb inside the vapor cell also ensures that the interatomic collision rate is faster than the precession frequency and with it the suppression of dephasing due to spin-exchange collisions between the atoms[13,14]. The result is a high field sensitivity of the magnetometer. The atomic orientation is a direct measure of the magnetic field strength, which is probed by monitoring the intensity of the pump light transmitted through the cell. At zero magnetic field, the atomic magnetization is aligned along the light direction and the absorption reaches minimum. When the magnetization is reoriented by a magnetic field perpendicular to the light direction, the light absorption increases. This DC transmission is a symmetric function of the magnetic field and does not reveal the direction of the field. By applying a small modulating magnetic field perpendicular to the laser beam at 1.8 kHz and detecting the resulting oscillating signal at this frequency in a phase-sensitive way, the line-shape becomes dispersive and, for small magnetic fields, is proportional to the component of the magnetic field parallel to the modulation field. The phase-sensitive detection improves the signal-to-noise ratio as compared to a recording at DC.

*MEG Measurement Setup*

A distributed-feedback laser (DFB) was used to pump and probe the atoms in three sensors simultaneously. The light was coupled into a polarization-maintaining fiber and split into three arms, one for each sensor, by means of a fiber splitter with manually adjustable attenuation. The heating light was provided by a second DFB laser and split into three channels with a single-mode fiber splitter. The heat power for each sensor was adjusted individually with variable optical attenuators. The signal from the photodiode was amplified and processed with a digital signal processor (DSP)-based lock-in amplifier. A low-pass filter of 8$^{th}$ order at 400 Hz and notch filters at 60 Hz and 180 Hz were applied digitally.

The sensor heads were mounted in a 3D-printed plastic holder such that all fibers were pointing into the vertical direction. The holder was mounted to a Delrin† platform. The platform was slid into a Plexiglas cylinder used as a manifold to hold a set of magnetic field coils to control the magnetic-field environment. The coil set could create three orthogonal magnetic fields homogenous to 1:100 over a volume of 5 cm. In addition, a field gradient along the cylinder axis could be applied to the field along this axis. The coil manifold was housed in a three-layer magnetic shield made of mu-metal. The rat was positioned on a slider bed with a 3D-printed nose clamp and two ear bars. The bed could be shifted in two horizontal directions under the sensor array and the sensors could be lowered to touch the head of the animal. Two sensors were mounted in the vertical direction with a separation of 1 cm, while the third sensor was 10 cm away to monitor the background magnetic fields. All sensors measured the field component along the cylinder axis.

The intrinsic sensitivity of the μAM was measured to be below 25 $fT/Hz^{1/2}$, averaged between 10 and 50 Hz. The noise from the magnetic shield was estimated to be around 12 $fT/Hz^{1/2}$, and the total sensitivity inside the shield can was at 30 $fT/Hz^{1/2}$ during the experiment. The intrinsic bandwidth of the sensor was approximately 250 Hz, rolling off similar to a first-order low-pass filter to a frequency set by the steep DSP low-pass filter. The demodulated signals from the three μAMs and the ECoG electrodes were recorded with a 24-bit ADC system at a 10 kHz sampling frequency.

*Animals and Surgery*

All procedures were conducted within the guidelines established by the University of Colorado Institutional Animal Care and Use Committee. Adult male Sprague-Dawley rats (n = 3; 510-515 g) were anesthetized to surgical levels using subcutaneous injections of ketamine (71 mg/kg of body weight), xylazine (14 mg/kg) and acepromazine (2.4 mg/kg). Additional doses were administered every 60 minutes to maintain an anesthetic depth where the corneal and flexor withdrawal reflexes could barely be elicited. Animals were placed on a regulated heating pad to maintain normal body temperature (37 ºC). Skin, fascia, and parts of the masseter muscle were removed to expose the dorsal and lateral aspects of the skull. Bilateral cranial windows (2 mm x 2 mm) were surgically opened on the lateral side of the skull at the junction of the squamosal and parietal bones by use of a small Dremel† tool with a 1 mm burr tip under a surgical microscope. The dura was reflected and the exposed cortex regularly doused with Ringer Solution containing: NaCl 135 mM; KCl 3 mM; MgCl 2 mM; and CaCl 2 mM – pH 7.4 at 37 ºC. At the conclusion of the experiment, the animals were euthanized by anesthetic overdose without ever regaining consciousness.

*Electrical Recording*

Electrophysiology was performed using Ag wire ball-electrodes (ball diameter: ~1 mm; bare wire diameter: 250 μM, Teflon† coated diameter: 330 μM). The electrodes were positioned epipially through the cranial window in the squamosal bone. Recordings were referenced to a similar electrode secured over the occipital bone, and were amplified (×500; DAM80, World Precision Instruments, Sarasota, FL, USA†), analog filtered (band-pass: 1 to 1000 Hz) and digitized at 10 kHz. Both MEG and ECoG signals were subsequently digitally band-pass filtered (1 to 100 Hz) using a zero-phase, second-order, Butterworth design. To evoke epileptiform spikes, the $GABA_A$ antagonist bicuculline methiodide (BMI; Tocris Bioscience, Bristol, UK†) (100 uL, 4 mM, in 0.9 % saline) was applied to the cortical surface subsequent to ketamine spike data collection. Epileptiform spiking from BMI application stabilized after 10 minutes, at which point data were collected in 5-minute blocks.

**References**


1. Cohen, D. in Biomagnetism an Interdisciplinary Approach (Williamson, S. J., Romani, G. L., Kaufman, L. & Modena, I.) 5–16 (Plenum Press, 1983).
2. Barth, D. S., Sutherling, W., Engel, J. & Beatty, J., Science 218, 891–894 (1982).
3. Barth, D. S., Sutherling, W., Engle, J. & Beatty, J., Science 223, 293–296 (1984).
4. Engel, J., *Seizures and epilepsy*. Vol. 83. Oxford University Press, 2013.
5. Schwindt, P.D.D., Lindseth, B., Knappe, S., Shah, V. & Kitching, J., Appl. Phys. Lett. 90, 081102 (2007).
6. Preusser, J., Gerginov, V., Knappe, S. & Kitching, J., IEEE Sensors 344-346 (Lecce, Italy, 2008).
7. Mhaskar, R., Knappe, S. & Kitching, J., Appl. Phys. Lett. 101, 241105-241104 (2012).
8. Kayama, Y. & Iwama, K., Anesthesiology 36, 316 (1972).
9. Barth, D. S., Sutherling, W. & Beatty, J., Brain Res 368, 36–48 (1986).
10. Nowak, H., Gießler, F., Huonker, R. & Haueisen, J., Medical engineering & Physics 21, 563-568 (1999).
11. Zwiener, U., Eiselt, M., Gießler, F. & Nowak, H., Neurosci Lett 289, 103–106 (2000).
12. Sheng, D., Li, S., Dural, N. & Romalis, M. V., Phys. Rev. Lett. 110, (2013).
13. Happer, W. & Tang, H., Phys. Rev. Lett. 31, 273 (1973).
14. Allred, J.C., Lyman, R.N., Kornack, T.W. & Romalis, M.V., Phys. Rev. Lett. 89, 130801 (2002).

**Acknowledgements**

This work was supported by the U.S. Army Medical Research and Material Command (grant PR100040) and NIST. We thank John LeBlanc (Draper Laboratories) for the fabrication of sensor heads and Vishal Shah (QuSpin Inc.) for providing signal processing algorithms for the μAMs. This work is a contribution of NIST, an agency of the U.S. Government, and is not subject to copyright.

[†]Trade name is stated for technical clarity and does not imply endorsement by NIST. Products from other manufacturers may perform as well or better**.**

**Figure Captions**

**Figure 1** | Theory and operation of the microfabricated atomic magnetometer (μAM). (**a**) Rubidium ($^{87}$Rb) atoms are spin-polarized by transferring the spin of resonant laser light. (**b**) Precession, or wobble, of electron spin is imparted by external magnetic fields, changing the light transmitted through the atomic vapor. (**c**) Plot of light transmission with magnetic field strength (black, right) and the demodulated signal (red, left). (**d**) μAM (right) with photodiode removed to expose $^{87}$Rb vapor cell inside of vacuum package. The μAM is shown in comparison to a standard scalp EEG electrode (left) and grain of rice (top).

**Figure 2** | Simultaneous magnetic and electric recording of spontaneous spikes in the rat. (**a**) Sagittal view of the rat skull (caudal is toward the right) showing positions of the $^{87}$Rb cell for MEG, and parietal cranial window for ECoG, recording in experiment 1. The circle with arrows indicates the direction of magnetic fields expected during the negative peak of spikes in the left hemisphere ECoG. At the level of the MEG sensor, the tangential component of the magnetic field is pointed caudally. (**b**) Upper traces are raw MEG (red) and ECoG (blue) of non-epileptiform ketamine spikes ("*"). Lower traces are five superimposed ketamine spikes (light traces) and their average (dark traces). (**c**) Similar to (**b**) but showing an example of a single epileptiform spike following focal injection of bicuculline methiodide via the cranial window. Both upper and lower traces are single un-averaged spikes. (**d**) Dorsal view showing bilateral placement of magnetrodes over the parietotemporal ridges and bilateral parietal ECoG electrodes. (**e**) Averaged ($n$ = 20) ketamine spikes using the left MEG response peak (arrow) to align the average. The MEG spike (red) is lateralized to the left hemisphere and attenuated over the right. The averaged ECoG spike is confined to the left hemisphere. (**f**) Similar to (**e**) but using the right MEG response peak (arrow) to align averaging. Note a complete shift of the MEG and ECoG response to the right hemisphere. The magnetic field is reversed to a rostral direction, as expected for a right hemisphere equivalent dipole reflecting intra-dendritic current flowing away from the cortical surface toward the deeper cortical layers.

Figure 1

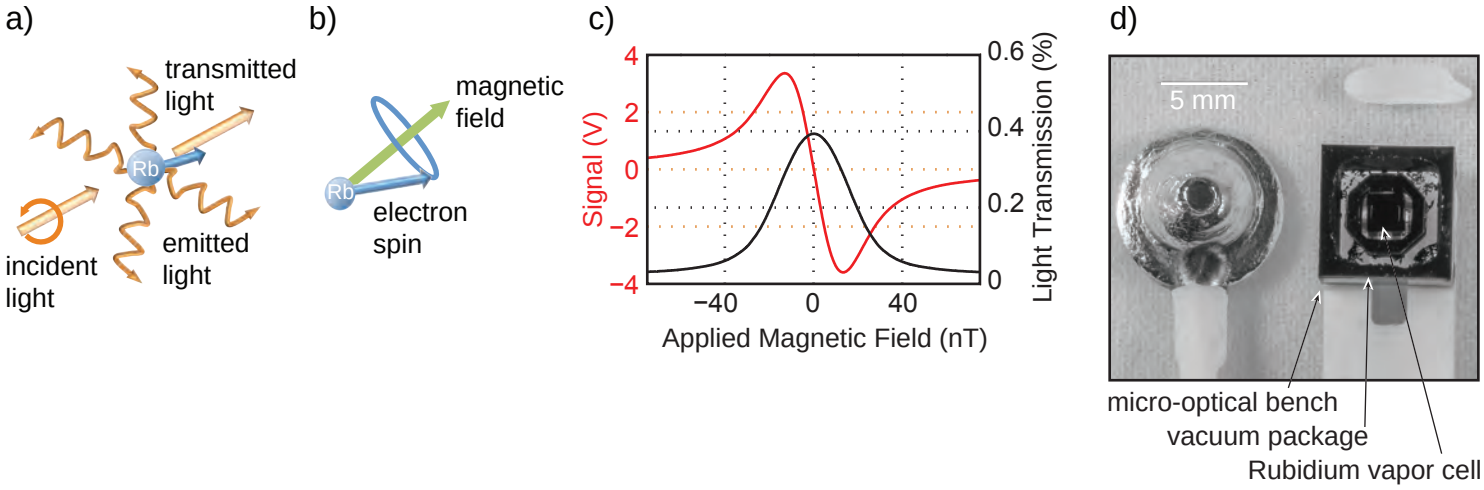
a)
transmitted light
Rb
incident light
emitted light
b)
magnetic field
Rb
electron spin
c)
Signal (V)
4
2
0
−2
−4
−40
0
40
Applied Magnetic Field (nT)
0.6
0.4
0.2
0
Light Transmission (%)
d)
5 mm
micro-optical bench
vacuum package
Rubidium vapor cell

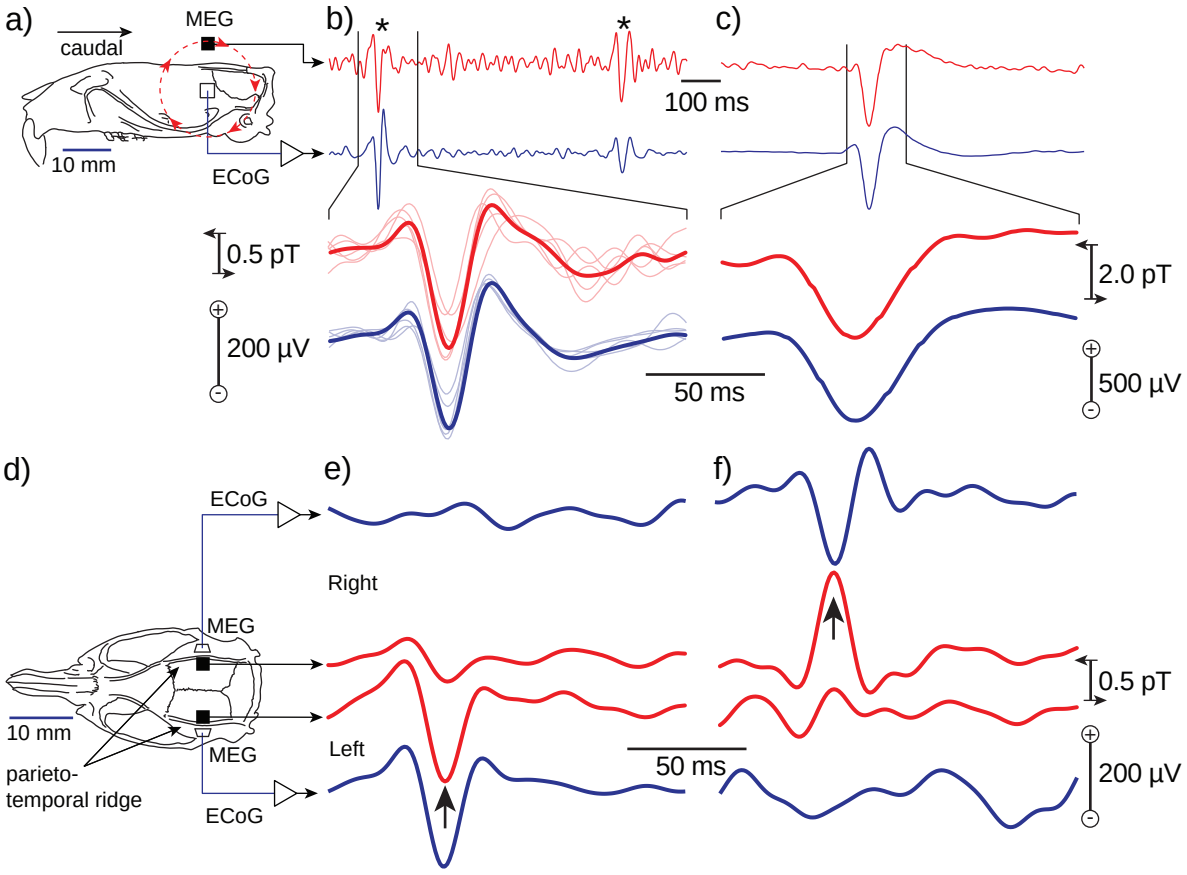
a)
caudal
MEG
10 mm
ECoG
b)
*
*
100 ms
0.5 pT
200 µV
50 ms
c)
2.0 pT
500 µV
d)
ECoG
MEG
10 mm
parieto-
temporal ridge
MEG
ECoG
e)
Right
Left
50 ms
f)
0.5 pT
200 µV

Title: Pattern recognition and quantification of spike-and-wave discharge in normal and brain-injured Sprague-Dawley rats

Presentation preference: poster only

Theme: C. Disorders of the Nervous System.

Subtheme: C.07. Epilepsy

Topic: C.07.g. Animal Models

Author: Krista M. Rodgers[1], F. Edward Dudek[2] and Daniel S. Barth[1]

[1]Department of Psychology and Neuroscience, University of Colorado, Boulder, CO 80309

[2]Department of Neurosurgery, University of Utah School of Medicine, Salt Lake City, UT 84108

Abstract:

Spike-and-wave discharge (SWD) has long been recognized in inbred rat strains as the electrographic hallmark of non-convulsive episodes that mimic *absence* seizures in humans. Similar patterns have also been reported in the electrocorticogram (ECoG) of rats undergoing lateral fluid percussion injury (LFPI), a leading model of post-traumatic epilepsy, and thought to reflect early signs of epileptogenesis preceding spontaneous convulsive seizures. However, it has been recently reported that SWD are observed in uninjured Sprague-Dawley rats used as controls in these and other models of acquired epilepsy. The presence of SWD in control rats raises the possibility of confounds in the interpretation of results from acquired epilepsy models if they are thought to also reflect epileptogenesis.

The present study quantified features of SWD episodes throughout the lifetime of normal "control" rats with the objective of distinguishing normal brain activity from that heralding the development of non-convulsive and convulsive seizures. These results were compared to the same timeline in brain-injured rats receiving moderate to severe LFPI. A support vector machine was trained on the fully developed SWD of each rat and used to detect and quantify subsequent episodes.

A majority (approximately 80%) of older (8-12 mo) control rats displayed large-amplitude and frequent SWD bouts at parietal recording sites. These events occurred in bursts of 1-30 sec duration with a typical repetition frequency of approximately 1-4/hr. Earlier recordings in the same rats also revealed clear SWD at 3-6 mo age that were of shorter duration and less frequent, and occasional "larval" SWD detected as early as 1 mo of age. All features of SWD quantified for control rats were evident in LFPI animals, including a marked increase in the frequency of occurrence, duration and amplitude with age. Initial analysis indicated that the prevalence of SWD at earlier time-points (3-6 mo) close to the time of injury may be greater in LFPI rats, but this was too variable to reach significance. These results suggest that the presence, duration, amplitude, and frequency of occurrence of SWD may not unambiguously reflect epileptogenesis in acquired epilepsy with moderate to severe LFPI. However, none of our LFPI rats developed convulsive seizures across 1-12 mo of video/EEG monitoring. Work is underway to examine LFPI animals undergoing more severe impact pressures to determine parameters of SWD that may be uniquely associated with epileptogenesis.

Support: U.S. Army Medical research and Material Command (grant PR100040)

Title: A micro-fabricated atomic magnetometer for magnetoencephalography of epilepsy

Presentation preference: poster only

Theme: C. Disorders of the Nervous System.

Subtheme: C.07. Epilepsy

Topic: C.07.g. Animal Models

Author: Alex M. Benison[1], Orang Alem[2], Svenja Knappe[1,2], John Kitching[2] and Daniel S. Barth[1]

[1]Department of Psychology and Neuroscience, University of Colorado, Boulder, CO 80309

[2]Time and Frequency Division, National Institute of Standards and Technology, Boulder, CO 80305

Abstract:

Magnetoencephalography (MEG) has long presented the promise of providing noninvasive images of brain activity with a spatial and temporal resolution rivaling that obtained only through penetrating the skull using electrodes placed within the brain. Nowhere is the potential of MEG more clinically relevant than in the surgical treatment of human epilepsy, where the origin of seizures cannot always be adequately determined from the scalp electroencephalogram (EEG) and intracranial electrical recording is still used in many cases. Yet, the use of MEG to replace invasive recording of epilepsy has remained elusive over the past 30 years, due largely to the fact that cryogenic sensors must be housed within a large Dewar "helmet" which decreases sensitivity and spatial resolution, and more importantly, eliminates the ability to capture single rare events (seizures), which require days of continuous monitoring.

We have used Micro-Electro-Mechanical Systems (MEMS) technology to fabricate a miniature atomic magnetometer smaller than a standard EEG electrode. The atomic magnetometer is optically pumped and operates at room temperature. We report here the first use of this device to measure spontaneous brain activity and epileptiform (bicuculline) spikes in the rat. With a magnetometer attached to the rat's skull, we recorded spikes with a sensitivity and signal to noise ratio rivaling that obtained with simultaneously performed electrocorticography. Single epileptiform spikes and smaller spontaneous neuronal magnetic fields were reliably recorded without the need of averaging. In addition, the small sensor size and close proximity of the magnetometer to the brain provided a spatial resolution sufficient to discriminate individual spikes in the opposite hemispheres of the rat.

With these performance characteristics, along with simplicity of design, small size for high spatial resolution mapping, easy expansion to high channel counts, flexible fiber optic coupling, and the ability to be attached to the cranium like EEG electrodes, room temperature micro-fabricated atomic magnetometers may ultimately replace cryogenic sensing technology for localizing brain pathology such as epileptic seizures. There are still technical obstacles to overcome before atomic MEG can be used for chronic epilepsy monitoring, particularly concerning shielding and noise cancelation for use in moving patients. Yet, the present results justify and motivate overcoming these obstacles. The atomic magnetometer may represent a technological advance sufficient to realize the originally anticipated potential of MEG for non-invasive pre-surgical evaluation of seizure disorders.

Support: U.S. Army Medical Research and Material Command (grant PR100040) and NIST. We would like to thank John LeBlanc (Draper Laboratories) for the fabrication of sensor heads.

Emails:

Alex: abenison@gmail.com

Orang: oranga@gmail.com

Svenja: sknappe@gmail.com

John: john.kitching@nist.gov